INTERACTION OF LEPTOSPIRAL MICROBIAL SURFACE COMPONENTS RECOGNIZING ADHESIVE MATRIX MOLECULES WITH HOST EXTRACELLULAR MATRIX

A Dissertation

Presented to the Faculty of the Graduate School

of Cornell University

In Partial Fulfillment of the Requirements for the Degree of

Doctor of Philosophy

by

Yi-pin Lin

February 2010

INTERACTION OF LEPTOSPIRAL MICROBIAL SURFACE COMPONENTS RECOGNIZING ADHESIVE MATRIX MOLECULES WITH HOST EXTRACELLULAR MATRIX

Yi-pin Lin, Ph. D.

Cornell University 2010

Adhesion through microbial surface components recognizing adhesive matrix molecules (MSCRAMM) is an essential step of infection for most pathogenic bacteria. *Leptospira spp.* are pathogenic spirochetes that cause a zonootic disease and express several important virulence factors on their surface including immunoglobulin-like (Ig-like) proteins, LigA and LigB. In this dissertation, both LigA and LigB were discovered as MSCRAMMs to bind to some extracellular matrices such as fibronectin (Fn), elastin, tropoelastin, laminin, and collagen. The Fn binding sites are located on LigBCen, C-terminal unique Ig-like domains and LigBCtv, C-terminal non-Ig-like region. In addition, those Fn-binding fragments can also mediate leptospiral adhesion to host cells.

A high affinity Fn-binding site was identified on LigBCen2, and the domains of Fn those contribute to the binding were N-terminal domain (NTD) and gelatin binding domain (GBD). Apart from Fn, LigBCen2 can interact with laminin, collagen, and fibrinogen. Interestingly, LigBCen2 was also found as a calcium-binding protein, and calcium-induced conformational change can assist LigB-NTD interactions.

Furthermore, LigBCen2 was found to contained a well folded region, LigBCen2R containing 12th and partial 11th Ig-like domains, and a disorered region, LigBCen2NR. LigBCen2R and LigBCen2NR bind to GBD and NTD, respectively. There would be a disordered to ordered transition on LigBCen2NR upon NTD binding. In addition to LigBCen2R, most of Ig-like domains on LigA (7'-8th, 10th, 11th, 12th,

13th) and LigB (7'-8th, 9th) can bind to GBD. The binding affinity of GBD or MDCK cells become greater if the Lig proteins contain more Ig-like domains especilly including the terminal Ig-like domain (LigA13 or LigB12). It suggests that Lig-GBD interaction is enhanced by multivalency to mediate leptospiral adhesion to host cells. Interestingly, Lig proteins with terminal Ig-like domains (LigAVar7'-13 or LigBCen7'-12) bind GBD with 40-fold greater affinities than it without terminal Ig-like domains (LigAVar7'-12 or LigBCen7'-11). The compact structure possessed by LigAVar7'-12 or LigBCen7'-11 instead of LigAVar7'-13 or LigBCen7'-12 suggested the relevance to their strong binding affinities with GBD and host cells.

Moreover, the Fn-binding sites of LigBCtv was also identified and located on amino acids 1708-1712, LIPAD containing region, and 15th type III modules of Fn ($15F_3$) is characterized to be the slow and moderate binding partner of LIPAD containing region. LIPAD containing region was proved to be surface exposed and possesses a nacent helix and β-strand structure.

Elastin and tropoelastin were also discovered to interact with Ig-like domains of Lig proteins. Interestingly, elastin and tropoelastin can bind to conserved region of Lig, which other ECMs don't bind. Tropoelastin-Lig interaction is attributed to charge-charge interactions, and ASP341 on 4th Ig-like domain (LigCon4) serves as an imporant role for the binding. The binding of Lig proteins to tropoelastin might be elicited to inhibit elastogenesis, then, to help the leptospiral entry by preventing tissue repair and reorganization.

Fibrinogen (Fg), a plasma rich protein can be also associated with several Ig-like domains of Lig proteins. LigBCen2R including partial 11th and full 12th Ig-like domains of LigB, can bind to FgαCC, the C-terminal αC domain of Fg. By binding to LigBCen2R, the RGD motif of FgαCC can be blocked and prevent its further interaction with integrin αIIbβ3 for platelet adhesion and aggregation. LigBCen2R-

FgαCC can also inhibit thrombin-induced fibrin clot formation but not influence the binding of plasminogen or tissue plasminogen activator. To sum up, Lig-Fg interaction blocking platelet adhesion, aggregation and clot formation might be the one of the reasons to lead pulmonary hemorrhage in *Leptospira* infected patients.

BIOGRAPHICAL SKETCH

Yi-Pin Lin was born in Taipei, Taiwan on November 20, 1979 and lived there until 1997. He entered National Cheng Kung University in Taiwan, finished his bachelors thesis on purification of prourokinase, a plasminogen activator, guided by Dr. Shyh-yu Shaw. Yi-Pin double majored in Biology and Chemical Engineering, and earned both bachelors degrees in four years on 2001. Then, he attended in National Taiwan University majoring in Biochemistry under Dr. Po-Huang Liang's supervision investigating the mechanism of antibiotics resistance and susceptibility and was granted a masters degree in 2003. After serving a military obligation for one and half years, he worked as a research assistant with Dr. Po-Huang Liang in Academia Sinica, Taiwan.

In, 2005, Yi-Pin came to Cornell University and joined Dr. Yung-Fu Chang's lab. In October of 2009, he successfully accomplished his Ph D. degree major in Comparative Biomedical Science and minor in Immunology, Biochemistry and Molecular and Cell Biology.

ACKNOWLEDGMENTS

It is a long journey for me to finish the work eventually to obtain the Ph.D. degree in Cornell University. Though only my name appears on the cover of this dissertation, a great many people have contributed to its production.

First of all, I'd like to appreciate my advisor, Prof. Yung-Fu Chang, who gave me a great of freedom to study, tolerated my rarely bad temper, and suggested me a lot the future planning especially since he is not originally from United States like me. This is also a great opportunity to express my respect to Prof. Linda Nicholson to discuss my experiment with me, gave me plenty of novel ideas, and, the most important of all, assist me to perform and analyze NMR spectra. Prof. Marci Scidmore was not only my advisor when I rotated in her lab but also taught me both cell biology techniques and seriously and carefully recorded and looked at all of the results. I also want to thank Prof. Moonsoo Jin nicely to let me use his SPR equipment and provide his insightful comments for my experiment based on his rich background of cell adhesion molecules such as fibronectin and integrin. Thanks also to Prof. Theodore Clark, Prof. Patrick McDonough, and Prof. Sean McDonough to read and correct my dissertation for me and give me some instrumental advice in committee meeting, A exam, and B exam.

I am also indebted to the members of the *Leptopspira group* in Dr. Chang's lab including Syed and Weiwei for lots of valuable discussions, and other former and current lab members such as Maria Cida, Sen, Dr. Shin, Kumanan, Rani, Li-Hsuen. Thanks also extended to my undergraduate student, Danny and Chris for all of the technical supports. Especially, I'd like to acknowledge my best American friend, Peter Rafe Harpending, although he sometimes makes trouble for making common stuff such as Rafe style LB, he still shares lots of fun and airplane knowledge with me to make me not frustrated by the failed experiments and restart my progress with full

enthusiasm.

I am grateful to Dr. Delores Tseng, my postdoctoral advisor when I was a rotation student in Prof. Scidmore's lab for her conscientious training on the designing and performing experiments. Based on those, I start to know what the real academic research is in Cornell University. Thanks also to Prof. John Helmann and Dr. Bronwyn Butcher to guide me for experiments, to learn a lot in bacterial genetics, and publish a paper eventually.

I am also thankful to other collaborators including Alex Greenwood, who generously provided his help in NMR experiments and always comment on my views of the paper and Dr. Sandra Dias who patiently instructed me the knowledge of X-ray crystallography and selflessly provided all of the necessities of that experiment. Thanks also extended to Prof. Yogendra Sharma and his student Rajeev Raman, who nicely evaluated my studies and offered the helpful discussions in calcium binding experiments, and, furthermore, enrich my ideas.

I'd like to show my gratitude to those people who have provided me with essential assistance in all of the equipments I need to use including Drs. Bhargavi Jayaraman and Charlene Mottler for ITC, Anthony Condo for DSC, Jeremiah Hanes for Stopped Flow, John Hunt for EDS, Robert Sherwood for Mass spectra, Roisen Owen for SPR, Yuanmng Zhang and Graham Kerslick for DLS, Christopher Umbach for Raman spectrophotometer, John Grazul for TEM, Timothy Foster, Hiroshi Washi, Deane Mosher, Cynthia Kinsland, and Prof. Bendicht Pauli for different clones. I'd also like to acknowledge Prof. John Leong, Prof. Magnus Höök, and Prof. Robert Oswald to give us their valuable opinions for the published papers including in this dissertation.

Many friends including Lynn, Joy, Hung-Yen, Liyang, Allen, and Wen-Hsiang, have helped me stay sane through these difficult years. Their support and care helped

me overcome setbacks and stay focused on my graduate study. I greatly value their friendship and deeply appreciate their belief in me. Particularly, I want to say thank you to Grace, Dr. Chang's wife, because of her warm-heartedly assistance in all respects, which helped me to adjust myself to this new country initially. Thanks also to Prof. Tsai-Ling Lauderdale for her consistent help before and after coming to Cornell. On the other hand, I also want to thank Brenda Payne, the administrative in department office, due to her frequent encouragement and practical advice curing my disappointment sometimes.

Most importantly, none of this would have been possible without the love and patience of my family, my father Ching-Chuan, mother You-Fan, and sister Yi-Chen. Due to their constant source of love, concern, support and strength all these years, I can smoothly finish my study and obtain Ph.D. Therefore, I would like to express my heart-felt gratitude and dedicate this dissertation to them because any of my accomplishment could not be completed without them.

Finally, I appreciate the financial support from CAT and BRDC that funded parts of the research discussed in this dissertation.

TABLE OF CONTENTS

Biographical Sketch iii

Acknowledgements iv

List of Figures xi

List of Tables xvi

Chap 1: Literature review and introduction 1

Biology of Leptospires 1

Leptospirosis in human 2

Leptospirosis in Cattle 3

Leptospirosis in horses 4

Equine uveitis, a major concern 5

Leptospirosis in swine 6

Leptospirosis in Dogs 6

Leptospirosis in sheep and goats 7

The virulence potential of leptospiral adhesins 9

The functions of Ca^{2+} in leptospires 11

References 13

Chap 2: The C-terminal variable domain of LigB from *Leptospira* mediates binding to fibronectin 30

Introduction 30

Materials and Methods 32

Results 41

Discussions 53

References 56

Chap 3: A domain of *Leptospira* LigB contributes to high affinity binding of fibronectin **65**

Introduction 65

Materials and Methods 66

Results 72

Discussions 78

References 80

Chap 4: Calcium binds to Leptospiral Immunoglobulin-like protein, LigB, and modulates fibronectin binding **83**

Introduction 83

Materials and Methods 85

Results 91

Discussions 109

References 113

Chap 5: Fibronectin binds to and induces conformational change in a disordered region of *Leptospira interrogans* immunoglobulin-like protein LigB **119**

Introduction 119

Materials and Methods 121

Results 133

Discussions 150

References 154

Chap 6: Enhancing the binding affinity to gelatin binding domain of fibronectin by Ig-like domains of *Leptospira* Lig proteins through multivalency 161

Introduction 161

Materials and Methods 162

Results 179

Discussions 194

References 201

Chap 7: Fibronectin binding activity on a surface-exposed domain within the C-terminal variable region of *Leptospira interrogans* LigB protein 208

Introduction 208

Materials and Methods 212

Results 226

Discussions 241

References 247

Chap 8: The Leptospiral Immunoglobulin-like protein repeated domains of Lig proteins interacting with elastin and tropoelastin 254

Introduction 254

Materials and Methods 259

Results 269

Discussions 285

References 291

Chap 9: *Leptospira* Immunogobulin-like proteins bind to the C-terminal fibrinogen αC domain inhibiting fibrin clot formation and platelet

adhesion **298**

Introduction 298

Materials and Methods 299

Results 313

Discussions 332

References 338

Chap 10: Conclusion **347**

LIST OF FIGURES

Figure 1.1 Schematic representation of *Leptospira* MSCRAMM including Lig proteins, Len proteins, Lsa21, Lsa27, LipL32, Lp95, and TlyC. 8

Figure 2.1 The binding of *L. interrogans* serovar Pomona to Fn. 39

Figure 2.2 The interaction between LigB and Fn by GST-pull down assay. 43

Figure 2.3 LigBCen or LigBCtv binds to Fn and inhibits the binding of *Leptospira* to Fn. 45

Figure 2.4 Isothermal titration calorimetry (ITC) profile of LigBCtv with Fn as a typical ITC profile in this study. 47

Figure 2.5 The binding of LigBCen or LigBCtv to MDCK cells reduces leptospiral adhesion. 48

Figure 2.6 The binding of LigBCen or LigBCtv to Fn siRNA transfected MDCK cells was reduced. 50

Figure 3.1 A schematic diagram showing the structure of LigB, the truncated LigB protein, Fn, and truncated Fn used in this study. 68

Figure 3.2 NTD and GBD bind on LigBCen2 at different binding site 74

Figure 3.3 LigBCen2 bind to Fn, laminin, and fibrinogen. 75

Figure 3.4 Binding of LigBCen2 to MDCK cells reduces leptospiral adhesion. 77

Figure 4.1 Schematic representation of various domains and regions of LigB and Sequence alignment of LigBCen2 with C-type lectin like domain 90

Figure 4.2 Ca^{2+}-binding characterized by EDS and MALDI-TOF mass spectroscopy. 93

Figure 4.3 Stoichiometry of Ca^{2+} binding. 96

Figure 4.4 Conformational changes of LigBCen2 after addition of Ca^{2+} monitored by CD and fluorescence. 97

Figure 4.5 Thermal stability measured by CD and DSC. 101

Figure 4.6 Calcium influences the interaction of LigBCen2 with NTD of fibronectin, monitored by fluorescence and CD. 102

Figure 4.7 Ca^{2+} influence Fn binding to LigBCen2 analyzed by near-UV CD, ELISA and Stains-all 104

Figure 5.1 A schematic diagram showing the location of the truncated LigBCen2 protein including the LigBCen2R and LigBCen2NR constructs used in this study. 123

Figure 5.2 NMR provides evidence for distinct structured and disordered regions of LigBCen2. 130

Figure 5.3 Determination of binding constant and thermodynamics of the LigBCen2NR/NTD interaction by ELISA and ITC. 136

Figure 5.4 Analysis of LigBCen2, LigBCen2R, or LigBCen2NR by Far-UV CD, GPC, DLS, and viscometry. 138

Figure 5.5 Thermal unfolding transitions of LigBCen2, LigBCen2R, or LigBCen2NR as measured by CD and DSC. 144

Figure 5.6 Modification of the Far-UV CD spectrum of LigBCen2NR upon NTD binding. 145

Figure 5.7 SPR sensograms of LigBCen2/NTD binding. 1 μM of Recombinant Histdine-tag LigBCen2 was immobilized on the surface of Ni-NTA chip. 147

Figure 5.8 The intrinsic tryptophan fluorescence of NTD in the absence and presence of LigBCen2NR. 148

Figure 6.1 A schematic diagram showing the structure of truncated LigA, LigB , and Fn used in this study. 168

Figure 6.2 Determination of binding constant, kinetics and thermodynamics of the

LigBCen2R/NTD interaction by ELISA, SPR, and ITC. 177

Figure.6.3 Localization of the GBD-binding domains on Lig proteins. 180

Figure 6.4 ITC isotherms showing the binding of GBD to various length LigA constructs 184

Figure 6.5 ITC isotherms showing the binding of GBD to various length LigB constructs. 185

Figure 6.6 Multivalent binding of Lig proteins to MDCK cells reduces leptospiral adhesion. 186

Figure 6.7 Terminal Ig-like domains contribute to the compact structure of Lig proteins 190

Figure 6.8 Terminal Ig-like domains contribute to the round shape of Lig proteins. 195

Figure 6.9 W1073C mutation cannot affect the structure of LigBCen2R. 196

Figure 7.1 Identification of the LigB C-terminal Fn-binding region and its Fn-binding residues. 210

Figure 7.2 Binding affinity determined by the ITC profile of $LigB_{1706-1716}$ with Fn. 225

Figure 7.3 The binding of $LigB_{1706-1716}$ to MDCK cells reduces leptospiral adhesion. 228

Figure 7.4 LigBCtv residues encompassing the LIPAD domain are surface-exposed. 229

Figure 7.5 LIPAD Fn-binding motif distributed in LigB and LigC from different *Leptospira* serovars show similar Fn-binding activity. 231

Figure 7.6 Mapping the LIPAD binding site in Fn. 233

Figure 7.7 Kinetic analysis of the binding of LIPAD Fn-binding motif and 15^{th} type III modules of Fn. 235

Figure 7.8 H^N-H^N region of the homonuclear NOESY spectrum of $LigB_{1703-1717}$ in PBS in H_2O and the Plot of the difference in H^α chemical shifts, or $\Delta\delta_{H\alpha}$, between observed and random coil values for $LigB_{1703-1717.}$ 237

Figure 8.1 Binding of *L. interrogans* serovar Pomona to elastin and tropoelastin. 268

Figure 8.2 A schematic diagram showing the structure of Lig proteins and the truncated Lig proteins used in this study. 270

Figure 8.3 Localization of the elastin or HTE-binding domains on Lig proteins. 271

Figure 8.4 Soluble elastin peptide or HTE inhibited LigBCon4, LigBCen7'-8, LigBCen9, LigBCen12 binding to immobilized elastin or HTE. 273

Figure 8.5 Mapping the binding site of LigBCon4, LigBCen7'-8, LigBCen9, LigBCen12 on HTE. 276

Figure 8.6 Interaction of 17-27HTE and LigBCon4 by steady state fluorescence spectroscopy and isothermal titration calorimetry (ITC). 277

Figure 8.7 The effect of different pH values on the binding of LigBCon4 to 17-27HTE. 279

Figure 8.8 Asp341 is one of the important residues contributing to the LigBCon4-17-27HTE interaction. 281

Figure 8.9 Environmental pH cannot affect the secondary structures of 17-27HTE and LigBCon4. 283

Figure 8.10 D341N mutation cannot affect the structure of LigBCon4. 284

Figure 9.1 A schematic diagram showing the structure of truncated LigA, LigB, and Fg used in this study. 304

Figure 9.2 Determination the binding sites of Fg and fibrin on LigBCen2. 314

Figure 9.3 Localization of the Fg-binding domains on Lig proteins. 316

Figure 9.4 Characterization the LigBCen2R binding site on Fg exhibited by ELISA, ITC, and steady state fluorescence spectroscopy. 319

Figure 9.5 LigBCen2R prevents the binding of FgαCC to integrin on platelets by altering the conformation close to RGD motif on FgαCC. 322

Figure 9.6 Platelet aggregation inhibited by LigBCen2R-FgαCC interaction. 325

Figure 9.7 Effect of LigBCen2R on thrombin-induced fibrin clot. 327

Figure 9.8 Competition experiments on the binding of LigBCen2 and PLG or tPA to the immunoblized FgαCC performed by ELISA. 330

LIST OF TABLES

Table 2.1 Thermodynamic parameters for the interaction of Fn and truncated LigB. 42

Table 3.1 Dissociation constant (K_d values) for the interaction of a range of truncated LigBCen with full length human Fn or NTD, GBD, or 70kDa from human Fn. 73

Table 4.1 The concentration of the metal ions detected by ICP-optical emission 92

Table 4.2 Thermodynamic and Ca^{2+}-binding parameters obtained for LigBCen2 by ITC. 95

Table 4.3 Dissociation constant (K_d values) for the interaction of NTD of Fn and LigBCen2 in the presence or absence of Ca^{2+} calculated by ELISA. 107

Table 5.1 Thermodynamic parameters for the interaction of NTD and LigBCen2R or LigBCen2NR. 135

Table5.2 Estimated radii of recombinant LigBCen2, LigBCen2R, and LigBCen2NR 140

Table5.3 Intrinsic viscosity of recombinant LigBCen2, LigBCen2R, and LigBCen2NR 143

Table 6.1 The sources of the clones used in this study 164

Table 6.2 Primer Table 166

Table 6.3 The Dissociation constants and Kinetic data of GBD-Lig interactions determined by ELISA and SPR. 175

Table 6.4 Thermodynamic parameters for the interaction of GBD and truncated Lig proteins 183

Table 6.5 Estimated radii of recombinant truncated Lig proteins 189

Table 7.1 Primers. 214

Table 7.2 Peptides used in this study 220

Table 7.3 Thermodynamic parameters for the interaction of Fn and $LigB_{1706-1716}$ 222

Table 7.4 Proton chemical shift assignments for $LigB_{1703-1717}$ 238

Table 8.1 Primers. 258

Table 8.2 The dissociation constant (K_D) obtained from the Elastin and HTE binding by Lig proteins determined by ELISA. 262

Table 8.3 Thermodynamic parameters for the interaction of 17-27 HTE and LigBCon4 or LigBCon4D341N 266

Table 9.1 The sources of clones used in this study. 301

Table 9.2 Primer Table. 302

Table 9.3 The dissociation constant (K_D) obtained from the Fibrinogen binding by Lig proteins determined by ELISA 308

CHAPTER 1

INTRODUCTION AND LITERATURE REVIEW

Leptospirosis in humans and livestock is caused by spirochetes belonging to the genus *Leptospira* and is manifested by various syndromes such as acute or chronic interstitial nephritis, pulmonary hemorrhage, myocarditis and hemolytic crisis. Leptospirosis also causes abortions, stillbirths and reproductive failure in cattle, pigs, horses and dogs, and there is an increasing prevalence of leptospirosis in humans who have come in contact with infected animals. The involvement of *Leptospira* in autoimmune disease has also been reported in horses and humans (64, 92, 96). Leptospirosis is identified as an emerging infectious disease, exemplified by recent large outbreaks in several countries, including Nicaragua, Brazil, India, Malaysia, and the United States (69). In 1992, Lederberg *et al* used leptospirosis as an example of an infection that in the past caused significant morbidity in military personnel deployed in tropical areas (68).

Biology of Leptospires: Leptospires are approximately 0.1 by 6 μm to 0.1 by 20 μm tightly coiled spirochetes, but occasional cultures may contain much longer cells. The helical amplitude and the wavelength are approximately 0.1 to 0.15 μm and 0.5 μm, respectively (40). The genus *Leptospira* comprises of saprophytic and pathogenic species and belongs to the phylum of spirochaetes. Saprophytic leptospires, such as *L. biflexa,* are free-living organisms found in water and soil and unlike pathogenic *Leptospira* spp., do not infect human or animal hosts (40). The organisms have pointed ends on either side, which are usually bent into a distinctive hook. The periplasmic space contains two axial filaments (periplasmic flagella) with polar insertions (111). Morphologically all leptospires are indistinguishable *in vivo* but the structure of individual isolates varies with subculture *in vitro*. Interestingly, the original

morphology of leptospires can be restored by passage in hamsters (26). Leptospires have a typical double membrane structure in common with other spirochetes, in which the cytoplasmic membrane and peptidoglycan cell wall are closely associated and are overlain by an outer membrane (46). Leptospiral lipopolysaccharide (LPS) has a composition similar to that of other Gram-negative bacteria (127), but has lower endotoxic activity (104, 105). Also, leptospiral LPS activates cells through a toll-like receptor 2 (TLR2)-dependent mechanism (129).

Leptospirosis in human: Leptospirosis caused by *Leptospira interrogans* is a re-emerging zoonosis occurring as large outbreaks throughout the world and US and is considered to be the most geographically widespread zoonosis (8, 70, 81, 125). This disease affects humans in both urban and rural areas and in temperate and tropical climates (9, 125). However, leptospirosis is a sporadic disease, restricted to risk exposure associated with specific occupational groups, such as farmers, miners, abattoir, sewer workers (9), athletes (45, 83, 103), military (15, 42) or recreational exposure (47, 86, 113). Leptospirosis is a major urban pathogen causing epidemics in South America with 10%-15% mortality (9, 66, 98, 102). The transmission of this disease to humans is through direct contact with the urine or infected tissues of mammalian reservoirs or indirectly through contaminated water, soil, or vegetation (5, 69). These spirochetes usually enter through injured skin and/or intact mucous membranes and then disseminate through blood vessels to various organs, such as the kidney, liver and lungs (20, 21). The clinical signs of human infection range from subclinical infection to jaundice, renal failure, and potentially fatal lung disease (9, 69, 101, 102, 124, 131). Although leptospirosis is typically a biphasic illness (anicteric), a fulminant disease can also be found in 5–10% of all patients (40, 69). Fatalities typically result from renal,

cardiac, or pulmonary failure (21, 69, 75, 101, 102). In the biphasic illness, the initial acute or septicemic phase is characterized by bacteremia that typically lasts about one week. Most of the cases present with a febrile illness of sudden onset. Fever, chills, headache, severe myalgia, conjunctival suffusion, anorexia, nausea, vomiting, and prostration usually characterize acute leptospirosis (21). A substantial proportion of people infected by *Leptospira* may have subclinical disease or very mild symptoms, and do not seek medical attention (9, 131). In this leptospiremic phase, leptospires may be found in the blood and cerebrospinal fluid (76). The resolution of symptoms may coincide with the second or immune phase, when circulating immunoglobulin M (IgM) antibodies begin to be produced, accompanied by excretion of spirochetes in the urine (21). However, fever may recur after a remission of 3 to 4 days, producing a biphasic illness (21). Weil's syndrome can develop after the acute phase as the second phase of a biphasic illness, or can simply present as a single, progressive illness. It is characterized by high fever, intense jaundice, bleeding, renal and lung dysfunction, neurologic alterations, and cardiovascular collapse, with a variable clinical course (69, 125, 126).

Leptospirosis in Cattle. Most serovars of *Leptospira* that infect cattle cause acute, subacute or inapparent leptospirosis. The most common cause of leptospirosis among cattle, especially the dairy cow, is *L. borgpetersenii* serovar Hardjo. Cattle are the maintenance host for serovar Hardjo and shedding from infected animals is responsible for the spread of this bacterium in nature. *L. borgpetersenii* serovar Hardjo (type hardjoprajitino) is isolated primarily from cattle in the United Kingdom, while *L. borgpetersenii* serovar Hardjo (type hardjobovis) is common among cattle in the US and other parts of the world (50, 118). After infection, leptospires localize in the kidneys (44, 87, 94, 115, 130) and are excreted intermittently in the urine (34). Serovar Hardjo causes outbreaks of mastitis (38) and abortion (35, 38) and is found in aborted

fetuses and premature calves (28, 38, 43, 54). In addition, hardjo has been isolated from normal fetuses (36), the genital tracts of pregnant cattle (39), vaginal discharge after calving (37), and the genital tract and urinary tract of >50% of cows (39) and bulls (31) in that area. In Australia, both serovars Hardjo and Pomona were demonstrated in bovine abortions, but serological evidence suggested that the incidence of hardjobovis infection was much higher (25, 62, 108). In the United States, serovar hardjobovis is the most commonly isolated serovar in cattle (39), but pomona also occurs. A recent serologic survey indicated that 22% and 15% of 1193 Texas slaughterhouse cattle serum samples were positive for Pomona and Hardjobovis, respectively (112). The leptospiral vaccine for cattle in use today is an inactivated whole-cell vaccine containing *L. borgpetersenii* serovar Hardjo (type hardjoprajitno), Canicola, Pomona, and Icterohaemorrhagiae and *L. kirschneri* serovar grippotyphosa (52). This vaccine is ineffective and provides only short-term immunity. Recently, it has been reported that a new *L. borgpetersenii* serovar Hardjo (hardjobovis) vaccine (SPIROVAC^{TM}, Pfizer Animal Health) could induce a Th1 immune response and protect against maternal and fetal infection in cattle (84, 85). Since there are a number of reports on the involvement of *Leptospira* in triggering autoimmunity in horses and humans, the administration of whole cells as a vaccine needs to be thoroughly studied.

Leptospirosis in horses: The prevalence of leptospiral infection in horses may be greater than any other host (117). However horses are considered to be accidental hosts, because they are not typically carriers of the disease but are susceptible to leptospiral infection only under certain circumstances (like direct exposure to a reservoir host). The bacterium is believed to be transmitted through direct contact with blood, urine or tissues of affected animals and may enter the accidental host through the mucous membranes of the eyes, nose, and mouth, or an abrasion of the skin (116). The clinical syndromes in

horses are uveitis (periodic ophthalmia) (64, 92), corneal opacity (92), abortion (22, 23), and renal diseases (19). Leptospiral infection of horses is a significant problem for the equine industry. In recent years, an increase of systemic leptospiral infection resulting in abortions has been reported (59, 60, 65). The number of confirmed leptospiral abortion cases increased from 0.6% in 1987 to 5.9% in 1990 (93). Donahue, et al. demonstrated that most isolates from aborted fetal tissues are *L. interrogans* serovar Pomona type Kennewicki with occasional isolates of serovar *grippotyphosa* (22, 23). Hong, et al. demonstrated that leptospiral placentitis is one of the most important emerging causes of equine abortion (59). Equine leptospirosis is an emerging infectious disease possibly because vaccination with a leptospiral vaccine for cattle has generally been ineffective.

Equine uveitis, a major concern: Equine uveitis is a leading cause of blindness in horses and mules in many parts of the world (48). Post leptospiral uveitis has been confirmed in a natural outbreak of leptospirosis on a small farm near Ithaca, NY (97). Five of the 16 horses showed fever and recurrent uveitis. A positive correlation between the finding of leptospiral serum agglutinins and uveitis has been reported (106). In addition, 56% of 112 horses with uveitis and only 9% of 260 horses without uveitis were sero-positive for *L. interrogans* serovar Pomona in western New York (24). Some of these latter seropositive horses subsequently developed signs of uveitis. Experimental infection with *L. interrogans* serovar Pomona results in a transient, mild systemic disease characterized by fever, leptospiremia, and leptospiuria of 120 days duration after infection. These findings have also been observed in natural infection with *Leptospira*. In the horse, the inflammatory response is characterized by a large infiltration of lymphocytes and plasma cells (30). The pathogenesis of uveitis remains to be elucidated, but clinical and experimental data strongly suggest that it is an immune-mediated disease

(64). Parma,et al. have reported that leptospiral-associated uveitis is due to the sharing of an antigenic epitope between the equine cornea and *Leptospira* (74, 91, 92, 122).

Leptospirosis in swine: Leptospirosis in swine is predominantly a chronic, asymptomatic disease, which may go unnoticed in a herd for a long time (49, 51). When it manifests itself, it is characterized primarily by the occurrence of abortions, infertility, and the birth of premature and weak piglets. Serovars Pomona and Grippotyphosa are recognized as the major contributors of infertility in pigs (27, 53). However, serogroups like Canicola, Hebdomandis, Icterohaemorrhagiae, Autumnalis and Australis have also been implicated (27) Acute systemic disease characterized by a haemolytic crisis and death is rarely encountered (27).

L. interrogans serovar Pomona is the most important cause of porcine leptospirosis in the world (27). This serovar also causes an asymptomatic chronic interstitial nephritis which is usually only identified at slaughter. Natural and experimental infections by *L. interrogans* serovar Canicola cause abortions, mummification, stillbirths, neonatal mortality and low conception rates. Serovars of the Australis serogroup are similarly associated with infertility, and have been isolated from the genital tracts of sows and boars. Pigs infected with *L. interrogans* serovar Bratislava, another important serovar that causes porcine reproductive failure in Europe and in the US, display clinical signs such as stillborn pigs, weak neonatal pigs, and abortions (10, 11, 27, 32, 33).

Leptospirosis in Dogs: In the past, serovars Icterohaemorrhagiae and Canicola were responsible for the acute forms of canine leptospirosis (2). However, serovars Australis, Pyrogenes, Autumnalis, Pomona and Grippotyphosa can induce typical acute leptospirosis, with icterus, acute renal failure, and other clinical signs. (2). A recent outbreak of acute canine lepotspirosis caused by serovars Pomona and

Grippotyphosa has been reported (http://www.ivis.org/advances/Infect_Dis_Carmichael/mcdonough). Chronic canine leptospirosis is less frequently described and is often more difficult to diagnose, simply because clinical signs can be observed in vaccinated animals (1). The present vaccine can protect the animal against acute signs but may not prevent infection if the dog is exposed to a high infectious challenge or to a highly invasive strain (3). However, subacute or chronic disease can also occur following infection by less virulent serovars. After delayed treatment of an acute form of leptospirosis, surviving bacteria within kidney or liver cells can escape host defenses, which after several weeks may lead to subacute or chronic hepatitis or renal failure. Many cases of polyuria–polydipsia syndrome of unknown etiology are probably associated with chronic leptospirosis in dogs. Reproductive failure (abortion) can also occur following infection (2).

Leptospirosis in sheep and goats: Leptospirosis of sheep manifests as two distinct clinical syndromes: an acute and often fatal systemic disease, and genital disease. The acute systemic disease in lambs is characterized by icterus, hemoglobinemia, hemoglobinuria, fever, and death, and has been associated with infections by the Pomona serogroup in particular, but rarely by the Hebdomadis, Ballum and Grippotyphosa serogroups (29). *L. borgpetersenii* serovar Hardjo infections in sheep cause agalactia, abortion, stillbirths, and the birth of weak lambs. Abortion rates of up to 20% have been recorded. Serovars such as Hebdomadis, Australis and Pomona have been reported to be the causative agent in cases of abortion. Ewes manifesting "agalactia" clinically show partial or total loss of milk production, which resolves itself without treatment within three to four days. The syndrome is usually only noticed when lambs with a normal birth weight die of malnutrition (80). The Serjoe serogroup has also been isolated from

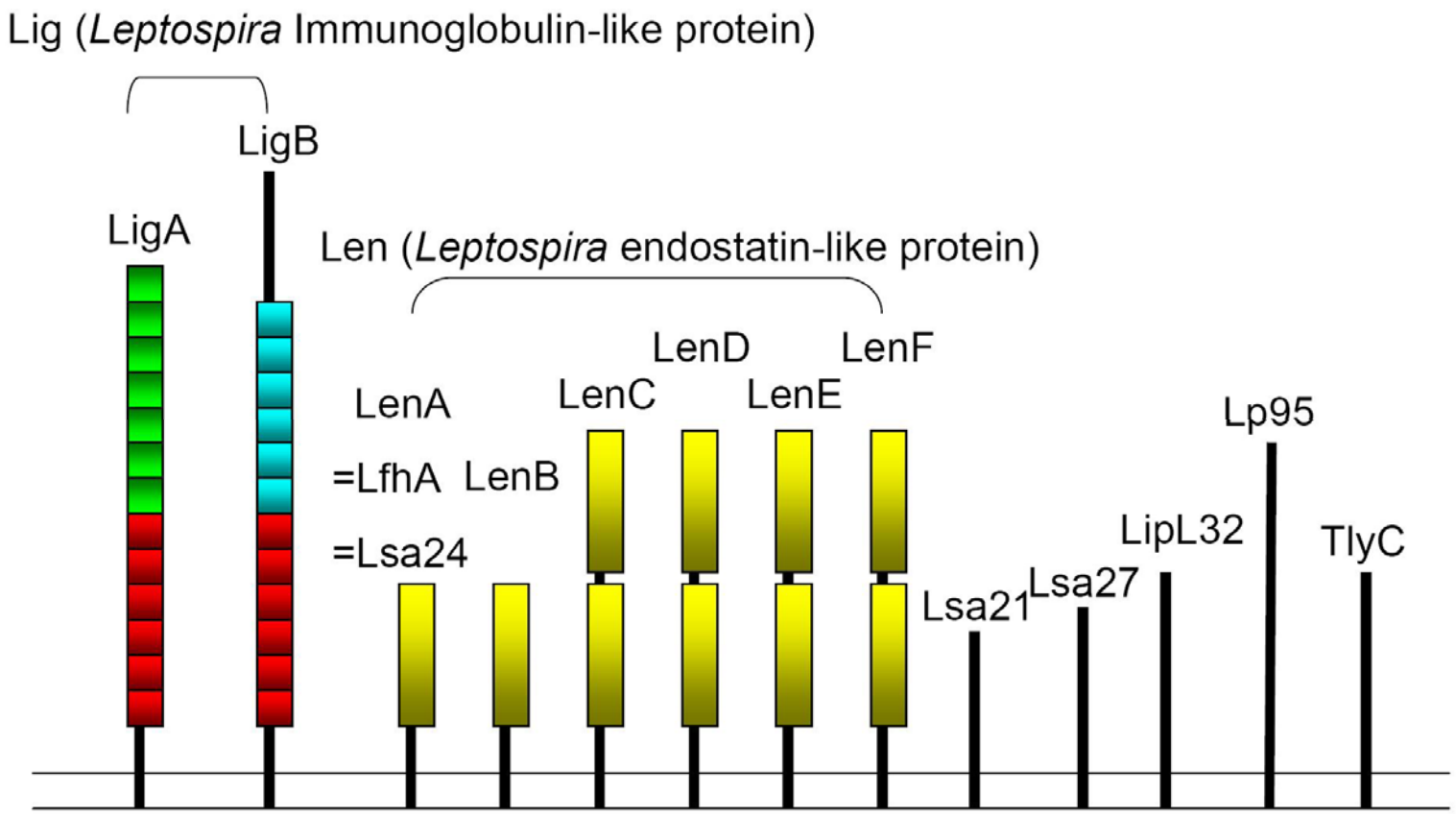

Figure 1. Schematic representation of Leptopsira MSCRAMM including Lig proteins, Len proteins, Lsa21, Lsa27, LipL32, Lp95, and TlyC

kidneys of infected sheep suffering from subclinical chronic interstitital nephritis (29) . Goats are susceptible to infection by *L. interrogans* serovar Grippotyphosa, which causes an acute disease characterized by hemoglobinuria, icterus, anemia, and death in severe cases (63). Serovars Pomona, Sejroe, Icterohaemorrhagiae and Grippotyphosa have been associated with death from interstitial nephritis (63).

The virulence potential of leptospiral adhesins: *Leptospira spp.* are highly adaptive, versatile pathogens and are cause of a wide range of clinical diseases in humans and animals (69). These spirochetes have the ability to adhere to extracellular matrix (ECM) and/or plasma proteins, which is crucial in order for the leptospires to colonize and disseminate in the host (4, 7, 14, 55, 57, 71, 72, 109) (Figure. 1). Like other pathogenic bacteria, the first step in the infective process is adherence to the host matrix (injured ski or mucous membrane). Adherence to host tissues is mediated by bacterial surface adhesins referred to as MSCRAMMs (microbial surface components recognising adhesive matrix molecules) (99, 100) or as SERAMs (secretable expanded repertoire adhesive molecules)(13). The first recognized leptospiral adhesin genes, *ligA* and *ligB* have been cloned and sequenced (77, 88, 89). Lig proteins, which include LigA and LigB, possess bacterial immunoglobulin-like (Big) domains with 90 amino acid tandem repeats. LigA is secreted into the extracellular milieu (SERAM), and it may not mediate bacterial adhesion (14, 78, 79). The N-terminal sequence of 630 amino acids are identical, but the C-terminals of LigA and LigB are variable (77, 88, 89). LigB also encodes a C-terminal, non-repeat domain of 771 amino acid residues (77, 88). LigA and LigB may serve as a SERAM and MSCRAMM, respectively, that allow pathogenic *Leptospira* to bind to host extracellular matrix components such as fibronectin (Fn), fibrinogen, laminin, and collagen (14, 71, 72). Lig proteins may also serve as good vaccine candidates and/or as diagnostic antigens (16, 41, 88, 90, 107) and

their expression is regulated by osmolarity (78). A high affinity Fn binding region of LigB, designated LigBCen2, contains 152 amino acids that include part of an immunoglobulin-like domain and a non-repeated region has also been identified (72).

Barbosa, et al. subsequently identified a Leptospiral surface adhesin (Lsa24) that binds to laminin (7). This protein has been previously reported by Verma, et al. as a factor H-binding protein of *Leptospira* (LfhA) that may be responsible for resistance of pathogenic leptospires to complement-mediated killing (123). Stevenson, et al. later found that Lsa24 or LfhA belongs to an endostatin-like outer membrane protein family that they renamed Len (Leptospiral endostatin-like) proteins that contained 6 genes (*lenA-F*). LenA and LenB are a single gene while LenC-F contain a single gene with an intragenic duplication. Len proteins bind to fibronectin, laminin, and human factor H (109). Another novel MSCRAMM, Lsa21 has recently reported by Atzingen, et al. that also binds to Fn, collagen IV, and laminin (4). LipL32 is a surface protein of *Leptospira* that has been recently found to bind to several ECMs by two different groups (55, 57). However, there is some conflict about their findings in that that the group found that LipL32 binds to Fn, but not laminin (56), while the other group claims that it binds to laminin and collagen, but not Fn (58). So far, several leptospiral MSCRAMMs have been found to have a significant functional overlap with the capacity to bind the same host factors (4, 7, 14, 56, 58, 71, 72, 109). The reason of such binding plasticity in the pathogenesis of leptospiral infection is not well understood. Each leptospiral adhesin has such a wide range of adhesive capability that may allow *Leptospira* spp. to produce specific adhesins under a broad span of environmental conditions and, in particular niches, to allow them to tailor its interaction with the host. This seems likely, given that *Leptospira spp.* causes disease in a wide range of hosts, an extensive diversity of tissues (lung, kidney, liver, etc…) and causes a wide variety of tissue damage (nephritis, hepatitis, pneumonia, and/or

meningitis). Most leptospiral MSCRAMMs described to date are outer surface proteins. The roles of these adhesins in pathogenesis are still unknown. However, it is clear that *Leptospira* spp. produce multiple ECM-binding proteins. Although many of these proteins may employ distinct mechanisms of ECM-binding, the end result is to manipulate ECM's biology to enhance the microbe's survival in the host. We may find more leptospiral ECM-binding MSCRAMMs as more pathogenic *Leptospira* spp. are sequenced in the near future. Our knowledge of how these leptospiral proteins interact with ECM is still very meager and little is known about the importance of these interactions within the disease process after *Leptospira* spp. infection.

The functions of Ca^{2+} in leptospires. Calcium plays a pivotal role in bacterial physiological activities, such as cell cycle, cell division (132), competence (121),pathogenesis (110), signal transduction (128), motility and chemotaxis (119, 120). Apart from these functions, it is also known that host-pathogen interactions of some bacteria are affected by calcium (18, 61). Several types of Ca^{2+} -binding motifs in bacterial proteins have been identified and include the well-known helix-loop-helix or EF-hand motif (82), annexin type, C2 domain of protein kinase C (67) or βγ-crystallin or Protein S type motif (6, 95, 114), leukotoxin or hemolysin-type calcium-binding domain that contains glycine rich repeats (12, 17), and orphan motifs in which oxygen atoms provided by several charged glutamate or aspartate residues are used in ligation (82). It appears that Lig proteins do not have any of these known Ca^{2+}-binding motifs. LigBCen2 shows sequence similarity to the c-type lectin domain of other adhesins including invasin of *Yersinia pseudotuberculosis* and intimin of *Escherichia coli* (88). We have found that LigBcen2 binds to Ca^{2+} (73) and it would be important to identify Ca^{2+} the binding sites in order to learn about their role in binding to ECMs.

Since Lig proteins bind to host ECM, are expressed only in vivo, are regulated by environmental cues, and are good vaccine candidates, I have focused my thesis study on the interaction of Lig proteins and host cells. The purpose of the present study was four-fold: 1). To determinate whether LigA/LigB are ECM or fibrinogen binding proteins; 2). To elucidate the role of Ca^{++} in the binding of LigA/B to fibronectin; 3). To study the conformational changes of LinBcen2 when it binds to fibronectin; and 4). To analyze whether LigA/B binds to fibronectin through multivalency.

REFERENCES

1. **Adamus, C., M. Buggin-Daubie, A. Izembart, C. Sonrier-Pierre, L. Guigand, M. T. Masson, G. Andre-Fontaine, and M. Wyers.** 1997. Chronic hepatitis associated with leptospiral infection in vaccinated beagles. Journal of comparative pathology **117:**311-328.
2. **Andre-Fontaine, G.** 2006. Canine leptospirosis--do we have a problem? Vet Microbiol **117:**19-24.
3. **Andre-Fontaine, G., C. Branger, A. W. Gray, and H. L. Klaasen.** 2003. Comparison of the efficacy of three commercial bacterins in preventing canine leptospirosis. Vet Rec **153:**165-169.
4. **Atzingen, M. V., A. S. Barbosa, T. De Brito, S. A. Vasconcellos, Z. M. Morais, D. M. Lima, P. A. Abreu, and A. L. Nascimento.** 2008. Lsa21, a novel leptospiral protein binding adhesive matrix molecules and present during human infection. BMC Microbiol **8:**70.
5. **Ayanegui-Alcerreca, M. A., P. R. Wilson, C. G. Mackintosh, J. M. Collins-Emerson, C. Heuer, A. C. Midwinter, and F. Castillo-Alcala.** 2007. Leptospirosis in farmed deer in New Zealand : A review. New Zealand veterinary journal **55:**102-108.
6. **Bagby, S., T. S. Harvey, S. G. Eagle, S. Inouye, and M. Ikura.** 1994. Structural similarity of a developmentally regulated bacterial spore coat protein to beta gamma-crystallins of the vertebrate eye lens. Proc Natl Acad Sci U S A **91:**4308-4312.
7. **Barbosa, A. S., P. A. Abreu, F. O. Neves, M. V. Atzingen, M. M. Watanabe, M. L. Vieira, Z. M. Morais, S. A. Vasconcellos, and A. L. Nascimento.** 2006. A newly identified leptospiral adhesin mediates attachment to laminin. Infect. Immun. **74:**6356-6364.

8. **Bharadwaj, R.** 2004. Leptospirosis--a reemerging disease? The Indian journal of medical research **120:**136-138.

9. **Bharti, A. R., J. E. Nally, J. N. Ricaldi, M. A. Matthias, M. M. Diaz, M. A. Lovett, P. N. Levett, R. H. Gilman, M. R. Willig, E. Gotuzzo, and J. M. Vinetz.** 2003. Leptospirosis: a zoonotic disease of global importance. Lancet Infect Dis **3:**757-771.

10. **Bolin, C. A., and J. A. Cassells.** 1990. Isolation of **Leptospira interrogans** serovar Bratislava from stillborn and weak pigs in Iowa. J Am Vet Med Assoc **196:**1601-1604.

11. **Bolin, C. A., and J. A. Cassells.** 1992. Isolation of *Leptospira interrogans* serovars Bratislava and Hardjo from swine at slaughter. J. Vet. Diagn. Invest. **4:**87-89.

12. **Chang, Y. F., J. Shi, D. P. Ma, S. J. Shin, and D. H. Lein.** 1993. Molecular analysis of the *Actinobacillus pleuropneumoniae* RTX toxin-III gene cluster. DNA Cell Biol.. **12:**351-362.

13. **Chavakis, T., K. Wiechmann, K. T. Preissner, and M. Herrmann.** 2005. *Staphylococcus aureus* interactions with the endothelium: the role of bacterial "secretable expanded repertoire adhesive molecules" (SERAM) in disturbing host defense systems. Thromb. Haemost. **94:**278-285.

14. **Choy, H. A., M. M. Kelley, T. L. Chen, A. K. Moller, J. Matsunaga, and D. A. Haake.** 2007. Physiological osmotic induction of *Leptospira interrogans* adhesion: LigA and LigB bind extracellular matrix proteins and fibrinogen. Infect. Immun. **75:**2441-2450.

15. **Corwin, A., A. Ryan, W. Bloys, R. Thomas, B. Deniega, and D. Watts.** 1990. A waterborne outbreak of leptospirosis among United States military personnel in Okinawa, Japan. International journal of epidemiology **19:**743-748.

16. **Croda, J., J. G. Ramos, J. Matsunaga, A. Queiroz, A. Homma, L. W. Riley, D. A. Haake, M. G. Reis, and A. I. Ko.** 2007. Leptospira immunoglobulin-like proteins as a serodiagnostic marker for acute leptospirosis. J Clin Microbiol **45:**1528-1534.

17. **Cruz, W. T., R. Young, Y. F. Chang, and D. K. Struck.** 1990. Deletion analysis resolves cell-binding and lytic domains of the *Pasteurella* leukotoxin. Mol Microbiol **4:**1933-1939.

18. **Dardanelli, M., J. Angelini, and A. Fabra.** 2003. A calcium-dependent bacterial surface protein is involved in the attachment of rhizobia to peanut roots. Can. J. Microbiol. **49:**399-405.

19. **Divers, T. J., T. D. Byars, and S. J. Shin.** 1992. Renal dysfunction associated with infection of *Leptospira interrogans* in a horse. J Am Vet Med Assoc **201:**1391-1392.

20. **Dolhnikoff, M., T. Mauad, E. P. Bethlem, and C. R. Carvalho.** 2007. Leptospiral pneumonias. Curr Opin Pulm Med **13:**230-235.

21. **Dolhnikoff, M., T. Mauad, E. P. Bethlem, and C. R. Carvalho.** 2007. Pathology and pathophysiology of pulmonary manifestations in leptospirosis. Braz. J. Infect. Dis. **11:**142-148.

22. **Donahue, J. M., B. J. Smith, J. K. Donahoe, C. L. Rigsby, R. R. Tramontin, K. B. Poonacha, and M. A. Wilson.** 1992. Prevalence and serovars of leptospira involved in equine abortions in central Kentucky during the 1990 foaling season. J. Vet. Diagn. Invest. **4:**279-284.

23. **Donahue, J. M., B. J. Smith, K. B. Poonacha, J. K. Donahoe, and C. L. Rigsby.** 1995. Prevalence and serovars of leptospira involved in equine abortions in central Kentucky during the 1991-1993 foaling seasons. J. Vet. Diagn. Invest. **7:**87-91.

24. **Dwyer, A. E., R. S. Crockett, and C. M. Kalsow.** 1995. Association of leptospiral seroreactivity and breed with uveitis and blindness in horses: 372 cases (1986-1993). J Am Vet Med Assoc **207:**1327-1331.

25. **Elder, J. K., P. M. Pepper, M. W. Hill, and W. H. Ward.** 1985. The significance of leptospiral titres associated with bovine abortion. Australian veterinary journal **62:**258-262.

26. **Ellis, T. M., G. M. Robertson, L. Hustas, and M. Kirby.** 1983. Detection of leptospires in tissue using an immunoperoxidase staining procedure. Australian veterinary journal **60:**364-367.

27. **Ellis, W. A. (ed.).** 1999. Leptospirosis, vol. Iowa State University Press, Iowa State.

28. **Ellis, W. A., D. G. Bryson, and J. B. McFerran.** 1976. Abortion associated with mixed Leptospira/equid herpesvirus 1 infection. The Veterinary record **98:**218-219.

29. **Ellis, W. A., D. G. Bryson, S. D. Neill, P. J. McParland, and F. E. Malone.** 1983. Possible involvement of leptospires in abortion, stillbirths and neonatal deaths in sheep. The Veterinary record **112:**291-293.

30. **Ellis, W. A., D. G. Bryson, J. J. O'Brien, and S. D. Neill.** 1983. Leptospiral infection in aborted equine foetuses. Equine Vet J **15:**321-324.

31. **Ellis, W. A., J. A. Cassells, and J. Doyle.** 1986. Genital leptospirosis in bulls. The Veterinary record **118:**333.

32. **Ellis, W. A., P. J. McParland, D. G. Bryson, and J. A. Cassells.** 1986. Prevalence of *Leptospira* infection in aborted pigs in Northern Ireland. Vet. Rec. **118:**63-65.

33. **Ellis, W. A., P. J. McParland, D. G. Bryson, and M. S. McNulty.** 1985. Leptospires in pig urogenital tracts and fetuses. Vet. Rec. **117:**66-67.

34. **Ellis, W. A., and S. W. Michna.** 1977. Bovine leptospirosis: experimental infection of pregnant heifers with a strain belonging to the Hebdomadis serogroup. Research in veterinary science **22:**229-236.

35. **Ellis, W. A., and S. W. Michna.** 1976. Bovine leptospirosis: infection by the Hebdomadis serogroup and abortion-A herd study. The Veterinary record **99:**409-412.

36. **Ellis, W. A., S. D. Neill, J. J. O'Brien, J. A. Cassells, and J. Hanna.** 1982. Bovine leptospirosis: microbiological and serological findings in normal fetuses removed from the uteri after slaughter. The Veterinary record **110:**192-194.

37. **Ellis, W. A., J. J. O'Brien, J. A. Cassells, S. D. Neill, and J. Hanna.** 1985. Excretion of Leptospira interrogans serovar hardjo following calving or abortion. Research in veterinary science **39:**296-298.

38. **Ellis, W. A., J. J. O'Brien, S. Neill, J. Hanna, and D. G. Bryson.** 1976. The isolation of a leptospire from an aborted bovine fetus. The Veterinary record **99:**458-459.

39. **Ellis, W. A., J. G. Songer, J. Montgomery, and J. A. Cassells.** 1986. Prevalence of Leptospira interrogans serovar hardjo in the genital and urinary tracts of non-pregnant cattle. The Veterinary record **118:**11-13.

40. **Faine, S. B., B. Adher, C. Bolin, and P. Perolat (ed.).** 1999. *Leptospira* and Leptospirosis., vol. 2nd edition. MedSci, Medbourne, Australia.

41. **Faisal, S. M., W. Yan, C. S. Chen, R. U. Palaniappan, S. P. McDonough, and Y. F. Chang.** 2008. Evaluation of protective immunity of *Leptospira* immunoglobulin like protein A (LigA) DNA vaccine against challenge in hamsters. Vaccine **26:**277-287.

42. **Gale, N. B., A. D. Alexander, L. B. Evans, R. H. Yager, and R. G. Matheney.** 1966. An outbreak of leptospirosis among U. S. army troops in the Canal Zone. The American journal of tropical medicine and hygiene **15:**64-70.

43. **Giles, N., S. C. Hathaway, and A. E. Stevens.** 1983. Isolation of Leptospira interrogans serovar hardjo from a viable premature calf. The Veterinary record **113:**174-176.

44. **Gregoire, N., R. Higgins, and Y. Robinson.** 1987. Isolation of leptospires from nephritic kidneys of beef cattle at slaughter. American journal of veterinary research **48:**370-371.

45. **Guarner, J., W. J. Shieh, J. Morgan, S. L. Bragg, M. D. Bajani, J. W. Tappero, and S. R. Zaki.** 2001. Leptospirosis mimicking acute cholecystitis among athletes participating in a triathlon. Human pathology **32:**750-752.

46. **Haake, D. A., G. Chao, R. L. Zuerner, J. K. Barnett, D. Barnett, M. Mazel, J. Matsunaga, P. N. Levett, and C. A. Bolin.** 2000. The leptospiral major outer membrane protein LipL32 is a lipoprotein expressed during mammalian infection. Infect. Immun. **68:**2276-2285.

47. **Haake, D. A., M. Dundoo, R. Cader, B. M. Kubak, R. A. Hartskeerl, J. J. Sejvar, and D. A. Ashford.** 2002. Leptospirosis, water sports, and chemoprophylaxis. Clin Infect Dis **34:**e40-43.

48. **Halliwell, R. E., T. A. Brim, M. T. Hines, D. Wolf, and F. H. White.** 1985. Studies on equine recurrent uveitis. II: The role of infection with Leptospira interrogans serovar pomona. Curr Eye Res **4:**1033-1040.

49. **Hanson, L. E.** 1972. Problems related to epizootiology of swine leptospirosis. Journal of the American Veterinary Medical Association **160:**631-634.

50. **Hanson, L. E., and B. O. Brodie.** 1967. Leptospira hardjo infections in cattle. Proceedings, annual meeting of the United States Animal Health Association **71:**210-215.

51. **Hanson, L. E., H. A. Reynolds, and L. B. Evans.** 1971. Leptospirosis in swine caused by serotype grippotyphosa. American journal of veterinary research **32:**855-860.

52. **Hanson, L. E., D. N. Tripathy, and A. H. Killinger.** 1972. Current status of leptospirosis immunization in swine and cattle. Journal of the American Veterinary Medical Association **161:**1235-1243.

53. **Hathaway, S. C., and T. W. Little.** 1981. Prevalence and clinical significance of leptospiral antibodies in pigs in England. Vet. Rec. **108:**224-228.

54. **Hathaway, S. C., T. W. Little, and A. E. Stevens.** 1982. Isolation of Leptospira interrogans serovar muenchen from a sow with a history of abortion. The Veterinary record **111:**100-102.

55. **Hauk, P., C. R. Guzzo, H. R. Ramos, P. L. Ho, and C. S. Farah.** 2009. Structure and Calcium-Binding Activity of LipL32, the Major Surface Antigen of Pathogenic *Leptospira* sp. J Mol Biol.

56. **Hauk, P., F. Macedo, E. C. Romero, S. A. Vasconcellos, Z. M. de Morais, A. S. Barbosa, and P. L. Ho.** 2008. In LipL32, the major leptospiral lipoprotein, the C terminus is the primary immunogenic domain and mediates interaction with collagen IV and plasma fibronectin. Infect. Immun. **76:**2642-2650.

57. **Hoke, D. E., S. Egan, P. A. Cullen, and B. Adler.** 2008. LipL32 is an extracellular matrix-interacting protein of Leptospira spp. and Pseudoalteromonas tunicata. Infection and immunity **76:**2063-2069.

58. **Hoke, D. E., S. Egan, P. A. Cullen, and B. Adler.** 2008. LipL32 is an extracellular matrix-interacting protein of *Leptospira* spp. and *Pseudoalteromonas tunicata*. Infect Immun **76:**2063-2069.

59. **Hong, C. B., J. M. Donahue, R. C. Giles, Jr., M. B. Petrites-Murphy, K. B. Poonacha, A. W. Roberts, B. J. Smith, R. R. Tramontin, P. A. Tuttle, and T. W. Swerczek.** 1993. Equine abortion and stillbirth in central Kentucky during 1988 and 1989 foaling seasons. J Vet Diagn Invest **5:**560-566.

60. **Hong, C. B., J. M. Donahue, R. C. Giles, Jr., M. B. Petrites-Murphy, K. B. Poonacha, A. W. Roberts, B. J. Smith, R. R. Tramontin, P. A. Tuttle, and T. W. Swerczek.** 1993. Etiology and pathology of equine placentitis. Journal of veterinary diagnostic investigation **5:**56-63.

61. **Izutsu, K. T., C. M. Belton, A. Chan, S. Fatherazi, J. P. Kanter, Y. Park, and R. J. Lamont.** 1996. Involvement of calcium in interactions between gingival epithelial cells and *Porphyromonas gingivalis*. FEMS Microbiol Lett **144:**145-150.

62. **Jerrett, I. V., S. McOrist, J. Waddington, J. W. Browning, J. C. Malecki, and I. P. McCausland.** 1984. Diagnostic studies of the fetus, placenta and maternal blood from 265 bovine abortions. The Cornell veterinarian **74:**8-20.

63. **Jubb, K. V., P. C. Kennedy, and N. Plamer (ed.).** 1985. Pathology of domestic animals., 3rd ed, vol. Academic Press, New Yrok.

64. **Kalsow, C. M., and A. E. Dwyer.** 1998. Retinal immunopathology in horses with uveitis. Ocular immunology and inflammation **6:**239-251.

65. **Kinde, H., S. K. Hietala, C. A. Bolin, and J. T. Dowe.** 1996. Leptospiral abortion in horses following a flooding incident. Equine Vet J **28:**327-330.

66. **Ko, A. I., M. Galvao Reis, C. M. Ribeiro Dourado, W. D. Johnson, Jr., and L. W. Riley.** 1999. Urban epidemic of severe leptospirosis in Brazil. Salvador Leptospirosis Study Group. Lancet **354:**820-825.

67. **Kretsinger, R. H., and C. E. Nockolds.** 1973. Carp muscle calcium-binding protein. II. Structure determination and general description. J. Biol. Chem. **248:**3313-3326.

68. **Lederberg, J., R. E. Shope, and S. C. Oaks (ed.).** 1992. Emerging infections:microbial threats to health in the United States., vol. National Academy Press,, Washington, D.C.

69. **Levett, P. N.** 2001. Leptospirosis. Clin Microbiol Rev **14:**296-326.

70. **Levett, P. N.** 1999. Leptospirosis: re-emerging or re-discovered disease? J Med Microbiol **48:**417-418.

71. **Lin, Y. P., and Y. F. Chang.** 2008. The C-terminal variable domain of LigB from *Leptospira* mediates binding to fibronectin. J. Vet. Sci. **9:**133-144.

72. **Lin, Y. P., and Y. F. Chang.** 2007. A domain of the *Leptospira* LigB contributes to high affinity binding of fibronectin. Biochem Biophys Res Commun **362:**443-448.

73. **Lin, Y. P., R. Raman, Y. Sharma, and Y. F. Chang.** 2008. Calcium binds to Leptospiral immunoglobulin-like protein, LigB and modulates fibronectin binding. J. Biol. Chem. **283:**25140-25149.

74. **Lucchesi, P. M., A. E. Parma, and G. H. Arroyo.** 2002. Serovar distribution of a DNA sequence involved in the antigenic relationship between Leptospira and equine cornea. BMC microbiology **2:**3.

75. **Luks, A. M., S. Lakshminarayanan, and J. V. Hirschmann.** 2003. Leptospirosis presenting as diffuse alveolar hemorrhage: case report and literature review. Chest **123:**639-643.

76. **Martinez Garcia, M. A., A. de Diego Damia, R. Menendez Villanueva, and J. L. Lopez Hontagas.** 2000. Pulmonary involvement in leptospirosis. European journal of clinical microbiology & infectious diseases **19:**471-474.

77. **Matsunaga, J., M. A. Barocchi, J. Croda, T. A. Young, Y. Sanchez, I. Siqueira, C. A. Bolin, M. G. Reis, L. W. Riley, D. A. Haake, and A. I. Ko.** 2003. Pathogenic *Leptospira* species express surface-exposed proteins belonging to the bacterial immunoglobulin superfamily. Mol Microbiol **49:**929-945.

78. **Matsunaga, J., M. Lo, D. M. Bulach, R. L. Zuerner, B. Adler, and D. A. Haake.** 2007. Response of *Leptospira interrogans* to Physiologic Osmolarity: Relevance in Signaling the Environment-to-Host Transition. Infect. Immun. **75:**2864-2874.

79. **Matsunaga, J., Y. Sanchez, X. Xu, and D. A. Haake.** 2005. Osmolarity, a key environmental signal controlling expression of leptospiral proteins LigA and LigB and the extracellular release of LigA. Infect. Immun. **73:**70-78.

80. **McKeown, J. D., and W. A. Ellis.** 1986. Leptospira hardjo agalactia in sheep. The Veterinary record **118:**482.

81. **Meites, E., M. T. Jay, S. Deresinski, W. J. Shieh, S. R. Zaki, L. Tompkins, and D. S. Smith.** 2004. Reemerging leptospirosis, California. Emerg Infect Dis **10:**406-412.

82. **Michiels, J., C. Xi, J. Verhaert, and J. Vanderleyden.** 2002. The functions of Ca(2+) in bacteria: a role for EF-hand proteins? Trends Microbiol **10:**87-93.

83. **Morgan, J., S. L. Bornstein, A. M. Karpati, M. Bruce, C. A. Bolin, C. C. Austin, C. W. Woods, J. Lingappa, C. Langkop, B. Davis, D. R. Graham, M. Proctor, D. A. Ashford, M. Bajani, S. L. Bragg, K. Shutt, B. A. Perkins, and J. W. Tappero.** 2002. Outbreak of leptospirosis among triathlon participants

and community residents in Springfield, Illinois, 1998. Clin Infect Dis **34:**1593-1599.

84. **Naiman, B. M., D. Alt, C. A. Bolin, R. Zuerner, and C. L. Baldwin.** 2001. Protective killed *Leptospira borgpetersenii* vaccine induces potent Th1 immunity comprising responses by CD4 and gammadelta T lymphocytes. Infect. Immun. **69:**7550-7558.

85. **Naiman, B. M., S. Blumerman, D. Alt, C. A. Bolin, R. Brown, R. Zuerner, and C. L. Baldwin.** 2002. Evaluation of type 1 immune response in naive and vaccinated animals following challenge with *Leptospira borgpetersenii* serovar Hardjo: involvement of WC1(+) gammadelta and CD4 T cells. Infect.Immun. **70:**6147-6157.

86. **Narita, M., S. Fujitani, D. A. Haake, and D. L. Paterson.** 2005. Leptospirosis after recreational exposure to water in the Yaeyama islands, Japan. The American journal of tropical medicine and hygiene **73:**652-656.

87. **Orr, H. S., and T. W. Little.** 1979. Isolation of Leptospira of the serotype hardjo from bovine kidneys. Research in veterinary science **27:**343-346.

88. **Palaniappan, R. U., Y. F. Chang, F. Hassan, S. P. McDonough, M. Pough, S. C. Barr, K. W. Simpson, H. O. Mohammed, S. Shin, P. McDonough, R. L. Zuerner, J. Qu, and B. Roe.** 2004. Expression of leptospiral immunoglobulin-like protein by *Leptospira interrogans* and evaluation of its diagnostic potential in a kinetic ELISA. J Med Microbiol **53:**975-984.

89. **Palaniappan, R. U., Y. F. Chang, S. S. Jusuf, S. Artiushin, J. F. Timoney, S. P. McDonough, S. C. Barr, T. J. Divers, K. W. Simpson, P. L. McDonough, and H. O. Mohammed.** 2002. Cloning and molecular characterization of an immunogenic LigA protein of *Leptospira interrogans*. Infect. Immun. **70:**5924-5930.

90. **Palaniappan, R. U., S. P. McDonough, T. J. Divers, C. S. Chen, M. J. Pan, M. Matsumoto, and Y. F. Chang.** 2006. Immunoprotection of recombinant leptospiral immunoglobulin-like protein A against *Leptospira interrogans* serovar Pomona infection. Infect. Immun. **74:**1745-1750.

91. **Parma, A. E., S. I. Cerone, S. A. Sansinanea, and M. Ghezzi.** 1992. C3 fixed in vivo to cornea from horses inoculated with Leptospira interrogans. Veterinary immunology and immunopathology **34:**181-187.

92. **Parma, A. E., M. E. Sanz, P. M. Lucchesi, J. Mazzonelli, and M. A. Petruccelli.** 1997. Detection of an antigenic protein of *Leptospira interrogans* which shares epitopes with the equine cornea and lens. Vet.J. **153:**75-79.

93. **Poonacha, K. B., J. M. Donahue, R. C. Giles, C. B. Hong, M. B. Petrites-Murphy, B. J. Smith, T. W. Swerczek, R. R. Tramontin, and P. A. Tuttle.** 1993. Leptospirosis in equine fetuses, stillborn foals, and placentas. Vet Pathol **30:**362-369.

94. **Prescott, J. F., R. B. Miller, and V. M. Nicholson.** 1987. Isolation of *Leptospira hardjo* from kidneys of Ontario cattle at slaughter. Can. J. Vet. Res. **51:**229-231.

95. **Rajini, B., P. Shridas, C. S. Sundari, D. Muralidhar, S. Chandani, F. Thomas, and Y. Sharma.** 2001. Calcium binding properties of gamma-crystallin: calcium ion binds at the Greek key beta gamma-crystallin fold. J Biol Chem **276:**38464-38471.

96. **Rathinam, S. R., S. Rathnam, S. Selvaraj, D. Dean, R. A. Nozik, and P. Namperumalsamy.** 1997. Uveitis associated with an epidemic outbreak of leptospirosis. Am J Ophthalmol **124:**71-79.

97. **Roberts, C. S., and L. W. Turner.** 1958. The susceptibility of the chinchilla (Chinchilla laniger) to *Leptospira pomona*. J Am Vet Med Assoc **132:**527-528.

98. **Sarkar, U., S. F. Nascimento, R. Barbosa, R. Martins, H. Nuevo, I. Kalafanos, I. Grunstein, B. Flannery, J. Dias, L. W. Riley, M. G. Reis, and A. I. Ko.** 2002. Population-based case-control investigation of risk factors for leptospirosis during an urban epidemic. Am. J. Trop. Med. Hyg. **66:**605-610.

99. **Schwarz-Linek, U., M. Hook, and J. R. Potts.** 2006. Fibronectin-binding proteins of gram-positive cocci. Microbes and infection / Institut Pasteur **8:**2291-2298.

100. **Schwarz-Linek, U., M. Hook, and J. R. Potts.** 2004. The molecular basis of fibronectin-mediated bacterial adherence to host cells. Mol Microbiol **52:**631-641.

101. **Segura, E. R., C. A. Ganoza, K. Campos, J. N. Ricaldi, S. Torres, H. Silva, M. J. Cespedes, M. A. Matthias, M. A. Swancutt, R. Lopez Linan, E. Gotuzzo, H. Guerra, R. H. Gilman, and J. M. Vinetz.** 2005. Clinical spectrum of pulmonary involvement in leptospirosis in a region of endemicity, with quantification of leptospiral burden. Clin Infect Dis **40:**343-351.

102. **Seijo, A., H. Coto, J. San Juan, J. Videla, B. Deodato, B. Cernigoi, O. G. Messina, O. Collia, D. de Bassadoni, R. Schtirbu, A. Olenchuk, G. D. de Mazzonelli, and A. Parma.** 2002. Lethal leptospiral pulmonary hemorrhage: an emerging disease in Buenos Aires, Argentina. Emerg Infect Dis **8:**1004-1005.

103. **Sejvar, J., E. Bancroft, K. Winthrop, J. Bettinger, M. Bajani, S. Bragg, K. Shutt, R. Kaiser, N. Marano, T. Popovic, J. Tappero, D. Ashford, L. Mascola, D. Vugia, B. Perkins, and N. Rosenstein.** 2003. Leptospirosis in "Eco-Challenge" athletes, Malaysian Borneo, 2000. Emerg Infect Dis **9:**702-707.

104. **Shimizu, T., E. Matsusaka, N. Nagakura, K. Takayanagi, T. Masuzawa, Y. Iwamoto, T. Morita, I. Mifuchi, and Y. Yanagihara.** 1987. Chemical properties of lipopolysaccharide-like substance (LLS) extracted from Leptospira interrogans serovar canicola strain Moulton. Microbiology and immunology **31:**717-725.

105. **Shimizu, T., E. Matsusaka, K. Takayanagi, T. Masuzawa, Y. Iwamoto, T. Morita, I. Mifuchi, and Y. Yanagihara.** 1987. Biological activities of lipopolysaccharide-like substance (LLS) extracted from Leptospira interrogans serovar canicola strain Moulton. Microbiology and immunology **31:**727-735.

106. **Sillerud, C. L., R. F. Bey, M. Ball, and S. I. Bistner.** 1987. Serologic correlation of suspected *Leptospira interrogans* serovar pomona-induced uveitis in a group of horses. J Am Vet Med Assoc **191:**1576-1578.

107. **Silva, E. F., M. A. Medeiros, A. J. A. McBride, J. Matsunaga, G. S. Esteves, J. G. R. Ramos, C. S. Santos, J. Croda, A. Homma, O. A. Dellagostin, D. A. Haake, M. G. Reis, and A. I. Ko.** 2007. The terminal portion of leptospiral immunoglobulin-like protien A confers protective immunity against lethal infection in the hamster model of leptospirosis. . Vaccine **25:**6277-6286.

108. **Slee, K. J., S. McOrist, and N. W. Skilbeck.** 1983. Bovine abortion associated with Leptospira interrogans serovar hardjo infection. Australian veterinary journal **60:**204-206.

109. **Stevenson, B., H. A. Choy, M. Pinne, M. L. Rotondi, M. C. Miller, E. Demoll, P. Kraiczy, A. E. Cooley, T. P. Creamer, M. A. Suchard, C. A. Brissette, A. Verma, and D. A. Haake.** 2007. Leptospira interrogans Endostatin-Like Outer Membrane Proteins Bind Host Fibronectin, Laminin and Regulators of Complement. PLoS ONE **2:**e1188.

110. **Straley, S. C., G. V. Plano, E. Skrzypek, P. L. Haddix, and K. A. Fields.** 1993. Regulation by Ca2+ in the Yersinia low-Ca2+ response. Mol Microbiol **8:**1005-1010.

111. **Swain, R. H. A.** 1957. The electron-microscopical anatomy of *Leptospira canicola*. J. Pahtol. Bacteriol. **73:**155-158.

112. **Talpada, M. D., N. Garvey, R. Sprowls, A. K. Eugster, and J. M. Vinetz.** 2003. Prevalence of leptospiral infection in Texas cattle: implications for transmission to humans. Vector borne zoonotic Dis. **3:**141-147.

113. **Teichmann, D., K. Gobels, J. Simon, M. P. Grobusch, and N. Suttorp.** 2001. A severe case of leptospirosis acquired during an iron man contest. Eur J Clin Microbiol Infect Dis **20:**137-138.

114. **Teintze, M., M. Inouye, and S. Inouye.** 1988. Characterization of calcium-binding sites in development-specific protein S of *Myxococcus xanthus* using site-specific mutagenesis. J. Biol. Chem. **263:**1199-1203.

115. **Thiermann, A. B.** 1983. Bovine leptospirosis: bacteriologic versus serologic diagnosis of cows at slaughter. American journal of veterinary research **44:**2244-2245.

116. **Thiermann, A. B.** 1984. Isolation of leptospires in diagnosis of leptospirosis. Modern veterinary practice **65:**758-759.

117. **Thiermann, A. B.** 1984. Leptospirosis: current developments and trends. Journal of the American Veterinary Medical Association **184:**722-725.

118. **Thiermann, A. B., A. L. Handsaker, J. W. Foley, F. H. White, and B. F. Kingscote.** 1986. Reclassification of North American leptospiral isolates belonging to serogroups Mini and Sejroe by restriction endonuclease analysis. American journal of veterinary research **47:**61-66.

119. **Tisa, L. S., and J. Adler.** 1992. Calcium ions are involved in *Escherichia coli* chemotaxis. Proc. Natl. Acad. Sci. U S A **89:**11804-11808.

120. **Tisa, L. S., and J. Adler.** 1995. Cytoplasmic free-Ca2+ level rises with repellents and falls with attractants in *Escherichia coli* chemotaxis. Proc. Natl. Acad. Sci. U S A **92:**10777-10781.

121. **Trombe, M. C., V. Rieux, and F. Baille.** 1994. Mutations which alter the kinetics of calcium transport alter the regulation of competence in *Streptococcus pneumoniae*. J Bacteriol **176:**1992-1996.

122. **Verma, A., S. Artiushin, J. Matsunaga, D. A. Haake, and J. F. Timoney.** 2005. LruA and LruB, novel lipoproteins of pathogenic *Leptospira interrogans* associated with equine recurrent uveitis. Infect. Immmun. **73:**7259-7266.

123. **Verma, A., J. Hellwage, S. Artiushin, P. F. Zipfel, P. Kraiczy, J. F. Timoney, and B. Stevenson.** 2006. LfhA, a novel factor H-binding protein of *Leptospira interrogans*. Infect. Immun. **74:**2659-2666.

124. **Vijayachari, P., A. P. Sugunan, S. Sharma, S. Roy, K. Natarajaseenivasan, and S. C. Sehgal.** 2008. Leptospirosis in the Andaman Islands, India. Trans R Soc Trop Med Hyg **102:**117-122.

125. **Vinetz, J. M.** 2001. Leptospirosis. Curr. Opin. Infect. Dis. **14:**527-538.

126. **Vinetz, J. M., G. E. Glass, C. E. Flexner, P. Mueller, and D. C. Kaslow.** 1996. Sporadic urban leptospirosis. Ann Intern Med **125:**794-798.

127. **Vinh, T., B. Adler, and S. Faine.** 1986. Ultrastructure and chemical composition of lipopolysaccharide extracted from Leptospira interrogans serovar copenhageni. Journal of general microbiology **132:**103-109.

128. **Werthen, M., and T. Lundgren.** 2001. Intracellular Ca(2+) mobilization and kinase activity during acylated homoserine lactone-dependent quorum sensing in Serratia liquefaciens. J. Biol. Chem. **276:**6468-6472.

129. **Werts, C., R. I. Tapping, J. C. Mathison, T. H. Chuang, V. Kravchenko, I. Saint Girons, D. A. Haake, P. J. Godowski, F. Hayashi, A. Ozinsky, D. M. Underhill, C. J. Kirschning, H. Wagner, A. Aderem, P. S. Tobias, and R. J. Ulevitch.** 2001. Leptospiral lipopolysaccharide activates cells through a TLR2-dependent mechanism. Nat Immunol **2:**346-352.

130. **White, F. H., K. R. Sulzer, and R. W. Engel.** 1982. Isolations of Leptospira interrogans serovars hardjo, balcanica, and pomona from cattle at slaughter. American journal of veterinary research **43:**1172-1173.

131. **Yang, C. W.** 2007. Leptospirosis in Taiwan--an underestimated infectious disease. Chang Gung Med J **30:**109-115.

132. **Yu, X. C., and W. Margolin.** 1997. Ca2+-mediated GTP-dependent dynamic assembly of bacterial cell division protein FtsZ into asters and polymer networks *in vitro*. Embo J **16:**5455-5463.

CHAPTER 2

THE C-TERMINAL VARIABLE DOMAIN OF LIGB FROM *LEPTOSPIRA* MEDIATES BINDING TO FIBRONECTIN

Introduction

Leptospirosis is a zoonotic disease caused by pathogenic spirochetes in the genus *Leptospira* [22]. The disease occurs widely in developing countries and is reemerging in the United States [28]. The clinical features are variable and include subclinical infection, self-limited anicteric febrile illness, and severe, potentially fatal disease [22]. In the severe form of leptospirosis (Weil's syndrome), the symptoms include an acute febrile illness associated with multi-organ damage including liver failure (jaundice), renal failure (nephritis), pulmonary hemorrhage and meningitis [10]. If not treated, the mortality rate may exceed 15% [48]. Furthermore, *Leptospira* infection can trigger autoimmune diseases in horses and people [35, 40]. Several virulence factors have been proposed for *Leptospira* spp., including the sphingomyelinases, serine proteases, zinc-dependent proteases, collagenase [3], LipL32 [58], the novel factor H-binding protein LfhA [53], and lipopolysaccharide [55].

Pathogenic spirochetes have evolved a variety of strategies to infect host cells such as evasion of the innate and adaptive immunity [53]. Attachment to host cells is an essential step for colonization by bacterial pathogens. *Leptospira* has been shown to bind to mammalian cells, such as Madin-Darby canine kidney (MDCK) cells [2] via extracellular matrix (ECM) [15]. Several adhesion molecules in pathogenic spirochetes have been identified including a Fn binding protein (36 kDa protein) [29], a laminin binding protein (Lsa24) [1], and Lig proteins [24, 32, 33] from *Leptospira spp*., decorin-binding proteins (Dbp A and B) [36] and Fn-binding proteins (BBK 32 and 47

kDa) [21, 37] from *Borrelia spp.* and MSP, Tp0155, Tp0483, Tp0751 from *Treponema* spp. [4, 5, 9]. Lig proteins (Lig A, B and C) possess immunoglobulin-like domains with 90 amino acid repeats that have been identified in other adhesion molecules, such as the intimin of *Escherichia coli* and the invasin of *Yersinia pseudotuberculosis* [14, 17]. Interestingly, the N-terminal 630 amino acid sequences of LigA and B are identical, but the C-terminal amino acid sequences are variable with only 34% homogeneity [32]. *ligB* also encodes a C-terminal, non-repeat domain of 771 amino acid residues [32]. On the other hand, the *ligA-ligB* intergenic regions from *L. kirschneri* and *L. interrogans* are 943 bp and 1347 bp in length respectively, and *ligC* is not linked to the *ligA-ligB* locus [24]. The expression of LigA and LigB is controlled by a key environmental signal, osmolarity, to enhance the binding of *Leptospira* to host cells [25, 26].

It has been shown that the *lig* genes are present exclusively in pathogenic *Leptospira* spp [24, 32]. LigA and LigB are weakly expressed in low passage, but not in high passage cultures of this organism [24, 32]. Importantly, we have shown that LigA and LigB expression is upregulated *in vivo* in the kidneys of *Leptospira*-infected hamsters [33]. Recently, LigA and LigB reportedly bind to extracellular matrix proteins including collagens type I and IV, laminin, fibronectin and fibrinogen [6]. These data indicate that Lig proteins may play an important role in attachment of pathogenic leptospires to host cells.

Although there are three copies of *lig* genes (*ligA, B* and *C*) in *L. interrogans* serovar Pomona and *L. interrogans* serovar Copenhageni [30, 32, 33], only *ligB* is present in most pathogenic *Leptospira* spp. *ligA* is absent in *L. interrogans* serovar Lai [41], *ligC* is truncated (a pseudogene) in *L. kirschneri* serovar Grippotyphosa [24] and both *ligA* and *ligC* are absent in *L. borgpetersenii* serovar Harjo [3]. Therefore, we focused on LigB in this study and report that the variable region of LigB binds with high

affinity to Fn, suggesting that this fragment is crucial for bacterial adhesion to the host cells.

Materials and Methods

Bacterial strains and cell culture

L. interrogans serovar Pomona (NVSL1427-35-093002) was used in this study [34]. All experiments were performed with virulent, low-passage strains obtained by infecting golden syrian hamsters as previously described [34]. *Leptospires* were grown in EMJH medium at 30 ^{o}C for less than 5 passages and growth was monitored by dark-field microscopy. MDCK cells (ATCC CCL34^{TM}) were cultured in Dulbecco minimum essential medium (DMEM) containing 10% fetal bovine serum (GIBCO Laboratories, Grand Island, NY) and were grown at 37^{o}C in a humidified atmosphere with 5% CO_2.

Reagents and antibodies

Horseradish peroxidase (HRP)-conjugated goat anti-hamster antibody, HRP-conjugated goat anti-mouse antibody, and HRP-conjugated goat anti-rabbit antibody were purchased from Zymed (San Diego, CA). Rabbit anti-GST antibody, Alexa 594-conjugated goat anti-hamster antibody, Alexa 488-conjugated goat anti-hamster antibody and FITC-conjugated goat anti-mouse antibody were purchased from Molecular Probe (Eugene, OR). Anti-Fn (MAB1932) and anti-actin mouse antibodies (MAB1501) were purchased from Chemicon International (Temecula, CA). Human plasma Fn was purchased from GIBCO (City, State). Anti-*L. interrogans* antibodies were prepared in hamsters as previously described [34].

Plasmid construction and protein purification

Constructs for the expression of glutathione S-transferase (GST), GST fused with the conserved region of LigB (LigBCon; amino acids 1-630), and GST fused with the central variable region of LigB (LigBCen; amino acids 631-1417) were previously generated using the vector pGEX-4T-2 (Amersham Pharmacia Biotech, Piscataway, NJ) [32]. GST fused with the C-terminal variable region of LigB (LigBCtv; amino acids 1418-1889) was generated using the vector pET41A (Novogen, San Diego, CA). Relevant fragments of DNA were amplified by PCR using primers based on the *ligB* sequence [32]. Primers were designed to introduce a *Sal*I site at the 5' end of each fragment and a stop codon followed by a *Not*I site at the 3' end of each fragment. PCR products were digested sequentially with *Sal*I and *Not*I and then ligated into pGEX-4T-2 or pET41A cut with *Sal*I and *Not*I. In this study, we purified the soluble form of GST-LigBCon, GST-LigBCen and GST-LigBCtv from *E. coli* as previously described [33, 34].

Binding assays by ELISA

To measure the binding of *Leptospira* to ECM components, 1mg of each ECM component (as indicated by Figure. 2.1. A) in 100 µl PBS (pH 7.2) was coated onto microtiter plate wells. For the dose-dependent binding experiments, different concentrations of Fn (as indicated by Figure. 2.1. B) were coated on microtiter plate wells. The plates were incubated at 4^{o}C for 16 h and subsequently blocked with blocking buffer (50 µl/well) containing 3.5% BSA in 50mM Tris (pH 7.5)-100mM NaCl-1mM $MgCl_2$, $MnCl_2$, and $CaCl_2$ at room temperature (RT) for 2 h. Then, *Leptospira* (10^7) were added to each well and further incubated at 37^{o}C for 6 h. To determine the inhibition of *Leptospira* binding to MDCK cells by Fn, *Leptospira* (10^7) were pre-incubated at 37 ^{o}C for 1 h with various concentrations of Fn (as indicated in

Figure. 2.1.C) prior to the addition of MDCK cells (10^5) and finally incubated for 6 h at 37 ^oC. The percentage of adhesion was determined relative to the attachment of untreated *Leptospira* binding to MDCK cells. For all experiments, the same concentration of BSA was used as a negative control. To determine the binding of LigBCen or LigBCtv to Fn, 10 nM of GST-LigBCen, GST-LigBCtv or GST (negative control) was added to 96 well microtiter plates coated with various concentrations of Fn (as indicated in Figure. 2.3. A) or BSA (negative control and data not shown) in 100µl PBS for 1 hour at 37 ^oC.

To measure the binding inhibition of *Leptospira* to Fn, various concentrations of GST-LigBCen, GST-LigBCtv (as indicated by Figure. 2.3. B) or GST (negative control) in 100µl PBS was added to Fn or BSA (negative control and data not shown) (1mg in 100 µl PBS) coated wells at 37 ^oC for 1 h, then *Leptospira* (10^7) were added to each well and incubated at 37 ^oC for 6 h. To measure the binding of LigBCen or LigBCtv to MDCK cells, MDCK cells (10^5) were incubated with various concentrations (as indicated in Figure. 2.4. A.) of GST-LigBCen, GST-LigBCtv or GST (negative control) in 100 µl PBS for 1 hour at 37 ^oC. To measure the binding inhibition of *Leptospira* to MDCK cells treated with LigBCen or LigBCtv, MDCK cells (10^5) were pretreated with various concentrations (as indicated in Figure. 2.4. B.) of GST-LigBCen, GST-LigBCtv or GST (negative control) in 100 µl PBS for 1 hour at 37 ^oC. Then, *Leptospira* (10^7) were added to each well and incubated for 6 hours at 37 ^oC. Following the incubation, the plates were washed three times with phosphate-buffered saline (PBS) containing 0.05% Tween-20 (PBST). To measure the binding of *Leptospira,* hamster anti-*Leptospira* (1:200x) and HRP-conjugated goat anti-hamster IgG (1:1,000x) were used as primary and secondary antibodies, respectively. To detect the binding of GST-LigBCen, GST-LigBCtv, or GST to Fn or MDCK cells, rabbit anti-GST (1:200x) and HRP-conjugated goat anti-rabbit IgG (1:1,000x) were used as primary and

secondary antibodies, respectively. After washing the plates thrice with PBST, 100µl of TMB (KPL, Gaithersburg, MD) was added to each well and incubated for 5 min. The reaction was stopped by adding 100 µl of 0.5% hydrofluoric acid in each well. Each plate was read at 630nm by ELISA plate reader (Bioteck EL-312, Winoski, VT). Each value represents the mean ± SEM of three trials in triplicate samples. Statistically significant ($P<0.05$) differences are indicated by asterisks.

Binding assays by epifluorescence microscopy (EPM) and confocal laser-scanning microscopy (CLSM)

To measure the binding of *Leptospira* to Fn by EPM, *Leptospira* (10^8) were added to each well (eight well culture slides) coated with 1mg Fn or BSA (negative control) in 100 µl of PBS and incubated at 37 ^oC for 6 h (Figure. 2.1. D). To measure the binding inhibition of *Leptospira* to MDCK cells by Fn, 10^8 *Leptospira* were pre-incubated with 10 µg of Fn or BSA (negative control) in 100 µl of PBS for 1 hour at 37 ^oC prior to the addition of 10^6 MDCK cells and incubated 6 h at 37 ^oC (Figure. 2.1. E). To measure the binding inhibition *Leptospira* to Fn by LigBCen or LigBCtv by EPM. Fifty nM of GST-LigBCen, GST-LigBCtv or GST (negative control) in 100 µl PBS was each added to coated Fn or BSA (negative control and data not shown) (1 mg per 100 µl) wells for 1 h at 37 ^oC, then, *Leptospira* (10^8) were added to each well and incubated for 6 h at 37 ^oC (Figure. 2.3. C). To determine the binding inhibition of *Leptospira* to MDCK cells by LigBCen or LigBCtv by CLSM, MDCK cell (10^6) was preincubated with 50 nM of GST-LigBCen, GST-LigBCtv or GST (negative control) in 100 µl of PBS for 1 h at 37 ^oC respectively. Then, *Leptospira* (10^8) were added to each well and incubated for 6 h at 37 ^oC (Figure. 2.4. C). For the detection of *Leptospira* binding in Figure. 2.1D. E. and Figure. 2.3C, hamster anti-*Leptospira* antibodies (1:100x) and Alexa 488-conjugated goat anti-hamster IgG (1:250x) were used as primary and secondary antibodies,

respectively. To determine the attachment of *Leptospira* and the binding of GST-LigBCen, GST-LigBCtv, or GST in Figure. 2.4C., rabbit anti-GST (1:250x) and hamster anti-*Leptospira* antibodies (1:100x) served as primary antibodies, and FITC conjugated goat anti-rabbit IgG (1:250x) and Alexa 594-conjugated goat anti-hamster IgG (1:250x) were used as secondary antibodies. Fixation and immunofluorescence staining were performed as previously described [43] with slight modifications. Briefly, *Leptopsira* and MDCK cells were fixed in 2% praformaldehyde for 60 min at RT. For antibody labeling, fixed bacteria were incubated in PBS containing 0.3% BSA for 10 min at RT. The primary and secondary antibodies in PBS containing 0.3% BSA were incubated sequentially for 60min at RT. After incubation with primary and secondary antibodies, the glass slides were mounted with coverslips using Prolong Antifade (Molecular Probe, Eugene, OR) and viewed with a 60x objective by EPM (Nikon Inc., Avon, MA) or CLSM (Olympus, America, Inc., Melville, NY). An Olympus Fluoview 500 confocal laser-scanning imaging system equipped with krypton, argon, and He-Ne lasers on an Olympus IX70 inverted microscope with a PLAPO 60X objective was used. The settings were identical for all captured images. Images were processed using Adobe Photoshop CS2. For counting the attachment of *Leptospira* to the MDCK cells or Fn, three fields were selected to count the number of binding organisms. All studies were repeated three times and the number of leptospria attached to MDCK cells were counted by an operator who was blinded to the treatment group.

GST pulldown assay

The GST pull-down assay was performed as previously described [56]. Purified proteins or GST (negative control) were loaded onto 0.5 ml glutathione-Sepharose beads (Amersham Biosciences Piscataway, NJ) at 4^{o}C overnight. The beads were then washed three times with the lysis buffer containing 30 mM Tris acetate, 10 mM sodium

phosphate, pH 7.4, 0.1% Tween 20, 1mM EDTA, 2 μg/ml leupeptin, 4 μg/ml aprotinin, 1 μg/ml pepstatin A, and 1 mM phenylmethylsulfonyl fluoride (PMSF). MDCK cells (10^6) were lysed in the lysis buffer and used immediately after lysis. A 500 μl aliquot of cell lysate or human plasma Fn (40 μg/ml) was incubated with purified proteins immobilized on glutathione-Sepharose beads at 4^{o}C for 3 h. After incubation, the beads were separated by centrifugation, washed three times with the lysis buffer, and boiled in Laemmli sample loading buffer consisting of 50 mM Tris-HCl (pH6.8), 100 mM dithiothreitol, 2% sodium dodecyl sulfate, 0.25 mM PMSF, and 0.1% bromophenol blue in 20% glycerol. The eluted proteins were subjected to 6% SDS-PAGE and electroblotted onto polyvinylidene difluoride membranes. The membranes were incubated in 5% skim milk in PBS/T overnight and then incubated with mouse anti-Fn antibody (1:1,000x). The immunocomplexes were detected with an HRP-conjugated goat anti-mouse IgG antibody (1:5,000x).

Small interfering RNA (siRNA) inhibition of LigB binding

siRNA duplexes directed against the sequence 5'-gcagcacaacuuccaauua-3' of Fn and negative siRNA duplex, 5'-auucuaucacuagcgugac- 3', were selected by a software, si*DESIGN*^{TM} [42] and synthesized by Dharmacon (Lafayette, CO). RNA duplexes were introduced into MDCK cells by the method of lipofection [18], and 8×10^5 cells were transfected with 0.4 μg negative siRNA and Fn-siRNA. Adhesion assays were performed 72 h after lipofection [50]. The knocking down efficiency of endogeneous Fn expression was determined as previously described [56] with slight modification. Total protein contents of MDCK cells (10^6) were analyzed using Western immunoblotting as described under 'GST pulldown assays'. The protein bands of actin derived from MDCK cells were measured as a control using a mouse anti-actin antibody (1:5,000x). The band intensity was measured by densitometry using the Image J software

(National Institutes of Health, Bethesda, MD, USA) [52]. LigB binding assay was performed 72 h after lipofection. To determine the binding of Lig B fragments to Fn, each fragment (50nM) was added to MDCK cells (10^6) transfected with Fn or negative siRNA. To determine the binding of each fragment and the expression of Fn on MDCK cells, rabbit anti-GST (1:250x) and mouse anti-Fn (1:250x) served as the primary antibodies, and FITC-conjugated goat anti-mouse IgG (1:250x) and Texas Red-conjugated goat anti-rabbit IgG (1:250x) were used as secondary antibodies. Fixation, immunofluorescence staining, image detection and processing were described in the previous sections. All the experiments were performed in triplicate.

Isothermal titration calorimetry

The experiments were carried out with CSC 5300 microcalorimeter (Calorimetry Science Corp. Lindon, UT, USA) at 25^{o}C as previously described [46]. In a typical experiment, the cell contained 1ml of a solution of proteins, and the syringe contained 250 µl of a solution of Fn at a concentration that was 20 times higher than the protein concentration in the cell. Both solutions were in PBS pH 7.5. The titration was performed as follows: 15 to 25 injections of 10 µl (Table 2.1) with a stirring speed of 250rpm, and the delay time between the injections was 5 min. Data were analyzed using Titration BindingWork 3.1 software (Calorimetry Science Corp. Lindon, UT, USA) fitting them to an independent binding model. The concentration of Fn and LigB used in this study was based on our preliminary titration experiment (data not shown).

Figure 2.1 The binding of *L. interrogans* serovar Pomona (NVSL 1427-35-093002) to Fn. (A). Binding of *Leptopsira* to various immobilized ECM components. *Leptospira* (10^7) were added to wells coated with each ECM (1mg in 100 µl PBS) including Fn, chondroitin-6-sulfate (C6S), chondroitin sulfate A (CSA), chondroitin sulfate B (CSB), gelatin A (GA), gelatin B (GB), heparin (HP), keratin (KR), or BSA (negative control). (B). Binding of *Leptospira* (10^7) to a series concentration of Fn (0, 10, 100 or 1000 µg in 100 µl PBS). BSA was coated and used as negative control. (C). Fn inhibits the binding of *Leptospira* to MDCK cells. *Leptospira* (10^7) were treated with a series concentration of Fn (0, 0.01, 0.1, 0.2, 1, 2, or 10µg) or BSA (negative control) prior to the addition of MDCK cells (10^5). The percentage of adhesion was determined relative to the attachment of untreated *Leptospira* on MDCK cells. (D). Binding of *Leptospira* to immobilize Fn. *Leptospira* (10^8) were cultured in Fn or BSA (negative control) coated (1mg in 100 µl PBS) or un-coated wells (negative control). (E). Fn inhibits the binding of *Leptospira* to MDCK cells. *Leptospira* (10^8) were pre-treated with 10µg of Fn or BSA (negative control) prior to the addition of MDCK cells (10^6). The un-treated *Leptospira* was used as negative control. The binding of *Leptospira* to ECMs or Fn or the adhesion of *Leptospira* to MDCK cells was measured by ELISA (A, B, and C) or EPM (D and E). For all experiments, each value represents the mean ± SEM of three trials in triplicate samples. Statistically significant ($P<0.05$) values are indicted by an asterisk. The EPM settings were identical for all captured images (D and E).

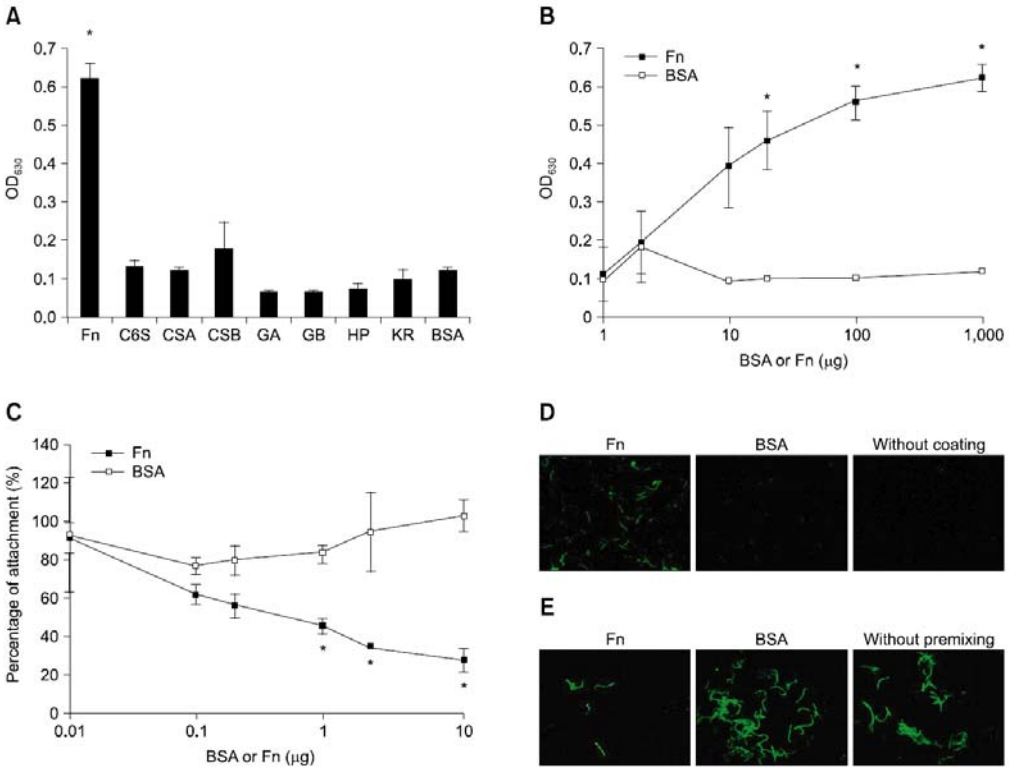
A
B
C
D
E
Fn
C6S
CSA
CSB
GA
GB
HP
KR
BSA
OD450
BSA or Fn (μg)
Percentage of attachment (%)
Without coating
Without premixing

Statistical analysis

Statistically significant differences between samples was determined using the Student's t-test following logarithmic transformation of the data. Two-tailed *P*-values were determined for each sample, and a $P < 0.05$ was considered significant. Each data point represents the mean ± standard error of the mean (SEM) of a sample tested in triplicate. An asterisk indicates the result was statistically significant.

Results

Attachment of *Leptospira* to MDCK cells was mediated by fibronectin

The binding of leptospiral cells to various ECM components was determined using ELISA. As shown in Figure. 2.1A, *Leptospira* strongly bound to Fn, but not to other ECM molecules (Figure. 2.1A). Furthermore, the binding of *Leptospira* to Fn was dose dependent (Figure. 2.1B). When *Leptospira* were pretreated with Fn, binding to MDCK cells decreased (Figure. 2.1C). Approxximately 3.5-fold increase in immobilization of *Leptospira* on Fn-coated wells was found compared to the control (Figure. 2.1D). Moreover, Fn could also block the attachment of *Leptospira* by approximately 47% when Fn treated *Leptospira* were added to MDCK cells (Figure. 2.1 E). Thus, Fn can mediate the attachment of *Leptospira* to MDCK cells.

Interaction between LigB and Fn

To determine whether LigB interacts with Fn, we truncated the LigB protein into three parts, LigBCon, LigBCen and LigBCtv, (Figure. 2.2A) due to the difficulty of expressing and purifying full length LigB [32]. First, we analyzed the interaction of each LigB fragment with Fn using a GST-pull down assay. Our results showed that both human plasma Fn and Fn derived from MDCK cell lysates could bind both LigBCen and LigBCtv, but not LigBCon (Figure. 2.2B and 2.2C). Since LigBCen and LigBCtv

Table 2.1 Thermodynamic parameters for the interaction of Fn and truncated LigB.

Macromolecule	LigB Residues	[Macromolecule]	[Fn]	ΔH	ΔS	K_d
		μM	μM	kcal mol^{-1}	cal mol^{-1} K^{-1}	μM
LigBCon	1-630	1.25	25	n/f[a]	n/f[a]	n/f[a]
LigBCen	631-1,417	2	40	-2,002.67±14	-6.68	0.011±0.003
LigBCtv	1,418-1,861	2.82	56.4	-12,140±1557	-40.71	8.55±0.75

[a] n/f, non-fittable

Figure. 2.2 The interaction between LigB and Fn by GST-pull down assay. (A) A schematic diagram showing the structure of LigB and the truncated LigB protein used in this study. (B). Human plasma Fn (lane 2 to lane 5) or cell lysate of MDCK cells (lane 7 to lane 10) was applied to GST beads preimmobilized by GST, GST-LigBCon, GST-LigBCen, or GST-LigBCtv at 4^{o}C for 3 hours. The pull down complex was analyzed by immunoblot analysis using Fn antibody. Lane 1 and lane 6 contain 1 μg of human plasma Fn and the cell lysate from 1 x 10^{6} MDCK cells, respectively, to serve as a positive reference. Lane 2 and lane 7 are GST-LigBCen, lane 3 and lane 8 are GST-LigBCtv, lane 4 and lane 9 are GST-LigBCon, and lane 5 and lane 10 are GST. The molecular mass of human Fn and canine Fn (MDCK cells) is 261 kDa and 271 kDa, respectively, and the relative positions of the standards are given in kDa on the left.

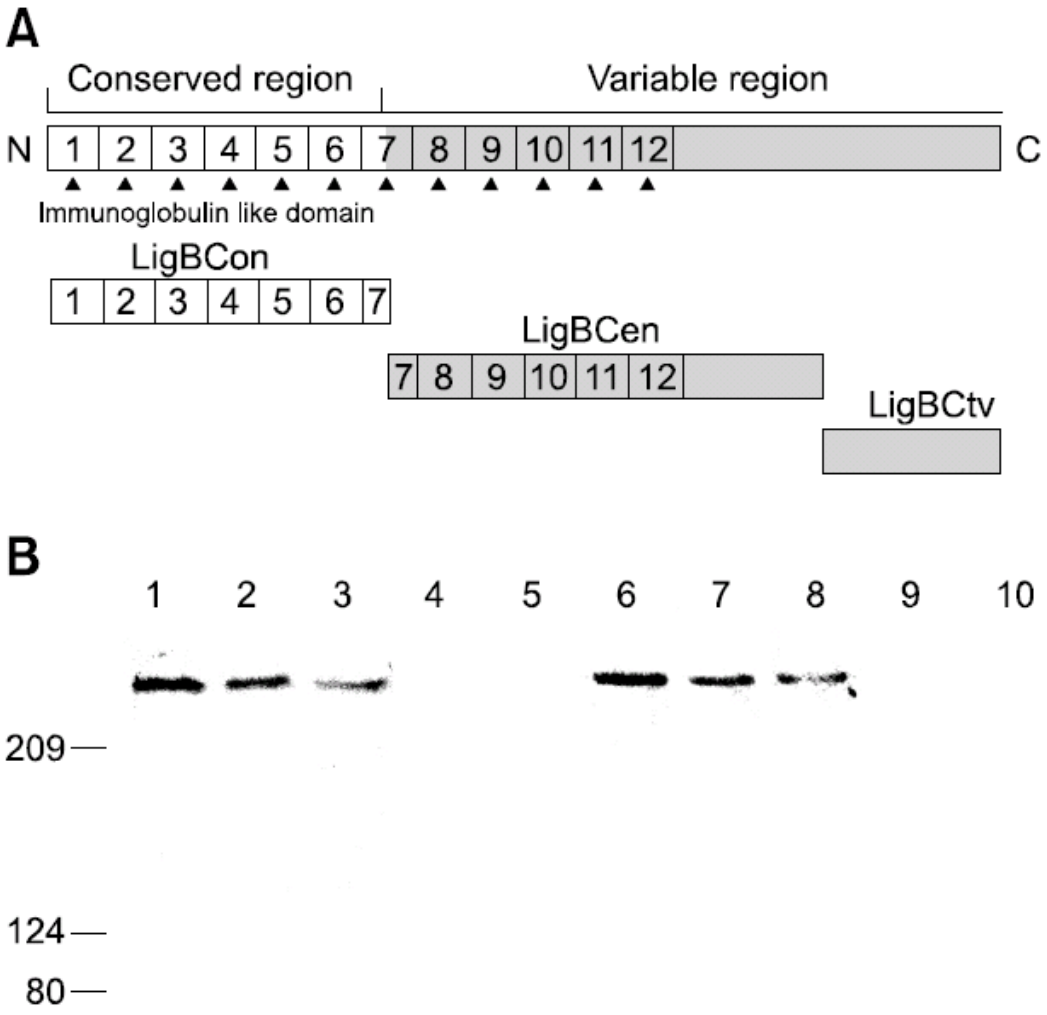
A
Conserved region
Variable region
N
1 2 3 4 5 6 7 8 9 10 11 12
C
Immunoglobulin like domain
LigBCon
1 2 3 4 5 6 7
LigBCen
7 8 9 10 11 12
LigBCtv
B
1 2 3 4 5 6 7 8 9 10
209
124
80

Figure 2.3 LigBCen or LigBCtv binds to Fn and inhibits the binding of *Leptospira* to Fn. (A). Binding of LigBCen or LigBCtv to a series concentration of immobilized Fn. Ten nM of GST-LigBCen, GST-LigBCtv, or GST (negative control) was added to wells coated with a series concentration of Fn (0, 0.27μM, 0.45μM, 2.7μM, 4.5μM, 27μM, or 45μM) in 100 μl PBS. . The binding of each of these proteins to Fn was measured by ELISA. (B). LigBCen or LigBCtv inhibits the binding of *Leptospira* to immobilized Fn. A series concentration (0, 2, 4, 6, or 8 nM) of GST-LigBCen, GST-LigBCtv, or GST (negative control) were added to each well coated with Fn (1mg in 100 μl PBS) prior to the addition of *Leptospira* (10^7). The attachment of *Leptopsira* to wells was measured by ELISA. The percentage of attachment was determined relative to the attachment of *Leptopsira* on untreated Fn. (C). LigBCen or LigBCtv inhibits the binding of *Leptospira* to Fn. Fifty nM of GST-LigBCen, GST-LigBCtv, or GST (negative control) was added to wells coated with Fn (1mg in 100 μl PBS) prior to the addition of *Leptospira* (10^8). The binding of *Leptospira* to wells were detected by EPM. In (A) and (B), each value represents the mean± SEM of three trials in triplicate samples. Statistically significant values ($P<0.05$) are indicted by *. In (C), The EPM settings were identical for all captured images. Images were processed using Adobe Photoshop CS2.

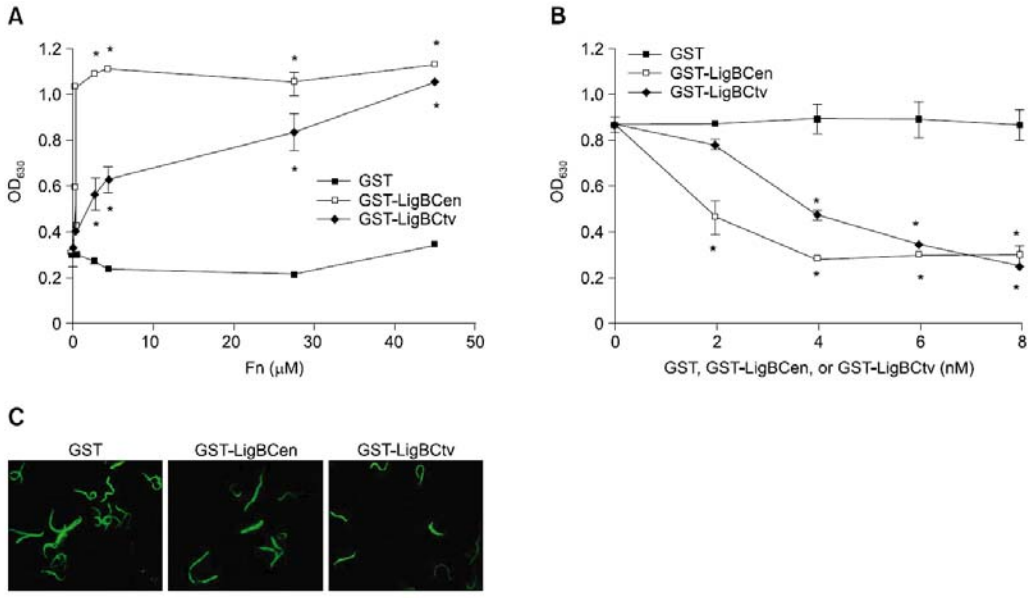
A
1.2
1.0
0.8
0.6
0.4
0.2
0
OD630
0
10
20
30
40
50
Fn (μM)
GST
GST-LigBCen
GST-LigBCtv
B
1.2
1.0
0.8
0.6
0.4
0.2
0
OD630
0
2
4
6
8
GST, GST-LigBCen, or GST-LigBCtv (nM)
GST
GST-LigBCen
GST-LigBCtv
C
GST
GST-LigBCen
GST-LigBCtv

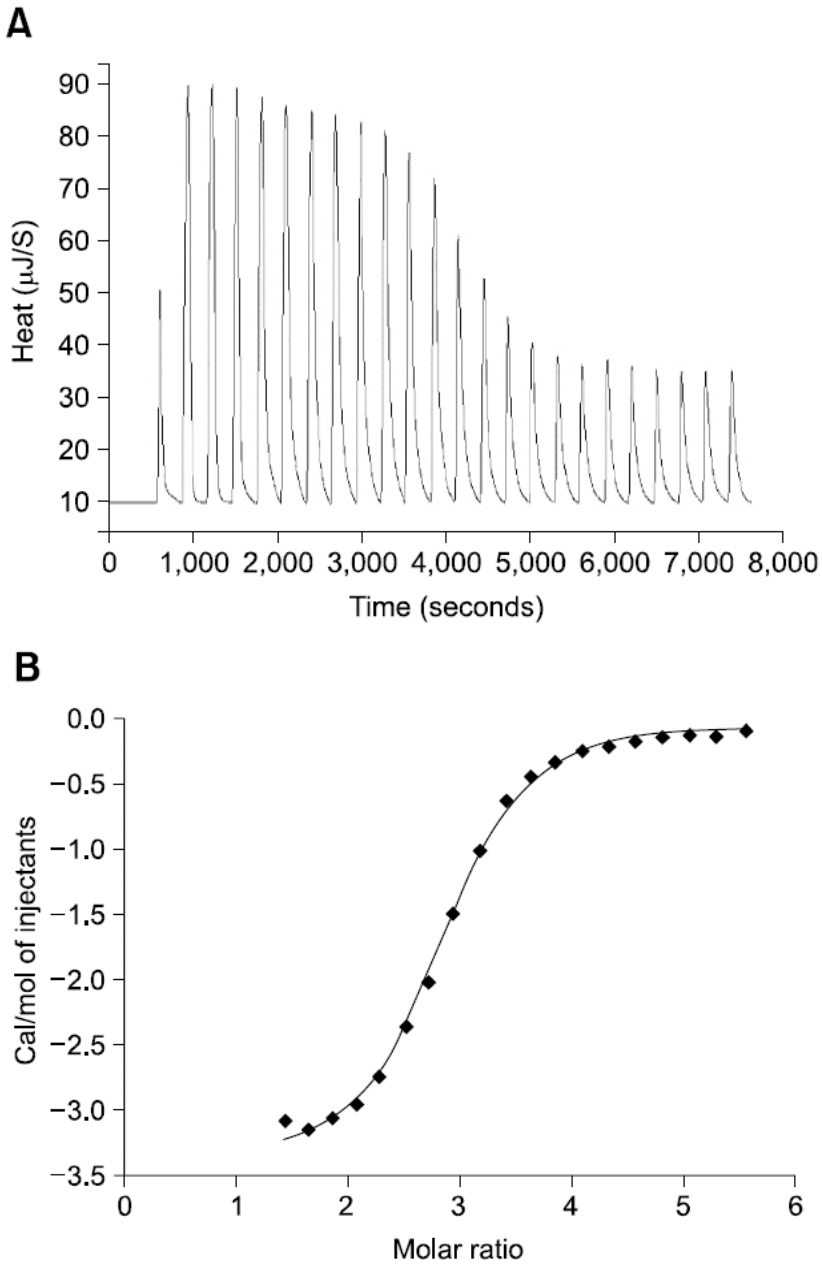

Figure. 2.4 Isothermal titration calorimetry (ITC) profile of LigBCtv with Fn as a typical ITC profile in this study. A; heat differences obtained from 25 injections. B: Integrated curve with experimental point (◆) and the best fit (—). The thermodynamic parameters are shown in Table 2.1

Figure 2.5 The binding of LigBCen or LigBCtv to MDCK cells reduces leptospiral adhesion. (A) Binding of LigBCen or LigBCtv to MDCK cells. A series concentration (0, 2, 4, 6, or 8 nM) of GST-LigBCen, GST-LigBCtv, or GST (negative control) was added to MDCK cells (10^5). The binding of each of these proteins to MDCK cells were measured by ELISA. (B) LigBCen or LigBCtv inhibits the binding of *Leptopsira* to MDCK cells. MDCK cells were incubated with a series concentration (0, 2, 4, 6, or 8 nM) of GST-LigBCen, GST-LigBCtv, or GST (negative control) prior to the addition of *Leptopsira* (10^7). The ashesion of *Leptospira* to MDCK cells (10^5) were detected by ELISA. The reduced percentage of attachment was determined relative to the attachment of *Leptopsira* on untreated MDCK cells. (C). LigBCen or LigBCtv inhibits the binding of *Leptopsira* to MDCK cells. MDCK cells (10^6) were pre-treated with 50nM of GST-LigBCen, GST-LigBCtv, and GST (negative control) prior to the addition of *Leptopsira* (10^8). The adhesion of *Leptospira* or the binding of these proteins to MDCK cells were detected by CLSM. In (A) and (B), each value represents the mean± SEM of three trials in triplicate samples. Statistically significant values ($P<0.05$) are indicted by *. In (C), the CLSM settings were identical for all the captured images. Images were processed using Adobe Photoshop CS2.

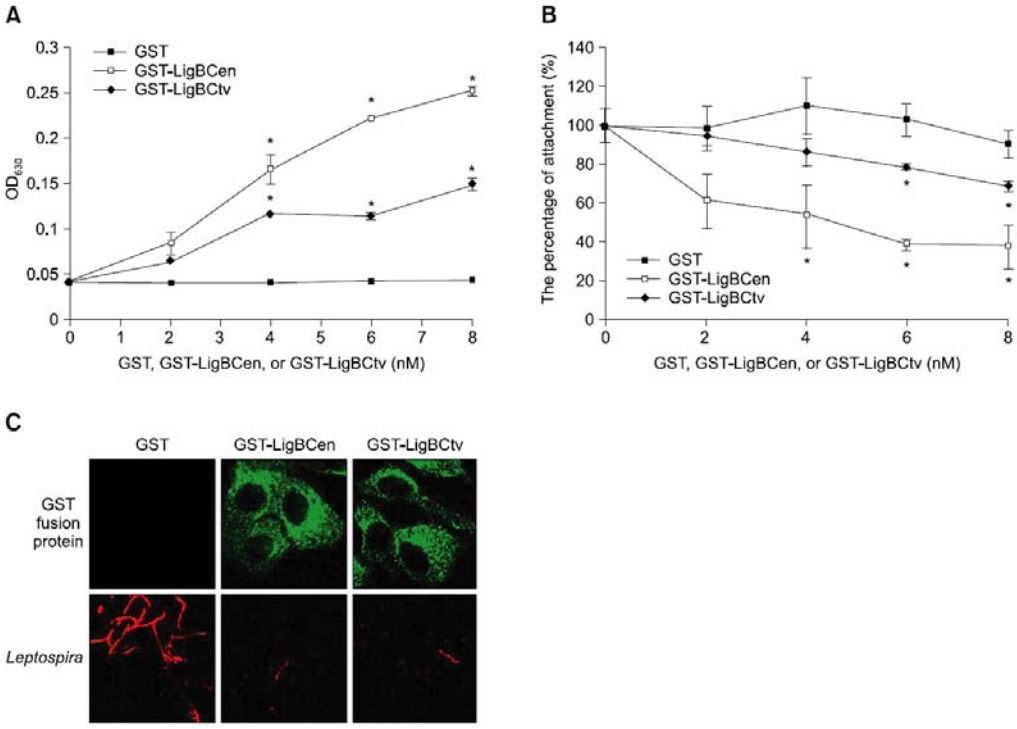
A
GST
GST-LigBCen
GST-LigBCtv
OD630
GST, GST-LigBCen, or GST-LigBCtv (nM)
B
The percentage of attachment (%)
GST
GST-LigBCen
GST-LigBCtv
GST, GST-LigBCen, or GST-LigBCtv (nM)
C
GST
GST-LigBCen
GST-LigBCtv
GST fusion protein
Leptospira

Figure 2.6 The binding of LigBCen or LigBCtv to Fn siRNA transfected MDCK cells was reduced. (A). Detection of the expression of Fn and actin in MDCK cells 72 h after transfected by Fn or negative siRNA. Fn and α-actin were detected by immunoblotting probed by actin antibody or Fn antibody. (B) Binding of GST-LigBCen or (C) GST-LigBCtv was reduced by the siRNA transfected cells. (D) GST was served as negative control. Fifty nM of GST-LigBCen, GST-LigBCtv, or GST was added to Fn or negative siRNA transfected MDCK cells. Expression of Fn and the binding of these proteins to MDCK cells were detected by CLSM. The CLSM settings were identical for all the captured images. Images were processed using Adobe Photoshop CS2.

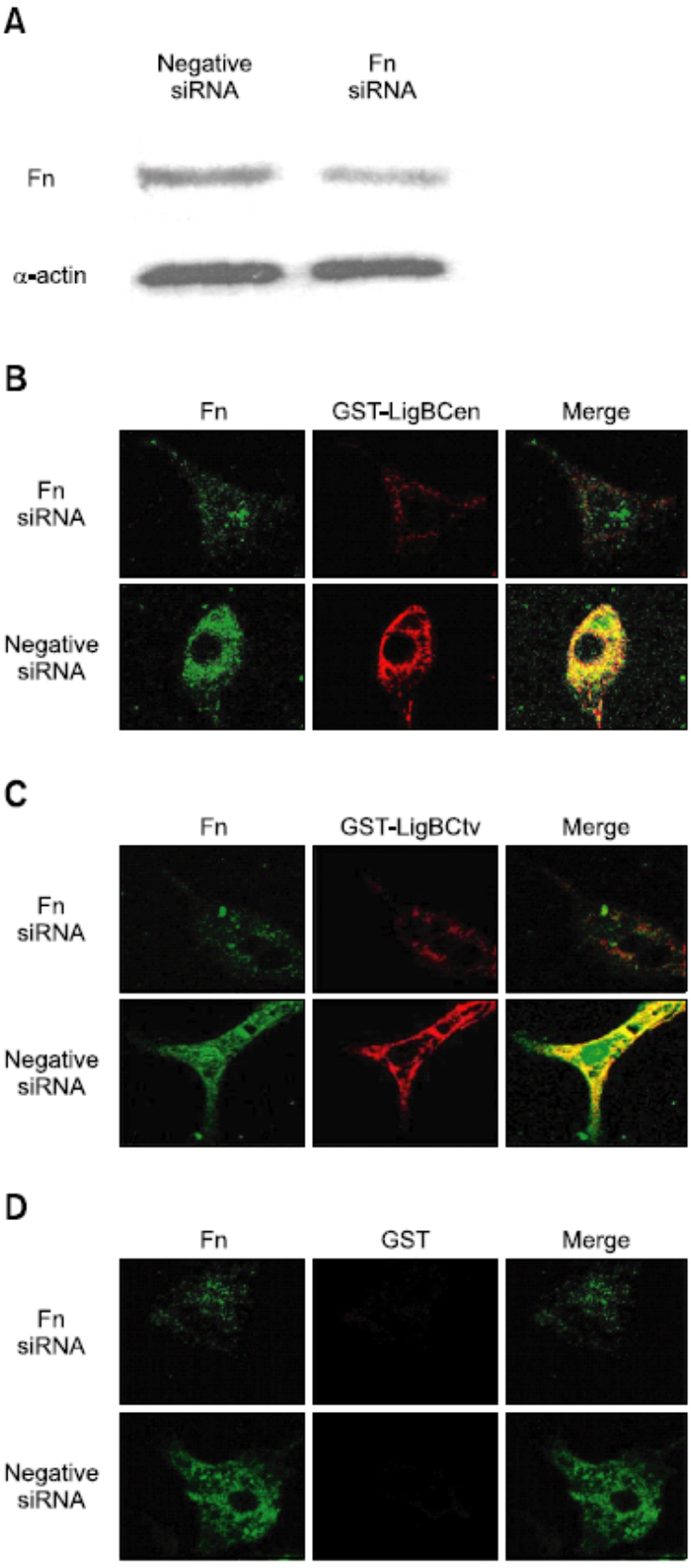
A
Negative siRNA
Fn siRNA
Fn
α-actin
B
Fn
GST-LigBCen
Merge
Fn siRNA
Negative siRNA
C
Fn
GST-LigBCtv
Merge
Fn siRNA
Negative siRNA
D
Fn
GST
Merge
Fn siRNA
Negative siRNA

showed a positive pull down result, the interaction between LigBCen and LigBCtv with Fn was further studied using ELISA. We found that both the binding of LigBCen and LigBCtv to Fn and the inhibition of the attachment of *Leptospira* to Fn by LigBCen and LigBCtv was dose-dependent (Figure. 2.3A and 2.3B). Moreover, the EPM images revealed up to 40% reduction in the attachment of *Leptospira* to Fn in the presence of LigBCen and LigBCtv (Figure. 2.3C). Finally, in order to quantitatively evaluate the binding affinity between Fn and LigB fragments, the dissociation constants (K_d) were measured by ITC (Table 2.1). Figure. 2.4 shows data of a typical ITC experiment. The interaction appears to be exothermic with a favorable enthalpy and unfavorable entropy. The calculated K_d values for Fn binding to LigBCen and LigBCtv were 0.01μM and 8.55μM, respectively (Table 2.1). Binding of LigBCon could not be detected by ITC (data not shown). These studies are in agreement with our previous results. Altogether, these data indicate that Fn specifically interacts with LigBCen and LigBCtv fragments.

LigBCen and LigBCtv mediate the attachment of *Leptospira* to MDCK cells

To determine if LigB is used by *Leptospira* to adhere to MDCK cells, various concentrations of LigBCen or LigBCtv were added to MDCK cells, and binding was detected by ELISA and immunofluorescence staining. Our results clearly showed that LigBCen and LigBCtv bound to MDCK cells in a dose dependent manner (Figure. 2.5A). Pretreatment of MDCK cells with LigBCen or LigBCtv reduced the attachment of *Leptospira* by ~32%. The reduction of *Leptospira* attachment was also dose-dependent (Fig. 2.5B and 2.5C). We further elucidated the receptor role of Fn on MDCK cells for its possible ligand, LigB, on the surface of *Leptospira*, by RNA interference to decrease endogeneous Fn expression in MDCK cells. As shown in Fig. 2.6A, transfection of cells with siRNA duplex specific for canine Fn resulted in ~36% reduction in Fn expression, relative to the control cells. The binding of LigBCen and

LigBCtv to Fn siRNA-transfected MDCK cells was significantly reduced (Fig. 2.6B, 2.6C). The data suggest that Fn serves as a receptor for LigB, which mediates *Leptospira* adhesion.

Discussion

Adhesion to host cells is pivotal for many pathogenic bacteria including *Leptospira* spp. Since pathogenic *Leptospira* spp. can infect a variety of tissues including liver, kidney and lung, the study of host-pathogen interaction is extremely important in leptospirosis. Recently, the leptospiral genome has been sequenced and a number of tentative virulence factors have been proposed [3, 30, 41]. However, their exact roles in leptospiral pathogenesis remain to be established. To date, several leptospiral adhesins have been identified. These include a 36 kDa Fn-binding protein [29], a 24 kDa laminin-binding protein [1] and LigA, LigB and LigC proteins [24, 32, 33]. These molecules may play an important role in the pathogenesis of leptospiral infection since they are able to bind to ECMs such as collagens I and IV, laminin and fibronectin [6].

Pathogenic *Leptospira* spp. have been previously reported to adhere to extracellular matrices [15, 16] including Fn. Fns are dimers of two similar peptides linked at their C-termini by two disulfide bonds [8] and serve as a receptor for several bacteria, including spirochetes [20, 27, 31, 45, 54] [7, 11, 12, 19, 23, 37, 39, 49]. Our results showed that Fn immobilized *Leptospira* (Fig. 2.1A, B and D). We also found that Fn blocked the attachment of *Leptospira* to MDCK cells if *Leptospira* were pre-treated with Fn (Fig. 2.1C and E). These results confirmed a recent report that Fn could be an important molecule by which all pathogenic *Leptospira* spp. adhere to host cells [6].

We demonstrated the interaction between LigB and Fn. It was shown that the LigBCen and LigBCtv fragments bound to Fn using a GST-pulldown assays (Fig.

2.2), ELISA (Fig. 2.3), and ITC measurements (Fig. 2.6). The low K_d values for LigBCen indicated that the LigB-Fn interaction is specific. This evidence strongly suggests that LigB is a Fn-binding protein (Fbp). A similar study has been reported by Choy *et al* that LigB U1 and LigB U2 (LigBCen equivalent) could strongly bind to Fn, while the LigB CTD (LigBCtv equivalent) binds weakly to Fn [6]. However, the K_d values of LigBCen and LigBCtv to Fn that we obtained are slightly different to those reported by Choy *et al* [6]. The differences in the obtained K_d values could be explained by (i) the protein fragments in this study (LigBCen and LigBCtv) were not exactly the same length fragments used by Choy *et al* (LigBU1, LigBU2, and LigBCTD) and (ii) the method we used (ITC) to measure the K_d differs from that of Choy, et al (ELISA).

Since pathogenic *Leptospira* spp. adhere to renal tubular epithelial cells and induce severe tubulointerstitial nephritis leading to renal failure [57], it is possible that LigB is responsible for the binding of *Leptospira* to renal tubular epithelium. Our results indicated that LigB binds to MDCK cells via LigBCen or LigBCtv fragments (Fig. 2.4A, B and C). However, LigBCen could bind to both MDCK cells and Fn with greater affinity than could LigBCtv (Fig. 2.3A, Fig. 2.4A and 2.4 B, Table 2.1). The microscopic images also showed that not all of the Fn was co-localized with LigB (Fig. 2.5B and 2.5C). This result suggests that LigB might bind to two or more receptors. Our results elucidate how *Leptospira* attach to MDCK cells, as shown in a previous study [51], and indicate why Fn can block leptospiral attachment to MDCK cells, as shown in this study (Fig. 2.1D and E).

Our results clearly confirm that LigB is one of the MSCRAMM members that binds to ECM including Fn. The transmembrane domain of LigB is predicted to reside within the conserved region, and only the variable region is exposed on the surface[32, 33]. These results support our data that Fn-binding domains of LigB are localized in

the variable regions. This is not surprising since similar findings have been reported for other MSCRAMMs [13, 36, 38]. In *Borrelia*, the binding motifs in the decorin-binding proteins, DbpA and B are located in the central regions, which vary among different *Borrelia* strains (*B. burgdorferi, B. garnii,* and *B. afzeli*) [36]. The Fn-binding domain of the Fn-binding protein, BBK32 is also variable among different *Borrelia* strains [38]. The repetitive D1, D2 and D3 elements of *Staphylococcus aureus* Fn-binding protein, which bind the N-terminal 29 kDa of Fn, also vary [13].

Since both LigBCen and LigBCtv bind to Fn but with different affinities, it suggests that there is more than one potential Fn-binding domain. In *Mycobacterium avium*, two Fn-binding domains are located on two non-contiguous 24 amino acids of the Fn attachment protein-A (FAP-A) [44]. The FnBA of *Staphylococcus aureus* contains three repetitive elements, D1, D2, and D3 and each binds the N-terminal 29 kDa fragment of Fn [13]. Seven additional Fn-binding elements are located in the N-terminal of the D repeats [47]. In *Streptococcus dysgalactiae*, there are five Fn-binding segments within the C-terminus of the Fn binding protein F1/(FnBB) [46, 47]. Therefore, it is likely that several binding sites might be present in the LigB variable region. However, we are unable to identify a similar Fn-binding motif from other known Fn-binding proteins.

In conclusion, we have shown that LigBCen and LigBCtv bind to Fn and have proved that LigB is a member of MSCRAMMs. Since pathogenic *Leptospira* spp. initially attach to mucosal epithelial cells prior to entry into the bloodstream and subsequent dissemination to multiple organs such as the kidney, liver, and lung, Lig proteins may play a pivotal role in the pathogenesis of leptospirosis. Fn is one of the most important ECMs on epithelial cells and serves as a receptor for leptospiral adherence [6, 15]. Thus, further studies into the interaction of Lig proteins and ECMs are warranted.

REFERENCES

1. **Barbosa, AS, Abreu, PA, Neves, FO, Atzingen, MV, Watanabe, MM, Vieira, ML, Morais, ZM, Vasconcellos, SA, and Nascimento, AL.** 2006. A newly identified leptospiral adhesin mediates attachment to laminin. Infect. Immun. **74 :** 6356-6364.

2. **Barocchi, MA, Ko, AI, Reis, MG, McDonald, KL, and Riley, LW.** 2002. Rapid translocation of polarized MDCK cell monolayers by *Leptospira interrogans*, an invasive but nonintracellular pathogen. Infect. Immun. **70 :** 6926-6932.

3. **Bulach, DM, Zuerner, RL, Wilson, P, Seemann, T, McGrath, A, Cullen, PA, Davis, J, Johnson, M, Kuczek, E, Alt, DP, Peterson-Burch, B, Coppel, RL, Rood, JI, Davies, JK, and Adler, B.** 2006. Genome reduction in *Leptospira borgpetersenii* reflects limited transmission potential. Proc. Natl. Acad. Sci. USA. **103 :** 14560-14565.

4. **Cameron, CE, Brouwer, NL, Tisch, LM, and Kuroiwa, JM.** 2005. Defining the interaction of the *Treponema pallidum* adhesin Tp0751 with laminin. Infect. Immun. **73 :** 7485-7494.

5. **Cameron, CE, Brown, EL, Kuroiwa, JM, Schnapp, LM, and Brouwer, NL.** 2004. *Treponema pallidum* fibronectin-binding proteins. J. Bacteriol. **186 :** 7019-7022.

6. **Choy, HA, Kelley, MM, Chen, TL, Moller, AK, Matsunaga, J, and Haake, DA.** 2007. Physiological osmotic induction of *Leptospira interrogans* adhesion: LigA and LigB bind extracellular matrix proteins and fibrinogen. Infect. Immun. **75 :** 2441-2450.

7. **Coburn, J, Fischer, JR, and Leong, JM.** 2005. Solving a sticky problem: new genetic approaches to host cell adhesion by the Lyme disease spirochete. Mol. Microbiol. **57 :** 1182-1195.

8. **Darnell, J, Lodish, H, and Baltimore, D (ed.).** 1990. Chaperter 23. Multicellularity: cell-cell and cell-matrix interactions., 2nd ed. , vol. Scientific American Books,, New York.

9. **Edwards, AM, Jenkinson, HF, Woodward, MJ, and Dymock, D.** 2005. Binding properties and adhesion-mediating regions of the major sheath protein of *Treponema denticola* ATCC 35405. Infect. Immun. **73 :** 2891-2898.

10. **Faine, SB, Adher, B, Bolin, C, and Perolat, P (ed.).** 1999. *Leptospira* and Leptospirosis., vol. 2nd edition. MedSci, Medbourne, Australia.

11. **Fischer, JR, LeBlanc, KT, and Leong, JM.** 2006. Fibronectin binding protein BBK32 of the Lyme disease spirochete promotes bacterial attachment to glycosaminoglycans. Infect. Immun. **74 :** 435-441.

12. **Grab, DJ, Givens, C, and Kennedy, R.** 1998. Fibronectin-binding activity in *Borrelia burgdorferi*. Biochim. Biophys. ACTA. **1407 :** 135-145.

13. **Ingham, KC, Brew, S, Vaz, D, Sauder, DN, and McGavin, MJ.** 2004. Interaction of *Staphylococcus aureus* fibronectin-binding protein with fibronectin: affinity, stoichiometry, and modular requirements. J. Biol. Chem. **279 :** 42945-42953.

14. **Isberg, RR, Voorhis, DL, and Falkow, S.** 1987. Identification of invasin: a protein that allows enteric bacteria to penetrate cultured mammalian cells. Cell **50 :** 769-778.

15. **Ito, T, and Yanagawa, R.** 1987. Leptospiral attachment to extracellular matrix of mouse fibroblast (L929) cells. Vet. Microbiol. **15 :** 89-96.

16. **Ito, T, and Yanagawa, R.** 1987. Leptospiral attachment to four structural components of extracellular matrix. Nippon. juigaku. zasshi. **49 :** 875-882.

17. **Jerse, AE, Yu, J, Tall, BD, and Kaper, JB.** 1990. A genetic locus of enteropathogenic *Escherichia coli* necessary for the production of attaching and effacing lesions on tissue culture cells. Proc. Natl. Acad. Sci. USA. **87 :** 7839-7843.

18. **Jiang, ST, Chiang, HC, Cheng, MH, Yang, TP, Chuang, WJ, and Tang, MJ.** 1999. Role of fibronectin deposition in cystogenesis of Madin-Darby canine kidney cells. Kidney intl. **56 :** 92-103.

19. **Kim, JH, Singvall, J, Schwarz-Linek, U, Johnson, BJ, Potts, JR, and Hook, M.** 2004. BBK32, a fibronectin binding MSCRAMM from *Borrelia burgdorferi*, contains a disordered region that undergoes a conformational change on ligand binding. J. Biol. Chem. **279 :** 41706-41714.

20. **Konkel, ME, Christensen, JE, Keech, AM, Monteville, MR, Klena, JD, and Garvis, SG.** 2005. Identification of a fibronectin-binding domain within the *Campylobacter jejuni* CadF protein. Mol. Microbiol. **57 :** 1022-1035.

21. **Kopp, PA, Schmitt, M, Wellensiek, HJ, and Blobel, H.** 1995. Isolation and characterization of fibronectin-binding sites of *Borrelia garinii* N34. Infect. Immun. **63 :** 3804-3808.

22. **Levett, PN.** 2001. Leptospirosis. Clin. Microbiol. Rev. **14 :** 296-326.

23. **Li, X, Liu, X, Beck, DS, Kantor, FS, and Fikrig, E.** 2006. *Borrelia burgdorferi* lacking BBK32, a fibronectin-binding protein, retains full pathogenicity. Infect. Immun. **74 :** 3305-3313.

24. **Matsunaga, J, Barocchi, MA, Croda, J, Young, TA, Sanchez, Y, Siqueira, I, Bolin, CA, Reis, MG, Riley, LW, Haake, DA, and Ko, AI.** 2003. Pathogenic

Leptospira species express surface-exposed proteins belonging to the bacterial immunoglobulin superfamily. Mol. Microbiol. **49 :** 929-945.

25. **Matsunaga, J, Lo, M, Bulach, DM, Zuerner, RL, Adler, B, and Haake, DA.** 2007. Response of *Leptospira interrogans* to Physiologic Osmolarity: Relevance in Signaling the Environment-to-Host Transition. Infect. Immun. **75 :** 2864-2874.

26. **Matsunaga, J, Sanchez, Y, Xu, X, and Haake, DA.** 2005. Osmolarity, a key environmental signal controlling expression of leptospiral proteins LigA and LigB and the extracellular release of LigA. Infect. Immun. **73 :** 70-78.

27. **May, M, Papazisi, L, Gorton, TS, and Geary, SJ.** 2006. Identification of fibronectin-binding proteins in *Mycoplasma gallisepticum* strain R. Infect. Immun. **74 :** 1777-1785.

28. **Meites, E, Jay, MT, Deresinski, S, Shieh, WJ, Zaki, SR, Tompkins, L, and Smith, DS.** 2004. Reemerging leptospirosis, California. Emerg. Infect. Dis. **10 :** 406-412.

29. **Merien, F, Truccolo, J, Baranton, G, and Perolat, P.** 2000. Identification of a 36-kDa fibronectin-binding protein expressed by a virulent variant of *Leptospira interrogans* serovar icterohaemorrhagiae. FEMS. Microbiol. Lett. **185 :** 17-22.

30. **Nascimento, AL, Ko, AI, Martins, EA, Monteiro-Vitorello, CB, Ho, PL, Haake, DA, Verjovski-Almeida, S, Hartskeerl, RA, Marques, MV, Oliveira, MC, Menck, CF, Leite, LC, Carrer, H, Coutinho, LL, Degrave, WM, Dellagostin, OA, El-Dorry, H, Ferro, ES, Ferro, MI, Furlan, LR, Gamberini, M, Giglioti, EA, Goes-Neto, A, Goldman, GH, Goldman, MH, Harakava, R, Jeronimo, SM, Junqueira-de-Azevedo, IL, Kimura, ET, Kuramae, EE, Lemos, EG, Lemos, MV, Marino, CL, Nunes, LR, de**

Oliveira, RC, Pereira, GG, Reis, MS, Schriefer, A, Siqueira, WJ, Sommer, P, Tsai, SM, Simpson, AJ, Ferro, JA, Camargo, LE, Kitajima, JP, Setubal, JC, and Van Sluys, MA. 2004. Comparative genomics of two *Leptospira interrogans* serovars reveals novel insights into physiology and pathogenesis. J. Bacteriol. **186 :** 2164-2172.

31. **Nyberg, P, Sakai, T, Cho, KH, Caparon, MG, Fassler, R, and Bjorck, L.** 2004. Interactions with fibronectin attenuate the virulence of *Streptococcus pyogenes*. EMBO J. **23 :** 2166-2174.

32. **Palaniappan, RU, Chang, YF, Hassan, F, McDonough, SP, Pough, M, Barr, SC, Simpson, KW, Mohammed, HO, Shin, S, McDonough, P, Zuerner, RL, Qu, J, and Roe, B.** 2004. Expression of leptospiral immunoglobulin-like protein by *Leptospira interrogans* and evaluation of its diagnostic potential in a kinetic ELISA. J. Med. Microbiol. **53 :** 975-984.

33. **Palaniappan, RU, Chang, YF, Jusuf, SS, Artiushin, S, Timoney, JF, McDonough, SP, Barr, SC, Divers, TJ, Simpson, KW, McDonough, PL, and Mohammed, HO.** 2002. Cloning and molecular characterization of an immunogenic LigA protein of *Leptospira interrogans*. Infect. Immun. **70 :** 5924-5930.

34. **Palaniappan, RU, McDonough, SP, Divers, TJ, Chen, CS, Pan, MJ, Matsumoto, M, and Chang, YF.** 2006. Immunoprotection of recombinant leptospiral immunoglobulin-like protein A against *Leptospira interrogans* serovar Pomona infection. Infect. Immun. **74 :** 1745-1750.

35. **Parma, AE, Cerone, SI, and Sansinanea, SA.** 1992. Biochemical analysis by SDS-PAGE and western blotting of the antigenic relationship between *Leptospira* and equine ocular tissues. Vet. Immunol. Immunopathol. **33 :** 179-185.

36. **Pikas, DS, Brown, EL, Gurusiddappa, S, Lee, LY, Xu, Y, and Hook, M.** 2003. Decorin-binding sites in the adhesin DbpA from *Borrelia burgdorferi*: a synthetic peptide approach. J. Biol. Chem. **278 :** 30920-30926.

37. **Probert, WS, and Johnson, BJ.** 1998. Identification of a 47 kDa fibronectin-binding protein expressed by *Borrelia burgdorferi* isolate B31. Mol. Microbiol. **30 :** 1003-1015.

38. **Probert, WS, Kim, JH, Hook, M, and Johnson, BJ.** 2001. Mapping the ligand-binding region of *Borrelia burgdorferi* fibronectin-binding protein BBK32. Infect. Immun. **69 :** 4129-4133.

39. **Raibaud, S, Schwarz-Linek, U, Kim, JH, Jenkins, HT, Baines, ER, Gurusiddappa, S, Hook, M, and Potts, JR.** 2005. *Borrelia burgdorferi* binds fibronectin through a tandem beta-zipper, a common mechanism of fibronectin binding in staphylococci, streptococci, and spirochetes. J. Biol. Chem. **280 :** 18803-18809.

40. **Rathinam, SR, Rathnam, S, Selvaraj, S, Dean, D, Nozik, RA, and Namperumalsamy, P.** 1997. Uveitis associated with an epidemic outbreak of leptospirosis. Am. J. ophthalmol. **124 :** 71-79.

41. **Ren, SX, Fu, G, Jiang, XG, Zeng, R, Miao, YG, Xu, H, Zhang, YX, Xiong, H, Lu, G, Lu, LF, Jiang, HQ, Jia, J, Tu, YF, Jiang, JX, Gu, WY, Zhang, YQ, Cai, Z, Sheng, HH, Yin, HF, Zhang, Y, Zhu, GF, Wan, M, Huang, HL, Qian, Z, Wang, SY, Ma, W, Yao, ZJ, Shen, Y, Qiang, BQ, Xia, QC, Guo, XK, Danchin, A, Saint Girons, I, Somerville, RL, Wen, YM, Shi, MH, Chen, Z, Xu, JG, and Zhao, GP.** 2003. Unique physiological and pathogenic features of *Leptospira interrogans* revealed by whole-genome sequencing. Nature **422 :** 888-893.

42. **Reynolds, A, Leake, D, Boese, Q, Scaringe, S, Marshall, WS, and Khvorova, A.** 2004. Rational siRNA design for RNA interference. Nat. biotechnol. **22,** 326-330.

43. **Rzomp, KA, Scholtes, LD, Briggs, BJ, Whittaker, GR, and Scidmore, MA.** Rab 2003. GTPases are recruited to chlamydial inclusions in both a species-dependent and species-independent manner. Infect. Iimmun. **71 :** 5855-5870.

44. **Schorey, JS, Holsti, MA, Ratliff, TL, Allen, PM, and Brown, EJ.** 1996. Characterization of the fibronectin-attachment protein of *Mycobacterium avium* reveals a fibronectin-binding motif conserved among mycobacteria. Mol. Microbiol. **21 :** 321-329.

45. **Schroder, A, Schroder, B, Roppenser, B, Linder, S, Sinha, B, Fassler, R, and Aepfelbacher, M.** 2006. *Staphylococcus aureus* fibronectin binding protein-A induces motile attachment sites and complex actin remodeling in living endothelial cells. Mol. Biol. Cell. **17 :** 5198-5210.

46. **Schwarz-Linek, U, Pilka, ES, Pickford, AR, Kim, JH, Hook, M, Campbell, ID, and Potts, JR.** 2004. High affinity streptococcal binding to human fibronectin requires specific recognition of sequential F1 modules. J. Biol. Chem. **279 :** 39017-39025.

47. **Schwarz-Linek, U, Werner, JM, Pickford, AR, Gurusiddappa, S, Kim, JH, Pilka, ES, Briggs, JA, Gough, TS, Hook, M, Campbell, ID, and Potts, JR.** 2003. Pathogenic bacteria attach to human fibronectin through a tandem beta-zipper. Nature **423 :** 177-181.

48. **Segura, ER, Ganoza, CA, Campos, K, Ricaldi, JN, Torres, S, Silva, H, Cespedes, MJ, Matthias, MA, Swancutt, MA, Lopez Linan, R, Gotuzzo, E, Guerra, H, Gilman, RH, and Vinetz, JM.** 2005. Clinical spectrum of

pulmonary involvement in leptospirosis in a region of endemicity, with quantification of leptospiral burden. Clin. Infect. Dis. **40 :** 343-351.

49. **Seshu, J, Esteve-Gassent, MD, Labandeira-Rey, M, Kim, JH, Trzeciakowski, JP, Hook, M, and Skare, JT.** 2006. Inactivation of the fibronectin-binding adhesin gene bbk32 significantly attenuates the infectivity potential of *Borrelia burgdorferi*. Mol. Microbiol. **59 :** 1591-1601.

50. **Shi, J, Scita, G, and Casanova, JE.** 2005. WAVE2 signaling mediates invasion of polarized epithelial cells by *Salmonella typhimurium*. J. Biol. Chem. **280,** 29849-29855.

51. **Thomas, DD, and Higbie, LM.** 1990. In vitro association of leptospires with host cells. Infect. Immun. **58 :** 581-585.

52. **Vendrame, F, Segni, M, Grassetti, D, Tellone, V, Augello, G, Trischitta, V, Torlontano, M, and Dotta, F.** 2006. Impaired caspase-3 expression by peripheral T cells in chronic autoimmune thyroiditis and in autoimmune polyendocrine syndrome-2. J. Clin. Endocrinol. Metabol. **91 :** 5064-5068.

53. **Verma, A, Hellwage, J, Artiushin, S, Zipfel, PF, Kraiczy, P, Timoney, JF, and Stevenson, B.** 2006. LfhA, a novel factor H-binding protein of *Leptospira interrogans*. Infect. Immun. **74 :** 2659-2666.

54. **Wann, ER, Gurusiddappa, S, and Hook, M.** 2000. The fibronectin-binding MSCRAMM FnbpA of *Staphylococcus aureus* is a bifunctional protein that also binds to fibrinogen. J. Biol. Chem. **275 :** 13863-13871.

55. **Werts, C, Tapping, RI, Mathison, JC, Chuang, TH, Kravchenko, V, Saint Girons, I, Haake, DA, Godowski, PJ, Hayashi, F, Ozinsky, A, Underhill, DM, Kirschning, CJ, Wagner, H, Aderem, A, Tobias, PS, and Ulevitch, RJ.** 2001. Leptospiral lipopolysaccharide activates cells through a TLR2-dependent mechanism. Nat. immunol. **2 :** 346-352.

56. **Xu, Q, Yan, B, Li, S, and Duan, C.** 2004. Fibronectin binds insulin-like growth factor-binding protein 5 and abolishes Its ligand-dependent action on cell migration. J. Biol. Chem. **279 :** 4269-4277.

57. **Yang, CW, Wu, MS, and Pan, MJ.** 2001. Leptospirosis renal disease. Nephrol Dialysis. Transplant. **16 Suppl 5 :** 73-77.

58. **Yang, CW, Wu, MS, Pan, MJ, Hsieh, WJ, Vandewalle, A, and Huang, CC.** 2002. The Leptospira outer membrane protein LipL32 induces tubulointerstitial nephritis-mediated gene expression in mouse proximal tubule cells. J. Am. Soc. Nephrol. **13 :** 2037-2045.

CHAPTER 3

A DOMAIN OF THE *LEPTOSPIRA* LIGB CONTRIBUTES TO HIGH AFFINITY BINDING OF FIBRONECTIN

Introduction

The interaction between bacteria and host cells is the first step in the establishment of a productive infection. Various bacterial adhesion molecules including afimbrial and fimbrial adhesins contribute to either extracellular colonization or invasion to the host cells [1]. Microbial surface components recognizing adhesive matrix molecules (MSCRAMM), defined to bind extracellular matrix (ECM) such as Fn, laminin, elastin, or collagen, is one of the strategies that bacterium uses to attach on the host cells [2]. In pathogenic *Leptospira* spp., it was also known that different ECMs within the host were bound by several MSCRAMM including a 36kDa Fn binding protein [3], a laminin binding protein (Lsa24) [11] and Lig proteins which bind to several receptors (Fn, laminin, collagen and fibrinogen) [4, 5].

Leptospiral immunoglobulin-like proteins, LigA, LigB and LigC possess 12, 13 and 12 immunoglobulin-like (Ig-like) domains, respectively, and these Ig-like domains is similar to some known bacteria adhesion proteins including intimin from *Escherichia coli* and invasin from *Yersinia pseudotuberculosis* [6-8]. Interestingly, the N-terminal 630 amino acids of LigA and LigB are identical, but the C-terminal amino acid sequences are only 34% similarity, while LigC is only about 38% identity to that of LigA and LigB (serovar Pomona) [14-15]. The expression of *ligA* and *ligB* is controlled by a key environmental signal, osmolarity to enhance the binding of

leptospira to host cells [9, 10]. These data indicated that Lig proteins may be pivotal virulence factors of pathogenic *Leptospira* spp.

In a previous study, we have identified two regions, LigBCen and LigBCtv, in the C-terminal of LigB which were able to bind to Fn [5]. The aim of the present study was to localize the binding site of LigBCen to Fn as fine as possible and we have identified a domain containing 152 amino acids of LigB with a strong binding affinity to N-terminal domain (NTD), gelatin binding domain (GBD) of Fn, fibrinogen and laminin.

Materials and Methods

Bacterial strains and Cell Culture

L. interrogans serovar Pomona (NVSL1427-35-093002) was used as previously described [11]. All experiments were performed with virulent, low-passage strains obtained by passage to golden syrian hamsters as previously described [16]. *Leptospires* were grown in EMJH medium at 30 ^{o}C for less than 5 passages and growth was monitored by dark-field microscopy. Madin-Darby canine kidney (MDCK) cells (ATCC CCL34^{TM}) were cultured in Dulbecco minimum essential medium (DMEM) containing 10% fetal bovine serum (GIBCO Laboratories, Grand Island, NY). Cells were grown at 37^{o}C in a humidified atmosphere with 5% CO_2.

Reagents and antibodies

Horseradish peroxidase (HRP)-conjugated goat anti-hamster antibody and HRP-conjugated goat anti-rabbit antibody were ordered from Zymed (San Diego, CA). FITC-conjugated goat anti-rabbit antibody, Alexa594-conjugated goat anti-hamster antibody, and Rabbit anti-GST antibody were obtained from Molecular Probe (Eugene,

OR). Hamster anti-*Leptospira* was previously prepared in our laboratory [11]. Human plasma fibronectin was purchased from GIBCO (Carlsbad, CA). N-terminal domain (NTD), gelatin binding domain (GBD), and N-terminal domain (70kDa, including NTD and GBD) of Fn, fibrinogen (F3879), laminin (L2020), type I (C7774) and type IV collagens (C5533) were ordered from Sigma-Aldrich (St. Louis, MO) and cell binding/DNA domain (CBD) and heparin binding domain-2 (Hep-2) of Fn were ordered from Chemicon International (Temecula, CA).

Plasmid construction and Protein purification

Constructs for the expression of Histidine-tag fused with LigBCen1 (amino acids 631-1013) was generated using the vector pQE30 (Qiagen, Alencia, CA)(Figure. 3.1A). Constructs for the expression of GST, GST fused with LigBCen2 (amino acids 1014-1165), and GST fused with of LigBCen3 (amino acids 1166-1417) were generated using the vector pGEX-4T-2 (Amersham Pharmacia Biotech, Piscataway, NJ) (Figure. 3.1A) . To perform the PCR reactions, the following forward and backward primers were utilized based on the *ligB* sequence [17]. These included LigBCen1 forward primer 5' GGATCCATTGCTGAAATTAAAAAT 3' and backward primer 5' AAGCTTTTAAGTGATTTTGCTCTT 3'; LigBCen2 forward primer 5' GGATCCACTGCGACTTACAAT 3' and backward primer 5' GTCGACTTAATTGGAACTATT 3'; LigBCen3 forward primer 5' GGATCCTTTATAGGACATTGT 3' and backward primer 5' GTCGACTTAGTTTCCTTTTAC 3'. Primers were engineered to introduce a *BamH*I site at the 5' end of each fragment and a stop codon followed by a *Sal*I site at the 3' end of each fragment. PCR products were sequentially digested with *BamH*I and *Sal*I and

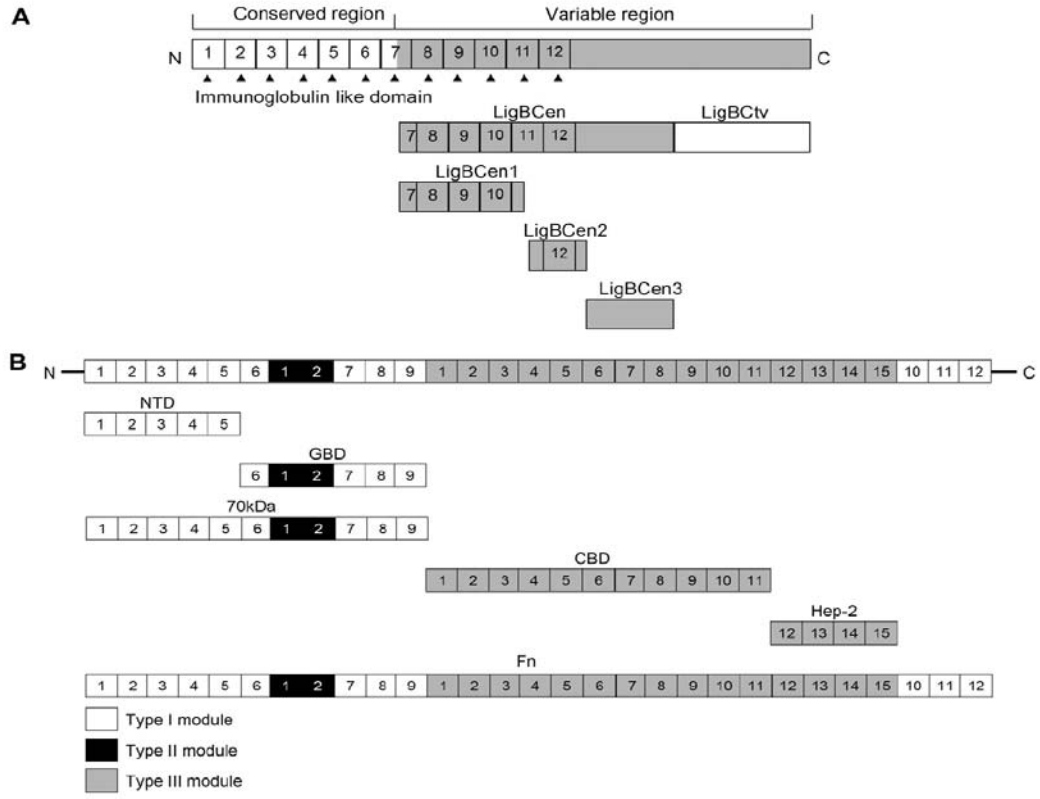

Figure. 3.1 (A) A schematic diagram showing the structure of LigB and the truncated LigB protein including LigBCen1, LigBCen2, and LigBCen3 used in this study. (B) A chart presenting the location of Fibronectin (Fn) and truncated Fn including N-terminal domain (NTD), Gelatin binding domain (GBD), 70kDa domain (70kDa), Cell binding domain (CBD), and Heparin binding domain 2 (Hep-2) used in this study.

then ligated into pQE30 or pGEX-4T-2 cut with *BamH*I and *Sal*I, respectively. In this study, we purified the soluble form of the histidine-tag fused with LigBCen1 and the GST fused with LigBCen2, and LigBCen3 from *E. coli* as previously described [11].

Isothermal Titration Calorimetry

The experiments were carried out with CSC 5300 microcalorimeter (Calorimetry Science Corp. Lindon, UT, USA) at 25℃ as previously described [5]. In a typical experiment the cell contained 1ml of a solution of LigBCen1, LigBCen2, or LigBCen3 and the syringe contained 250μl of a solution of full length Fn, N-terminal or gelatin binding domain of Fn at a concentration that was 20 times higher than the protein concentration in the cell. Both solutions were in phosphate based saline, pH 7.5. The titration was performed as follows: 25 injections of 10 μl (Table 3.1) with an stirring peed of 250rpm, and the delay time between the injections was 5min. Data were analyzed using Titration BindingWork 3.1 software (Calorimetry Science Corp. Lindon, UT, USA) fitting them to an independent binding model. The concentration of Fn and LigB used in this study was based on our preliminary dose titration experiment (data not shown).

Fn binding assays by ELISA

To determine the binding of LigBCen2 to full length Fn (positive control), N-terminal 70kDa region (70kDa), NTD, GBD, CBD, or Hep-2 of Fn (Figure. 3.1B), a series amounts (as indicated by Figure. 3.2. A) of full length Fn or Fn were coated on microtiter plate wells, incubated at 4^{o}C for 16 hours and blocked with blocking buffer (100 μl/well) containing 3% BSA in PBS at RT for 2 hours. Then, 10 nM of GST-LigBCen2 or GST in 100μL PBS was added onto microtiter plate wells for 1 hour at 37^{o}C.

For determination whether GBD and NTD have the same binding site on LigBCen2, 10nM GST-LigBCen2 or GST in 100μL PBS were incubated with a series concentration (0, 0.0625, 0.125, 0.25, 0.5, or 1μM) of GBD or NTD for 1 hour at 37^{o}C prior to be added to 100μl of 1μM NTD or BSA coated on microtiter plate wells. To evaluate the binding of LigBCen2 to other ECMs including full length Fn (positive control), fragments of Fn, laminin, or fibrinogen (Figure. 3.1B), a series amounts (as indicated by Figure. 3.3) of these ECMs were coated on microtiter plate wells incubated at 4^{o}C for 16 hours and blocked with blocking buffer (100 μl/well) containing 3% BSA in PBS at RT for 2 hours. Then, 10 nM of GST-LigBCen2 or GST in 100μL PBS was added into microtiter plate wells for 1 hour at 37^{o}C. BSA or GST with the same concentration was used in all experiments as a negative control through the study (data not shown).

To detect the binding of LigBCen2 to MDCK cells, MDCK cells (10^5) were incubated with 0, 1.25, 2.5, 5, or 10 nM of GST-LigBCen2 or GST (negative control) in 100 μl PBS for 1 hour at 37^{o}C. For measuring the binding inhibition of *Leptospira* to MDCK cells by LigBCen2, MDCK (10^5) cells were treated with 0, 1.25, 2.5, 5, or 10 nM of GST-LigBCen2 or GST (negative control) in 100 μl PBS for 1 hour at 37^{o}C prior to the addition of *Leptospira* (10^7) for 6 hours at 37^{o}C. To detect the binding of GST-LigBCen2 or GST, rabbit anti-GST (1:200x) and HRP-conjugated goat anti-rabbit IgG (1:1,000x) were used as primary and secondary antibodies, respectively. To measure the binding of *Leptospira*, hamster anit-*Leptospira* (1:200 x) and HRP-conjugated goat anti-hamster IgG (1:1,000 x) were used as primary and secondary antibodies, respectively. The percentage of attachment was determined relative to the attachment of serovar Pomona on untreated MDCK cells. After washing the plates thrice with PBST, (0.05% Tween 20 in PBS) 100μL of TMB (KPL, Gaithersburg, MD) was added to each well and incubated for 5 min. The reaction was stopped by adding

100µl of 0.5% hydrofluoric acid in each well. Each plate was read at 630nm by ELISA plate reader (Bioteck EL-312, Winoski, VT). Each value represents the mean ± SEM of three trials in triplicate samples. Statistically significant ($P<0.05$) differences are indicated by *.

Binding assays by Confocal Laser Scanning Microscopy (CLSM)

To determine the binding inhibition of *Leptospira* to MDCK cells by LigBCen2, 10^6 MDCK cell was treated by 50 nM of GST-LigBCen2 or GST (negative control) in 100 µl of PBS for 1 hour at 37°C prior to be added by 10^8 *Leptospira* for 6 hours at 37°C. Fixation and immunofluorescence staining were followed as previously described with slight modification [5]. Briefly, *Leptospira* and MDCK cells were fixed in 2% praformaldehyde for 60min at room temperature (RT). Fixed bacteria were incubated in PBS containing 0.3% BSA for 10min at RT. The primary and secondary antibodies in PBS containing 0.3% BSA were incubated sequentially for 60min at RT. For detecting the adhesion of *Leptospira* and the binding of GST-LigBCen2 or GST, rabbit anti-GST (1:250x) and hamster anti-*Leptospira* antibodies (1:250x) served as primary antibodies, and FITC conjugated goat anti-rabbit IgG (1:250x) and Alexa 594-conjugated goat anti-hamster IgG (1:250x) were used as secondary antibodies. The glass slides were mounted with coverslips using Prolong Antifade (Molecular Probe, Eugene, OR) viewed by Olympus Fluoview 500 confocal laser-scanning imaging system equipped with krypton, argon, and He-Ne lasers on an Olympus IX70 inverted microscope with a PLAPO 60X objective was used (Olympus, America, Inc., Melville, N.Y.). Confocal images were processed using Adobe Photoshop CS2 (San Jose, CA). The settings were identical for all captured images. For counting the attachment of *Lepotspira* to the MDCK cells, three fields were selected to count the number of binding organisms. All

studies were repeated three times and the attachment of *Leptospira* to MDCK cells was blindly counted which was statistically significant.

Statistical analysis

Significance between samples was determined using the Student's t-test following logarithmic transformation of the data. Two-tailed P-values were determined for each sample and a P-value <0.05 was considered significant. Each data point represents the meaṇ standard error of the mean (SEM) of sample tested in triplicate. An (*) indicates the result was statistically significant.

Results

LigBCen2, contributed to high affinity of Fn binding

To localize the Fn-binding site on central variable region of LigBCen, three truncated LigBCen including LigBCen1, LigBCen2 and LigBCen3 (Figure. 3.1A) were expressed and purified to apply to isothermal titration calorimetry (ITC) titrated by Fn. (Table 3.1). As shown on Table 3.1, the dissociation constant (K_d) for Fn binding to LigBCen1 and LigBCen2 were 7,200nM and 170nM, respectively. Binding of LigBCen3 was not detected by ITC (data not shown). The interaction appeared to be exothermic with a favorable enthalpy and unfavorable entropy. LigBCen2 showed stronger Fn binding affinity than LigBCen1.

NTD and GBD bind to LigBCen2

To determine whether LigBCen2 could bind to fragments of Fn, GST-LigBCen2 or GST (data not shown) were added to a series concentration of full length Fn and Fn fragments such as 70kDa, NTD, GBD, CBD, Hep-2, or BSA coated microtiter plate wells. As shown on Figure. 3.2A, LigBCen2 bound to 70kDa of Fn including NTD and

Table 3.1 Dissociation constant (K_d values) for the interaction of a range of truncated LigBCen with full length human Fn or NTD, GBD, or 70kDa from human Fn.

Truncated LigB	LigB Residues	K_d for the interaction with			
		Full length Fn	NTD	GBD	70kDa
		nM			
LigBCen1	631-1013	7200±170	[b]n/d	[b]n/d	[b]n/d
LigBCen2	1014-1165	170±20	272±25	1200±108	148±9
LigBCen3	1166-1417	[a]n/f	[b]n/d	[b]n/d	[b]n/d

[a]n/f, non-fittable

[b]n/d, not determined

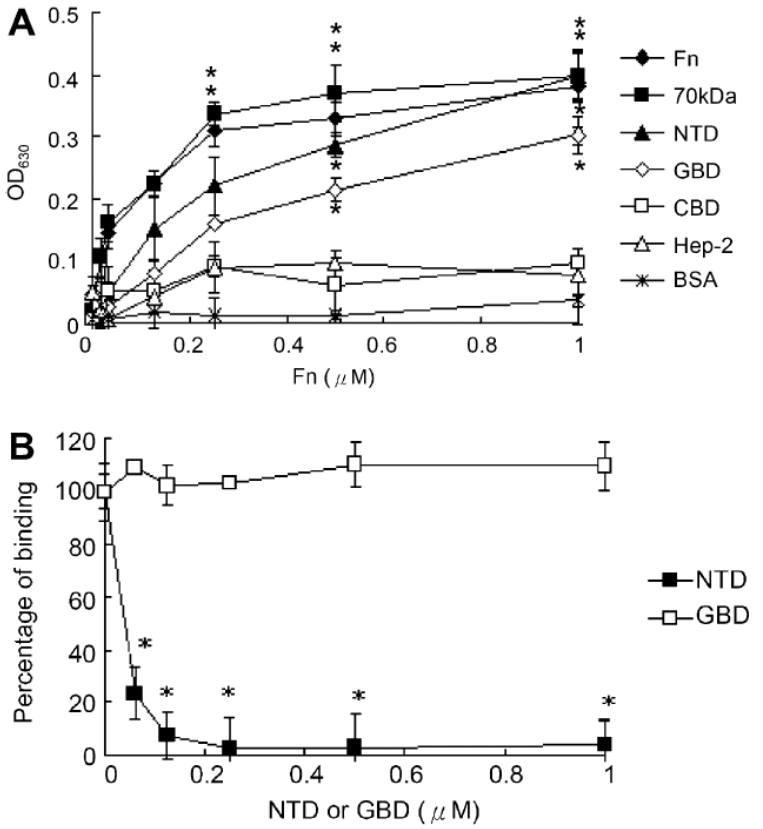

Figure. 3.2 NTD and GBD bind on LigBCen2 at different binding site (A). Binding of LigBCen2 to a series concentration of immobilized 70kDa, NTD, or GBD. Ten nM of GST-LigBCen2 and GST (negative control and data not shown) were added to different concentration of full length Fn, 70kDa, NTD, GBD, CBD, Hep-2, or BSA coated wells (negative control). Bound proteins were measured by ELISA. (B). GBD couldn't block the binding of LigBCen2 on immobilized NTD. Ten nM of GST-LigBCen2 and GST (negative control and data not shown) were pre-treated with different concentration of NTD or GBD prior to be added on NTD or BSA (negative control) coated wells. Bound proteins were measured by ELISA. The percentage of binding was determined relative to the binding of untreated LigBCen2 on NTD. Each value represents the mean± SEM of three trials in triplicate samples. Statistically significant ($P<0.05$) is indicted by *. In (B), the mean of the value obtained from the NTD-BSA or GBD-BSA coated wells subtracted from all other data points.

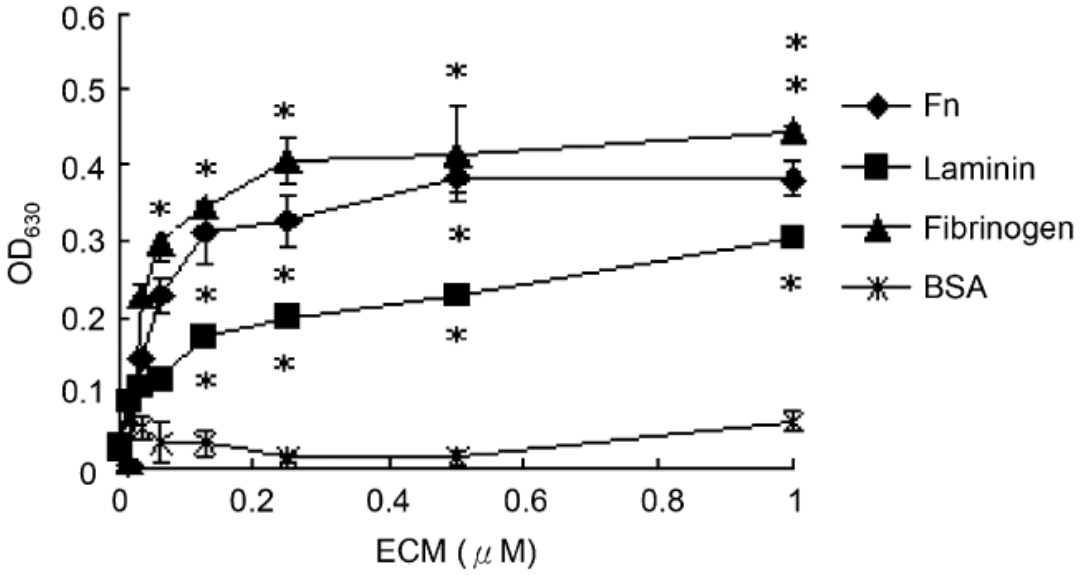

Figure 3.3 LigBCen2 bind to Fn, laminin, and fibrinogen. Ten nM of GST-LigBCen2 and GST (negative control and data not shown) were added to different concentration of full length Fn, laminin, fibrinogen, or BSA coated wells (negative control). Bound proteins were measured by ELISA. Each value represents the mean± SEM of three trials in triplicate samples. Statistically significant ($P<0.05$) is indicted by *.

GBD and full length Fn with high affinity than to that of NTD or GBD individually. However, LigBCen2 bound to NTD stronger than to GBD. The dissociation constant (K_d) for LigBCen2 binding to 70kDa, NTD, and GBD were 148nM, 272nM and 1,200nM, respectively (Table 3.1). This result was in agreement to our ELISA results (Figure. 3.2A). To reveal whether NTD and GBD bind to LigBCen2 on the same binding site, LigBCen2 were pre-treated with different concentrations of NTD, GBD or BSA (data not shown) prior to be incubated to NTD coated wells. As presented on Figure. 3.2B, pre-treatment of GBD could not reduce the binding of LigBCen2 on NTD and vice versa (data not shown). This result suggested that NTD and GBD bound to LigBCen2 on different binding site.

Laminin and fibrinogen also bind to LigBCen2

In order to reveal if there were other ECMs bind to LigBCen2, GST and GST-LigBCen2 were added into Fn, laminin or fibrinogen coated wells. As shown on Figure. 3.3, LigBCen2 was bound by Fn, laminin, and fibrinogen, and the binding to these ligands was dose dependent. We also performed the binding assays on type I or type IV collagen, but with negative results (data not shown).

LigBCen2 mediate the attachment of Leptospira to MDCK cells

To reveal whether LigBCen2 could bind on MDCK cells, a series amount of GST-LigBCen2 or GST were added to MDCK cells, and the binding of LigBCen2 to MDCK cells was detected by ELISA and immunofluorescence staining. Our results clearly showed that LigBCen2 bound to MDCK cells in a dose dependent manner (Figure. 3.4A). Pretreatment of MDCK cells with LigBCen2 approximately reduced the attachment of *Leptospira* by 45%. The reduction of *Leptospira* attachment was also

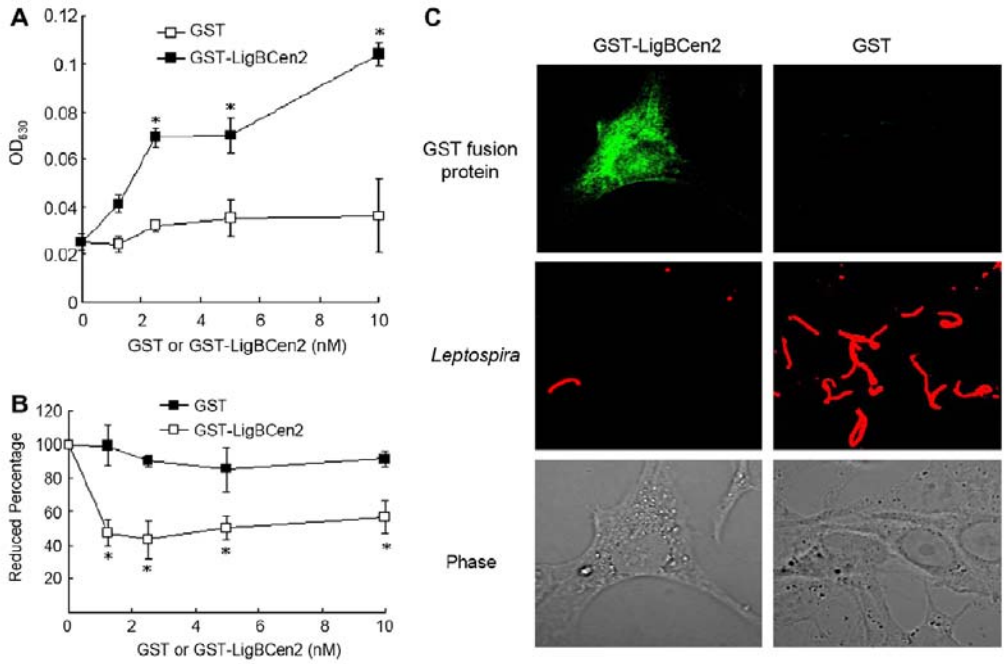

Figure. 3.4 Binding of LigBCen2 to MDCK cells reduces leptospiral adhesion. (A) Binding of LigBCen2 to MDCK cells. Different concentration of GST-LigBCen2 and GST (negative control) were added to MDCK cells. The binding of LigBCen2 to MDCK cells was measured by ELISA. (B) LigBCen2 inhibits the binding of *Leptospira* to MDCK cells. MDCK cells were pre-treated with different concentration of GST-LigBCen2 and GST (negative control) prior to be addition of *Leptospira*. The binding of *Leptospira* to MDCK cells was detected by ELISA. The reduced percentage of attachment was determined relative to the attachment of *Leptospira* on untreated MDCK cells. (C). LigBCen2 inhibits the binding of *Leptospira* to MDCK cells by CLSM. MDCK cells were pre-treated with 50nM of GST-LigBCen2 and GST (negative control) prior to be addition of *Leptospira*. The binding of *Leptospira* or LigBCen2 to MDCK cells was examined by CLSM. In (A) and (B), each value represents the mean± SEM of three trials in triplicate samples. Statistically significant ($P<0.05$) is indicted by *. In (C), the CLSM settings were identical for all the captured images. Images were processed using Adobe Photoshop CS2

dose dependent (Figure. 3.4B &C). Thus, LigBCen2 region may mediate the binding of *Leptospira* on MDCK cells.

Discussion

A pivotal factor for bacterial pathogenesis is the ability of the pathogenic organism to colonize host tissues. *Leptospira* spp. possess on their cell surface a number of MSCRAMMs [3-5, 12] that may promote the binding of the *Leptospira* to components of the host ECMs and play a pivotal role in leptospiral virulence. LigB, a *Leptospira* outer membrane protein proved to be an adhesin molecule, was reported to have significant Fn binding activities [4, 5]. LigB also showed sequence similarity with known bacteria adhesins, invasin from *Y. pseudotuberculosis* and intimin from *E coli* [13]. Moreover, both adhesins contained immunoglobin-like domain similar to LigB and interact with integrin, the receptor of host [14, 15]. The integrin binding site on the intimin was located on C-terminal 190 amino acids including its immunoglobulin like domain D3 and domain D4 [16], and the integrin binding site on the invasin was located on C-terminal 192 amino acids including an immunoglobulin like domain domain [13]. We truncated the LigBCen into three subconstructs, LigBCen1, 2 and 3. By using ITC, we found that LigBCen2 (containing 152 amino acids) could bind Fn with high affinity (Table 3.1).

It was recognized that LigB possess a strong Fn binding region on its immunoglobulin (Ig) like repeated motifs and a weaker Fn binding site on its c-terminal non-repeated region [4, 5]. To perform a further fine binding site mapping on LigB, LigCen was truncated into LigBCen1, 2 and 3 and we found that LigBCen2 could bind to both NTD and GBD of Fn, but with a higher affinity to NTD than to GBD (Figure. 3.2. A &Table 3.1). However, we are unable to identify a similar Fn-binding motif on LigBCen2 from other known Fn-binding proteins.

Lig proteins also bound to type 1 and type IV collagen, laminin and fibrinogen [4]. Therefore, it is important to determine whether LigBCen2 binds these ligands. In this study, we found that LigBCen2 also bound to laminin and fibrinogen, but not type I and type IV collagens (Figure. 3.3). This is not surprising since it has been reported that fibrinogen and elastin bound to the same region within the A domain of Fn binding protein A of *Staphylococcus aureus* [17]. The interaction with various ligands may enhance the binding of leptospires to host cells.

Since pathogenic *Leptospira* spp. adhere to renal tubular epithelial cells and induce severe tubulointerstitial nephritis leading to renal failure [18], it is possible that LigB is responsible for the binding of *Leptospira* to renal tubular epithelium by interacting with ECMs. Our results indicated that a region with 152 amino acid (LigBCen2) also bound (Figure. 3.4A and C) and blocked the binding of *Leptospira* on MDCK cells (Figure. 3.4B and C). These results could elucidate the region of LigB mediating the *Leptospira* adhesion on host cells.

REFERENCES

1. **G. E. Soto, and S. J. Hultgren,** 1999. Bacterial adhesins: common themes and variations in architecture and assembly, J. Bacteriol. **181**: 1059-1071.
2. **J. M. Patti, B. L. Allen, M. J. McGavin, and M. Hook,** 1994. MSCRAMM-mediated adherence of microorganisms to host tissues, Annu. Rev. Microbiol. **48:** 585-617.
3. **F. Merien, J. Truccolo, G. Baranton, and P. Perolat,** 2000. Identification of a 36-kDa fibronectin-binding protein expressed by a virulent variant of *Leptospira interrogan*s serovar icterohaemorrhagiae, FEMS Microbiol. Lett. **185:** 17-22.
4. **H. A. Choy, M. M. Kelley, T. L. Chen, A. K. Moller, J. Matsunaga, and D. A. Haake,** 2007. Physiological osmotic induction of *Leptospira interrogans* adhesion: LigA and LigB bind extracellular matrix proteins and fibrinogen, Infect. Immun. **75:** 2441-2450.
5. **Y. P. Lin, and Y. F. Chang,** 2008. The C-terminal variable domain of LigB from *Leptospira* mediates binding to fibronectin. J. Vet. Sci. **9:** 133-144.
6. **J. Matsunaga, M. A. Barocchi, J. Croda, T. A. Young, Y. Sanchez, I. Siqueira, C. A. Bolin, M. G. Reis, L. W. Riley, D. A. Haake, and A. I. Ko**, 2003. Pathogenic *Leptospira* species express surface-exposed proteins belonging to the bacterial immunoglobulin superfamily, Mol. Microbiol. **49:** 929-945.
7. **R. U. Palaniappan, Y. F. Chang, F. Hassan, S. P. McDonough, M. Pough, S. C. Barr, K. W. Simpson, H. O. Mohammed, S. Shin, P. McDonough, R. L. Zuerner, J. Qu, and B. Roe** 2004. Expression of leptospiral immunoglobulin-like protein by *Leptospira interrogans* and evaluation of its diagnostic potential in a kinetic ELISA, J. Med. Microbiol. **53:** 975-984.
8. **R. U. Palaniappan, Y. F. Chang, S. S. Jusuf, S. Artiushin, J. F. Timoney, S. P. McDonough, S. C. Barr, T. J. Divers, K. W. Simpson, P. L. McDonough, and H.**

O. Mohammed, 2002. Cloning and molecular characterization of an immunogenic LigA protein of *Leptospira interrogans*, Infect. Immun. **70:** 5924-5930.

9. **J. Matsunaga, M. Lo, D. M. Bulach, R. L. Zuerner, B. Adler, and D. A. Haake,** 2007. Response of *Leptospira interrogans* to Physiologic Osmolarity: Relevance in Signaling the Environment-to-Host Transition, Infect. Immun. **75:** 2864-2874.
10. **J. Matsunaga, Y. Sanchez, X. Xu, and D. A. Haake,** 2005. Osmolarity, a key environmental signal controlling expression of leptospiral proteins LigA and LigB and the extracellular release of LigA, Infect. Immun. **73:** 70-78.
11. **R. U. Palaniappan, S. P. McDonough, T. J. Divers, C. S. Chen, M. J. Pan, M. Matsumoto, and Y. F. Chang**, 2006. Immunoprotection of recombinant leptospiral immunoglobulin-like protein A against *Leptospira interrogans* serovar Pomona infection, Infect. Immun. **74:** 1745-1750.
12. **A. S. Barbosa, P. A. Abreu, F. O. Neves, M. V. Atzingen, M. M. Watanabe, M. L. Vieira, Z. M. Morais, S. A. Vasconcellos, and A. L. Nascimento**, 2006. A newly identified leptospiral adhesin mediates attachment to laminin, Infect. Immun. **74:** 6356-6364.
13. **J. M. Leong, R. S. Fournier, and R. R. Isberg,** 1990. Identification of the integrin binding domain of the *Yersinia pseudotuberculosis* invasin protein, Embo J. **9:** 1979-1989.
14. **R. R. Isberg, D. L. Voorhis, and S. Falkow,** 1987. Identification of invasin: a protein that allows enteric bacteria to penetrate cultured mammalian cells, Cell **50:** 769-778.
15. **A. E. Jerse, J. Yu, B. D. Tall, and J. B. Kaper,** 1990. A genetic locus of enteropathogenic *Escherichia coli* necessary for the production of attaching and effacing lesions on tissue culture cells, Proc. Natl.Acad. Sci. USA **87:** 7839-7843.

16. **M. Batchelor, S. Prasannan, S. Daniell, S. Reece, I. Connerton, G. Bloomberg, G. Dougan, G. Frankel, and S. Matthews**, 2000 Structural basis for recognition of the translocated intimin receptor (Tir) by intimin from enteropathogenic *Escherichia coli*, EMBO J. **19:** 2452-2464.

17. **F. M. Keane, A. Loughman, V. Valtulina, M. Brennan, P. Speziale, and T. J. Foster**, Fibrinogen and elastin bind to the same region within the A domain of fibronectin binding protein A, an MSCRAMM of *Staphylococcus aureus*, Mol. Microbiol. **63:** 711-723.

18. **C. W. Yang, M. S. Wu, and M. J. Pan,** 2001. Leptospirosis renal disease, Nephrol Dial Transplant 16 Suppl **5:** 73-77.

CHAPTER 4

CALCIUM BINDS TO LEPTOSPIRAL IMMUNOGLOBULIN-LIKE PROTEIN, LIGB AND MODULATES FIBRONECTIN BINDING

Introduction

Leptospira spp. are spirochetes including pathogenic species, *Leptospira interrogans* as well as saprophytic species, *Leptospira biflexa*. Leptospirosis, a zoonotic disease caused by *Leptospira* spp., is widely distributed in developing countries and has reemerged in the United States (1). The severe form of leptospirosis, Weil's syndrome, includes an acute febrile illness associated with multi-organ damage such as liver failure (jaundice), renal failure (nephritis), pulmonary hemorrhage and meningitis (2) with a mortality rate up to 15% if not treated (3). Several virulence factors of this organism have been identified including the sphingomyelinases, serine proteases, zinc-dependant proteases, collagenase (4), LipL32 (5), lipopolysaccharide (6), a novel factor H, laminin and Fn-binding protein (Lsa24 or Len) (7-9), Loa22 (10), and immunoglobulin-like proteins, Lig proteins (11-13).

Lig proteins include LigA and LigB, possess bacterial immunoglobulin-like (Big) domains with 90 amino acid repeats, have identical 630 amino acid residues at the N-terminal of LigA and LigB, but their C-terminals are variable (11-13). In addition, LigB also encodes a C-terminal, non-repeat domain with 771 amino acid residues (11, 12). LigA and LigB may serve as Microbial Surface Components Recognizing Adhesive Matrix Molecules that allow pathogenic *Leptospira* to bind to host extracellular matrix components such as Fn, fibrinogen, laminin, and collagen (14, 15). A high affinity Fn binding region of LigB, designated LigBCen2, contains 152 amino acids that include part of an immunoglobulin-like domain and a non-repeated region

(16). The expression of Lig proteins are regulated by osmolarity (17). Lig proteins may also serve as good vaccine candidates and/or diagnostic antigens (12, 18, 19).

Calcium plays a pivotal role in bacterial physiological activities such as cell cycle, cell division (20), competence (21), pathogenesis (22), signal transduction (23), motility and chemotaxis (24, 25). Apart from these functions, it is also known that host-pathogen interactions of some bacteria are affected by calcium (26, 27). Several types of calcium-binding regions have been identified which include EF-hand domain, leukotoxin or hemolysin-type calcium-binding domain (28, 29), and orphan motifs in which oxygen atoms provided by several charged glutamate or aspartate residues are used in ligation (30). Lig proteins do not contain any of the known Ca^{2+}-binding domains. However, LigBCen2 shows sequence similarity to the c-type lectin domain of other adhesins including invasin of *Yersinia pseudotuberculosis* and intimin of *Escherichia coli* (12).

Even though Lig proteins likely play a significant role in pathogenicity, little is known about the mechanisms of action of these Lig proteins. We undertook this study to identify novel properties of Lig proteins. Based on the structural homology of immunoglobulin-like fold with lens β -crystallins type Greek key motif (31), we wondered if Lig proteins would bind Ca^{2+}. We, therefore performed these studies and report that calcium binds to the high affinity Fn binding region of LigB, LigBCen2. Ca^{2+}-binding increases the stability of the protein and significantly influences the conformation of LigBCen2. Further, we demonstrate that Ca^{2+}-binding modulates the binding of LigB to NTD of Fn, suggesting that it has a significant role in bacterial infection.

Materials and Methods

Reagents and antibodies

Calcium Green^{TM}-1 was obtained from Molecular Probe (Eugene, OR). Fibronectin (human plasma fibronectin), NTD of Fn, ethylene glycol tetraacetic acid (EGTA), sodium chloride, sodium phosphate monobasic, sodium phosphate dibasic, and calcium chloride were from Sigma-Aldrich (St. Louis, MO).

Plasmid construction and Protein purification

The construct for the expression of Histidine-tag fused with LigBCen2 (amino acids 1014-1156) was generated using the vector pQE30 (Qiagen, Alencia, CA). Construction, expression, and purification procedures were as previously described (16, 19).

Inductively Coupled Plasma Optical Emission Spectrometry (ICP-OES)

Standard analysis procedures were performed by the Soil and Plant Laboratory, Cornell University to analyze the total mineral and heavy metal content by using ICP-OES (Varian, Inc., Palo Alto, CA). Prepared samples included fresh, phosphate buffered saline (PBS) and 70 μM of LigBCen2 either untreated or treated with 2 mM $CaCl_2$ or 5 mM EGTA, pH 7.0 for 1 hour at room temperature. Unbound calcium and EGTA were removed to trace levels (< 0.1 μg/ml) via dialysis against PBS buffer.

^{45}Ca overlay

Calcium-binding to protein was done by ^{45}Ca overlay method as described previously (32). Basically, 150-200 μg of protein was spotted onto a nitrocellulose membrane using a dot-blot apparatus. The membrane was rinsed three times in a solution containing 10 mM imidazole-HCl (pH 6.8), 60 mM KCl and 5 mM $MgCl_2$ for one hour and then incubated for 15 minutes at 25°C in the same buffer containing 1 mCi/liter of ^{45}Ca. The

membrane was then rinsed twice in 45% ethanol, blotted, dried and exposed to a phosphorimager screen. The signal was read in a PhosphorImager (Fuji Bas-1800).

Matrix Assisted Laser Desorption Ionization-Time of Flight (MALDI-TOF) mass spectrometry

The molecular weight of purified LigBCen2 protein was analyzed using MALDI-TOF mass spectrometer recorded on an Applied Biosystem 4700 Mass Spectrometer (Applied Biosystem. Foster City, CA). Prepared samples included 70 μM of LigBCen2 untreated or treated with 2 mM $CaCl_2$, pH 7, for 1 hour at room temperature. Unbound calcium was removed via dialysis against deionized water.

Energy Dispersive Spectrometry (EDS)

EDS analyses were performed with a JEOL 8900 Electron Probe Microanalyzer (JEOL, Ltd. Tokyo, Japan). The operating conditions were 10 kV acceleration voltages. Sample preparation was described as mentioned in the section 'MALDI-TOF mass spectrometry'. Water was removed by lyophilization (Labconco, Kansas City, MS) from all of the samples, and a powder form of each sample was applied to EDS.

Isothermal Titration Calorimetry (ITC)

The experiments were carried out with CSC 5300 microcalorimeter (Calorimetry Science Corp. Lindon, UT, USA) at 25°C as previously described (16). Before the ITC experiment, traces of calcium from LigBCen2 solution were removed via dialysis. In a typical ITC experiment, the cell contained 1 ml of a solution of $MgCl_2$ or $CaCl_2$ treated or untreated LigBCen2 and the syringe contained 250 μl of a solution of NTD, calcium chloride or magnesium chloride at a concentration that was indicated on table 4.2. Both solutions were in phosphate based saline (pH 7.5). The titration was performed as

follows: 25 injections of 10 µl with a stirring speed of 250 rpm, and the delay time between the injections was 5 minutes. Data were analyzed using Titration Binding Work 3.1 software (Calorimetry Science Corp. Lindon, UT, USA) fitting them to an independent binding model.

Differential Scanning Calorimetry (DSC)

Excess heat capacity $C_p(T)$ of LigBCen2 with or without $CaCl_2$ was measured using a DSC Q1000 microcalorimeter (Waters. New Castle, DE). Degassed samples containing 3 µM of LigBCen2 with or without 2 mM of $CaCl_2$ or buffer were heated at 10 K/h scan rate. Heat Capacity, Cp(T) data were recorded, corrected for buffer baseline, and normalized to the amount of the sample. The TA Universal Analysis software (Waters, New Castle, DE) was used for the data analysis and display. All calorimetric experiments in this study were repeated 3 times to ensure reproducibility.

Circular dichroism (CD) spectrometry

CD spectra were recorded on a Jasco J-815 spectropolarimeter under N_2 atmosphere at room temperature (25°C) in a 0.02 and 0.5 cm path length quartz cell for far- and near-UV respectively with 8 accumulations. Aliquots of calcium chloride solution were added to the protein solution and incubated for 5 minutes. All spectra were recorded in 50 mM Tris buffer, pH 7, containing 50 mM KCl. In a melting temperature experiments, 2 µM of LigBCen2 in the absence or presence of 2 mM $CaCl_2$ was subjected to thermal unfolding, and data were collected at 1°C/minute increments from 25°C to 70°C recording the ellipticity at 215 nm, with 30 seconds temperature equilibrations, followed by 30 second data averaging. In order to measure the melting point, a first order derivative was applied to the results from the melting experiment. In all CD

experiments, the background spectrum of buffer without protein was subtracted from the protein containing spectra.

Fluorescence Spectrometry

Fluorescence emission spectra were measured on a Hitachi F4500 spectrofluorometer (Hitachi. San Jose, CA). All spectra were recorded in correct spectrum mode of the instrument using excitation and emission band passes of 5 nm. The intrinsic Trp fluorescence of protein was recorded by exciting the solution at 295 nm and measuring the emission in the 300-400 nm regions. For calcium or magnesium titration, 0.1, 0.3, 0.5, 0.8, 1.0 mM of calcium chloride or magnesium chloride was mixed with 10 μM of LigBCen2 and spectra were recorded after 3 minutes. Calcium- or magnesium-saturated LigBCen2 protein was further titrated with magnesium or calcium, respectively and spectra were recorded as mentioned above, until saturation was reached.

For the ANS fluorescence experiment, ANS binding was checked by adding 100 μM ANS solution (10 mM stock in 100% methanol) to a protein solution (18 μM), incubated for two minutes and spectra were recorded between 400 and 600 nm. Next, LigBCen2 was treated with 100 μM EGTA or 100 μM $CaCl_2$, after that four titration of fibronectin (1 mg/ml), 0.5 μl each, was done, after 5 minutes of incubation and spectra were measured at an excitation wavelength of 295 nm.

In a calcium competition experiment, 20 μM of Calcium Green™-1 was mixed with or without 30 μM of LigBCen2 and 100 μl per well was dispensed into a micro titer plate and incubated with 0.1, 0.2, 0.4, 1, 2, 4, 10, 20, 40 μM of $CaCl_2$ in PBS pH 7.0 for 5 minutes. Enhanced fluorescence due to binding of free calcium and Calcium Green™-1 was monitored at 528 nm with excitation at 485 nm using a Synergy™ HT multi-detection micro plate reader (Bio-TEK instruments, Inc. Winooski, VT). The association constant, K_A, was deduced using Scatchard plot and rearrangement of the

Chang-Prusoff equation was used to calculate the dessociation constant (K_D) of LigBCen2 and calcium (33).

$$K_{app} = K_{Ddye}\left(1 + \frac{[LigBCen2]}{K_{DLigBCen2}}\right)$$

K_{app} is the apparent dissociation constant measured in the presence of a concentration of LigBCen2 in Calcium Green^{TM}-1 solution with calcium, K_{Ddye} or $K_{DLigBCen2}$ is the K_D of calcium with Calcium Green^{TM}-1 or LigBCen2. All spectra were recorded in the correct spectrum mode excitation and emission band passes of 5 nm each and corrected for volume changes before further analysis. All measurements were performed at 25ºC.

Fn binding assays by ELISA

To determine the binding of untreated or calcium treated LigBCen2 to NTD, a serial concentrations of NTD or BSA (negative reference) were coated on microtiter plate wells and blocked subsequently as previously described (16). 10 nM of untreated or 2 mM of $CaCl_2$ treated GST-LigBCen2 or GST in 100 µl PBS was added onto microtiter plate wells and incubated for 1 hour at 37°C.

To detect the binding of GST-LigBCen2 or GST, rabbit anti-GST (1:200x) and HRP-conjugated goat anti-rabbit IgG (1:1,000x) were used as primary and secondary antibodies, respectively (16). After washing the plates thrice with PBST, (0.05% Tween20 in PBS) 100 µl of TMB (KPL, Gaithersburg, MD) was added to each well and incubated for 5 min. The reaction was stopped by adding 100 µl of 0.5% hydrofluoric acid in each well. Each plate was read at 630 nm using an ELISA plate reader (Bioteck EL-312, Winoski, VT). Each value represents the mean ± SEM of three trials in triplicate samples. Statistically significant ($P<0.05$) differences are indicated by *.

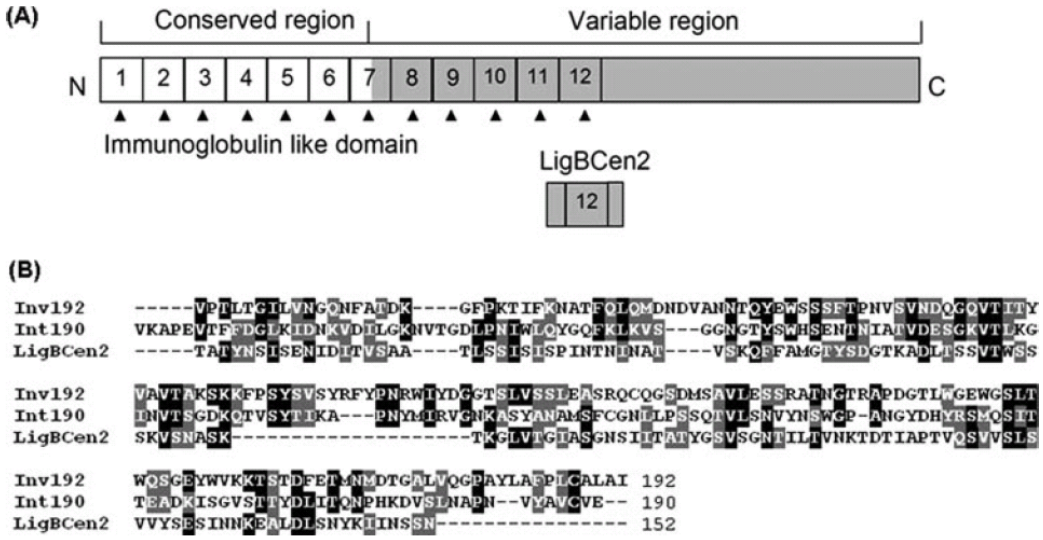

Figure 4.1 (A) Schematic representation of various domains and regions of LigB. Boxes 1-12 indicate various bacterial immunoglobulin-like domains. (B) Sequence alignment of LigBCen2 with C-type lectin like domain. Fn binding site and C-type lectin like domains (CTLD) of *L. interrogans* serovar Pomona LigB (LigBCen2), integrin binding site and CTLD of *Y. pseudotuberculosis* invasin (Inv192), and Tir binding site and CTLD of enteropathogenic *E. coli* intimin (Int190) were aligned, with gaps introduced to maximize the alignment. Black and gray colored residues indicated the conserved residues, and the homology was performed with EMBL-EBI ClustalW. (http://www.ebi.ac.uk/clustalw/)

Statistical analysis

Each data point represents the mean standard error of the mean (SEM) of sample tested in triplicate. Data were analyzed by Student's t test and statistically significant differences were claimed at p values < 0.05.

Results

The sequence of LigBCen2 is similar to C-type lectin domains of invasin and intimin

Previously, Lig proteins including LigA and LigB have been shown to bind to ECM (14, 15) and LigBCen2, the central region of LigB, annotated as LigBCen2 (Figure. 4.1A) was selected for further functional studies (16). The sequence was selected from amino acids 1014 to 1165 residue of LigB as seen in Figure. 4.1B. Interestingly, this region contains the bacterial Ig like (Big) domain and the non-repeat region of 46 amino acids (16). Proteins that contain this domain are found in a variety of bacterial and phage surface proteins such as intimins or invasins, which is a bacterial cell-adhesion molecule that mediates intimate bacterial host-cell interaction (34, 35). It contains three domains; two immunoglobulin-like domains and a C-type lectin-like module implying that carbohydrate recognition may be important in intimin-mediated cell adhesion. However, the exact functions of these proteins, barring some studies on fibronectin interactions, are not known (16).

Rationale of Ca^{2+}-binding

As mentioned above, nothing is known about the function of Lig proteins, except that they are thought to play a role in virulence or infection. We were, therefore, interested in identifying the functions of these important proteins. Structurally, these proteins belong

Table 4.1 The concentration of the metal ions detected by ICP-optical emission

	Ca	Mn	Co	Cu	Cd	Mg	Zn
LigBCen2 with Ca^{2+}	4.505 μg/mL	below[a]	below[a]	below[a]	below[a]	below[a]	below[a]
LigBCen2 with EGTA	below[a]	below[a]	below[a]	below[a]	below[a]	below[a]	below[a]
LigBCen2	below[a]	below[a]	below[a]	below[a]	below[a]	below[a]	below[a]

[a]below, the concentration below 0.1 μg/mL

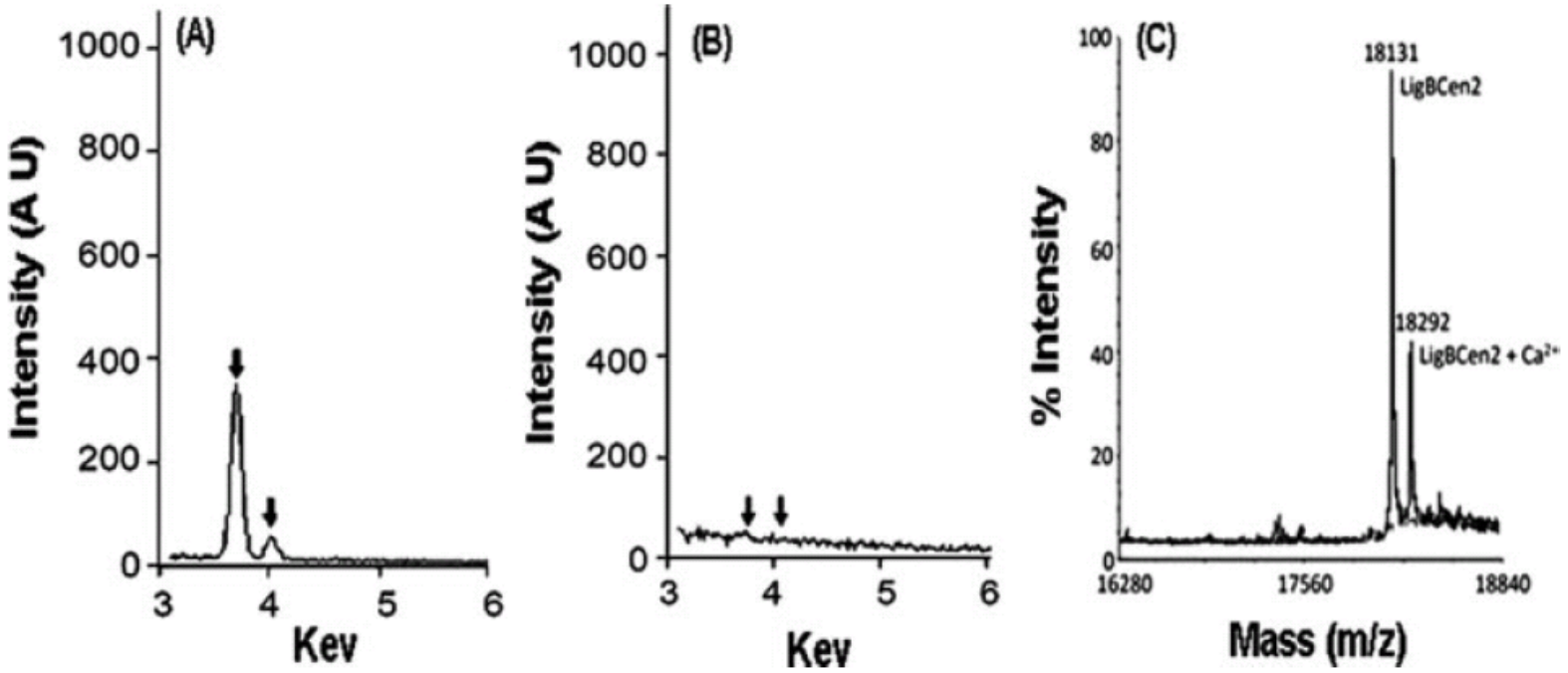

Figure 4.2 Ca^{2+}-binding characterized by EDS and MALDI-TOF mass spectroscopy. EDS analysis of the lyophilized (A) calcium-treated LigBCen2 or (B) untreated LigBCen2. Arrows indicate the locations of signal for calcium. The live time and accumulative voltage were 60 seconds and 10 kV respectively. (C) MALDI-TOF mass spectra of LigBCen2 in the absence (LigBCen2) or presence (LigBCen2 + Ca^{2+}) of 1 mM of $CaCl_2$. The number indicated on the peaks represents the molecular weight of LigBCen2.

to the immunoglobulin fold also called the bacterial immunoglobulin (BIG) fold. In one of the earlier studies, the structural and functional similarities were assessed between various proteins of Greek key/immunoglobulin fold (31). Among the proteins selected for functional prediction, lens γ-crystallins and immunoglobulin functions were chosen. It is important to mention that both proteins possess the Greek key type fold (31). This prompted us to look for the function of Lig proteins in the context of lens γ-crystallins. The exact function of lens γ-crystallins is not known. However, we have shown earlier that β -crystallins belong to a different family of low affinity Ca^{2+}-binding proteins (36, 37). Based on the fold similarities, we predicted that these Lig proteins might bind Ca^{2+}. Therefore, we assessed Ca^{2+}-binding to LigBCen2 by a number of methods as described below.

Probing of Ca^{2+}-binding to LigBCen2 by ICP-OES, EDS, ^{45}Ca overlay and MALDI-TOF mass spectrometric analysis

Since there is no known motif in LigBCen2 for Ca^{2+}-binding, it was necessary to probe Ca^{2+}-binding by a number of methods to examine the specificity of Ca^{2+} binding. First, we probed Ca^{2+}-binding to LigBCen2 by ICP-OES. Untreated or EGTA or calcium chloride treated LigBCen2 were applied to ICP-OES. As shown in Table 4.1, calcium was found only in calcium chloride treated LigBCen2, and not in untreated or EGTA treated LigBCen2. The results indicate that calcium binds to LigBCen2 since there was no Ca^{2+}-binding to EGTA treated or untreated LigBCen2. To further confirm the Ca^{2+}-binding activity revealed by ICP-OES, Ca^{2+}-binding to LigBCen2 was assessed by EDS. As seen in Figure. 4.2(A) and 2(B), a prominent calcium signal was seen in Ca^{2+}-bound LigBCen2 instead of the apo form of LigBCen2. We also performed ^{45}Ca binding to LigBCen2 using a well known method of overlay (38). Seen as a dark spot on the membrane, radioactive calcium ^{45}Ca binds to LigBCen2, thereby confirming the

Table 4.2 Dissociation constant (K_d values) for the interaction of calcium or magnesium and LigBCen2 in the presence or absence of 2 mM calcium chloride or magnesium chloride.

[LigBCen2] mM	[$CaCl_2$] mM	[$MgCl_2$] mM	ΔH kcal mol^{-1}	ΔS cal mol^{-1} K^{-1}	K_D μM	n
0.03	1	-	-0.73±0.03	-0.02	6.09±0.1	3.75±0.1
0.02[a]	0.48	-	-80.43±9.59	-0.24	5.34±0.9	4.04±0.1
0.02	-	0.42	-244.42±57.7	-0.79	9.17±0.2	1.05±0.05
0.02[b]	-	0.20	-63.38±4.13	-0.18	8.64±0.2	1.37±0.1

[a] in the presence of 2 mM magnesium chloride.

[b] in the presence of 2 mM calcium chloride.

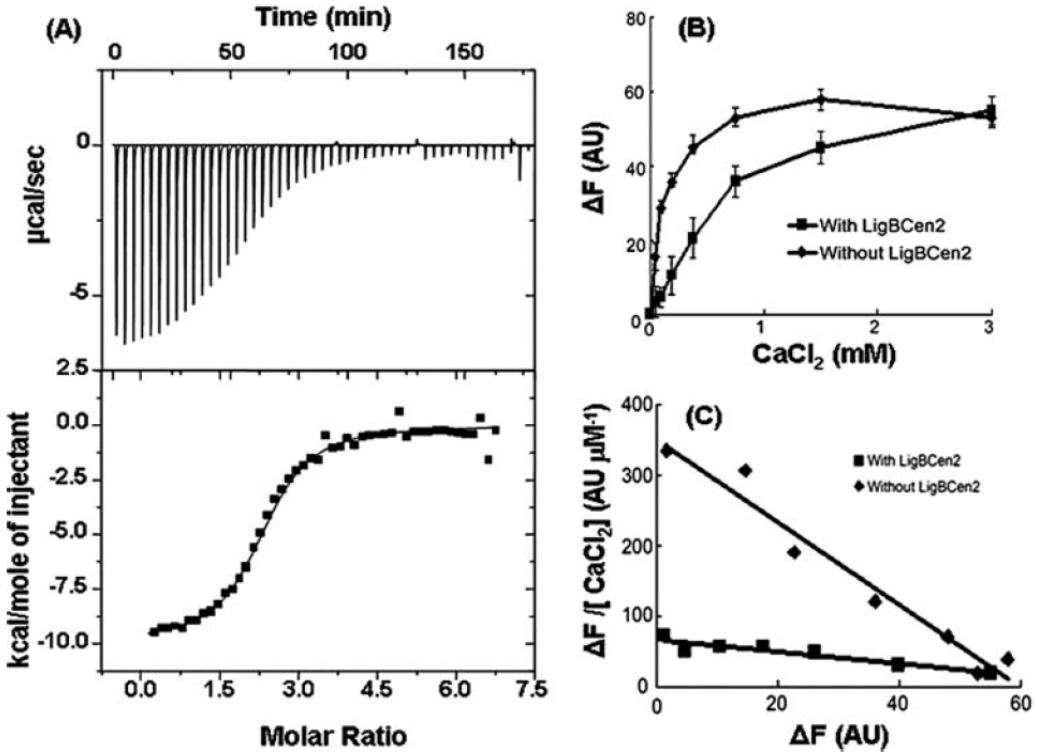

Figure 4.3 Stoichiometry of Ca^{2+} binding. (A) Binding affinity determined by the ITC profile of LigBCen2 with calcium chloride. Data of heat change obtained with ligand (Ca^{2+}) titration shown in the upper panel. In the lower panel, the solid lines represent the best fits to a single-site binding model data after peak (■) integration, subtraction of blank titration data (not shown), and concentration normalization. Molar heats of binding are plotted vs the molar ratio of Ca^{2+} to protein. Binding potency of protein with ligand K_D is 7.5µM. The thermodynamic data that were obtained from ITC are shown in Table 4.2. (B) and (C) represent the competition experiment between Calcium Green^{TM}-1 interacting with calcium mixed with 30 µM of LigBCen2 or without LigBCen2. (B) The increase of fluorescence intensity as a function of calcium concentration. ΔF represents the difference in the values of the emitted spectra upon addition of various concentrations of calcium. (C) Scatchard plot for the calculation of association constant for Calcium Green^{TM}-1 binding by holo form of Ca^{2+}-boundLigBCen2 or with Ca^{2+} alone, rearrangement of the Chang-Prusoff equation

Figure 4.4 Conformational changes of LigBCen2 after addition of Ca^{2+} monitored by CD and fluorescence. (A) Far-UV CD spectra of LigBCen2 were recorded in presence of calcium. Protein concentration was 80 μg/ml in 50 mM Tris-HCl (pH 7.0) and 50 mM KCl. Spectra were recorded with a 0.02 cm path length cuvette. Aliquots of calcium chloride solution were added to a final concentration of 0, 50, 150, 250, 400 and 750 μM to the protein solution and CD spectra recorded. (B) Near-UV CD spectra of LigBCen2. Protein concentration of 1 mg/ml in buffer containing 50 mM Tris-HCl (pH 7.0) and 50 mM KCl was used in a 0.5 cm pathlength cuvette. Calcium chloride was added to the final concentrations of 150, 400, 500 and 750 μM. Direction of arrows indicates increasing order of calcium addition. (C) Intrinsic fluorescence spectrum of LigBCen2 in the presence and absence of Ca^{2+}. 10 μM of LigBCen2 in 50 mM Tris (pH 7.0), 50 mM KCl and 1 mM DTT was excited at 295 nm. The figure shows Trp fluorescence in the presence of 0, 0.1, 0.3, 0.5, 0.8 and 1.0 mM of calcium. (D) Fluorescence emission spectra of ANS-LigBCen2 complex in the presence of 0, 0.1, 0.2, 0.3, 0.4, 0.5, 0.7, and 1.0mM of calcium chloride. The excitation wavelength was set at 375 nm. The buffer consisted of 50 mM Tris (pH 7.0), 50 mM KCl and 1 mM DTT.

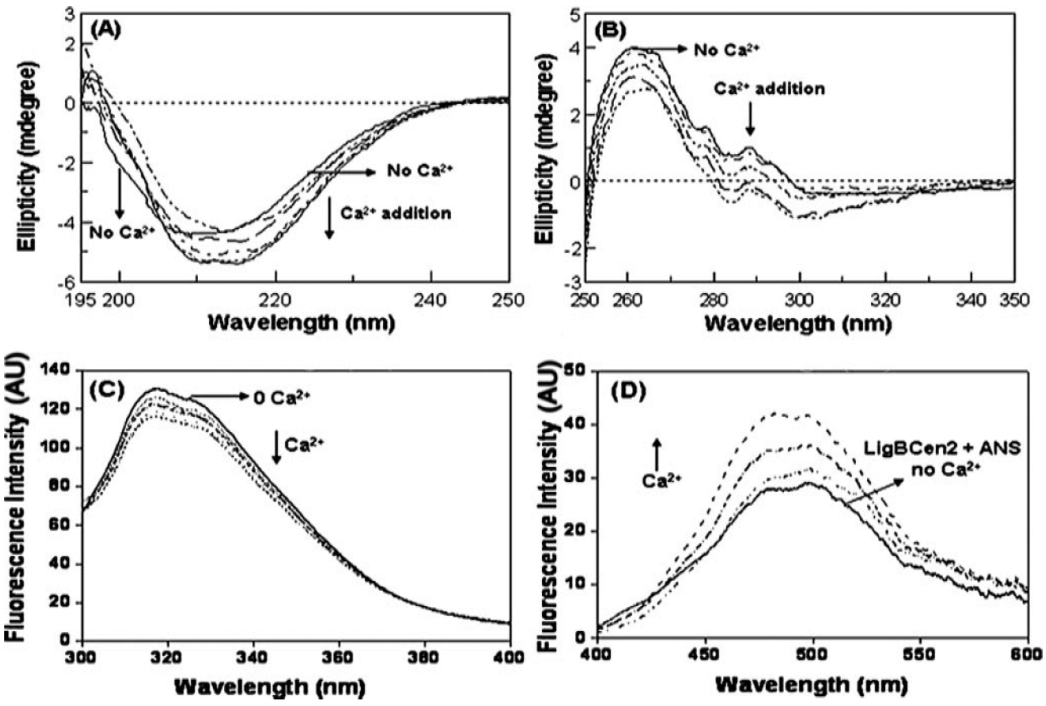
(A)
Ellipticity (mdegree)
Wavelength (nm)
No Ca2+
Ca2+ addition
No Ca2+
(B)
Ellipticity (mdegree)
Wavelength (nm)
No Ca2+
Ca2+ addition
(C)
Fluorescence Intensity (AU)
Wavelength (nm)
0 Ca2+
Ca2+
(D)
Fluorescence Intensity (AU)
Wavelength (nm)
Ca2+
LigBCen2 + ANS
no Ca2+

specificity of Ca^{2+}-binding to the protein (Figure. 4.2C). Further, the molecular weight of holo form of LigBCen2 (LigBCen2 + Ca^{2+} in Figure. 4.2D) is higher (18,292 Da) than that of apo form of LigBCen2 (18,131 Da) (LigBCen2 in Figure. 4.2D) further indicating that calcium binds to LigBCen2 (Figure. 4.2D). Since there was a 161 Da difference in the molecular weight between holo and apo forms, it is likely that at least four Ca^{2+} molecules were bound to LigBCen2. (see materials and methods) was used to obtain the K_D of calcium and LigBCen2 (K_d = 6.01 ± 0.2 μM).

Stoichiometry of Ca^{2+}-binding to LigBCen2 by ITC

The above results of mass spectroscopy and ^{45}Ca binding demonstrate that LigBCen2 is a Ca^{2+}-binding protein. We next assessed the affinity and stoichiometry of the Ca^{2+}-binding to LigBCen2 by ITC. To measure the Ca^{2+}-binding affinity to LigBCen2 quantitatively, a titration of calcium chloride to LigBCen2 was performed by ITC (Figure. 4.3A and 3B). As shown in Table 4.2, the dissociation constant (K_D) for calcium binding to LigBCen2 was 6 μM. The binding appeared to be an exothermic reaction with a favorable enthalpy and unfavorable entropy. Next, we examined if LigBCen2 also binds Mg^{2+}. As presented in Figure. 4.3C, 4.3D, and Table 4.2, Mg^{2+} also binds to LigBCen2 (K_D = 9 μM) (Figure. 4.3). We also examined if Mg^{2+} can replace Ca^{2+} using ITC. We did not see any competition of Mg^{2+} to replace Ca^{2+} bound to LigBCen2, which is possibly due to higher affinity of LigBCen2 for Ca^{2+} than Mg^{2+}. (Table 4.2)

Ca^{2+} and Calcium Green dye competition experiments

A calcium competition experiment using the dye, Calcium Green™-1 was performed to quantitatively confirm the binding of calcium to LigBCen2. When calcium chloride was added either to the dye or dye mixed with LigBCen2, the fluorescence was significantly

reduced, indicating that LigBCen2 was able to compete with the dye by binding calcium (Figure. 4.4A). The binding data were plotted using Scatchard plot (Figure. 4.4B) and analyzed by Rearrangement of the Chang-Prusoff equation. K_D of calcium-binding to LigBCen2 was calculated as 6 μM. The K_d value thus obtained was close to that calculated from ITC (K_d = 6 μM, Table 4.2).

Conformational studies of Ca^{2+} binding to LigBCen2

Ca^{2+} binding influences the secondary and tertiary structure monitored by circular dichroism

In the far-UV CD spectrum of the apo form of LigBCen2, a broad negative peak at 215-208 nm is seen (Figure. 4.5A), suggesting that LigBCen2 is largely in a β-sheet conformation. However, the cross over point is below 200 nm suggesting that the protein is partially unstructured. Addition of Ca^{2+} increases the negative value of ellipticity as well as red shift the cross over points suggesting that upon binding Ca^{2+}, the protein is folded and gains more β-sheet conformation (Figure. 4.5A).

Near-UV CD of LigBCen2 is shown in Figure 5B. There are one Trp, five Tyr and two Phe in this protein domain. In the near-UV CD, there are distinct bands (peaks) at 288 and 278 nm with a broad but strong peak at about 258-266 nm. The strong ellipticity of this peak (258-266 nm) suggests that Phe residues are either immobilized or interacting with neighboring residues. Two peaks at 288 and 292 nm represent the ^1L_b bands of Trp, whereas the peak at 278 is due to Tyr. Addition of Ca^{2+} brings significant changes in the near-UV CD spectrum (Figure. 4.5B). The ellipticity decreases over the entire range and a band for Trp transition appeared at about 302 nm, and some bands (at 288 and 302) becomes negative in Ca^{2+} bound protein. These data suggest that Ca^{2+} binding imparts significant changes in the protein conformation.

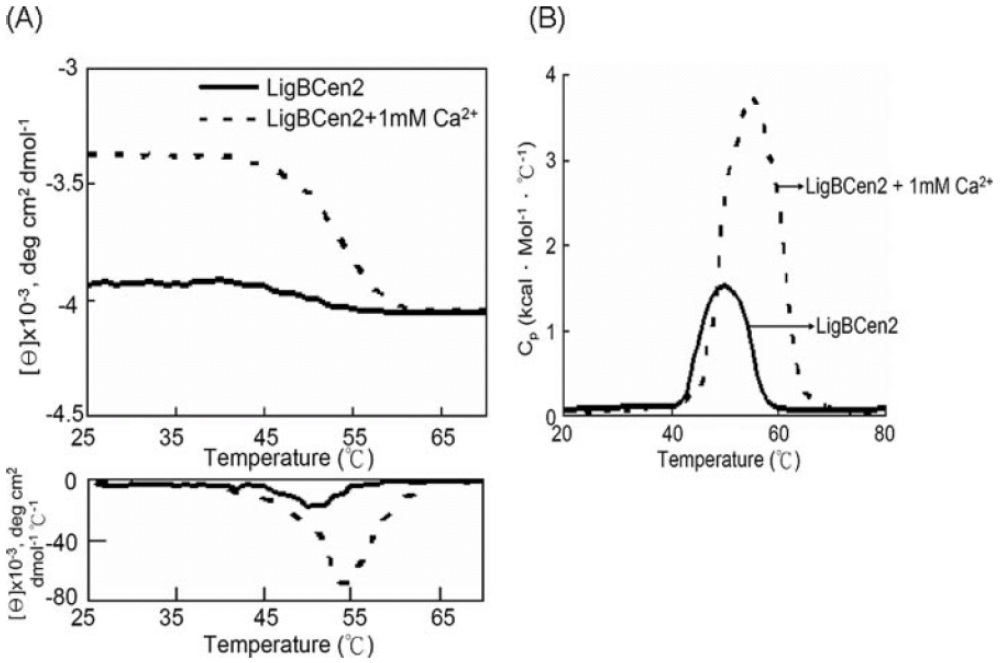

Figure 4.5 Thermal stability measured by CD and DSC. (A) Thermal unfolding transitions of apo and holo forms of LigBCen2 monitored by CD. Unfolding of 2 μM of LigBCen2 either in the presence of 1 mM calcium chloride or absence was followed by CD, measuring ellipticity at 215 nm from 25 to 70°C. A transition point was obtained found in both apo- and holo-proteins. The melting temperatures were determined by the location of the peak in the plot of the derivative of ellipticity versus temperature. The midpoints of transitions for apo and holo proteins are 50.7 ± 0.9°C and 54.8 ± 0.5°C respectively. (B) Molar heat capacity [kcal/(mol.K)] was plotted against the temperature (°C) for thermal denaturation of 3 μM of LigBCen2 in the absence or in the presence of calcium chloride (1 mM) was monitored by DSC. Transitions occur with midpoint temperatures of 50.02 ± 0.34°C and 55.71 ± 0.88°C for apo and holo proteins respectively.

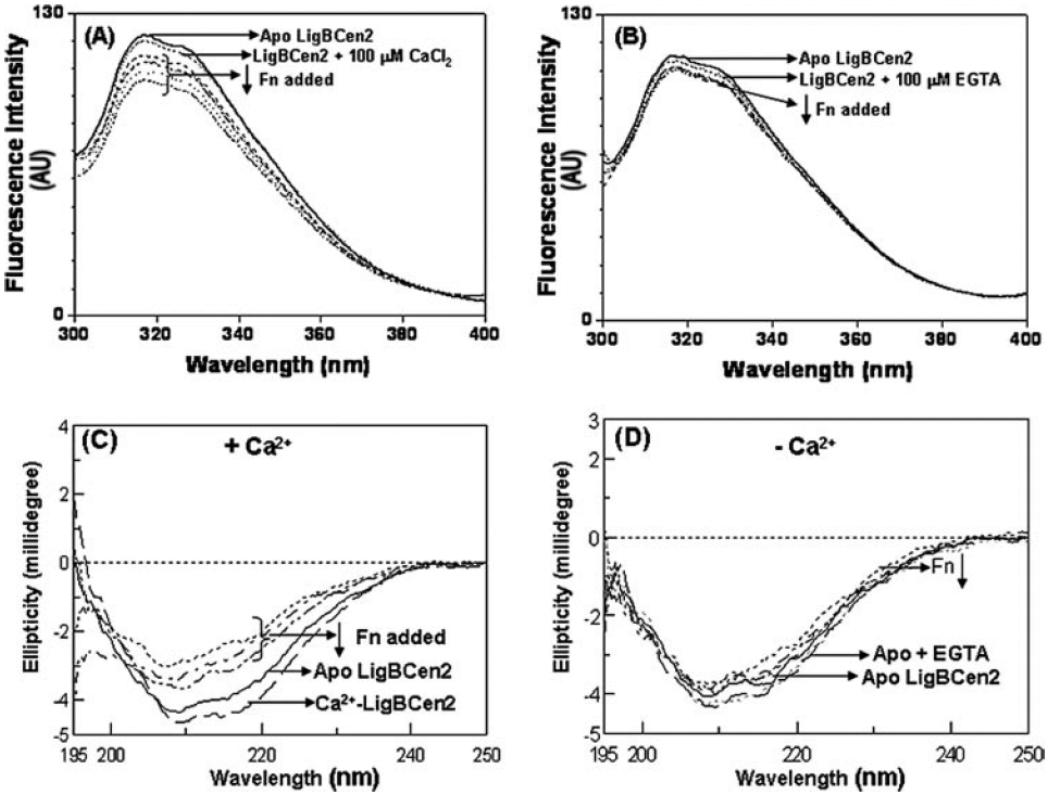

Figure 4.6 Calcium influences the interaction of LigBCen2 with NTD of fibronectin, monitored by fluorescence and CD. (A) Titration of NTD of Fn with LigBCen2 in the presence of Ca^{2+}. Decrease in fluorescence intensity was observed after addition of 0.5, 1.0, 1.5 and 2.0 µg of NTD (1 mg/ml) to LigBCen2 (10 µM) in the presence of 500 µM calcium chloride. (B) Similar experiment in the presence of 100 µM EGTA (in the absence of Ca^{2+}) (C) Far-UV CD spectra of LigBCen2 with NTD of Fn in the presence, or (D) in the absence of calcium. 0.5, 1.0, 1.5 and 2.0 µl of 1 mg/ml NTD was incubated

Ca^{2+} binding influences the fluorescence spectra of LigBCen2

Intrinsic Trp fluorescence of LigBCen2 is unusual in the sense that it shows a doublet or two peaks at 318 and 328 nm in its emission spectra (Figure. 4.6). Maximum emission by Trp fluorescence is seen at 318 nm suggesting that this single Trp is buried in a highly hydrophobic core of the protein. This unique phenomenon is rarely observed in with LigBCen2 for 15 minutes along with either 250 μM $CaCl_2$ or 100 μM EGTA and spectra were recorded using 0.2 mm path length cuvette. proteins but has been documented in -crystallin (39) and RNaseP (40) In the case of RNaseP, it has been demonstrated that the emission doublet is due to the hydrophobic interaction of Trp with two Phe residues in the excited state (40). Therefore, in case of LigBCen2, it appears that hydrophobic interaction among the lone Trp60 and two Phe residues at positions 41 and 42 can form a complex when excited. When titrated with Ca^{2+}, fluorescence intensity decreases significantly (10-15% decrease at 318 nm) suggesting that upon binding Ca^{2+}, there are conformational changes in the protein and Trp moves towards a more non-polar environment.

We also examined the influence of Mg^{2+} on LigBCen2 conformation. As seen in Figure. 4.6B, addition of Mg^{2+} decreases the Trp fluorescence in the same way as Ca^{2+} suggesting that upon binding Mg^{2+}, the protein undergoes conformational changes. Mg^{2+}-saturated LigBCen2 was further titrated with Ca^{2+}. Ca^{2+} was able to induce further changes in the fluorescence emission spectra of Mg^{2+}-saturated protein (Figure. 4.6C), suggesting that Ca^{2+} is able to replace Mg^{2+} owing to higher affinity. The surface hydrophobicity of LigBCen2 was assessed by ANS binding. There was a weak fluorescence emission suggesting that the protein is largely hydrophilic and binds ANS very weakly. In order to further characterize if there is any change in hydrophobicity upon Ca^{2+}-binding, the ANS-LigBCen2 complex was titrated by Ca^{2+}. There was an

Figure 4.7 Ca^{2+} influence Fn binding to LigBCen2 analyzed by near-UV CD, ELISA and Stains-all (A) Near-UV CD spectra of LigBCen2 and NTD in the presence of 250 μM $CaCl_2$. 0.5, 1.0, 1.5 and 2.0 μl of 1 mg/ml NTD was added to 0.5 mg/ml LigBCen2 in presence of 250 μM $CaCl_2$ and CD spectra were recorded and corrected for buffer and Fn. (B) Fn binding to LigBCen2 assayed by ELISA. Binding of GST-LigBCen2 or GST in the presence or absence of Ca^{2+} to varying concentrations (1.0, 0.5, 0.25, 0.12, 0.062, 0.037 μM) of immobilized NTD or BSA (negative control and data not shown). 10 nM of apo or holo GST-LigBCen2 or GST were added to a serial dilution of NTD or BSA coated wells. Bound proteins were estimated by ELISA. Each value represents the mean± SEM of three trials in triplicate samples. Statistically significant ($P<0.05$) is indicted by *. (C) and (D): The induced CD spectrum of the dye Stains-all (60μM) in 2 mM MOPS, pH 7.2 containing 30% ethylene glycol. 5 μM protein was incubated with dye for 10 min, (C) in presence of 200 M $CaCl_2$ and (D) in absence of $CaCl_2$ (presence of 100 μM EDTA), followed by addition of 0.5, 1.0 and 2 μl of NTD (1 mg/ml) to 1.6ml protein solution and CD spectrum recorded from 700 to 400 nm.

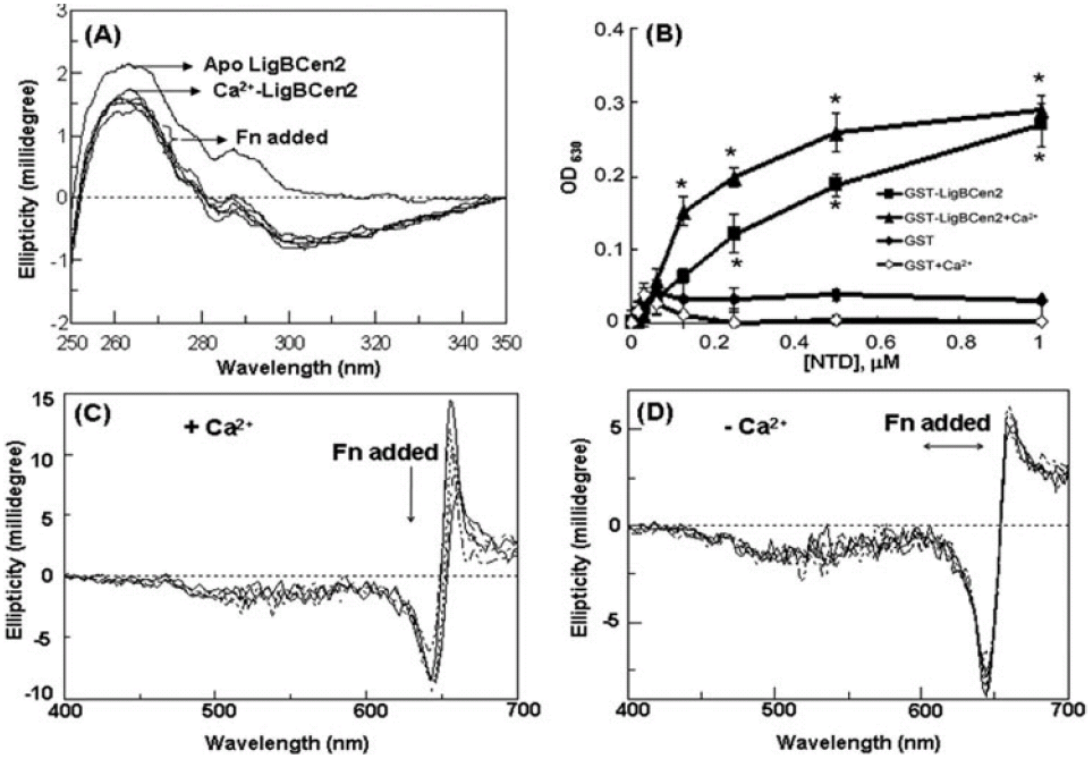
(A)
Apo LigBCen2
Ca2+-LigBCen2
Fn added
Ellipticity (millidegree)
Wavelength (nm)
(B)
OD 638
[NTD], μM
GST-LigBCen2
GST-LigBCen2+Ca2+
GST
GST+Ca2+
(C)
+ Ca2+
Fn added
Ellipticity (millidegree)
Wavelength (nm)
(D)
- Ca2+
Fn added
Ellipticity (millidegree)
Wavelength (nm)

increase in ANS binding intensity with a blue shift of about 4-5 nm suggesting that Ca^{2+} binding changes the surface hydrophobicity of the protein (Figure. 4.6D).

Ca^{2+} binding increases the conformational stability of LigBCen2

In order to gain more insight into the possible role of Ca^{2+} binding on protein stability, thermodynamic properties of thermal unfolding of LigBCen2, with or without calcium, were obtained by CD and DSC. The midpoint of unfolding was calculated by monitoring the change in ellipticity (in the CD) at 215 nm. As shown in Figure. 4.7A, the mid-point of LigBCen2 unfolding increased from 47.8 ± 1.2°C to 53.9 ± 0.8°C when Ca^{2+} was added. On the other hand, a shift in the midpoint of transition curves from 50.08 ± 1.05°C for apo-LigBCen2 to 55.00 ± 1.01°C for Ca^{2+}-bound LigBCen2 was also calculated by DSC (Figure. 4.7B). Taken together, these data indicate that Ca^{2+}-binding stabilizes the overall structure of LigBCen2 significantly.

Implications of Ca^{2+}-binding to the functions of LigBCen2

Our results confirm the hitherto unknown property of Ca^{2+}-binding by Lig proteins, whose functions are not yet fully understood. This is the first report confirming that a bacterial immunoglobulin domain is a Ca^{2+}-binding domain. We have recently shown that LigBCen2 binds strongly to the N-terminal domain (NTD), but very weak to the gelatin binding domain (GBD) of fibronectin (16). We, therefore studied if this binding is Ca^{2+}-dependent or is modulated by Ca^{2+}.

Calcium modulates NTD of fibronectin binding to LigBCen2

LigBCen2 possesses a high affinity Fn binding site and binds to the NTD of Fn (16). Since Ca^{2+}-binding stabilizes LigBCen2 conformation, we assayed for NTD binding to LigBCen2 by ELISA in the presence and absence of Ca^{2+}. As shown in Figure. 4.7A,

Table 4.3 Dissociation constant (K_d values) for the interaction of NTD of Fn and LigBCen2 in the presence or absence of calcium chloride.

Dissociation constant	LigBCen2 and Fn in the presence of $CaCl_2$	LigBCen2 and Fn in the absence of $CaCl_2$
K_D (nM)	85±2	272±25[a]

[a]reported previously (16)

holo-LigBCen2 binds the NTD more strongly than apo-LigBCen2. Similarly, the binding affinity of the NTD to holo-LigBCen2 was increased (K_d = 85 nM) compare to apo-protein (K_d = 272 nM) (Table 4.3) (16). These results suggest that Ca^{2+}-binding to LigBCen2 assists the interaction with the NTD of Fn.

Ca^{2+} influences the binding of LigBCen2 with fibronectin as monitored by fluorescence

It is known that LigBCen2 strongly binds to Fn (16). In order to determine if Fn binding to LigBCen2 is Ca^{2+}-dependent or independent, we performed Trp fluorescence titration of LigBCen2 by Fn in the presence or absence of Ca^{2+}. As seen in Figure 4.7B, there was a significant decrease in fluorescence (up to 20%) in performed in the presence of Ca^{2+}. There was an insignificant decrease when titration was performed in the absence of Ca^{2+}. These data suggest that Fn interaction with LigBCen2 depends on the presence of Ca^{2+}. In the absence of Ca^{2+}, there is only a weak interaction between these two proteins.

Fn binding to LigBCen2 monitored by CD

We monitored the binding of the NTD of Fn with LigBCen2 using far-UV CD. Varying concentrations of NTD were added to the LigBCen2 solution in the presence of Ca^{2+}. The spectra were corrected for the NTD signal by subtracting the appropriate blank as mentioned in the experimental section. Addition of NTD decreases the ellipticity to a great extent (Figure. 4.7C). The ellipticity in the region below 200 nm was more negative (as seen for a coiled protein) at the Lig:NTD ratio of about 1:2. When these experiments were performed in the absence of Ca^{2+} (in the presence of EGTA), the influence was comparatively very weak (Figure. 4.7C). It is interesting to note that there is no significant change in the tertiary structure upon binding NTD when monitored by

near-UV CD (Figure. 4.7D). Only minor changes were seen when the interaction was performed in the presence of Ca^{2+}. The above results suggest that the NTD of Fn influences the conformation of LigBCen2 significantly in the presence of Ca^{2+}.

Discussion

A number of studies on various Lig proteins have investigated their physiological roles and functions in pathogenicity still their functions and structural properties are not yet known (12, 13, 18, 19). This work was undertaken to understand the conformational and unique features of these proteins by which they are involved in pathogenesis. We for the first time, demonstrate a novel feature of Lig proteins, i.e., Ca^{2+}-binding. Since there is no known Ca^{2+}-binding motif in these proteins, this is a novel and significant finding. Furthermore, we demonstrate that Ca^{2+}-binding modulates the protein structures and the interaction of Lig with extra cellular matrix proteins, such as Fn.

LigB is a Ca^{2+}-binding protein

Our results confirm Lig proteins as a Ca^{2+}-binding protein despite the lack of a known Ca^{2+}-binding motif in these proteins such as an EF-hand motif, C2 domain or hemolysin-type motif (30). Besides these known motifs, some bacterial proteins also bind Ca^{2+} through oxygen atoms provided by several charged glutamate or aspartate residues (30). Interestingly, there are five Asp and three Glu residues present in the tandem repeats of LigBCen2. However, often these motifs are less well defined and not easy to specify because of the absence of structural data for these proteins. It appears that Lig has a novel, orphan Ca^{2+}-binding motif which needs to be identified. Taking into account the similarities between various Greek key motifs (31), we suggest that Lig proteins should have a motif for Ca^{2+}-binding similar to that seen in lens -crystallins (32). This motif is shown to bind Ca^{2+} in many proteins, such as Protein

S (41), spherulin 3a (42), caulollin (43), yersinia crystallins (44), though this motif still needs to be more clearly defined by structural studies on various diverse proteins. We suggest that a motif similar to that of -crystallins is present in LigB protein though it needs to be verified by structural means. Extensive structural studies to identify this motif and its comparison with crystallin-type Greek key motif are underway. There is a possibility that proteins of the Big domain would bind Ca^{2+}, thus forming a new family of Ca^{2+}-binding proteins.

LigBCen2 is partially unstructured in apo form

Significant changes in LigBCen2 conformation occur upon binding Ca^{2+}. It appears that this Lig domain is partially unstructured and folds upon binding Ca^{2+}. Similar results have been noted in some members of the lens βγ-crystallin superfamily, such as microbial crystallins (36, 43-44). Another similarity of LigBCen2 with -crystallin domain is the tendency of domain-domain interaction or homodimerization. There is a significant tertiary fold in apo-LigBCen2, suggesting that this protein is globally well folded. However, upon binding Ca^{2+}, there are significant changes in the tertiary structure of LigBCen2. These changes may differ those seen in many calcium sensors, such as neuronal calcium sensor-1 (45), since these sensors have poor tertiary structures in the apo form.

The concentration of calcium in *Leptospira* spp. infected hosts (*in vivo*) is generally higher than in the environment, and LigB is an essential virulence factor required by *Leptospira* spp. to infect the host (13). Thus, a higher concentration of calcium inside the host tissues is available to bind to LigB, which would fold the protein and increase its structural stability, and thus help in the protection of the bacterium. This also explains the fifty year old observation of Johnson and Gary (1963) about the absolute requirement of calcium and magnesium for the growth and survival of the bacterium

(46). This might explain how *Leptospira* spp. adapt and survive *in vivo* and highlights the importance of LigB for leptospiral infection.

Leptospirosis is intervened by Ca^{2+} via Lig proteins

We present a novel case of Lig interaction with Fn which is Ca^{2+} dependent. It has been reported that ClfA, a fibrinogen-binding MSCRAMM serving as a clumping factor of S*taphylococcus aureus*, has a Ca^{2+}-dependent inhibitory site for the interaction of ClfA and fibrinogen (47). However, in this case, Ca^{2+} was found to enhance the binding affinity of LigBCen2 to the NTD of Fn significantly. LigB has been shown to be an adhesin of *Leptospira* spp., and assists bacterial attachment to some ECMs including Fn to mediate their adhesion (15, 16). Thus, the increase of binding affinity of LigBCen2 to the NTD in the presence of Ca^{2+} indicates that the interaction between LigB and Fn would be stronger *in vivo* due to the presence and ever availability of calcium in the host. Thus *Leptospira* spp. would bind to Fn and other ECMs strongly or weakly to the infected host depending on the presence of calcium within the tissues. Therefore, we can readily propose a hypothetical but largely acceptable mechanism of infection involving Ca^{2+} and Lig proteins. Furthermore, our data suggest that these factors should be considered while designing optimum therapy for the treatment of leptospirosis, such as inclusion of calcium chelators, which might minimize the interaction between Lig and extracellular matrix proteins.

In conclusion, we demonstrate that LigB is a novel Ca^{2+}-binding protein which binds Ca^{2+} with high affinity. Ca^{2+}-binding stabilizes its structure, and influences its local as well as global conformation. This work would add one more class of bacterial Ca^{2+}-binding protein to list of proteins in bacteria (30). The physiological impact of this study is on the identification of Ca^{2+} as a factor for modulating Fn binding to LigB, and possibly with other ECMs, thus would have implications in pathogenesis. Our work

presents a case of a novel bacterial Ca^{2+}-binding protein, and would help in designing better therapy using calcium chelators for bacterial infection.

REFERENCES

1. **Levett, P. N.** Leptospirosis 2001 Clin. Microbiol. Rev. **14**: 296-326

2. **Faine, S. B., Adher, B., Bolin, C., and Perolat, P.** (eds). 1999 *Leptospira and Leptospirosis.*, MedSci, Medbourne, Australia

3. **Segura, E. R., Ganoza, C. A., Campos, K., Ricaldi, J. N., Torres, S., Silva, H., Cespedes, M. J., Matthias, M. A., Swancutt, M. A., Lopez Linan, R., Gotuzzo, E., Guerra, H., Gilman, R. H., and Vinetz, J. M.** 2005 Clinical spectrum of pulmonary involvement in Leptospirosis in a region of endemicity, with quantification of *Leptopsira* burden. Clin. Infect. Dis. **40**: 343-351

4. **Bulach, D. M., Zuerner, R. L., Wilson, P., Seemann, T., McGrath, A., Cullen, P. A., Davis, J., Johnson, M., Kuczek, E., Alt, D. P., Peterson-Burch, B., Coppel, R. L., Rood, J. I., Davies, J. K., and Adler, B.** 2006 Genome reduction in *Leptospira borgpetersenii* reflects limited transmission potential Proc. Natl. Acad. Sci. U S A **103**: 14560-14565

5. **Yang, C. W., Wu, M. S., Pan, M. J., Hsieh, W. J., Vandewalle, A., and Huang, C. C.** 2002 The *Leptospira* outer membrane protein LipL32 induces tubulointerstitial nephritis-mediated gene expression in mouse proximal tubule cells J. Am. Soc. Nephrol. **13**: 2037-2045

6. **Werts, C., Tapping, R. I., Mathison, J. C., Chuang, T. H., Kravchenko, V., Saint Girons, I., Haake, D. A., Godowski, P. J., Hayashi, F., Ozinsky, A., Underhill, D. M., Kirschning, C. J., Wagner, H., Aderem, A., Tobias, P. S., and Ulevitch, R. J.** 2001 Leptopsira lipopolysaccharide activates cell through a TLR2-dependent mechanism. Nat. Immunol. **2**: 346-352

7. **Barbosa, A. S., Abreu, P. A., Neves, F. O., Atzingen, M. V., Watanabe, M. M., Vieira, M. L., Morais, Z. M., Vasconcellos, S. A., and Nascimento, A. L.** 2006 A

newly identified *Leptospira* adhesin mediates attachment to laminin. Infect. Immun. **74**: 6356-6364

8. **Stevenson, B., Choy, H. A., Pinne, M., Rotondi, M. L., Miller, M. C., Demoll, E., Kraiczy, P., Cooley, A. E., Creamer, T. P., Suchard, M. A., Brissette, C. A., Verma, A., and Haake**, D. A. 2007 Leptospira interrogans endostatin-like outer membrane proteins bind host fibronectin, laminin, and regulators of complement. PLoS ONE **2**: e1188

9. **Verma, A., Hellwage, J., Artiushin, S., Zipfel, P. F., Kraiczy, P., Timoney, J. F., and Stevenson, B**. 2006. LfhA, a novel factor-H binding protein of Leptospira interrogans. Infect. Immun. **74**: 2659-2666

10. **Ristow, P., Bourhy, P., McBride, F. W., Figueira, C. P., Huerre, M., Ave, P., Girons, I. S., Ko, A. I., and Picardeau, M**. 2007. The OmpA-like protein Loa22 is essential for leptospiral virulence. PLoS Pathog. **3**: e97

11. **Matsunaga, J., Barocchi, M. A., Croda, J., Young, T. A., Sanchez, Y., Siqueira, I., Bolin, C. A., Reis, M. G., Riley, L. W., Haake, D. A., and Ko, A. I.** 2003 Pathogenic Leptospira species express surface-exposed proteins belonging to the bacterial immunoglobulin superfamily. Mol. Microbiol. **49**: 929-945

12. **Palaniappan, R. U., Chang, Y. F., Hassan, F., McDonough, S. P., Pough, M., Barr, S. C., Simpson, K. W., Mohammed, H. O., Shin, S., McDonough, P., Zuerner, R. L., Qu, J., and Roe, B.** 2004 Expression of leptospiral immunoglobulin-like protein by *Leptospira interrogans* and evaluation of its diagnostic potential in a kinetic ELISA. J. Med. Microbiol. **53**: 975-984

13. **Palaniappan, R. U., Chang, Y. F., Jusuf, S. S., Artiushin, S., Timoney, J. F., McDonough, S. P., Barr, S. C., Divers, T. J., Simpson, K. W., McDonough, P. L., and Mohammed, H. O.** 2002 Cloning and molecular characterization of an immunologic LigA protein of *Leptospira interrogans*. Infect. Immun. **70**: 5924-5930

14.**Choy, H. A., Kelley, M. M., Chen, T. L., Moller, A. K., Matsunaga, J., and Haake, D. A.** 2007 Physiological osmotic induction of *Leptospira interrogans* adhesion: LigA and LigB bind extracellular matrix proteins and firbrinogen. Infect. Immun. **75**: 2441-2450

15.**Lin, Y. P., and Chang, Y. F.** 2007 A domain of *Leptospira* LigB contribute to high affinity binding of fibronectin. Biochem. Biophys. Res. Commun. **362**: 443-448

16. **Lin, Y. P., and Chang, Y. F.** 2008 The C-terminal variable domain of LigB from *Leptospira* mediates binding to fibronectin. J. Vet. Sci. **9:**133-144.

17.**Matsunaga, J., Lo, M., Bulach, D. M., Zuerner, R. L., Adler, B., and Haake, D. A.** 2007 Response of *Leptospira interrogans* to physiologic osmolarity: relevance in signaling the environment-to-host transition. Infect. Immun. **75**: 2864-2874

18.**Palaniappan, R. U., McDonough, S. P., Divers, T. J., Chen, C. S., Pan, M. J., Matsumoto, M., and Chang, Y. F.** 2006 Immunoprotection of recombinant leptospira immunoglobulin-like protein A against Leptospira interrogans serovar Pomona infection. Infect. Immun. **74**: 1745-1750

19. **Faisal, S. M., Yan, W., Chen, C. S., Palaniappan, R. U., McDonough, S. P., and Chang, Y. F.** 2008 Evaluation of protective immunity of Leptospira immunoglobulin-like protein A (LigA) DNA vaccine against challenge in hamsters. Vaccine **26**: 277-287

20.**Yu, X. C., and Margolin, W.** 1997 Calcium-mediated GTP-dependent dynamic assembly of bacterial cell division protein FtsZ into polymer networks in vitro Embo J **16**: 5455-5463

21.**Trombe, M. C., Rieux, V., and Baille, F.** 1994 Mutation which alter the kinetics of calcium transport alter the regulation of competence in *Streptococcus pneumoniae*. J. Bacteriol. **176**: 1992-1996

22.**Straley, S. C., Plano, G. V., Skrzypek, E., Haddix, P. L., and Fields, K. A.** 1993 Regulation by calcium in *Yersinia* low-Ca^{2+} response Mol Microbiol **8**: 1005-1010

23.**Werthen, M., and Lundgren, T.** 2001 Intracellular calcium mobilization and kinase activity during acylated homoserine lactone-dependent quorum sensing in *Serratia liquefaciens* J. Biol. Chem. **276**: 6468-6472

24.**Tisa, L. S., and Adler, J.** 1992 Calcium ions are involved in *Escherichia coli* chemotaxis. Proc. Natl. Acad. Sci. U S A **89**: 11804-11808

25.**Tisa, L. S., and Adler, J.** 1995 Cytoplasmic free calcium level rises with repellents and falls with attractants in *Escherchia coli* chemotaxis. Proc. Natl. Acad. Sci. U S A **92**: 10777-10781

26.**Dardanelli, M., Angelini, J., and Fabra, A.** 2003 A calcium–dependent bacterial surface protein is involved in the attachment of rhizobia to peanut roots. Can. J. Microbiol. **49**: 399-405

27.**Izutsu, K. T., Belton, C. M., Chan, A., Fatherazi, S., Kanter, J. P., Park, Y., and Lamont, R. J.** 1996 Involvement of calcium in interactions between gingival epithelial cells and Porphyromonas gingivalis. FEMS Microbiol Lett **144**: 145-150

28.**Cruz, W. T., Young, R., Chang, Y. F., and Struck, D. K.** 1990 Deletion analysis resolves cell-binding and lytic domains of Pasteurella leukotoxin. Mol. Microbiol. **4**: 1933-1939

29.**Chang, Y. F., Shi, J., Ma, D. P., Shin, S. J., and Lein, D. H.** 1993 Molecular analysis of the Actinobacillus pleuropneumoniae RTX-toxin III gene cluster. DNA Cell Biol. **12**: 351-362

30.**Michiels, J., Xi, C., Verhaert, J., and Vanderleyden, J.** 2002 The functions of Ca2+ in bacteria: A role for EF-hand proteins? Trends Microbiol. **10**: 87-93

31.**Goode, D., and Crabbe, M. J.** 1995 Modelling molecular stability in gamma B crystallin. Comput. Chem. **19**: 65-74

32. **Rajini, B., Shridas, P., Sundari, C. S., Muralidhar, D., Chandani, S., Thomas, F., and Sharma, Y.** 2001. Calcium binding properties of gamma-crystallin: calcium ion binds at the Greek key beta gamma-crystallin fold. J. Biol. Chem. **276**: 38464-38471

33. **Cheng, Y., and Prusoff, W. H.** 1973 Relationship between the inhibition constant (K1) and the concentration of the inhibitor which causes 50 percent inhibition (I50) of an enzymatic reaction. Biochem Pharmacol **22**: 3099-3108

34. **Isberg, R. R., Voorhis, D. L., and Falkow, S.** 1987 Identification of invasion: a protein that allows enteric bacteria to penetrate cultured mammalian cells. Cell **50**: 769-778

35. **Jerse, A. E., Yu, J., Tall, B. D., and Kaper, J. B.** 1990. A genetic locus of enteropathogenic *Escherichia coli* necessary for the production of attaching and effacing lesions on tissue culture cells. Proc. Natl. Acad. Sci. U S A **87**: 7839-7843

36. **Jobby, M. K., and Sharma**, Y. 2007 Calcium binding to lens betaB2- and betaA3-crystallins suggests that all beta-crystallins are calcium-binding proteins. FEBS J. **274**: 4135-4147

37. **Rajini, B., Graham, C., Wistow, G., and Sharma, Y.** 2003 Stability, homodimerization, and calcium-binding properties of a single variant betagamma-crystallin domain of the protein absent in melanoma 1 (AIM1) Biochemistry **42**: 4552-4559

38. **Maruyama, K., Mikawa, T., and Ebashi, S.** 1984 Detection of calcium binding proteins by 45Ca autoradiography on nitrocellulose membrane after sodium dodecyl sulfate gel electrophoresis. J. Biochem. **95**: 511-519

39. **Piatigorsky, J.** 1984. Delta crystallins and their nucleic acids Mol Cell Biochem **59**: 33-56

40. **Gopalan, V., Baxevanis, A. D., Landsman, D., and Altman, S.** 1997 Analysis of the functional role of conserved residues in the protein subunit of ribonuclease P from *Escherichia coli.* J. Mol. Biol. **267**, 818-829

41. **Bagby, S., Harvey, T. S., Eagle, S. G., Inouye, S., and Ikura, M.** 1994 Structural similarity of a developmentally regulated bacterial spore coat protein to beta gamma crystallin of the vertebrate eye lens. Proc. Natl. Acad. Sci. U S A **91**: 4308-4312

42. **Clout, N. J., Kretschmar, M., Jaenicke, R., and Slingsby, C.** 2001 Crystal structure of the calcium-loaded spherulin 3a dimer sheds light on the evolution of eye lens betagamma-crystallin domain fold Structure **9**: 115-124

43. **Jobby, M. K., and Sharma, Y.** 2007 Caulollins from *Caulobacter crescentus*, a pair of partially unstructured proteins of betagamma-crystallin superfamily, gain structure upon binding calcium. Biochemistry **46**: 12298-12307

44. **Jobby, M. K., and Sharma, Y.** 2005 Calcium-binding crystallins from *Yersinia pestis.* Characterization of two single betagamma crystallin domains of a putative exported protein J. Biol. Chem. **280**: 1209-1216

45. **Jeromin, A., Muralidhar, D., Parameswaran, M. N., Roder, J., Fairwell, T., Scarlata, S., Dowal, L., Mustafi, S. M., Chary, K. V., and Sharma, Y.** 2004 N-terminal myristoylation regulates calcium-induced conformational changes in neuronal calcium sensor-1 J. Biol. Chem. **279**: 27158-27167

46. **Johnson, R. C., and Gary, N. D.** 1963 Neutrition of Leptospira Pomona III calcium, magnesium, and potassium requirement. J Bacteriol **85**: 983-985

47. **O'Connell, D. P., Nanavaty, T., McDevitt, D., Gurusiddappa, S., Hook, M., and Foster, T. J.** 1998 The fibrinogen-binding MSCAMM (clumping factor) of *Staphylococcus aureus* has a Ca^{2+}-dependent inhibitory site. J. Biol. Chem. **273**: 6821-682

CHAPTER 5

FIBRONECTIN BINDS TO AND INDUCES CONFORMATIONAL CHANGE IN A DISORDERED REGION OF *LEPTOSPIRA INTERROGANS* IMMUNOGLOBULIN-LIKE PROTEIN LIGB

Introduction

Leptospira interrogans is a pathogenic spirochete that causes leptospirosis throughout the world, especially in developing countries but also in regions of the United States where it has reemerged (1). Weil's syndrome, a severe form of this disease, is an acute febrile illness associated with multi-organ damage including liver failure (jaundice), renal failure (nephritis), pulmonary hemorrhage and meningitis (1), and has a 15% mortality rate if not treated (2). The molecular pathogenesis of leptospirosis is poorly understood and the bacterial virulence factors involved are largely unknown. Recently, several potential *Leptospira* virulence factors have been described, including sphingomyelinases, serine proteases, zinc-dependent proteases, collagenase (3), LipL32 (4), lipopolysaccharide (5), a novel factor H, laminin and Fn-binding protein (Lsa24 or Len) (6-8), Loa 22 (9), and Leptospiral immunoglobulin-like (Lig) proteins (10-12).

Lig proteins, including LigA, LigB, and LigC, contain multiple immunoglobulin-like repeat domains (13 in LigA, 12 in LigB and LigC) (10-12). Interestingly, the first 630 residues, from the N-terminus to the first half of the seventh immunoglobulin-like domain, are conserved between LigA and LigB, but the rest of the immunoglobulin-like domains are variable (10-12) between the two proteins. Also, a non-immunoglobulin-like repeat region found on the C-terminal tail of LigB is not found in LigA (10-12). Lig proteins are categorized as microbial surface components recognizing adhesive matrix molecules (MSCRAMM) due to their ability to bind to

eukaryotic cells (13) through their interactions with extracellular matrix components including fibronectin (Fn), laminin, and collagens (13,14). Previously, a high-affinity Fn-binding region was localized to LigBCen2, which includes the partial 11^{th} and complete 12^{th} immunoglobulin-like repeat region and the first 47 amino acids of the non-repeat regions of LigB (15). LigBCen2 was shown to bind to both the N-terminal domain (NTD) and the gelatin binding domain (GBD) of Fn. The addition of calcium induces a conformational change in LigBCen2 and enhances binding between LigBCen2 and the NTD of Fn (15).

The first step in the process of bacterial infection is cellular adhesion, mediated by bacterial adhesins interacting with various components of the extracellular matrix (ECM) (16). Known interaction modes between Fn and bacterial Fn-binding proteins include the β-zipper (17,18) and the cationic cradle (19). It was recently discovered that the Fn-binding domains in certain Fn-binding proteins are disordered and extended but gain structure upon binding to the NTD of Fn (20-22).

We have performed a fine-mapping study of the NTD-binding site on LigBCen2 and identified this site as LigBCen2NR, a portion of the non-repeat region (AA 1119-1165). The addition of NTD promotes the folding of LigBCen2NR from a disordered and extended structure to a folded structure. This finding is notable since LigBCen2NR is located in the non-immunoglobulin-like region of LigB, as compared with other Fn-binding proteins such as *Staphylococcus aureus* FnbpA and FnbpB (23), *Streptococcus dysgalactiae* FnBB (17), and *S. pyogenes* SfbI and SfbII (24). Thus, the binding mode appears to be similar to the known β -zipper mechanism, but unique in sequence-specific interactions. This finding provides the fundamental groundwork for the development of a therapeutic agent to target this interaction in order to prevent or treat *Leptospira* infection.

Materials and Methods

Reagents and antibodies

rabbit anti-GST antibody and HRP-conjugated goat anti-rabbit antibody were ordered from Molecular Probe (Eugene, OR) and Zymed (San Diego, CA) respectively. NTD or GBD of Fn, aldolase, bovine serum albumin, ovalbumin, chymotrypsinogen A, ribonuclease A, aprotinin, insulin chain B, sodium chloride, sodium phosphate monobasic, and sodium phosphate dibasic were purchased from Sigma-Aldrich (St. Louis, MO).

Plasmid construction and Protein purification

The construction, expression, and purification of LigCon (amino acids 1-630) were performed as described previously (12). Constructs for the expression of histidine-tagged or GST fused LigBCen2 (amino acids 1014-1156) and GST were generated using the vector pQE30 (Qiagen, Alencia, CA) and/or pGEX-4T-2 (GE Healthcare Bio-Science Corp., Piscataway, NJ), respectively, as previously described (14). Constructs for the expression of histidine-tagged or GST fused LigBCen2R (amino acids 1014-1123) and LigBCen2NR (amino acids 1119-1165) were generated using the vector pQE30 and pGEX-4T-2 (Figure. 5.1). To perform the PCR reactions, the following forward and backward primers were utilized (14): LigBCen2R forward primer 5' GGATCCACTGCGACTTACAAT 3' and backward primer 5' GTCGACCGTGTCCGTTTTGTT 3'; LigBCen2NR forward primer 5' CGGGATCCAACAAAACGGACACG 3' and backward primer 5' CGGTCGACATTGGAACTATTAAT 3'. Primers were engineered to introduce a *BamH*I site at the 5' end of each fragment and a stop codon followed by a *Sal*I site at the 3' end of each fragment. PCR products were sequentially digested with *BamH*I and *Sal*I and then ligated into pQE30 or pGEX-4T-2 cut with *BamH*I and *Sal*I, respectively. In

this study, we purified the soluble form of the histidine-tag or GST fused with LigBCen2, LigBCen2R, or LigBCen2NR from *E. coli* as previously described (25). Tris buffer (25mM Tris and 150 mM sodium chloride at pH 7.0) containing 100 μM of calcium chloride was used in all experiments as we have previously shown that calcium enhances the binding of LigBCen2 to NTD (15) and that both LigBCen2R and LigBCen2NR bind calcium (data not shown).

NMR Sample Preparation and Experiments

E. coli harboring the expression plasmid for His-tagged LigBCen2 were cultured in M9 minimal media. The recombinant LigBCen2 (retaining the 6-His tag) was labeled with $^{15}NH_4Cl$ (Cambridge Isotopes, Cambridge, MA), expressed, and purified as previously described (26). The purified ^{15}N-labeled LigBCen2 was dialyzed against Tris buffer with 100 μM calcium chloride at pH 6.0 and concentrated to 0.95mM (0.3 mL) using the Amicon Ultra centrifugal filter (Millipore, Billerica, MA). For some spectra, ^{15}N-labeled LigBCen2 was also mixed with 1.44mM of (unlabeled) NTD.

NMR spectra were recorded at 25 ^{o}C on a Varian Inova 600 MHz spectrometer equipped with a triple-resonance [H,C,N] z-axis pulse-field gradient probe. Two-dimensional ^{15}N-^{1}H fast-HSQC spectra were recorded with spectral widths of 2.4 kHz in t1 (400 real + imaginary data points) and 10 kHz in t2 (2048 real + imaginary data points) (27), with 16 or 32 transients per free induction decay for LigBCen2 in the absence or presence of NTD, and a recycle delay of 1.0 sec. NMR data were processed and analyzed using the software tools nmrPipe, nmrDraw, and Pipp (28,29). Data were apodized using a phase-shifted sine-bell function and zero-filled prior to Fourier transformation.

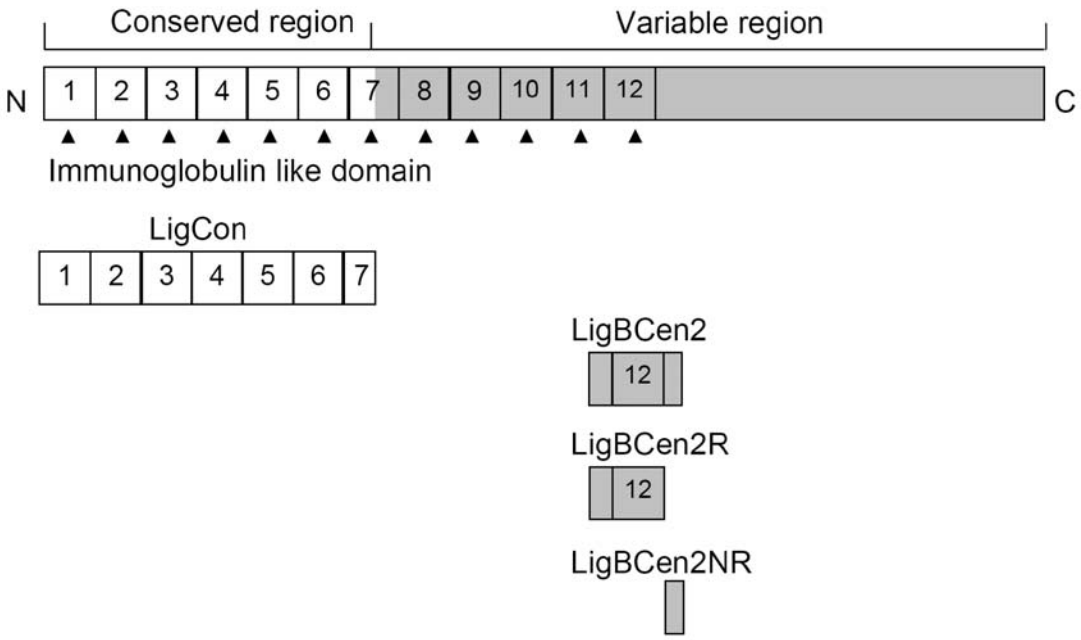

Figure 5.1 A schematic diagram showing the location of the truncated LigBCen2 protein including the LigBCen2R and LigBCen2NR constructs used in this study.

Surface Plasmon Resonance (SPR)

Association and dissociation rate constants for LigBCen2/NTD binding were measured by SPR analysis performed with a Biacore 2000 instrument (GE Healthcare Bio-Science, Piscataway, NJ) at 26.7^{o}C. 1 μM of His-tagged LigBCen2 in Tris buffer containing 100 μM $CaCl_2$ was immobilized on a NTA chip (GE Healthcare Bio-Science) conjugated with 500 μM nickel sulfate. Serial concentrations (100, 200, 400, 800 nM) of NTD were injected into the flow cells at a flow rate of 5 μL/min over the immobilized LigBCen2. All experiments are duplicated. All sensogram data have been corrected by subtracting data from a control cell injected with Tris buffer. Kinetic parameters were obtained by fitting the data to the one-step biomolecular association reaction model (1:1 Langmuir model) with the curve-fitting BIAevaluation software, version 3.0.

ELISA Fn binding assays

To determine the binding of GST-LigBCen2, GST-LigBCen2R, GST-LigBCen2NR, or GST-LigCon (negative control) to the NTD of Fn, 1 μM of NTD was coated on microtiter plate wells, incubated at 4^{o}C for 16 hours and blocked with blocking buffer (100 μl/well) containing 3% BSA in Tris buffer with 100 μM calcium chloride at room temperature (RT) for 2 hours. Then, serial concentrations (as indicated by Figure.

5.3A) of GST-LigBCen2, GST-LigBCen2R, GST-LigBCen2NR, or GST-LigCon in 100 μL Tris buffer with 100 μM calcium chloride were added to the microtiter plate wells for 1 hour at 37^{o}C. To detect the binding of GST-LigBCen2, GST-LigBCen2R, GST-LigBCen2NR, or GST-LigCon, rabbit anti-GST (1:200x) and HRP-conjugated goat anti-rabbit IgG (1:1,000x) were used as primary and secondary antibodies, respectively. After washing the plates thrice with TBST, (0.05% Tween 20 100 μM calcium chloride in Tris buffer) 100 μL of TMB (KPL, Gaithersburg, MD) was added to each well and incubated for 5 min. The reaction was stopped by adding 100 μl of 0.5%

hydrofluoric acid to each well. Each plate was read at 630nm using an ELISA plate reader (Bioteck EL-312, Winoski, VT). Each value represents the mean ± SEM of three trials in triplicate samples. Statistically significant ($P<0.05$) differences are indicated by *.

Isothermal Titration Calorimetry (ITC)

The experiments were carried out with a CSC 5300 microcalorimeter (Calorimetry Science Corp. Lindon, UT, USA) at 25^{o}C as previously described (14). In a typical experiment, the cell contained 1 ml of a solution of NTD and the syringe contained 250 µl of a solution of LigBCen2R or LigBCen2NR. The concentrations of LigBCen2R, LigBCen2NR, and NTD are described in Table 5.1. Both solutions were in Tris buffer with 100 µM calcium chloride. The titration was performed in 25 injections of 10 µl with a stirring speed of 250 rpm, and the delay time between the injections was 5 min. Data were analyzed using Titration Binding Work 3.1 software (Calorimetry Science Corp. Lindon, UT, USA) fitting them to an independent binding model.

Prediction of Protein Disorder

The LigBCen2NR folding prediction was carried out using PONDR, a software package containing VL-XT, XL1_XT, and VL3, which predict naturally disordered regions (30-32). PONDR can be used as a Web Service for remote and automatic data processing by accessing the following URL: www.pondr.com. The analyses were performed using default values.

Differential Scanning Calorimetry (DSC)

The excess heat capacity $C_p(T)$ of LigBCen2, LigBCen2R, or LigBCen2NR was measured using a DSC Q1000 microcalorimeter (Waters, New Castle, DE). Degassed

samples containing 3 μM of LigBCen2, LigBCen2R, LigBCen2NR or Tris buffer with 100 μM calcium chloride were heated at 10 K/h scan rate. Heat Capacities, cp(T), data were recorded, corrected for buffer baseline, and normalized to the amount of the samples. The TA Universal Analysis software (Waters, New Castle, DE) was used for the data analysis and display. All calorimetric experiments in this study were repeated 3 times to ensure reproducibility.

Gel Permeation Chromatography (GPC)

LigBCen2, LigBCen2R, and LigBCen2NR were analyzed for their partition coefficient (K_{av}) and effective radii (Stokes radii, R_s) in Tris buffer with 100 μM calcium chloride using a Superdex 200 HR 10/30 column (GE Healthcare Bio-Sceince) attached to a fast protein liquid chromatography (GE Healthcare Bio-Sceince) system. Protein samples were preequilibrated with Tris buffer with 100 μM calcium chloride, and eluted with the same buffer at a flow rate of 0.5 mL/min. The column was calibrated using a low molecular weight gel filtration calibration kit (GE Healthcare Bio-Sceince). The standard globular proteins contained in the kit were ribonuclease A (13,700 Da), chymotrypsinogen (25,000 Da), Ovalbumin (43,000 Da), and albumin (67,000 Da). Blue dextran 2000 (2,000,000Da) (GE Healthcare Bio-Sceince), and Aldolase (158,000 Da) were used to indicate the void volume (V_o) and the total volume (V_t), respectively. The elution volume (V_e) of each sample was measured. To define the relationships between the elution volumes of protein samples and their respective molecular weight, the K_{av} value for each protein was calculated using the equation

$$K_{av} = \frac{V_e - V_o}{V_t - V_o} \qquad \text{(Eq. 1)}$$

where V_o and V_t for the column used were 7.96 and 23.56 mL, respectively. K_{av} values of standard and LigBCen2, LigBCen2R, or LigBCen2NR were plotted against the logarithm of the protein molecular weights to fit the equation shown as follows (33).

$$\log M_w = a \cdot K_{av} + b \qquad \text{(Eq. 2)}$$

Where a and b are constants. R_s of the proteins were determined using sample elution volumes and standard curves as described in the calibration kit (Amersham Pharmacia Biotech, Piscataway, NJ).

Dynamic Light Scattering (DLS)

One mg per mL of LigBCen2, LigBCen2R, or LigBCen2NR was dialyzed against prefiltered (0.22 μm Millipore filters) Tris buffer with 100 μM calcium chloride. The samples were placed in a 1mL plastic cuvette. The standard globular proteins including albumin (67,000 Da), ovalbumin (43,000 Da), chymotrypsinogen A (25,000 Da), ribonuclease A (13,700 Da), aprotinin (6,500 Da), or insulin chain B (3,400 Da) were used to generate the calibration curve of globular proteins. The automated measurements were collected with a Zetasizer Nano ZS instrument (Malvern Instruments Ltd., Worcestershire, United Kingdom), using a 2 min equilibrium delay at each measurement. The data were adjusted using the method of cumulants to obtain the hydrodynamic radius (R_h). The logarithms of the R_h values of standards and LigBCen2, LigBCen2R, or LigBCen2NR were plotted against the logarithm of the protein molecular weights to fit the equation

$$\log M_W = a \cdot \log R_h + b \qquad \text{(Eq. 3)}$$

where a and b are constants.

Intrinsic Viscosity measurements

The viscosities of the LigBCen2, LigBCen2R, and LigBCen2NR were measured using a Cannon-Ubbelohde Semi-Micro Dilution Viscometer (No. 25 9722-H50, Cannon Instrument Co., State College, PA) with a viscometer constant, 0.002044 mm^2/s^2, at 25°C. Before measuring the viscosities, 1mL of each protein at concentrations of 0.5, 0.75, 1, and 1.5 mg/mL were dialyzed overnight against Tris buffer with 100 μM calcium chloride, with or without 6M guanidine hydrochloride, and the same buffer was used as a reference solution. The specific viscosity (η_{sp}) was determined as previously described (34). Specific viscosity / concentration of untreated or 6M guanidine hydrochloride-treated LigBCen2, LigBCen2R, or LigBCen2NR were plotted against the concentration of proteins, and the intrinsic viscosity [η] was calculated using the following equation:

$$\frac{\eta_{sp}}{C} = [\eta] + k[\eta]^2 C \qquad \text{(Eq. 4)}$$

Where c is protein concentration and k is a dimensionless constant. The values of [η] expected for a denatured protein shown in Table 5.3 were obtained from the following equation (34):

$$[\eta] = 0.716 n^{0.66} \qquad \text{(Eq. 5)}$$

where n is the number of residues in the protein.

Circular dichroism (CD) spectroscopy

CD analysis was performed on an Aviv 215 spectropolarimeter (Lakewood, NJ) under N_2 atmosphere. CD spectra were measured at RT (25°C) in a 1-cm path length quartz cell. Spectra of LigBCen2, LigBCen2R or LigBCen2NR were recorded in Tris buffer with 100 μM calcium chloride at a protein concentration of 10 μM. Three spectra were recorded for each condition from 190 to 250 nm for far-UV CD in 1 nm increments. In

the thermal denaturation experiment, 10 μM of LigBCen2, LigBCen2R, LigBCen2NR were used, and data were collected at 2°C/minute increments from 20°C to 100°C recording the ellipticity at 205 nm, with 30 second temperature equilibrations, followed by 30 second data averaging. In order to measure the melting point, the first order derivative of the melting curve was taken. Structural changes in LigBCen2R and LigBCen2NR upon binding to the NTD of Fn were examined by analyzing changes in the CD spectrum. LigBCen2R (10 μM) or LigBCen2NR (10 μM) was preincubated with or without the NTD (10 μM) of Fn for 1 hour at 25^{o}C, and the far-UV CD spectra were recorded as described above. The changes of the CD spectra upon NTD-LigBCen2R or NTD-LigBCen2NR interaction were determined by computationally subtracting the ellipticity of the NTD-LigBCen2R or NTD-LigBCen2NR complex from the added spectra of the free forms of interacting proteins. The deconvolution of the resulting spectra was performed as described above. In all CD experiments, the background spectrum of buffer without protein was subtracted from the protein spectra. CD spectra were initially analyzed by the software accompanying the spectrophotometer. Analysis of spectra to extrapolate secondary structures was performed by Dichroweb (35) (http://www.cryst.bbk.ac.uk/cdweb/html/home.html) using the K2D and Selcon 3 analysis programs (36,37).

Fluorescence Spectroscopy

Fluorescence emission spectra were measured on a Hitachi F4500 spectrofluorometer (Hitachi. San Jose, CA). All spectra were recorded in the correct spectrum mode of the instrument using excitation and emission band-passes of 5 nm. The intrinsic tryptophan fluorescence of the protein was recorded by exciting the solution at 295 nm and measuring the emission between 305-400 nm. For the LigBCen2NR/NTD binding

Figure 5.2 NMR provides evidence for distinct structured and disordered regions of LigBCen2. (A) The 1H-15N HSQC of apo LigBCen2 exhibits a set of well-dispersed peaks, indicative of folded, beta-rich residues, and a set of sharper peaks clustered toward the center, indicative of residues in an unstructured region. This is emphasized by (B) the HSQC viewed at a higher contour level. The number of peaks indicative of folded and unfolded residues roughly matches the number of residues expected to adopt the Ig-like fold of repeat regions 11 and 12 and the number of residues included from the non-repeat region, respectively. (C) When unlabeled NTD is added at an equimolar concentration, most of the sharp, clustered peaks either disappear or are greatly diminished in intensity while the well-dispersed peaks corresponding to folded protein remain largely unperturbed, as highlighted by (D) the overlay of this spectrum with the apo LigBCen2 spectrum. The disappearance of the peaks corresponding to the unstructured region(s) of the LigBCen2 construct suggests that the non-repeat sequence selectively binds to NTD. represents the meaṇ ± standard error of the mean (SEM) of samples tested in triplicate. An (*) indicates the result was statistically significant.

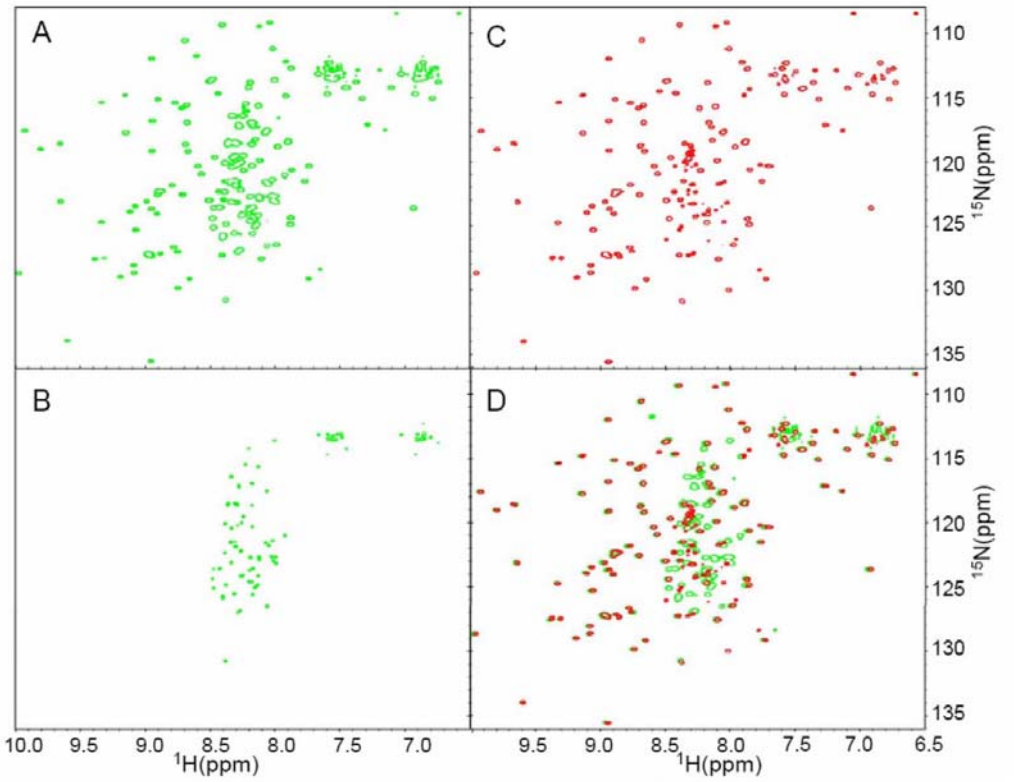
A
B
C
D
110
115
120
125
130
135
^{15}N(ppm)
10.0
9.5
9.0
8.5
8.0
7.5
7.0
6.5
^{1}H(ppm)

experiment, the emission spectra of untreated or LigBCen2NR (10 μM) treated with NTD (10 μM) were taken. LigBCen2NR contains no tryptophan; therefore, for the LigBCen2NR/NTD binding experiment, the spectrum of LigBCen2NR in isolation was essentially background and was subtracted from the spectrum for the mixture.

Matrix Assisted Laser Desorption Ionization-Time of Flight (MALDI-TOF) mass spectrometry

The molecular weight of samples of purified LigBCen2, LigBCen2R, or LigBCen2NR were analyzed using MALDI-TOF mass spectra recorded on an Applied Biosystems 4700 Mass Spectrometer (Applied Biosystems, Foster City, CA). Prepared samples included 10 μM of LigBCen2, LigBCen2R, or LigBCen2NR in deionized water.

Statistical analysis

Significance between samples was determined using the Student's t-test following logarithmic transformation of the data. Two-tailed P-values were determined for each sample and a P-value <0.05 was considered significant. Each data point fold predicted for repeat regions 11 and 12, which would place backbone N-H groups in unique chemical environments and would cause the corresponding ^{15}N-^{1}H correlation peaks to appear at widely varying positions in the NMR spectrum. In contrast, for a dynamically unstructured polypeptide, the corresponding ^{15}N-^{1}H correlation peaks are stronger due to increased motion, and cluster to similar regions of the spectrum due to the more uniform chemical environment of the solvent. A set of such peaks is clearly present, as highlighted by the LigBCen2 ^{15}N-^{1}H spectrum at a higher contour level (Figure. 5.2B). The number of peaks associated with folded and unfolded sets of N-H groups roughly matches the number of residues expected to adopt the -sheet rich fold of the 12th and

partial 11th Ig-like repeats (LigBCen2R) and the number of residues included from the non-repeat region (LigBCen2NR), respectively.

Results

Identification of the binding sites of NTD on LigBCen2

In order to investigate the general structural properties of LigBCen2 and its interactions with Fn, uniformly ^{15}N-labeled LigBCen2 was prepared, and two-dimensional ^{15}N-^{1}H chemical shift correlation NMR experiments were performed in the absence and presence of an equimolar amount of unlabeled NTD (Figure. 5.2. A-D).

The NMR spectrum of apo LigBCen2 shows evidence for distinct structured and unstructured regions, with a set of highly resolved peaks dispersed across both dimensions of the spectrum and another set of peaks of higher intensity clustered toward the center of the spectrum (Figure. 5.2A and B). The number of well-dispersed peaks and their positions are consistent with the β-sheet rich immunoglobulin-like When 1.44mM of unlabeled NTD was added to 0.95mM of ^{15}N-LigBCen2, the well-dispersed peaks corresponding to folded protein remained largely unperturbed, while most of the sharp, clustered peaks either disappeared or were greatly diminished in intensity (Figure. 5.2C) as highlighted by the overlay of this spectrum with the apo LigBCen2 spectrum (Figure. 5.2D). Interestingly, application of a TROSY-based ^{15}N-^{1}H HSQC experiment useful for very large proteins (38) did not recover the lost peaks (data not shown). These results demonstrate that NTD does not bind to the structured region of LigBCen2. The nature and number of peaks that are affected by NTD addition suggest that NTD specifically binds to LigBCen2NR and results in chemical exchange in the intermediate rate regime, where the peaks whose chemical environment changes between conformational states are broadened beyond the level of detection.

In order to test the possibility that the peak disappearance is due to sampling between free and bound states, surface plasmon resonance (SPR) was performed to measure the binding kinetics for the LigBCen2-NTD interaction at pH 6.0 and 26.7 °C to correspond to the NMR conditions (Fig. 5.7). Based on the rates obtained, (k_{on} = 2.28 × 10^5 ± 0.23 × $10^5 s^{-1}M^{-1}$, k_{off} = 2.47 × 10^{-2} ± 0.16 × 10^{-2} s^{-1}), the k_{ex} should be 112 ± 11 s^{-1} at the conditions of the NMR sample (1.44 mM NTD, 0.95 mM LigBCen2, $[NTD]_{free}$ = 0.49 mM). Resonances undergoing exchange broadening due to ligand binding usually refocus at saturation. Given the unusually slow off-rate of binding, at saturating concentrations of NTD the spectrum of LigBCen2 should show a single set of peaks reflecting the bound state. A saturation of >99% was predicted for the NMR sample, assuming simple two-state binding with a K_D of 93 nM (15). Therefore, the line-broadening observed for the NMR sample is not due to exchange between free and bound states. One possible explanation is the formation of a 'fuzzy complex,' or a dynamic ensemble of conformational states, upon binding NTD. This has been previously observed for other intrinsically disordered proteins, including the NTD-binding SfbI of *S. pyogenes* (39,40). Regardless of the origin of the peak disappearance, the NMR experiments indicate that NTD interacts specifically with the disordered region of LigBCen2 in the intact construct.

In order to evaluate the pH sensitivity of the LigBCen2-NTD interaction, the SPR measurements were performed at both pH 6.0 and 7.0. The dissociation constants calculated at each pH ($K_D = k_{off}/k_{on}$ = 109 ± 8 nM at pH 6.0, 95.5 ± 1.4 nM at pH 7.0) are in good agreement with each other, and the value at pH 7.0 is in excellent agreement with the previously reported K_D of 93 ± 8 nM at pH 7.0 (15). The kinetic rates at each pH were also in close agreement with each other (k_{on} = 2.72 ± 0.19 × 10^5 $s^{-1}M^{-1}$, k_{off} = 2.6 ± 0.22 × 10^{-2} $s^{-}1$ at pH 7.0). All subsequent biophysical measurements were performed at pH 7.0.

Table 5.1 Thermodynamic parameters for the interaction of NTD and LigBCen2R or LigBCen2NR

LigB	LigB Residues	[LigB]	[NTD]	ΔH	TΔS	ΔG	K_D	n
		μM	μM	kcal mol^{-1}	kcal mol^{-1}	kcal mol^{-1}	nM	
LigBCen2NR	1119-1165	362	61	13.13±1.55	22.25	-9.12	379±16	0.94±0.01
LigBCen2R	1014-1123	118	5.9	n/f[a]	n/f[a]	n/f[a]	n/f[a]	n/f[a]

n/f[a], non-fittable.

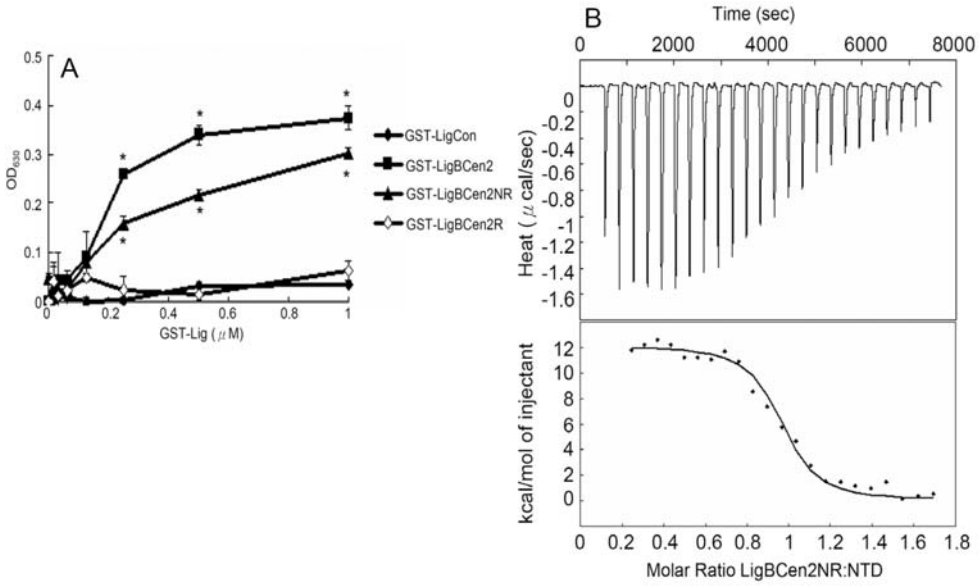

Figure. 5.3 Determination of binding constant and thermodynamics of the LigBCen2NR/NTD interaction by ELISA and ITC. (A) Binding of serial concentrations of LigBCen2NR to immobilized NTD by ELISA. Serial concentrations of GST-LigBCen2R, GST-LigBCen2NR, GST-LigBCen2 (positive reference), or GST-LigCon (negative reference) were added to 1μM of NTD or BSA coated wells (negative control, data not shown). (B) Determination of the binding affinity by ITC. The cell contained 1 ml of NTD and the syringe contained 250 μl of LigBCen2NR (upper panel) Heat differences obtained from 25 injections of LigBCen2NR; (lower panel) Integrated curve with experimental data (◆) and the best fit (—). The thermodynamic parameters are shown in Table 5.1.

In order to test the NMR-derived hypothesis that NTD interacts with specifically with LigBCen2NR, various concentrations of GST-LigCon (a truncation that cannot interact with Fn, used as a negative control) GST-LigBCen2 (positive control), GST-LigBCen2R, GST-LigBCen2NR, and GST were added to a NTD coated microtiter plate. As shown in Figure. 5.3A, LigBCen2NR binds NTD, but no NTD binding was observed for LigBCen2R or LigCon (Fig. 5.1) (13,14). These results were also confirmed by isothermal titration calorimetry (ITC) experiments. LigBCen2NR binding to NTD is an endothermic reaction (unfavorable enthalpy, favorable entropy) with a dissociation constant (K_D) of 379 nM (Fig. 5.3B and Table 5.1). The favorable entropy suggests that the complex formation of LigBCen2 and NTD involves significant hydrophobic interactions. By contrast, ITC experiments demonstrate that LigBCen2R does not bind to NTD (Table 5.1). Both ELISA and ITC results support the NMR-derived hypothesis that LigBCen2NR, the non-immunoglobulin-like domain 47-residue region of LigBCen2, selectively binds to NTD.

LigBCen2NR possesses a disordered and unfolded structure

To further characterize the structural properties of LigBCen2NR and investigate the NMR-derived hypothesis that this region is unstructured, the amino acid sequence of LigBCen2NR was analyzed by PONDR, a software tool used to predict naturally disordered protein regions. More than half of the residues in LigBCen2NR (all but residues 1146-1164) were predicted to be disordered by VLXT in the PONDR software package. In addition, a highly disordered structure was also predicted in LigBCen2NR by XL1_XT and VL3 in the PONDR software package (data not shown).

In order to confirm this sequence-based prediction, the secondary structure of LigBCen2, LigBCen2R, or LigBCen2NR was examined by far-UV CD. As presented in Figure. 5.4A, both LigBCen2 and LigBCen2R contain significant β-sheet structure

Figure. 5.4 Analysis of LigBCen2, LigBCen2R, or LigBCen2NR by Far-UV CD, GPC, DLS, and viscometry. (A) Far-UV CD analysis of LigBCen2, LigBCen2R, and LigBCen2NR. The molar ellipticity, Φ, was measured from 190 to 250 nm for 10 μM of each protein in Tris buffer with 100μM calcium chloride. (B) Gel Permeation chromatography of standard molecular mass markers, LigBCen2, LigBCen2R, and LigBCen2NR. The partition coefficient (K_{av}) is plotted as a function of the molecular weight of each individual protein on a log scale. (C) Dynamic light scattering of standard molecular mass markers, LigBCen2, LigBCen2R, and LigBCen2NR. The hydrodynamic radius (R_h) is plotted as a function of the molecular weight of each individual protein on a log-log scale. For (C) and (D), the molecular weights of the standards are indicated in Materials and Methods, and the molecular weight of LigBCen2, LigBCen2R, or LigBCen2NR are indicated in Table 5.2. (D) Determination of the intrinsic viscosity of proteins under native or denaturing conditions. The specific viscosity/concentration versus concentration is plotted for LigBCen2, LigBCen2R, and LigBCen2NR in Tris buffer with 100μM calcium chloride and with or without 6M guanidine hydrochloride. The intercept at the y axis is the intrinsic viscosity.

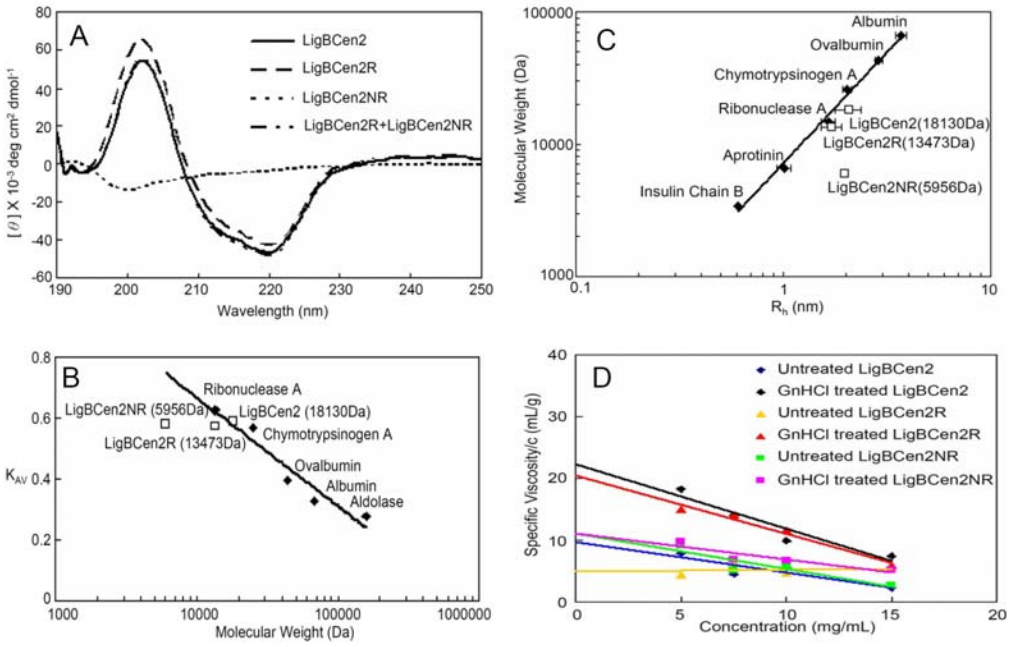
A
LigBCen2
LigBCen2R
LigBCen2NR
LigBCen2R+LigBCen2NR
[θ] X 10⁻³ deg cm² dmol⁻¹
Wavelength (nm)
B
Ribonuclease A
LigBCen2NR (5956Da)
LigBCen2 (18130Da)
Chymotrypsinogen A
LigBCen2R (13473Da)
Ovalbumin
Albumin
Aldolase
K_AV
Molecular Weight (Da)
C
Albumin
Ovalbumin
Chymotrypsinogen A
Ribonuclease A
LigBCen2(18130Da)
LigBCen2R(13473Da)
Aprotinin
Insulin Chain B
LigBCen2NR(5956Da)
Molecular Weight (Da)
R_h (nm)
D
Untreated LigBCen2
GnHCl treated LigBCen2
Untreated LigBCen2R
GnHCl treated LigBCen2R
Untreated LigBCen2NR
GnHCl treated LigBCen2NR
Specific Viscosity/c (mL/g)
Concentration (mg/mL)

Table 5.2 Estimated radii of recombinant LigBCen2, LigBCen2R, and LigBCen2NR

	Calculated mass	Mass Spectroscopy	Expected R_s from GPC calibration curve	R_s from GPC	Expected R_h from DLS calibration curve	R_h from DLS
	Da	Da	Nm	nm	Nm	nm
LigBCen2	18130.97	18131.60	2.05	1.95	2.04	2.07
LigBCen2R	13473.76	13416.81	1.67	2.07	1.75	1.71
LigBCen2NR	5956.57	5929.34	0.62	1.93	0.93	1.97

(40% in LigBCen2 and 55% in LigBCen2R). However, LigBCen2NR contains 65% random coil. Thus, compared to LigBCen2R, LigBCen2NR possesses a highly disordered and unfolded structure, in agreement with the NMR analysis of LigBCen2 presented above.

Gel permeation chromatography and dynamic light scattering indicate LigBCen2NR adopts an extended structure

Most proteins containing disordered structures are extended instead of globular and highly packed. Due to differences in the hydrodynamic properties (such as the Stokes radius, R_s, and the partition coefficient, K_{av}) of globular and extended proteins, gel permeation chromatography is a powerful technique to determine if a protein is unfolded. The K_{av} of LigBCen2, LigBCen2R, LigBCen2NR, and other globular protein standards were determined by the elution volume (V_e) obtained from gel permeation chromatography and calculated by equation 1 above. In addition, K_{av} was plotted against the logarithm of molecular weight, and a calibration curve of globular proteins was made by using the data from the globular protein standards. Compared to LigBCen2 and LigBCen2R, the value of K_{av} for LigBCen2NR was far from the calibration curve and less than expected for a globular protein with a similar molecular mass (Figure. 5.4B). These results indicate that LigBCen2NR is not a globular protein. Similarly, the R_s value of LigBCen2NR revealed by gel permeation chromatography (1.93nm) is significantly larger than expected for a globular protein (0.62 nm) (Table 5.2), suggesting that LigBCen2NR forms an extended structure.

The hydrodynamic radii (R_h) of LigBCen2, LigBCen2R, LigBCen2NR, and globular protein standards were measured using dynamic light scattering to confirm the results from the gel permeation chromatography measurements. The R_h value of LigBCen2 or LigBCen2R was close to the value of the globular proteins possessing a

similar molecular mass (Figure. 5.4C and Table 5.2). However, the R_h value of LigBCen2NR (1.97 nm) was significant larger than that of globular proteins with a similar molecular mass (0.94 nm) (Figure. 5.4C and Table 5.2). The distinctly larger R_h of LigBCen2NR suggested that it is a highly extended protein, consistent with the results obtained from gel permeation chromatography.

Intrinsic viscosity measurements suggest that LigBCen2NR is extended and denatured

Measurement of intrinsic viscosity is a well-known method to determine if a protein is denatured because of the direct relationship between the number of residues of a denatured protein and its intrinsic viscosity, as shown in equation 5 in Materials and Methods. For extended or denatured proteins, intrinsic viscosity is also generally larger than for folded proteins (21).

To further examine if LigBCen2NR is denatured and extended, the viscosities of LigBCen2, LigBCen2R, and LigBCen2NR were measured. The specific viscosity over protein concentration was plotted against concentration, as shown in Figure. 5.4D. The data were fitted to equation 4 in Materials and Methods to obtain intrinsic viscosities, and these values were compared to the values expected for denatured proteins, as calculated by equation 5. As shown in Figure. 5.4D and Table 5.3, the intrinsic viscosity of untreated LigBCen2 or LigBCen2R measured by viscometry was smaller than that of LigBCen2 or LigBCen2R treated with guanidine hydrochloride. However, the intrinsic viscosities of both guanidine hydrochloride-treated and untreated LigBCen2NR were close to the intrinsic viscosity expected for a denatured protein, as calculated by equation 5. Taken together, these results indicate that LigBCen2NR is denatured and extended.

Table 5.3 Intrinsic viscosity of recombinant LigBCen2, LigBCen2R, and LigBCen2NR

	measured [η] from viscometry		predicted [η] for denatured protein
	0M GnHCl	6M GnHCl	
LigBCen2	9.55	22.23	21.39
LigBCen2R	4.75	20.45	17.87
LigBCen2NR	10.76	10.98	10.20

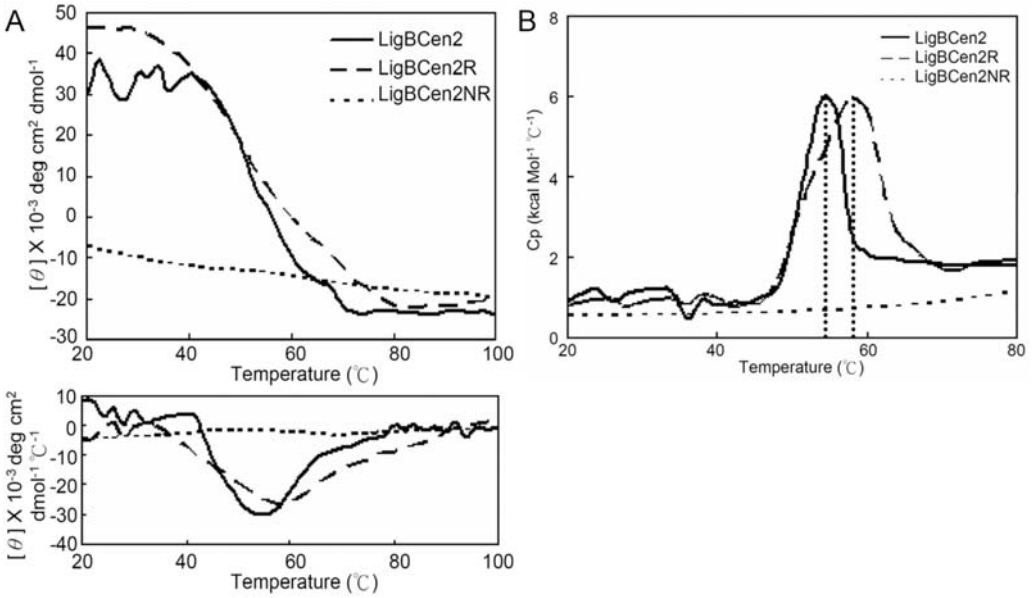

Figure. 5.5 Thermal unfolding transitions of LigBCen2, LigBCen2R, or LigBCen2NR as measured by CD and DSC. (A) Thermal unfolding of 10 μM of LigBCen2, LigBCen2R, or LigBCen2NR was observed by CD, measuring ellipticity at 205 nm from 20 to 100°C. A transition point was identified for LigBCen2 and LigBCen2R but not for LigBCen2NR. The melting temperatures were determined by the location of the peak in the derivative of the ellipticity curve, as shown in the lower panel. The transition midpoints of LigBCen2 and LigBCen2R are 54.0 ± 0.5°C and 58.1 ± 0.8°C, respectively. (B) Thermal unfolding transitions of LigBCen2, LigBCen2R, and LigBCen2NR measured by DSC. Molar heat capacity [kcal/(mol · K)] was plotted against temperature (°C) from 20 to 80°C for 3 μM of LigBCen2, LigBCen2R, or LigBCen2NR. The dot line indicated that the midpoint temperatures of the transitions for LigBCen2 and LigBCen2R are 54.2 ± 0.4 °C and 57.3 ± 0.2 °C, respectively.

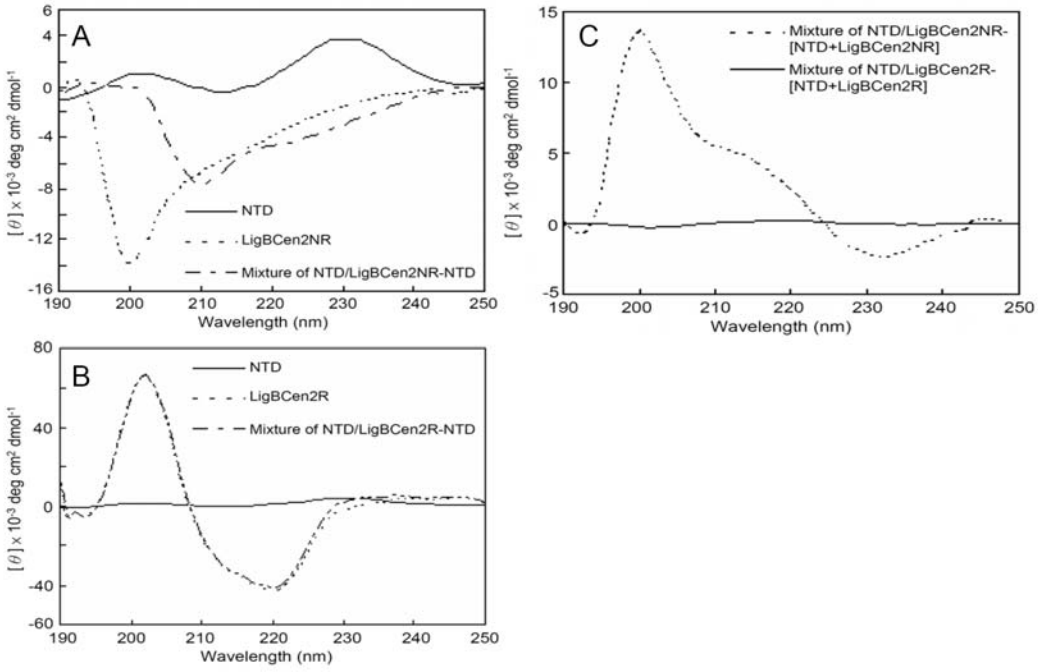

Figure 5.6 Modification of the Far-UV CD spectrum of LigBCen2NR upon NTD binding. Far UV spectra of the apo forms and mixtures of 10 μM of NTD and 10μM of either LigBCen2NR (A) or LigBCen2R (B). The ellipticities shown in (A) are those of uncomplexed LigBCen2NR (----), complexed NTD and LigBCen2NR after subtraction of the NTD CD spectrum (—-—), and the CD spectrum of 10 μM NTD (—). The ellipticities in (B) are those of LigBCen2R (----), a mixture of NTD and LigBCen2R after subtraction of the NTD CD spectrum (—-—), and the CD spectrum of 10 μM NTD (—). (C) The far UV spectra of mixtures of NTD and LigBCen2NR (---) or LigBCen2R (—) after subtraction of the CD spectra of both apo NTD and apo LigBCen2NR or LigBCen2R.

CD and DSC thermal unfolding experiments further indicate that LigBCen2NR has an unfolded structure

In order to gain more insight on the conformation of LigBCen2, LigBCen2, LigBCen2R, and LigBCen2NR were subjected to thermal unfolding experiments using CD spectrophotometry and DSC. As shown in Figure. 5.5A, the melting points of LigBCen2 and LigBCen2R are 54.0 ± 0.5^{o}C and 58.1 ± 0.8^{o}C, respectively, as measured by monitoring the CD signal at 205 nm from 20 to 80 ^{o}C. The higher melting temperature for LigBCen2R indicates that presence of LigBCen2NR reduces the thermal stability of LigBCen2R. The midpoint of the DSC transition curves for LigBCen2 (54.2 ± 0.4^{o}C) and LigBCen2R (57.3 ± 0.2 ^{o}C) are consistent with the CD-derived melting points (Figure. 5.5B). Compared with the results of LigBCen2 and LigBCen2R, no obvious cooperative unfolding transition of LigBCen2NR was observed (Figure. 5.5). Therefore, both thermal and chemical denaturation experiments indicate that LigBCen2NR has an unfolded structure.

The conformation of LigBCen2NR changes upon the addition of NTD

In order to determine if the binding of NTD affects the structure of LigBCen2NR, the CD spectra of NTD, LigBCen2NR (Figure. 5.6A), and NTD mixed with LigBCen2R or LigBCen2NR were recorded (Figure. 5.6B and C). The NTD spectrum and either the LigBCen2R or the LigBCen2NR spectrum were added as a comparison to assess conformational changes upon binding. Consistently, the far-UV CD spectrum of the NTD presented on Figure. 5.6A is similar to that published previously (20,21,41) since a minimum in intensity was located around 215 nm, and two peaks were located around 200 nm and 230 nm, respectively due to tyrosine side chains (42,43). As shown in Figure. 5.6A and B, the spectrum of apo LigBCen2NR and complexed NTD-LigBCen2NR after subtraction of the NTD CD spectrum are significantly

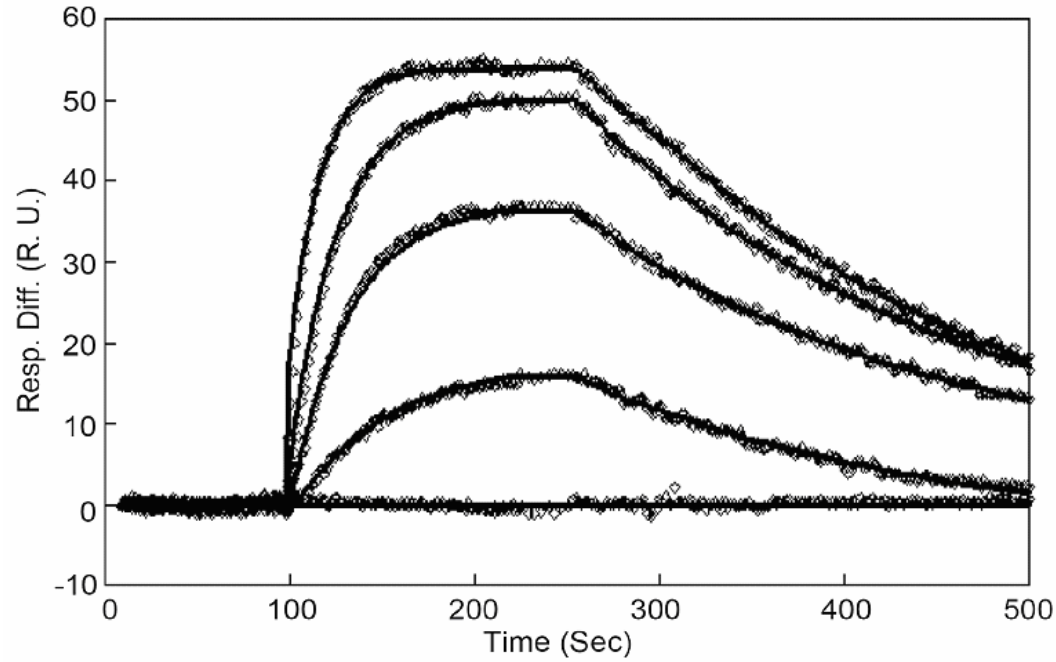

Figure 5.7 SPR sensograms of LigBCen2/NTD binding. 1 μM of Recombinant Histdine-tag LigBCen2 was immobilized on the surface of Ni-NTA chip. NTD was flowed through the chip in Tris Buffer containing 100μM $CaCl_2$ at pH 6, and the concentrations of NTD were ranging from 800 to 0 nM (from top to bottom). The average response of duplicate experiments (◇) and the fitted curve (—) are shown. The K_D, k_{on}, k_{off} were obtained from the average of duplicate experiments ($K_D = 109 \pm 8$ nM, $k_{on} = 2.28 \times 10^5 \pm 0.23 \times 10^5\ s^{-1}M^{-1}$ $k_{off} = 2.47 \times 10^{-2} \pm 0.16 \times 10^{-2}\ s^{-1}$).

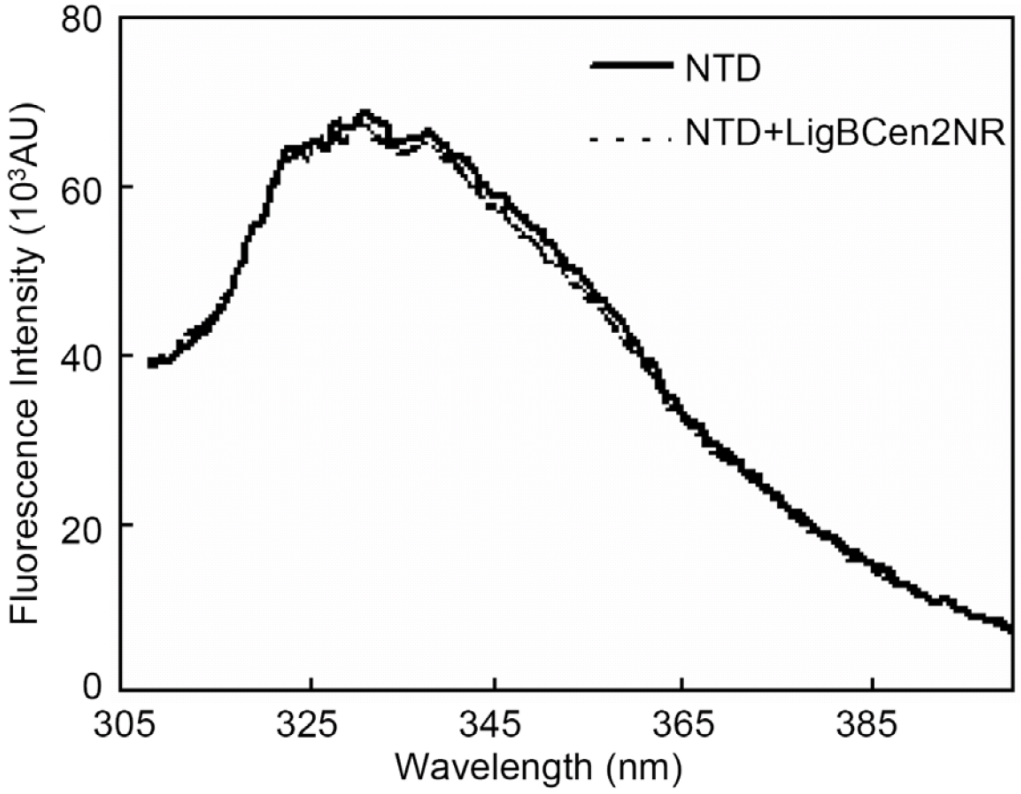

Figure. 5.8 The intrinsic tryptophan fluorescence of NTD (10 μM) in the absence (—) and presence (---) of LigBCen2NR (10 μM).

different, but the spectrum of apo LigBCen2R cannot be distinguished from a mixture of NTD and LigBCen2R after subtraction of the NTD CD spectrum. Therefore, conformational changes occur upon binding of NTD to LigBCen2NR. In order to clarify whether NTD or LigBCen2NR change conformation after binding, the intrinsic fluorescence spectra of unbound or LigBCen2NR-bound NTD were measured. In a previous study, it was shown that conformational changes in NTD are easily detected by intrinsic tryptophan fluorescence due to the presence of seven tryptophan residues in NTD that are sensitive to small changes in environment (20). Furthermore, because of the absence of tryptophan in LigBCen2NR, the intrinsic fluorescence spectrum of NTD-bound LigBCen2NR reflects only the conformation of NTD. The addition of LigBCen2NR did not significantly change the fluorescence spectrum of NTD (Figure 5.8), which suggests that binding of LigBCen2NR does not significantly alter the chemical environment of the tryptophan residues of NTD. This observation, which suggests that NTD does not undergo significant conformational rearrangement upon binding, has been reported previously for binding of a domain of FnbA from *S. dysgalactiae* to NTD, and it is thought to be generally true for many NTD-binding MSCRAMMs that NTD remains conformationally unchanged upon binding (20). Thus, the difference between the CD spectrum of the LigBCen2-NTD complex and the sum of the spectra of the individual components shown in Figure 5.6C is considered to be due to conformational changes in LigBCen2NR and not NTD. The CD spectra of free and complexed LigBCen2NR were analyzed by software to quantitate secondary structure before after binding of NTD (Figure 5.6 A). The results of analysis show that LigBCen2NR gains secondary structure upon the addition of NTD because the percentage of random coil dramatically decreases (from 65% to 46%), whereas the β-sheet composition increases (from 28 % to 48%). However, the α–helix composition

changes little (from 7% to 6%). This indicates that binding of NTD may cause LigBCen2NR to adopt a β-sheet rich structure.

Discussion

MSCRAMM is a class of well-known adhesin proteins that enable microbes to attach to host cells by binding to their ECMs. LigB binds to Fn, fibrinogen, laminin, elastin, proelastin and collagen, and hence likely plays a substantial role in adhesion for pathogenic *Leptospira* (13-15,44,45). We have shown that LigBCen2 strongly binds to the NTD, and weakly binds to the GBD, of Fn (14) (NTD, K_D = 272 nM; GBD, K_D = 1200 nM). LigBCen2 contains an immunoglobulin-like repeat region, LigBCen2R, and a non-repeat 47-residue region, LigBCen2NR. In this study, two-dimensional NMR spectroscopy revealed both folded and disordered regions of LigBCen2, demonstrated that the folded region does not bind to NTD, and indicated that the disordered region specifically interacts with NTD. Using ELISA and ITC, we found that LigBCen2NR indeed binds to NTD. However, the binding affinity of LigBCen2NR/NTD (K_D = 379 nM) (Table 5.1) is four-fold lower than LigBCen2/NTD (K_D = 93 nM) (15). It is not presently clear why this is true, but it may suggest that residues near the interface between LigBCen2R and LigBCen2NR may play a substantial role in binding and that severing the two regions reduces their binding capacity. In protein binding studies of intrinsically disordered proteins, it is not uncommon for regions flanking binding elements to contribute to binding without directly contacting the binding partner (40). A similarly unexplained reduction in binding affinity has previously been observed for truncated forms of BBK32 from *B. burgdorferi* (21). Further study is needed to clarify this result.

The N-terminal domain of BBK32 (AA56-205) from *B. burgdorferi* possesses Fn-binding activity but lacks secondary structure (21). Additional Fn-binding proteins

previously shown to be disordered include FNBD-D, the D1-D3 repeat region of FnbpA from *S. aereus*, FNBD-A and FNBD-B, the A1-A3 and B1-B3 repeat regions of FnbA and FnbB from *S. dysgalactiae*, FNBD-P, and the P1-P4 repeat regions of Sfb from *S. pyogens* (20). These Fn-binding regions change their conformation to a folded form upon binding to NTD (20,21,23). Similarly, upon binding to NTD LigBCen2NR folds into a β-strand rich structure, much like the D123 domain of FnbPA or the N-terminal of BBK32 (21). High-resolution structures of the complex between the B3 region of FnbB and the first and the second type I module of Fn (17,18), the complex between the first or the fifth Fn binding region of FnbpA, and the second to the fifth type I module of Fn (23,39,46) all indicate that a two β-strand complex, called a β-zipper, mediates those interactions. The binding of Sfb and BBK32 to NTD are also accomplished through the β-zipper interaction (23,39,46). The β-strand rich conformation formed by LigBCen2NR after binding NTD observed via far-UV CD spectroscopy suggests that the binding of LigBCen2NR to NTD might be also mediated by a β-zipper interaction. However, the entropy-driven interaction of LigBCen2NR and NTD is distinct from the enthalpy-driven binding of other bacterial proteins known to bind NTD via the β-zipper interaction (Table 5.1) (23,39,46). In addition, we are unable to identify substantial sequence similarity between LigBCen2NR and BBK32 or other Fn binding proteins, so additional study is needed to further characterized the binding between LigBCen2NR and NTD.

The on-rate of LigBCen2-NTD binding obtained from surface plasmon resonance (SPR) is on the order of 10^5 $M^{-1}s^{-1}$, three orders of magnitude below rates expected for diffusion-limited two state binding (10^8-10^9 $M^{-1}s^{-1}$) (47). This indicates that additional processes occur either before or concurrently with association of LigBCen2 with NTD. The observed increase in secondary structure of LigBCen2NR upon binding may account for this.

The off-rate of the NTD-LigBCen2 complex is also strikingly slow, yielding a residence time on the order of 40 s. This may be an important feature for the role of LigB in infection. Recent experiments (48,49) have suggested that a small k_{off} of a drug-target complex is an important predictor, in some cases more than a small K_D, of *in vivo* efficacy. This is because *in vivo* the concentration of ligand is often not constant, but instead influenced by absorption, distribution, metabolism, and excretion (ADME). In some cases, this leads to a greater dependence on k_{off} of the overall duration of the complex. Since a bacterial adhesin is challenged by many of the same limitations to concentration as a drug, it is interesting to speculate that the slow off-rate reported here is evolutionarily optimized to avoid clearance, while the slow on-rate may be optimized to facilitate movement through the host.

We have demonstrated that the region of LigBCen2 that mediates its interaction with the NTD of Fn is localized to LigBCen2NR. LigBCen2NR has a disordered structure that dramatically increases its β-strand content after binding to NTD. Disordered proteins often alter their conformations when binding their partners (50). One possible role of protein disorder in protein-protein interactions is the large accessible surface area per residue contributed by the disordered protein (18,51). The unfavorable decrease in the entropy of LigBCen2NR upon binding NTD due to the disorder-order transition is offset by a larger increase in entropy, possibly due to hydrophobic interactions, as demonstrated by ITC. Another advantage of protein disorder in binding is that coupled folding and binding usually contributes high specificity and low affinity to the interaction (50).

In conclusion, the moderate affinity and slow kinetics of the LigBCen2NR interaction with the NTD of Fn might aid in *Leptospira* infection of a host organism by increasing the time it remains adhered to cells while simultaneously facilitating efficient

transmission within the host. These intriguing results motivate further study of the role this disordered region plays in the pathogenesis of leptospiral infection.

REFERENCES

1. **Faine, S. B., Adher, B., Bolin, C., and Perolat, P**. (eds). 1999 *Leptospira and Leptospirosis.*, MedSci, Medbourne, Australia

2. .**Segura, E. R., Ganoza, C. A., Campos, K., Ricaldi, J. N., Torres, S., Silva, H., Cespedes, M. J., Matthias, M. A., Swancutt, M. A., Lopez Linan, R., Gotuzzo, E., Guerra, H., Gilman, R. H., and Vinetz, J. M.** 2005 Clinical spectrum of pulmonary involvement in Leptospirosis in a region of endemicity, with quantification of *Leptopsira* burden. Clin. Infect. Dis. **40**: 343-351

3. **Bulach, D. M., Zuerner, R. L., Wilson, P., Seemann, T., McGrath, A., Cullen, P. A., Davis, J., Johnson, M., Kuczek, E., Alt, D. P., Peterson-Burch, B., Coppel, R. L., Rood, J. I., Davies, J. K., and Adler, B.** 2006 Genome reduction in *Leptospira borgpetersenii* reflects limited transmission potential Proc. Natl. Acad. Sci. U S A **103**: 14560-14565

4. **Yang, C. W., Wu, M. S., Pan, M. J., Hsieh, W. J., Vandewalle, A., and Huang, C. C.** 2002 The *Leptospira* outer membrane protein LipL32 induces tubulointerstitial nephritis-mediated gene expression in mouse proximal tubule cells J. Am. Soc. Nephrol. **13**: 2037-2045

5. **Werts, C., Tapping, R. I., Mathison, J. C., Chuang, T. H., Kravchenko, V., Saint Girons, I., Haake, D. A., Godowski, P. J., Hayashi, F., Ozinsky, A., Underhill, D. M., Kirschning, C. J., Wagner, H., Aderem, A., Tobias, P. S., and Ulevitch, R. J.** 2001 Leptopsira lipopolysaccharide activates cell through a TLR2-dependent mechanism. Nat. Immunol. **2**: 346-352

6. **Barbosa, A. S., P. A. Abreu, F. O. Neves, M. V. Atzingen, M. M. Watanabe, M. L. Vieira, Z. M. Morais, S. A. Vasconcellos, and A. L. Nascimento.** 2006. A newly identified leptospiral adhesin mediates attachment to laminin. Infect. Immun. **74:**6356-6364.

7. **Stevenson, B., Choy, H. A., Pinne, M., Rotondi, M. L., Miller, M. C., Demoll, E., Kraiczy, P., Cooley, A. E., Creamer, T. P., Suchard, M. A., Brissette, C. A., Verma, A., and Haake**, D. A. 2007 Leptospira interrogans endostatin-like outer membrane proteins bind host fibronectin, laminin, and regulators of complement. PLoS ONE **2**: e1188

8. **Verma, A., Hellwage, J., Artiushin, S., Zipfel, P. F., Kraiczy, P., Timoney, J. F., and Stevenson, B**. 2006. LfhA, a novel factor-H binding protein of Leptospira interrogans. Infect. Immun. **74**: 2659-2666

9. **Ristow, P., Bourhy, P., McBride, F. W., Figueira, C. P., Huerre, M., Ave, P., Girons, I. S., Ko, A. I., and Picardeau, M**. 2007. The OmpA-like protein Loa22 is essential for leptospiral virulence. PLoS Pathog. **3**: e97

10. **Matsunaga, J., M. A. Barocchi, J. Croda, T. A. Young, Y. Sanchez, I. Siqueira, C. A. Bolin, M. G. Reis, L. W. Riley, D. A. Haake, and A. I. Ko.** 2003. Pathogenic *Leptospira* species express surface-exposed proteins belonging to the bacterial immunoglobulin superfamily. Mol Microbiol **49:**929-945.

11. **Palaniappan, R. U., Chang, Y. F., Hassan, F., McDonough, S. P., Pough, M., Barr, S. C., Simpson, K. W., Mohammed, H. O., Shin, S., McDonough, P., Zuerner, R. L., Qu, J., and Roe, B.** 2004 Expression of leptospiral immunoglobulin-like protein by *Leptospira interrogans* and evaluation of its diagnostic potential in a kinetic ELISA. J. Med. Microbiol. **53**: 975-984

12. **Palaniappan, R. U., Chang, Y. F., Jusuf, S. S., Artiushin, S., Timoney, J. F., McDonough, S. P., Barr, S. C., Divers, T. J., Simpson, K. W., McDonough, P. L., and Mohammed, H. O.** 2002 Cloning and molecular characterization of an immunologic LigA protein of *Leptospira interrogans*. Infect. Immun. **70**: 5924-5930

13. **Lin, Y. P., and Chang, Y. F.** 2008 The C-terminal variable domain of LigB from *Leptospira* mediates binding to fibronectin. J. Vet. Sci. **9:**133-144..

14. **Lin, Y. P., and Chang, Y. F.** 2007 A domain of *Leptospira* LigB contribute to high affinity binding of fibronectin. Biochem. Biophys. Res. Commun. **362**: 443-448

15. **Lin, Y. P., R. Raman, Y. Sharma, and Chang, Y. F..** 2008. Calcium binds to Leptospiral immunoglobulin-like protein, LigB and modulates fibronectin binding. J. Biol. Chem. **283:**25140-25149.

16. **Patti, J. M., B. L. Allen, M. J. McGavin, and M. Hook.** 1994. MSCRAMM-mediated adherence of microorganisms to host tissues. Annu Rev Microbiol **48:**585-617

17. **Schwarz-Linek, U., Werner, J. M., Pickford, A. R., Gurusiddappa, S., Kim, J. H., Pilka, E. S., Briggs, J. A., Gough, T. S., Hook, M., Campbell, I. D., and Potts, J. R.** 2003 Pathogenic bacteria attach to human fibronectin through a tandem beta-zipper Nature **423**: 177-181

18. **Bingham, R. J., Rudino-Pinera, E., Meenan, N. A., Schwarz-Linek, U., Turkenburg, J. P., Hook, M., Garman, E. F., and Potts, J. R.** (2008) Crystal structure of fibronectin-binding sites from *Staphylococcus aureus* FnBPA in complex with fibronectin domains Proc. Natl. Acad. Sci. U S A **105**: 12254-12258

19. **Kingsley, R. A., Keestra, A. M., de Zoete, M. R., and Baumler, A. J.** 2004 The ShdA adhesin binds to the cationic cradle of the fibronectin 13FnIII repeat module: evidence for molecular mimicry for heparin binding. Mol Microbiol **52**: 345-355

20. **House-Pompeo, K., Xu, Y., Joh, D., Speziale, P., and Hook, M**. (1996) J. Biol. Chem. Conformational change in the fibronectin binding MSCRAMMs are induced by ligand binding **271**, 1379-1384

21. **Kim, J. H., Singvall, J., Schwarz-Linek, U., Johnson, B. J., Potts, J. R., and Hook, M.** 2004 BBK32, a fibronectin binding MSCRAMM from Borrelia burgdorferi, contains a disordered region that undergoes a conformational change on ligand binding J. Biol. Chem. **279**, 41706-41714

22. **Penkett, C. J., Redfield, C., Jones, J. A., Dodd, I., Hubbard, J., Smith, R. A., Smith, L. J., and Dobson, C. M.** 1998 Structural and dynamical characterization of a biologically active unfolded fibronectin-binding protein from Staphylococcus aureus. Biochemistry **37**, 17054-17067

23. **Meenan, N. A., Visai, L., Valtulina, V., Schwarz-Linek, U., Norris, N. C., Gurusidappa, S., Hook, M., Speziale, P., and Potts, J. R.** 2007 The tandemβ-zipper model defines high affinity fibronectin-binding repeats within *Staphylococcus aureus* FnBPA J. Biol. Chem. **282:** 25893-25902.

24. **Schwarz-Linek, U., Hook, M., and Potts, J. R.** 2004 The molecular basis of fibronectin-mediated bacterial adherence to host cells. Mol Microbiol **52**, 631-641

25. **Palaniappan, R. U., McDonough, S. P., Divers, T. J., Chen, C. S., Pan, M. J., Matsumoto, M., and Chang, Y. F.** 2006 Immunoprotection of recombinant leptospira immunoglobulin-like protein A against Leptospira interrogans serovar Pomona infection. Infect. Immun. **74**: 1745-1750

26. **Jayaraman, B., and Nicholson, L. K.** 2007 Thermodynamic dissection of the Erzin FERM/CERMAD interface Biochemistry **46**: 12174-12189

27. **Mori, S., Abeygunawardana, C., Johnson, M. O., and van Zijl, P. C.** 1995 Improved sensitivity of HSQC spectra of exchanging protons at short interscan

delays using a new fast HSQC(FHSQC) detection scheme that avoids water saturation J Magn Reson B **108**: 94-98

28. **Delaglio, F., Grzesiek, S., Vuister, G. W., Zhu, G., Pfeifer, J., and Bax, A.** 1995 NMRPipe: a multidimentional spectral processing system based on UNIX pipes. J Biomol NMR **6**: 277-293

29. **Garrett, D., Powers, R., Gronenborn, A., and Clore, M.** 1991 J. Magn Reson *(1969)* **95:**, 214-220

30. **Li, X., Romero, P., Rani, M., Dunker, A. K., and Obradovic, Z.** 1999 Genome Inform. Ser. Workshop Genome Inform.
10: 30-40

31. **Romero, Obradovic, and Dunker, K.** 1997 Genome Inform. Ser. Workshop Genome Inform. **8**: 110-124

32. **Romero, P., Obradovic, Z., Li, X., Garner, E. C., Brown, C. J., and Dunker, A. K.** 2001 Sequence complexity of disordered protein. Proteins **42**: 38-48

33. **Ohno, H., Blackwell, J., Jamieson, A. M., Carrino, D. A., and Caplan, A. I.** 1986 Calibration of relative molecular mass of proteoglycan subunit by column chromatography on Sepharose CL-2B Biochem J **235**: 553-557

34. **Tanford, C., Kawahara, K., Lapanje, S., Hooker, T. M., Jr., Zarlengo, M. H., Salahuddin, A., Aune, K. C., and Takagi, T.** 1967 Protein as random coils. 3 Optical rotatory dispersion in 6M guanidine hydrochloride. J Am Chem Soc **89**: 5023-5029

35. **Lobley, A., Whitmore, L., and Wallace, B. A.** 2002 DICHROWEB: An interactive website for the analysis of protein secondary structure from circular dichroism spectra. Bioinformatics **18**: 211-212

36. **Bohm, G., Muhr, R., and Jaenicke, R.** 1992 Quantitative analysis of protein far UV circular dichroism spectra by neural network. Protein Eng **5**: 191-195

37. **Sreerama, N., and Woody, R. W.** 1994 Protein secondary structure from circular dichroism spectroscopy Combining variable selection principle and cluster analysis with neural network, ridge regression and self-consistent methods. J Mol Biol **242**: 497-507

38. **Pervushin, K., Riek, R., Wider, G., and Wuthrich, K.** 1997 Attenuated T2 relaxation by mutual cancellation of dipole-dipole coupling and chemical shift anisotropy indicates an avenue to NMR structure of very large biological macromolecules in solution. Proc Natl Acad Sci U S A **94**, 12366-12371

39. **Schwarz-Linek, U., Pilka, E. S., Pickford, A. R., Kim, J. H., Hook, M., Campbell, I. D., and Potts, J. R.** 2004 High affinity Streptococcal binding to human fibronectin requires specific recognition of sequential F1 modules. J. Biol. Chem. **279**: 39017-39025

40. **Tompa, P., and Fuxreiter, M.** 2008 Fuzzy complexes: polymorphism and structural disorder in protein-protein interactions. Trends Biochem. Sci. **33**: 2-8

41. **Odermatt, E., Engle, J., Richter, H., and Hormann, H.** 1982 Shape, conformation, and stability of fibronectin fragments determined by electron microscopy, circular dichroism, and ultracentrifugation. J Mol Biol **159**: 109-123

42. **Stevens, E. S., Morris, E. R., Charlton, J. A., and Rees, D. A.** 1987 Vacuum ultraviolet circular dichroism of fibronectin, Dominant tyrosine effects. J Mol Biol **197**: 743-745

43. **Welsh, E. J., Frangou, S. A., Morris, E. R., Rees, D. A., and Chavin, S. I.** 1983 Tyrosine optical activity as a probe of the conformation and interaction of fibronectin. Biopolymers **22**: 821-831

44. **Choy, H. A., Kelley, M. M., Chen, T. L., Moller, A. K., Matsunaga, J., and Haake, D. A.** 2007 Physiological osmotic induction of *Leptospira interrogans*

adhesion: LigA and LigB bind extracellular matrix proteins and firbrinogen. Infect. Immun. **75**: 2441-2450

45. **Lin, Y. P., Lee, D. W., McDonough, S. P., Nicholson, L. K., Sharma, Y., Chang, Y. F.** 2009 Repeated domains of Leptospira Immunoglobulin-like proteins interact with elastin and tropoelastin J. Biol. Chem. **284**: 19380-19391

46. **Raibaud, S., Schwarz-Linek, U., Kim, J. H., Jenkins, H. T., Baines, E. R., Gurusiddappa, S., Hook, M., and Potts, J. R.** 2005 Borrelia burgdorferi binds fibronectin through a tandem beta-zipper, a common mechanism of fibronectin binding in Staphylococci, streptococci, and spirochetes. J. Biol. Chem. **280**: 18803-18809

47. **Eigen, M., and Hammes, G. G.** 1963 Elementary steps in enzyme reactions (as studied by relaxation spectrometry) Adv. Enzymol. Relat. Areas Mol. Biol. **25**: 1-38

48. **Berezov, A., Zhang, H. T., Greene, M. I., and Murali, R.** 2001 Disabling erbB receptors with rationally designed exocyclic mimetics of antibodies: structure-function analysis. J. Med. Chem. **44**: 2565-2574

49. **Copeland, R. A., Pompliano, D. L., and Meek, T. D.** 2006 Drug target residence time and its implication for lead optimization. Nat. Rev. Drug Discov. **5**: 730-739

50. **Dyson, H. J., and Wright, P. E.** 2005 Intrinsically unstructured proteins and their functions. Nat. Rev. Mol. Cell. Biol. **6**: 197-208

51. **Dunker, A. K., Lawson, J. D., Brown, C. J., Williams, R. M., Romero, P., Oh, J. S., Oldfield, C. J., Campen, A. M., Ratliff, C. M., Hipps, K. W., Ausio, J., Nissen, M. S., Reeves, R., Kang, C., Kissinger, C. R., Bailey, R. W., Griswold, M. D., Chiu, W., Garner, E. C., and Obradovic, Z.** 2001 Intrinsically disordered protein J. Mol. Graph. Model. **19**: 26-59

CHAPTER 6

BINDING AFFINITY TO THE GELATIN BINDING DOMAIN OF FIBRONECTIN IS ENHANCED BY THE IG-LIKE REPEAT DOMAINS OF LEPTOSPIRA LIG PROTEINS THROUGH MULTIVALENCY

Introduction

Microbial Surface Components Recognizing Adhesive Matrix Molecules (MSCRAMMs) are a group of proteins located on the surface of microbes (1). They are able to contribute to microbial adhesion by binding to extracellular matrixes (ECMs) of host cells and initiate infection (1). Fibronectin (Fn), a 220 kDa ECM that forms a dimer by disulfide linkage, is composed of three different modules and several different domains including an N-terminal domain (NTD), a gelatin-binding domain (GBD), a cell binding domain (CBD), a heparin binding domain II, and a fibrin binding domain II (2,3). Fn plays a pivotal role in bacterial-host interaction by interacting with MSCRAMMs (4). These MSCRAMMs may bind to NTD, GBD (5-7) or heparin binding domain II (8,9).

In the past, several potential ECM binding proteins of *Leptospira* spp. have been identified; these include Lig proteins (10-16), LipL32 (17-20), Leptospira endostatin-like proteins (Len) (21,22), Lsa21 (23) and TLYC(24). Lig proteins, including LigA, LigB and LigC, contain 13, 12, and 13 Ig-like domains, respectively (25-27). The N-terminal 630 amino acid residues of LigA and LigB are identical, but the C-termini are variable (25-27). Unlike LigA, LigB and LigC possess a non-immunoglobulin (Ig)-like region in their C-termini (26,27). Lig proteins also serve as vaccine candidates and diagnostic antigens (26,28-32). Lig proteins are members of MSCRAMMs due to their ability to bind fibronectin (Fn), laminin, collagen, fibrinogen, elastin, and tropoelastin of host cells (10-16). Moreover, LigBCen2, which contains

LigBCen2R, the partial 11th and full 12th Ig-like domains, and LigBCen2NR, the C-terminal 47 non-Ig-like region, binds to NTD and GBD of Fn with high affinity that is enhanced by calcium binding (11,16). In a recent report, LigBCen2NR is found to be a disordered protein and is able to fold upon NTD binding (13).

Multivalency has advantages over monovalency for binding affinity through avidity (33,34). The off-rate of a multivalent species is much slower than that of a monomer, therefore, avidity is higher, and this may be advantageous for ligand binding receptors that require dimerization for activity (35). Because multivalency increases binding affinity through avidity, we engineered proteins containing 90 amino acid Ig-like repeats of the variable regions of LigA and LigB of *Leptospira* and studied their interaction with GBD of Fn. In this study, LigBCen2R was found to interact with GBD, and Isothermal Titration Calorimetry (ITC) and surface plasmon resonance (SPR) were used to monitor the binding of GBD to Fn by proteins containing different numbers of 90 amino acid Ig-like repeats of the variable region of LigA or LigB. In addition, the GBD binding activity expanded to most of the Ig-like repeats on the variable regions of LigA and LigB through multivalency. A large gain in affinity was achieved through an avidity effect, with the terminal domains, 13th or 12th Ig-like repeat of LigA or LigB (LigAVar7'-13 and LigBCen7'-12) enhancing binding affinity approximately 43 and 24 fold, respectively compared to recombinant proteins without this terminal repeat. The enhanced avidity might be due to the compact structures formed in LigAVar7'-13 and LigBCen7'-12 mediated by interdomain interaction.

Materials and Methods

Bacterial strains and cell culture

Leptospira interrogans serovar Pomona (NVSL1427–35–093002) was used as previously described (34). All experiments were performed with virulent, low-passage

strains obtained by passage through golden syrian hamsters as previously described (34). Leptospires were grown in EMJH medium at 30^{o}C for less than 5 passages and growth was monitored by dark-field microscopy. Madin–Darby canine kidney (MDCK) cells (ATCC CCL34) were cultured in Dulbecco minimum essential medium (DMEM) containing 10% fetal bovine serum (Gibco Laboratories, Grand Island, NY). Cells were grown at 37^{o}C in a humidified atmosphere with 5% CO_2.

Reagents and antibodies

rabbit anti-GST antibody was ordered from Molecular Probes (Eugene, OR). HRP-conjugated goat anti-rabbit antibody and HRP-conjugated streptavidin were ordered from KPL (Gaithersburg, MD). Alexa Fluor 488 C_5 maleimide and tris-(-2-carboxyethyl) phosphine (TCEP) were purchased from Molecular Probe (Carlsbad, CA). Gelatin binding domain of human plasma fibronectin (GBD) and bovine serum albumin (BSA), Tris-HCl, calcium chloride, sodium phosphate dehydrate, and sodium chloride were ordered from Sigma-Aldrich (St. Louis, MO). D_2O was ordered from Cambridge isotope Laboratories (Andover, MA)

Plasmid construction

All constructs used in this study were cloned into either a pGEX-4T-2 vector (GE Healthcare , Piscataway, NJ) or a pQE-30 vector (Qiagen, Alencia, CA) and purified as Glutathione-S-Transferase (GST) or Histidine tagged fusion proteins (Table 6.1 and Figure. 6.1) (15,16). To make all the above constructs, PCR reactions were performed by utilizing the primers described in Table 6.2. For constructing LigAVar7'-8, LigAVar7'-9, LigAVar7'-10, LigAVar7-11, LigAVar7'-12, LigAVar9, LigAVar10, LigAVar11, LigAVar12, and LigAVar13, primers were engineered to introduce a BamHI site at the 5' end and a SalI site at the 3' end of each fragment. For constructing

Table 6.1 The sources of clones used in this study

Clone	Vector	Source	Tag	Reference
LigBCon	pGEX4T2	Residues 1-630 of LigB from *L. interrogans*	GST-tag	33
LigAVar7'-8	pGEX4T2	Residues 631-765 of LigA from *L. interrogans*	GST tag	51
LigAVar7'-9	pGEX4T2	Residues 631-856 of LigB from *L. interrogans*	GST tag	This study
LigAVar7'-10	pGEX4T2	Residues 631-897 of LigB from *L. interrogans*	GST tag	This study
LigAVar7'-11	pGEX4T2	Residues 631-1038 of LigB from *L. interrogans*	GST tag	This study
LigAVar7'-12	pGEX4T2	Residues 631-1140 of LigB from *L. interrogans*	GST tag	This study
LigAVar7'-13	pGEX4T2	Residues 631-1224 of LigB from *L. interrogans*	GST tag	33
LigAVar9	pQE30	Residues 756-856 of LigA from *L. interrogans*	Histidine tag	51
LigAVar10	pQE30	Residues 847-946of LigA from *L. interrogans*	Histidine tag	51
LigAVar11	pQE30	Residues 938-1038 of LigA from *L. interrogans*	Histidine tag	51
LigAVar12	pQE30	Residues 1029-1140 of LigA from *L. interrogans*	Histidine tag	51
LigAVar13	pQE30	Residues 1131-1225 of LigA from *L. interrogans*	Histidine tag	51
LigBVar7'-8	pQE30	Residues 631-756 of LigB from *L. interrogans*	Histidine tag	27
LigBVar7'-9	pQE30	Residues 631-850 of LigB from *L. interrogans*	Histidine tag	This study
LigBVar7'-10	pQE30	Residues 631-941 of LigB from *L. interrogans*	Histidine tag	This study

Table 6.1 (Continued)

Clone	Vector	Source	Tag	Reference
LigBVar7'-11	pQE30	Residues 631-1033 of LigB from *L. interrogans*	Histidine tag	This study
LigBVar7'-12	pQE30	Residues 631-1124 of LigB from *L. interrogans*	Histidine tag	This study
LigBCen	pQE30	Residues 631-1417 of LigB from *L. interrogans*	Histidine tag	32
LigBVar9	pQE30	Residues 755-850 of LigB from *L. interrogans*	Histidine tag	27
LigBVar10	pQE30	Residues 846-941 of LigB from *L. interrogans*	Histidine tag	27
LigBVar11	pQE30	Residues 942-1028 of LigB from *L. interrogans*	Histidine tag	27
LigBCen2	pQE30	Residues 1014-1165 of LigB from *L. interrogans*	Histidine tag	23
LigBCen2R	pGEX4T2	Residues 1014-1124 of LigB from *L. interrogans*	GST-tag	24
LigBCen2NR	pGEX4T2	Residues 1120-1165 of LigB from *L. interrogans*	GST-tag	24

Table 6.2 Primer Table

Primer/Vector	Sequence*
LigAVar7'-8fp/pGEX4T2**	GCGGATCCCTTACCGTTTCCAAC
LigAVar7'-8rp	GCGTCGACATTGAAGTAAGAATT
LigAVar7'-9fp/pGEX4T2	GCGGATCCCTTACCGTTTCCAAC
LigAVar7'-9rp	GCGTCGACCTCAATAAGTTCCGC
LigAVar7'-10fp/pGEX4T2	GCGGATCCCTTACCGTTTCCAAC
LigAVar7'-10rp	GCGTCGACCGAAACTACTTTAGC
LigAVar7'-11fp/pGEX4T2	GCGGATCCCTTACCGTTTCCAAC
LigAVar7'-11rp	GCGTCGACGTAACGAAGAAGCGC
LigAVar7'-12fp/pGEX4T2	GCGGATCCCTTACCGTTTCCAAC
LigAVar7'-12rp	GCGTCGACATTTACTATACCACT
LigAVar9fp/pQE30***	GCGGATCCTACCGTTACTCCCGC
LigAVar9rp	GCGTCGACCTCAATAAGTTCCGC
LigAVar10fp/pQE30	GCGGATCCTTATCCGTTACCGCA
LigAVar10rp	GCGTCGACCGAAACTACTTTAGC
LigAVar11fp/pQE30	GCGGATCCTTCCAAGTTACTCCG
LigAVar11rp	GCGTCGACGTAACGAAGAAGCGC
LigAVar12fp/pQE30	GCGGATCCTTGAATGTCACTCCA
LigAVar12rp	GCGTCGACATTTACTATACCACT
LigAVar13fp/pQE30	GCGGATCCGTTACGGTTACGGAA
LigAVar13rp	GCGTCGACTTATGGCTCCGTTTT
LigBCen7'-9fp/pQE30	CGCGGATCCATTGCTGAAATT
LigBCen7'-9rp	CGCCCTGCAGAATCGGAATTGG
LigBCen7'-10fp/pQE30	CGCGGATCCATTGCTGAAATT
LigBCen7'-10rp	CGCCCTGCAGAAAATTTATTTTATT

Table 6.2 (Continued)

Primer/Vector	Sequence*
LigBCen7'-11fp/pQE30	CGCGGATCCATTGCTGAAATT
LigBCen7'-11rp	CGCCCTGCAGGACCGTTATGTC
LigBCen7'-12fp/pQE30	CGGCATGCATTGCTGAAATT
LigBCen7'-12rp	CGAAGCTTGTTTACTGTGAGAAT
LigBCen2RW1073Cf****	TCTTCGGTTACATGTTCCAGCTCAAAT
LigBCen2RW1073Cr	ATTTGAGCTGGAACATGTAACCGAAGA
[6]F1fp/pPICZα[#]	CGGAATTCTGTGTCACAGACAGT
[6]F1rp	CGGCGGCCGCCTCTTGGCAGCTGAC
[1]F2[2]F2fp/pPICZα	CGGAATTCACAGCTGTAACCCAG
[1]F2[2]F2rp	CGGCGGCCGCGATTTCCTCGTGGG
[7]F1fp/pET-THGT[$]	CGGAATTCTGCACAACCAATGAA
[7]F1rp	CGGCGGCCGCCTGATCTCGAAGCTG
[8]F1fp/pET-THGT	CGGAATTCTGCATTGTTGATGAC
[8]F1rp	CGGCGGCCGCTTGGTCGACGGGATC
[9]F1fp/pET-THGT	CGGAATTCTGCCAGGATTCAGAG
[9]F1rp	CGGCGGCCGCTGAGCTTGGATAGGT

* The restriction enzyme cutting sites are underlined. ** GE Healthcare, Piscataway, NJ, *** Qiagen Inc., Volencia, CA, **** Primers used for site directed mutagenesis. [#] Invitrogen, Carlsbad, CA, [$] Obtained from the Cornell protein production and characterization core facility, Cornell University.

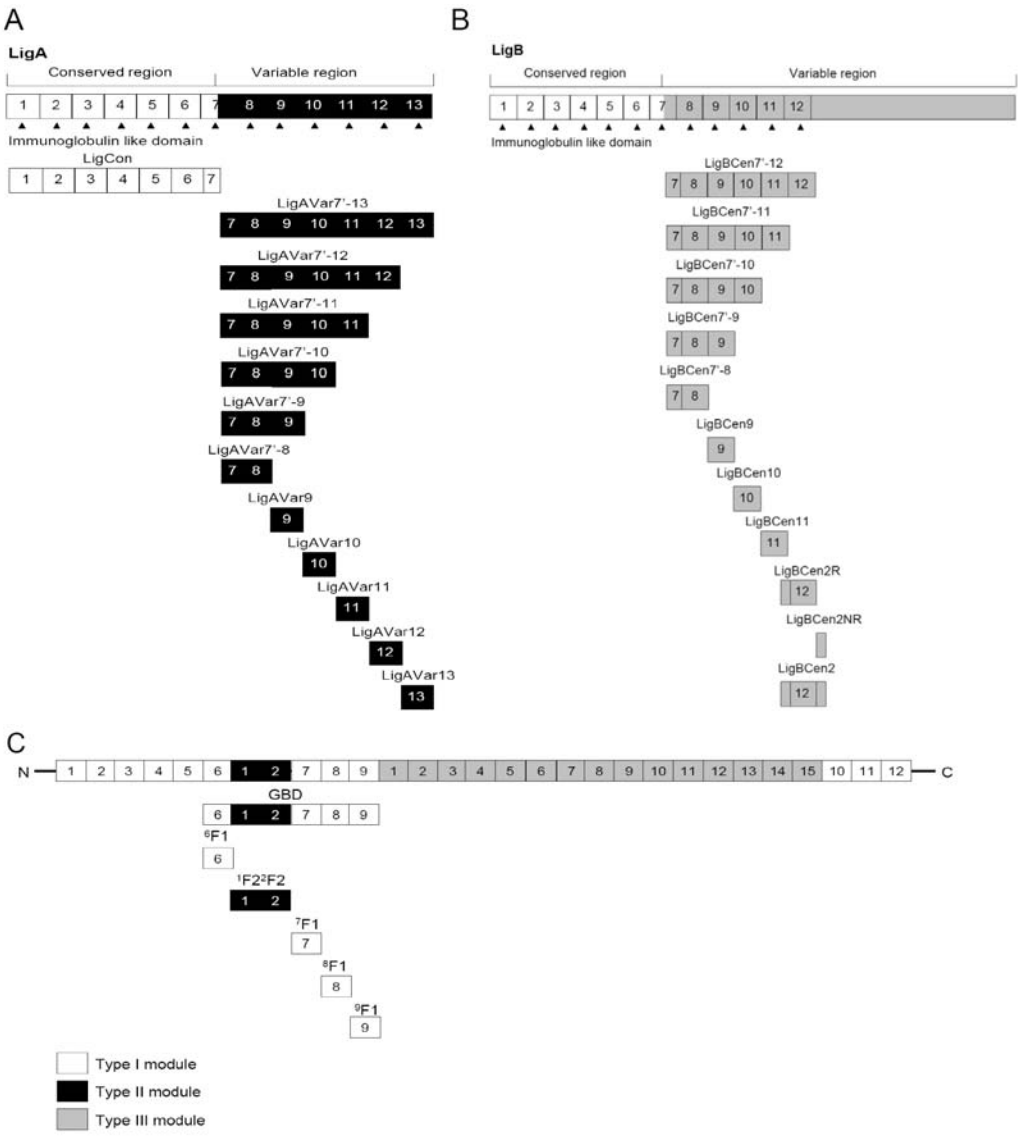

Figure 6.1 A schematic diagram showing the structure of truncated (A) LigA, (B) LigB , and (C) Fn used in this study.

^{6}F1, ^{1}F2^{2}F2, ^{7}F1, ^{8}F1, and ^{9}F1, primers were engineered to introduce an EcoRI site at the 5' end and a NotI site at the 3' end of each fragment. For constructing LigBCen7'-9, LigBCen7'-10, LigBCen7'-11, LigBCen7'-12, primers were engineered to introduce a BamHI site at the 5' end and a PstI site at the 3' end of each fragment. For constructing LigBCen7'-12, primers were engineered to introduce a SphI site at the 5' end and a HindIII site at the 3' end of each fragment. PCR products were sequentially digested with BamHI and SalI, EcoRI and NotI, BamHI and PstI, or SphI and HindIII and then ligated into pQE30, pGEX-4T-2, pPICZα or pET-THGT cut with BamHI and SalI, EcoRI and NotI, BamHI and PstI or, SphI and HindIII, respectively as previously described (15,31). For LigBCen2RW1073C mutant construction, the manufacturer's instructions of the Quickchange mutagenesis kit (Strategene, La Jolla, CA) were followed and has been described previously (15).

GBD binding assays by ELISA

1 μM of GBD or BSA (negative control and data not shown) in Tris buffer (25mM Tris and 150mM sodium chloride, pH 7.0) containing 100 μM of calcium chloride were coated onto microtiter plate wells as described previously (11). 100μL of different concentrations of GST fused LigBCon (negative control), LigBCen2 (positive control), LigBCen2R, or LigBCen2NR, (Figure. 6.2A), or biotinylated LigAVar7'-8, LigAVar9, LigAVar10, LigAVar11, LigAVar12, LigAVar13, LigBCen7'-8, LigBCen9, LigBCen10, LigBCen11, LigBCen7'-12 (positive control), LigAVar7'-13 (positive control), or LigCon (negative control) in Tris buffer containing 100 μM of calcium chloride were added subsequently (Figure. 6.3A and B). To measure the interaction of GBD and GST fusion proteins, rabbit anti-GST (1:200) and horseradish peroxidase-conjugated goat anti-rabbit IgG (1:1000) served as primary and secondary antibodies. To detect binding of the biotinylated proteins, HRP-conjugated streptavidin

(1:1000) was added to each well at RT for 1 hour prior to washing the wells thrice with TBST. The measurement of binding by ELISA was as described previously (15,16). To determine the dissociation constant (K_d), the data were fitted by the following equation using KaleidaGraph software (Version 2.1.3 Abelbeck software, Reading, PA), and the calculated K_d are listed in Table 6.3.

$$OD_{630} = \frac{OD_{630max}\,[\text{Lig proteins}]}{K_D + [\text{Lig proteins}]} \quad \text{(Eq. 1)}$$

Cell binding and inhibition assays by ELISA

To detect the binding of truncated Lig proteins to MDCK cells, MDCK cells (10^5) were incubated with 0, 0.08, 0.16, 0.3125, 0.625, 1.25, 2.5, or 5 μM of biotinylated LigBCen (positive control), GST (negative control), or truncated Lig proteins in 100 μL PBS for 1 h at 37℃ (Figure. 6.6A and B). For measuring the binding inhibition of *Leptospira* to MDCK cells by truncated Lig proteins, MDCK (10^5) cells were treated with 0, 0.08, 0.16, 0.3125, 0.625, 1.25, 2.5, or 5 μM of truncated Lig proteins, LigBCen (positive control), or GST (negative control) in 100 μL PBS for 1 h at 37℃ prior to the addition of Leptospira (107) for 6 h at 37℃ (Figure. 6.6C and D). To detect the binding of biotinylated Lig proteins, HRP-conjugated streptoavidine (1:1000 ×) was added subsequently. To measure the binding of *Leptospira*, hamster anit-Leptospira (1:200×) and HRP-conjugated goat anti-hamster IgG (1:1000×) were used as primary and secondary antibodies, respectively. The percentage of attachment was determined relative to the attachment of serovar Pomona on untreated MDCK cells. The measurement of binding by ELISA was as described previously (15,16). Each value represents the mean ± SEM of three trials in triplicate samples. Statistically significant ($P < 0.05$) differences are indicated by *.

Surface Plasmon Resonance (SPR)

Association and dissociation rate constants for the interaction of Lig proteins and GBD were measured by SPR analysis performed with a Biacore 2000 instrument (GE Healthcare) at 25^{o}C. 1.5μM of each His-tagged Lig protein, including LigAVar7'-8, LigVar10, LigAVar11, LigAVar12, LigAVar13, LigBCen7'-8, LigBCen9, or LigBCen2R in Tris buffer containing 100 μM calcium chloride, was immobilized on a NTA chip (GE Healthcare) conjugated with 500 μM nickel sulfate. Serial concentrations (0, 0.625, 1.25, 2.5, 5, 10, 20, 40μM) of GBD were injected into the flow cell at a flow rate of 5 μL/min over the immobilized Lig proteins. All experiments were duplicated. All sensogram data have been corrected by subtracting data from a control cell injected with Tris buffer containing 100 μM calcium chloride. Kinetic parameters were obtained by fitting the data to the one-step biomolecular association reaction model (1:1 Langmuir model) with the curve-fitting BIAevaluation software, version 3.0.

Isothermal Titration Calorimetry (ITC)

The experiments were carried out with a CSC 5300 microcalorimeter (Calorimetry Science Corp. Lindon, UT, USA) at 25^{o}C as previously described (15). In a typical experiment, the cell contained 1 ml of a GBD solution, ^{6}F1, ^{1}F2^{2}F2, ^{7}F1, ^{8}F1, or ^{9}F1 and the syringe contained 250 μl of a solution of LigBCen2R, LigAVar7'-8, LigAVar7'-9, LigAVar7'-10, LigAVar7'-11, LigAVar7'-12, LigAVar7'-13, LigBCen7'-8, LigBCen7'-9, LigBCen7'-10, LigBCen7'-11, or LigBCen7'-12. The concentration of LigBCen2R and GBD were 127μM and 6μM. The concentration of GBD and truncated Lig proteins are detailed in Table 6.4. Both solutions were in Tris buffer containing 100 μM of calcium chloride. The titration was performed as follows: 25 injections of 10 μl with a stirring speed of 250 rpm with a delay time between injections of 5min. Data

were analyzed using Titration Binding Work 3.1 software (Calorimetry Science Corp. Lindon, UT, USA) fitting them to an independent binding model.

Steady State Fluorescence Measurement

Steady state fluorescence emissions were measured on a Hitachi F7500 spectrofluorometer (Hitachi. San Jose, CA). All spectra were recorded in correct spectrum mode of the instrument using excitation and emission band passes of 2 nm. In order to measure the binding of GBD to LigBCen2R, LigBCen2RW1073C was expressed and labeled with Alexa-488. The labeling of Alexa-488 to LigBCen2RW1073C by the interaction of the cystein of LigBCen2RW1073 with Alexa Fluor 488 C_5 maleimide was performed following the manufacturer's instructions (Molecular probe). For the GBD titration, 1.62, 3.12, 6.25, 12.5, 25μM of GBD in Tris buffer containing 100μM of calcium chloride was mixed with 1μM of Alexa-488 labeled LigBCen2RW1073C in the same buffer. The fluorescence from Alexa-488 probe of Alexa-488 labeled LigBCen2RW1073C was recorded at the excitation wavelength of 490 nm, and the emission wavelength ranged from 500 to 600nm. All spectra were recorded at 25^{o}C after 5 minutes. Furthermore, the spectra of the various concentrations of GBD indicated above were also recorded and used to subtract the spectra of each Alexa-488 labeled LigBCen2RW1073C in the addition of certain concentrations of GBD. To determine the dissociation constant (K_D), the fluorescence intensities at 518nm were recorded and fitted by the following equation using KaleidaGraph software (Version 2.1.3 Abelbeck software):

$$F_{max}\text{-}F = \frac{(F_{max}\text{-}F_{min})\,[\,GBD]}{K_D + [\,GBD\,]} \quad \text{(Eq. 2)}$$

Where F_{max} is the fluorescence intensity of Alexa-488 labeled LigBCen2RW1073C protein in the absence of GBD, and F_{min} indicates the fluorescence intensity of

Alexa-488 labeled LigBCen2RW1073C saturated with GBD. In addition, F is the fluorescence intensity of Alexa-488 labeled LigBCen2RW1073C in the presence of various concentrations of GBD. All of the measurements were corrected for dilution and for inner filter effect.

Dynamic Light Scattering (DLS)

One mg per mL of LigAVar7'-8, LigAVar7'-9, LigAVar7'-10, LigAVar7'-11, LigAVar7'-12, LigAVar7'-13, LigBVar7'-8, LigBVar7'-9, LigBVar7'-10, LigBVar7'-11, or LigBVar7'-12 was dialyzed against prefiltered (0.22 μm Millipore filters) Tris buffer with 100 μM calcium chloride. The samples were placed in a 1mL plastic cuvette. The standard globular proteins including albumin (67,000 Da), ovalbumin (43,000 Da), chymotrypsinogen A (25,000 Da), ribonuclease A (13,700 Da), aprotinin (6,500 Da), or insulin chain B (3,400 Da) were used to generate the calibration curve of globular proteins. The automated measurements were collected with a Zetasizer Nano ZS instrument (Malvern Instruments Ltd., Worcestershire, United Kingdom), using a 2 min equilibrium delay at each measurement. The data were adjusted using the method of cumulants to obtain the hydrodynamic radius (R_h). The logarithms of the R_h values of standards and above proteins were plotted against the logarithm of the protein molecular weights to fit the equation

$$\log M_W = a \cdot \log R_h + b \quad \text{(Eq. 3)}$$

where a and b are constants.

Raman Spectroscopy

LigAVar7'-12, LigAVar7'-13, LigBCen7'-11, LigBCen7'-12 or the mixture of certain Ig-like domains of LigA or LigB was concentrated with an Amincon ultrafiltration device (Millipore, Billerica, MA) to the final concentration as 3mg/mL determined by

UV absorption spectrophotometry and dialyzed against Tris buffer with 100μM of calcium chloride (36). For the experiments performed in D_2O, the proteins were lyophilized, dissolved by D_2O, and stored at 4°C for 20 hours prior to acquisition of Raman spectra. A 10μL aliquot of the protein solution was applied to a Renishaw InVia micro-Raman spectrophotometer using long-range 50× objective, 30sec. integration, and 10% laser power (785nm excitation; 8mW at 100%)(37). The spectra were corrected by subtracting the buffer and background. Peak height was normalized to 1002cm^{-1} band of phenylalanine as the internal standard(36).

Circular dichroism (CD) spectroscopy

CD analysis was performed on an Aviv 215 spectropolarimeter (Lakewood, NJ) under N_2 atmosphere. CD spectra were measured at RT (25°C) in a 1-cm path length quartz cell. Spectra of 10 μM of LigBCen2R, and LigBCen2RW1073C were recorded in Tris buffer with 100μM calcium chloride. Structural changes in LigBCen2R upon binding to the GBD of Fn were examined by analyzing changes in the CD spectrum. To determine the secondary structure, three far-UV CD spectra of all those proteins mentioned above were recorded from 190 to 250 nm for far-UV CD in 1 nm increments at 25°C. The background spectrum of buffer without protein was subtracted from the protein spectra. CD spectra were initially analyzed by the software accompanying the spectrophotometer. Analysis of spectra to extrapolate secondary structures was performed by Dichroweb (http://www.cryst.bbk.ac.uk/cdweb/html/home.html) using the K2D and Selcon 3 analysis programs (11,12).

Transmission Electron Microscopy (TEM)

10μM of a small drop of LigAVar7'-12, LigAVar7'-13, LigBCen7'-11, or LigBCen7'-12 was added to an extremely thin copper grid. After drying for 5 min,

Table 6.3 The Dissociation constants and Kinetic data of GBD-Lig interactions determined by ELISA and SPR.

The association and dissociation data of the interactions were fitted locally using one the step biomolecular reaction model (1:1 Langmuir model : $A + B \leftrightarrows AB$), which resulted in optimum mathematical fits reflected by the lowest Chi values. The values for association rate constants (k_{on}), dissociation rate constants (k_{off}), and dissociation constants (K_D) were calculated from the binding data by BIAevaluation software.

Analyte	k_{on}	k_{off}	K_D[a]	K_D[b]
	$M^{-1}S^{-1}\times10^{3}$	$S^{-1}\times10^{-3}$	$M^{-1}\times10^{-6}$	$M^{-1}\times10^{-6}$
LigAVar7'-8	0.75±0.05	5.01±0.82	6.68±0.80	6.75±0.10
LigAVar9	n.d.[c]	n.d.[c]	n.d.[c]	n.b.[d]
LigAVar10	1.19±0.43	5.06±0.25	4.25±0.72	3.94±0.32
LigAVar11	1.19±0.49	5.99±0.13	5.04±0.32	4.70±0.24
LigAVar12	2.36±0.38	6.78±0.84	2.87±0.30	2.44±0.87
LigAVar13	0.51±0.09	5.30±0.43	10.40±2.53	10.96±0.41
LigBCen7'-8	3.57±0.25	9.63±0.18	2.69±0.70	2.27±0.15
LigBCen9	0.56±0.03	4.73±0.24	8.39±0.81	8.37±0.72
LigBCen10	n.d.[c]	n.d.[c]	n.d.[c]	n.b.[d]
LigBCen11	n.d.[c]	n.d.[c]	n.d.[c]	n.b.[d]
LigBCen2R	4.83±0.54	9.23±0.24	1.91±0.40	1.89±0.22

[a] determined by SPR

[b] determined by ELISA

[c] not determined

[d] no binding

Figure 6.2 Determination of binding constant, kinetics and thermodynamics of the LigBCen2R/NTD interaction by ELISA, SPR, and ITC. (A) Binding of serial concentrations of LigBCen2NR to immobilized NTD by ELISA. Serial concentrations of GST-LigBCen2R, GST-LigBCen2NR, GST-LigBCen2 (positive control), or GST-LigCon (negative control) were added to 1μM of GBD or BSA coated wells (negative control, data not shown). (B) SPR analysis of LigBCen2R interacting with GBD. 1.5μM of Recombinant Histidine-tagged LigBCen2R was immobilized on the surface of a Ni-NTA chip. GBD in Tris Buffer containing 100μM $CaCl_2$ at pH 7.5 flowed through the chip and the concentrations of GBD ranged from 40 to 0.625μM (from top to bottom). The K_D, k_{on}, and k_{off} were obtained from the average of duplicate experiments shown in Table 2. (C) Determination of the binding affinity by ITC. The cell contained 1 ml of GBD and the syringe contained 250 μl of LigBCen2R (upper panel). Heat differences obtained from 25 injections of LigBCen2R; (lower panel). Integrated curve with experimental data (◇) and the best fit (—). The thermodynamic parameters are shown as the average of duplicate experiments (K_D = 1.80 ± 0.14μM, ΔH = -26.72 ± 2.40 kcal mol^{-1}, TΔS = -18.91 ± 2.35 kcal mol^{-1} K^{-1}), and the molar ratio of LigBCen2R to GBD is 1:1. (D) Fluorescence spectrum of Alexa-488 labeled LigBCen2RW1073C in the presence and absence of GBD. One μM of Alexa-488 labeled LigBCen2RW1073C in Tris buffer was excited at 485 nm. Aliquots of GBD from respective stock solutions were added. The figure shows Alexa488 fluorescence in the presence of 0, 1.62, 3.12, 6.25, 12.5, 25μM of GBD (Inner plot). The determination of K_D of Alexa488 labeled LigBCen2RW1073C and GBD by monitoring the quenching fluorescence intensity of Alexa488 labeled LigBCen2RW1073C titrated by GBD. The emission wavelength recorded in this figure was 513nm, and K_D was revealed by fitting the data point into the equation described in materials and methods (K_D = 2.03±0.4μM).

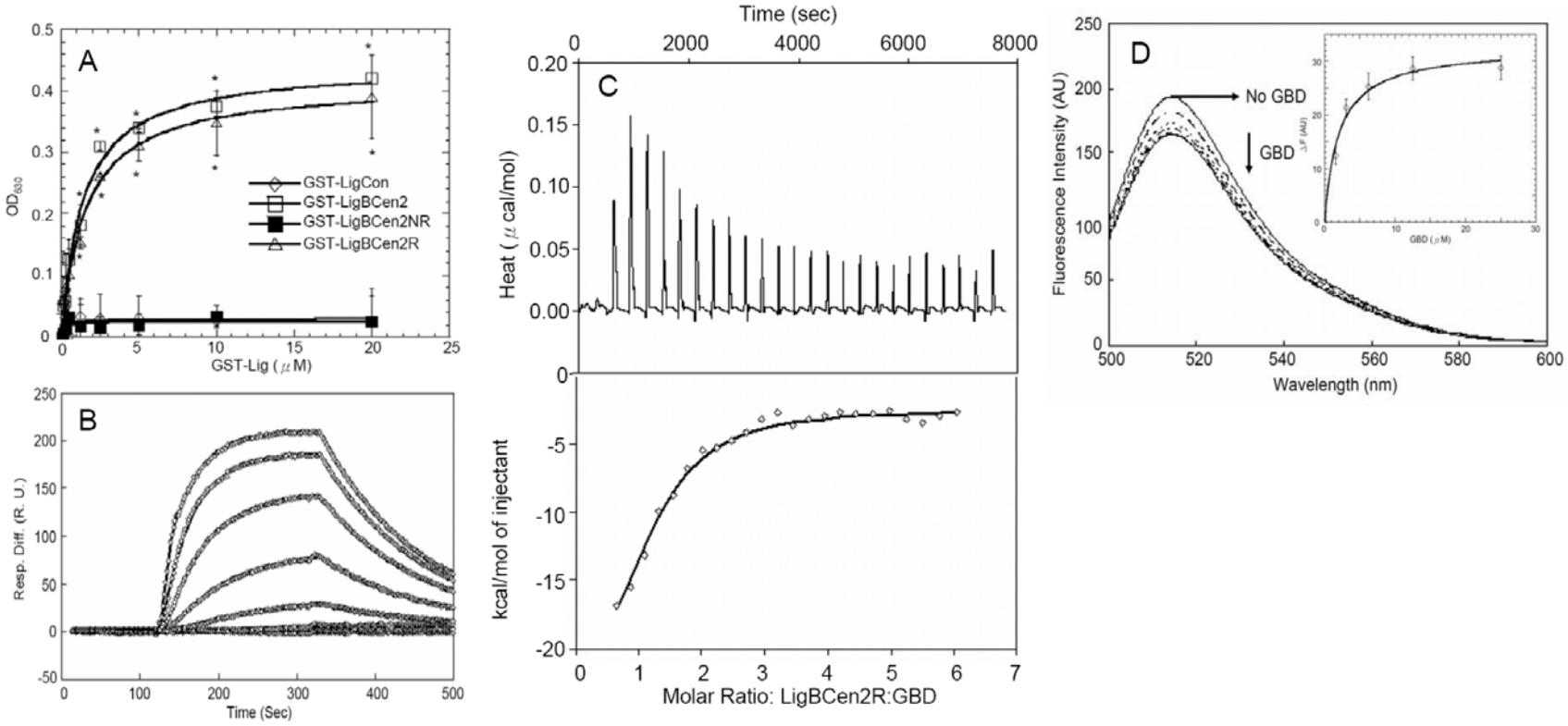
A
OD600
GST-Lig (μM)
GST-LigCon
GST-LigBCen2
GST-LigBCen2NR
GST-LigBCen2R
B
Resp. Diff. (R. U.)
Time (Sec)
C
Time (sec)
Heat (μcal/mol)
kcal/mol of injectant
Molar Ratio: LigBCen2R:GBD
D
No GBD
GBD
Fluorescence Intensity (AU)
Wavelength (nm)
ΔF (AU)
GBD (μM)

negative staining was performed by adding 5μL methylamine tungstate to the protein samples. The sample was examined in a FEI Tecnai G2 T12 Spirit TEM STEM (FEI, Hillsboro, OR). Typically, the magnification was 50,000×.

Statistical analysis

Significant differences between samples were determined using the Student's t-test following logarithmic transformation of the data. Two-tailed P-values were determined for each sample and a P-value <0.05 was considered significant. Each data point represents the meaṇ ± standard error of the mean (SEM) for each sample tested in triplicate. An (*) indicates the result was statistically significant.

Results

GBD binds to LigBCen2R

In order to fine map the GBD binding site of LigBCen2, LigBCen2 was truncated into LigBCen2R and LigBCen2NR (13). LigBCen2R and LigBCen2NR were then tested to determine if they can bind to GBD. LigCon, a conserved region of both LigA and B, was included as a negative control since it does not bind to Fn (11,12). GBD could immobilize LigBCen2R, but not LigBCen2NR (Figure. 6.2A). Moreover, ITC and SPR were also applied to measure the binding of LigBCen2R to GBD. The K_D obtained from both experiments (ITC, K_D = 1.80μM; SPR, K_D = 1.91μM) agreed with the binding affinity of LigBCen2R-GBD obtained by ELISA (K_D = 1.89μM) (Figure. 6.2B and C, Table 6.3). Moreover, the favorable enthalpy and unfavorable entropy obtained from the ITC experiment suggests the interaction is driven by enthalpy and mediated by hydrogen bonds or charge-charge interactions (Figure. 6.2C). Significant quenching (approximately16% decrease) was found in the Alexa-488 fluorescence spectra of Alexa-488 labeled LigBCen2RW1073C, a LigBCen2 mutant lacking its sole

Figure 6.3 Localization of the GBD-binding domains on Lig proteins. (A and B) Various concentrations (0, 0.3125, 0.625, 1.25, 2.5, 5, 10, 20μM) of biotinylated LigCon (negative control), and (A) LigAVar7'-13 (positive control), LigAVar7'-8, LigAVar9, LigAVar10, LigAVar11, LigAVar12, LigAVar13, (B) LigBCen7'-12 (positive control), LigBCen7'-8, LigBCen9, LigBCen10, LigBCen11 were added to wells coated with 1μM of GBD or BSA (negative control and data not shown) in Tris buffer. The binding of biotinylated proteins to GBD was measured by ELISA. For all experiments, each value represents the mean± SEM of three trials in triplicate samples. Statistically significant ($p < 0.05$) differences compared to the negative control are indicated by an asterisk. (C and D) SPR analysis of Ig-like domains of Lig interacting with GBD 1.5 μM of Recombinant Histdine-tag (C) LigAVar7'-8, LigAVar10, LigAVar11, LigAVar12, LigAVar13, (D) LigBCen7'-8, LigBCen9, or LigBCen2R was immobilized on the surface of Ni-NTA chip. GBD in Tris Buffer containing 100μM $CaCl_2$ at pH 7.5 was flowed through the chip and the concentration of GBD ranged from 40 to 0.625 μM. Only the response sensograms of the 40 μM of GBD are shown. The K_D, k_{on}, k_{off} were obtained from the average of duplicate experiments shown in Table 6.3.

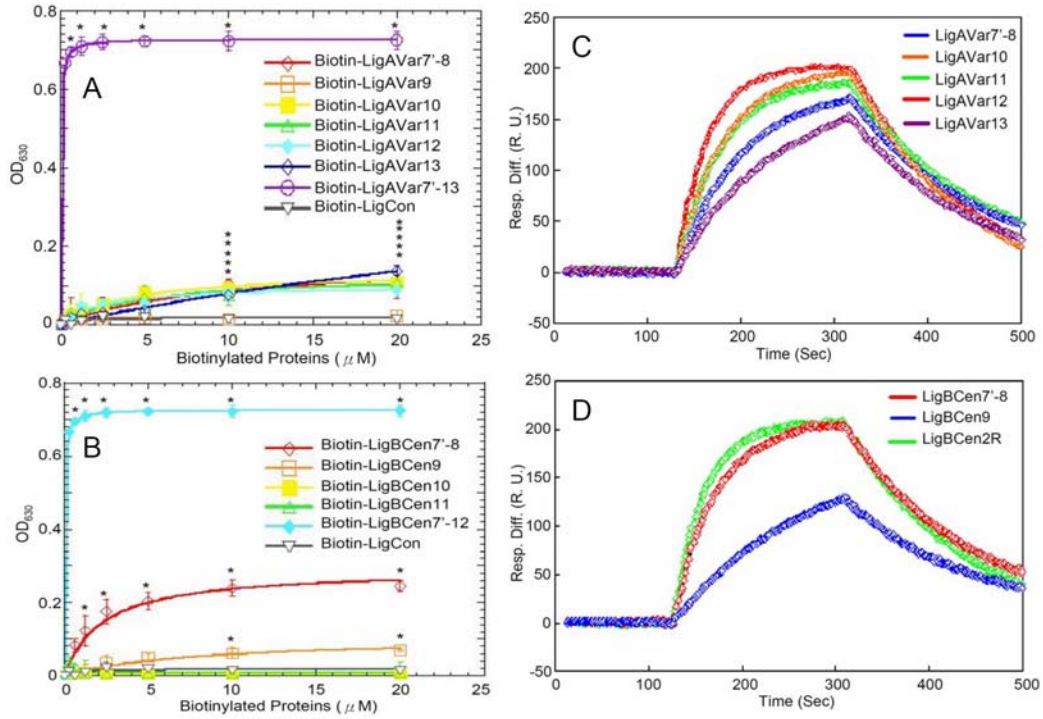
A
Biotin-LigAVar7'-8
Biotin-LigAVar9
Biotin-LigAVar10
Biotin-LigAVar11
Biotin-LigAVar12
Biotin-LigAVar13
Biotin-LigAVar7'-13
Biotin-LigCon
OD630
Biotinylated Proteins (μ M)
B
Biotin-LigBCen7'-8
Biotin-LigBCen9
Biotin-LigBCen10
Biotin-LigBCen11
Biotin-LigBCen7'-12
Biotin-LigCon
OD630
Biotinylated Proteins (μ M)
C
LigAVar7'-8
LigAVar10
LigAVar11
LigAVar12
LigAVar13
Resp. Diff. (R. U.)
Time (Sec)
D
LigBCen7'-8
LigBCen9
LigBCen2R
Resp. Diff. (R. U.)
Time (Sec)

tryptophan, when GBD was added with dose dependence confirming that GBD binding induces conformational changes in LigBCen2R (Figure. 6.2D). The undistinguished far-UV CD spectra of LigBCen2R and LigBCen2RW1073C (Figure. 6.9) and the K_D of the interaction of GBD-LigBCen2RW1073C determined by florescence spectroscopy (K_D = 1.93μM) is close to that of the GBD-LigBCen2R interaction determined above and rules out the possibility that the mutation alters the structure of LigBCen2R or the binding of LigBCen2R and GBD.

Determination that Ig-like domains interact with GBD

Since LigBCen2R containing the partial 11th and full 12th Ig-like domain of LigB shows GBD binding activity, we used ELISA to investigate whether the variable regions of LigA and LigB interact with GBD. As presented in Figure. 6.3A and B, LigAVar7'-8, LigAVar10, LigAVar11, LigAVar12, and LigAVar13 in LigA and LigBCen7'-8 and LigBCen9 of LigB are able to bind GBD (LigAVar7'-8, K_D = 6.75μM; LigAVar10, K_D = 3.94μM; LigAVar11, K_D = 4.70μM; LigAVar12, K_D = 2.44μM, LigAVar13, K_D = 10.96μM; LigBCen7'-8, K_D = 2.27μM; LigBCen9, K_D = 8.37μM) (Table 6.3). Furthermore, a similar K_D obtained from SPR also confirms the binding of certain variable regions of LigA and LigB with GBD (LigAVar7'-8, K_D = 6.68μM; LigAVar10, K_D = 4.25μM; LigAVar11, K_D = 5.04μM; LigAVar12, K_D = 2.87μM, LigAVar13, K_D = 10.39μM; LigBCen7'-8, K_D = 2.69μM; LigBCen9, K_D = 8.44μM)(Figure. 6.3C and D, Table 6.3). These results suggest that the GBD also binds to certain variable regions of LigA and LigB.

Table 6.4 Thermodynamic parameters for the interaction of GBD and truncated Lig proteins

	[Lig Proteins]	[GBD]	ΔH	TΔS	K_D	ΔG	n	1/n
	μM	μM	kcal mol^{-1}	kcal mol^{-1} K^{-1}	μM	kcal mol^{-1}	Lig: GBD	GBD: Lig
LigAVar7'-8	20	1	-28.65±5.14	-21.62	6.75±0.11	-7.02	1.010±0.04	0.99
LigAVar7'-9	20	1	-29.24±4.75	-22.15	6.11±0.12	-7.08	1.020±0.08	0.98
LigAVar7'-10	20	1	-25.32±2.27	-18.04	4.35±0.43	-7.28	0.510±0.02	1.96
LigAVar7'-11	10	1	-22.08±3.31	-14.60	3.13±0.48	-7.47	0.335±0.05	2.98
LigAVar7'-12	10	2	-30.79±1.74	-23.16	2.41±0.29	-7.63	0.255±0.09	3.92
LigAVar7'-13	10	2.5	-70.96±0.73	-62.47	0.055±0.02	-9.85	0.204±0.04	4.90
LigBCen7'-8	20	1	-20.37±3.62	-12.71	2.28±0.09	-7.66	0.985±0.03	1.01
LigBCen7'-9	20	1	-21.05±5.02	-13.06	1.31±0.19	-7.99	0.520±0.05	1.92
LigBCen7'-10	20	1	-26.72±1.92	-18.75	1.35±0.19	-7.97	0.510±0.04	1.96
LigBCen7'-11	20	1	-29.01±4.23	-21.06	1.39±0.08	-7.95	0.479±0.08	2.08
LigBCen7'-12	10	1	-57.93±2.74	-48.09	0.056±0.007	-9.84	0.320±0.018	3.12

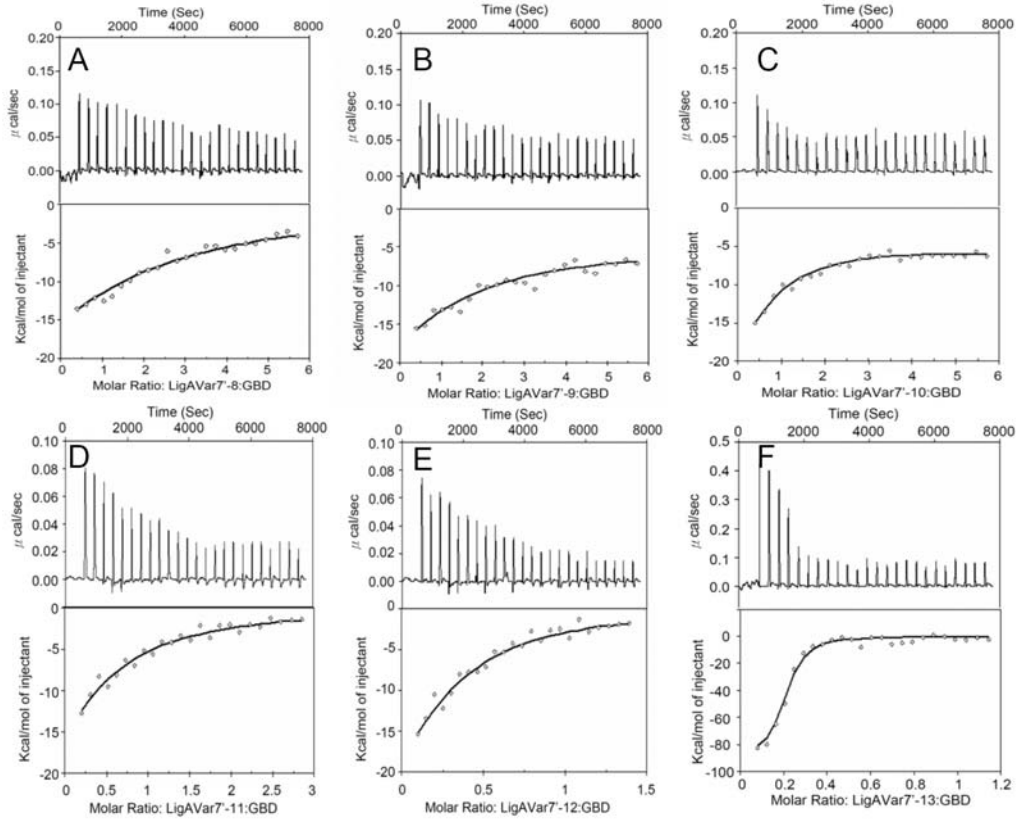

Figure. 6.4 ITC isotherms showing the binding of GBD to various length LigA constructs. The cell contained 1 ml of GBD and the syringe contained 250µl of (A) LigAVar7'-8, (B) LigAVar7'-9, (C) LigAVar7'-10, (D) LigAVar7'-11, (E) LigAVar7'-12, (F) LigAVar7'-13 (upper panel). Heat differences obtained from 25 injections of truncated LigA (lower panel); Integrated curve with experimental data (◇) and the best fit (—). The thermodynamic parameters are shown as the average of duplicate experiments in Table 6.4.

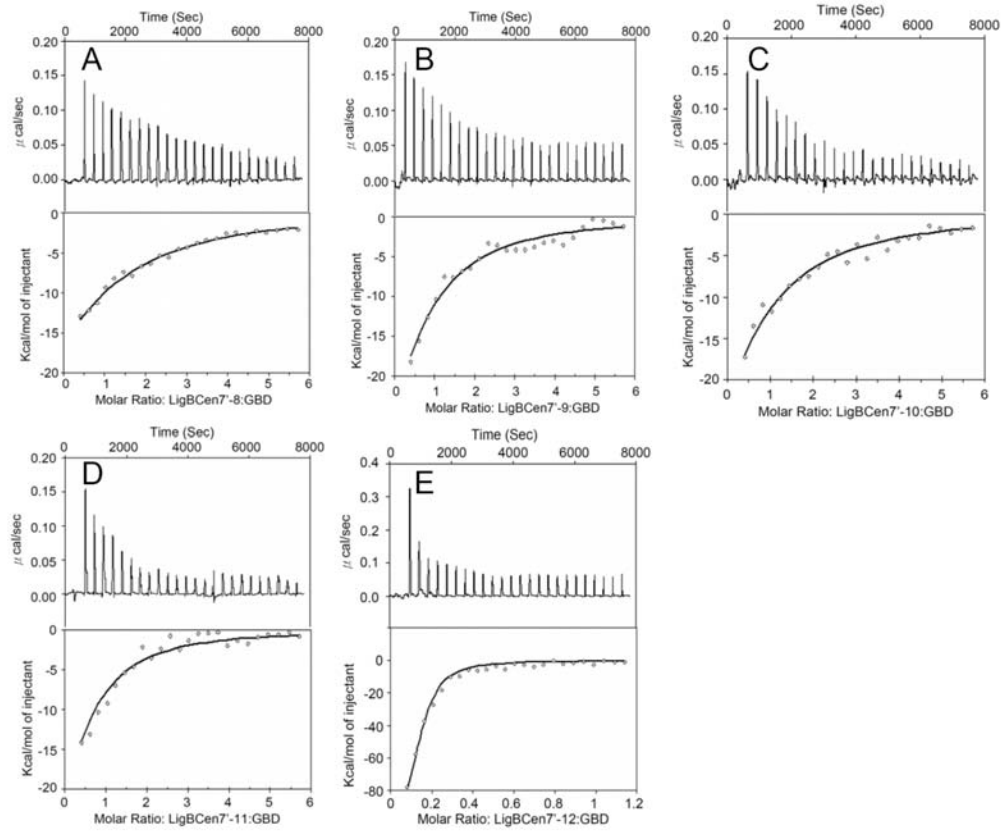

Figure. 6.5 ITC isotherms showing the binding of GBD to various length LigB constructs. The cell contained 1 ml of GBD and the syringe contained 250μl of (A) LigBCen7'-8, (B) LigBCen7'-9, (C) LigBCen7'-10, (D) LigBCen7'-11, (E) LigBCen7'-12 (upper panel). Heat differences obtained from 25 injections of truncated LigB (lower panel); Integrated curve with experimental data (◇) and the best fit (—). The thermodynamic parameters are shown as the average of duplicate experiments in Table 6.4.

Figure. 6.6 Multivalent binding of Lig proteins to MDCK cells reduces leptospiral adhesion. (A and B) Binding of truncated Lig proteins to MDCK cells. Various concentrations (0.08, 0.16, 0.3125, 0.625, 1.25, 2.5, 5μM) of biotinylated LigCon (negative control), LigBCen (positive control), and (A) LigAVar7'-13, LigAVar7'-12, LigAVar7'-11, LigAVar7'-10, LigAVar7'-9, LigAVar7'-8, (B) LigBCen7'-12, LigBCen7'-11, LigBCen7'-10, LigBCen7'-9, LigBCen7'-8 were added to MDCK cells (10^5), and binding was measured by ELISA. (C and D) Truncated Lig proteins inhibit the binding of *Leptospira* to MDCK cells. MDCK cells were incubated with various concentrations (0.08, 0.16, 0.3125, 0.625, 1.25, 2.5, 5μM) of biotinylated -$LigB_{1706\text{-}1716}$, or biotin (negative control) (C) LigAVar7'-13, LigAVar7'-12, LigAVar7'-11, LigAVar7'-10, LigAVar7'-9, LigAVar7'-8, (D) LigBCen7'-12, LigBCen7'-11, LigBCen7'-10, LigBCen7'-9, LigBCen7'-8 prior to the addition of *Leptospira* (10^7). The adhesion of *Leptospira* to MDCK cells (10^5) was detected by ELISA. The reduced percentage of attachment was determined relative to the attachment of *Leptospira* on untreated MDCK cells. Each value represents the mean± SEM of three trials in triplicate samples. Statistically significant values ($P<0.05$) are indicted by *.

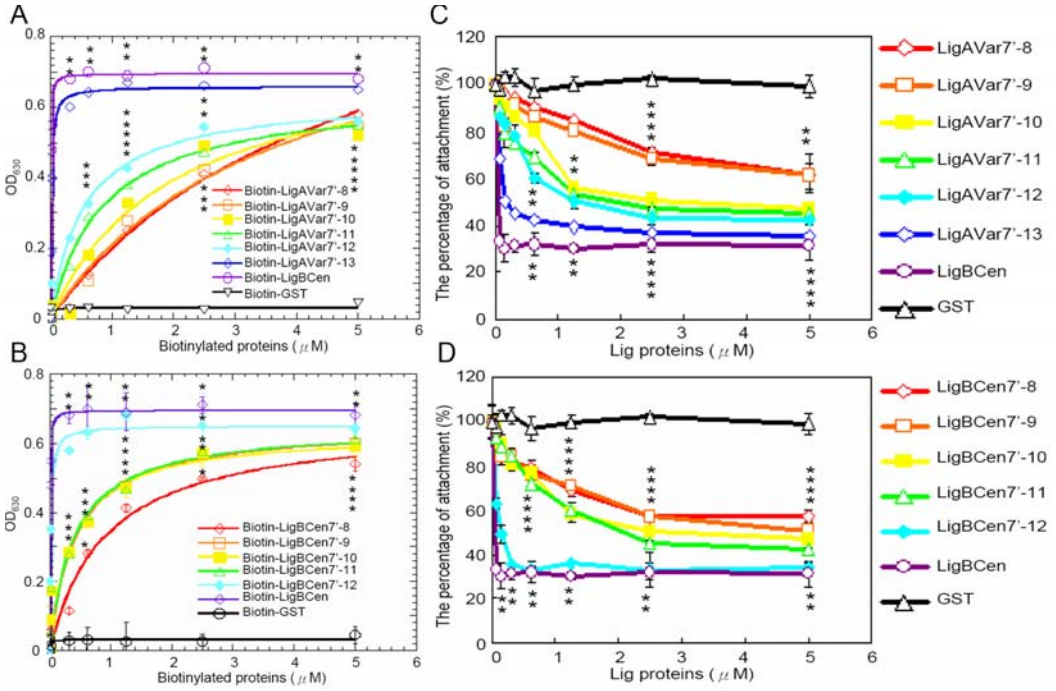
A
B
C
D
OD450
Biotinylated proteins (μM)
Biotin-LigAVar7'-8
Biotin-LigAVar7'-9
Biotin-LigAVar7'-10
Biotin-LigAVar7'-11
Biotin-LigAVar7'-12
Biotin-LigAVar7'-13
Biotin-LigBCen
Biotin-GST
Biotin-LigBCen7'-8
Biotin-LigBCen7'-9
Biotin-LigBCen7'-10
Biotin-LigBCen7'-11
Biotin-LigBCen7'-12
The percentage of attachment (%)
Lig proteins (μM)
LigAVar7'-8
LigAVar7'-9
LigAVar7'-10
LigAVar7'-11
LigAVar7'-12
LigAVar7'-13
LigBCen
GST
LigBCen7'-8
LigBCen7'-9
LigBCen7'-10
LigBCen7'-11
LigBCen7'-12

Ig-like domains of Lig proteins interact with GBD and MDCK cells through multivalency

Multivalency is a strategy by which a pathogen's virulence factors containing tandem repeated regions interact with their binding partners (33). In order to investigate if multivalency is adopted by the repeated Ig-like domains of Lig proteins to bind to GBD, the truncated proteins of each construct of the variable regions of LigA ad LigB were purified. The stoichiometry and binding affinities of those truncated proteins and GBD were measured by ITC. As shown in Figure. 6.4 and 6.5 a slight increase in affinity toward GBD was observed as the number of Ig-like domains increased. (LigAVar7'-8, K_D = 6.75μM; LigAVar7'-9, K_D = 6.11μM; LigAVar7'-10, K_D = 4.35μM; LigAVar7'-11, K_D = 3.13μM; LigAVar7'-12, K_D = 2.41μM; LigBCen7'-8, K_D = 2.28μM; LigBCen7'-9, K_D = 1.31μM; LigBCen7'-10, K_D = 1.35μM; LigBCen7'-11, K_D = 1.39μM) (Table 6.4). Interestingly, the last Ig-like domain of both LigA and LigB contributed more than the other Ig-like domains because the GBD binding affinity of LigAVar7'-13 and LigBCen7'-12 increased 43 fold and 24 fold, respectively compared to that of LigAVar7'-12 and LigBCen7'-11, the truncated proteins lacking the last Ig-like domain (LigAVar7'-13, K_D = 0.055μM; LigBCen7'-12, K_D = 0.056μM). This suggests the possibility of cooperative binding in each LigAVar7'-13-GBD and LigBCen7'-12-GBD interaction. On the other hand, based on the one-site binding model, the 1/n values are in agreement with the stoichiometry of GBD to Lig predicted by the different binding affinities of various Ig-like domains reported above (Table 6.4 and 6.4). These results indicate that Lig proteins bind to GBD through multivalency. In order to show the physiological relevance of the multivalent binding between Lig proteins and GBD, the interaction of truncated Lig proteins and MDCK cells was detected by ELISA. As shown in Figure. 6.6A and B, the more Ig-like domains included in the Lig constructs, the greater the binding of Lig proteins to MDCK cells.

Table 6.5 Estimated radii of recombinant truncated Lig proteins

Truncated Lig proteins	R_h	Truncated Lig proteins	R_h
	nm		nm
LigAVar7'-8	1.57	LigBCen7'-8	1.56
LigAVar7'-9	2.35	LigBCen7'-9	2.46
LigAVar7'-10	3.81	LigBCen7'-10	3.62
LigAVar7'-11	5.25	LigBCen7'-11	5.37
LigAVar7'-12	6.03	LigBCen7'-12	3.45
LigAVar7'-13	3.79		

Figure 6.7 Terminal Ig-like domains contribute to the compact structure of Lig proteins. (A) Dynamic light scattering of standard molecular mass markers, LigAVar7'-13, LigAVar7'-12, LigAVar7'-11, LigAVar7'-10, LigAVar7'-9, LigAVar7'-8, LigBCen7'-12, LigBCen7'-11, LigBCen7'-10, LigBCen7'-9, LigBCen7'-8. The hydrodynamic radius (R_h) is plotted as a function of the molecular weight of each individual protein on a log-log scale. The molecular weights of the standards are indicated in Materials and Methods, and the molecular weight of the truncated Lig proteins are indicated in Table 5. (B to E) Comparative Raman spectroscopy of full-length LigAVar7'-12, LigAVar7'-13, LigBCen7'-11, LigBCen7'-12 and a stoichiometic mixture of its composite domains. The Raman spectra of full length or stoichiometrically mixed separated Ig-like domains of (B) LigAVar7'-12, (C) LigAVar7'-13, (D) LigBCen7'-11, and (E) LigBCen7'-12 were recorded in D_2O and H_2O.

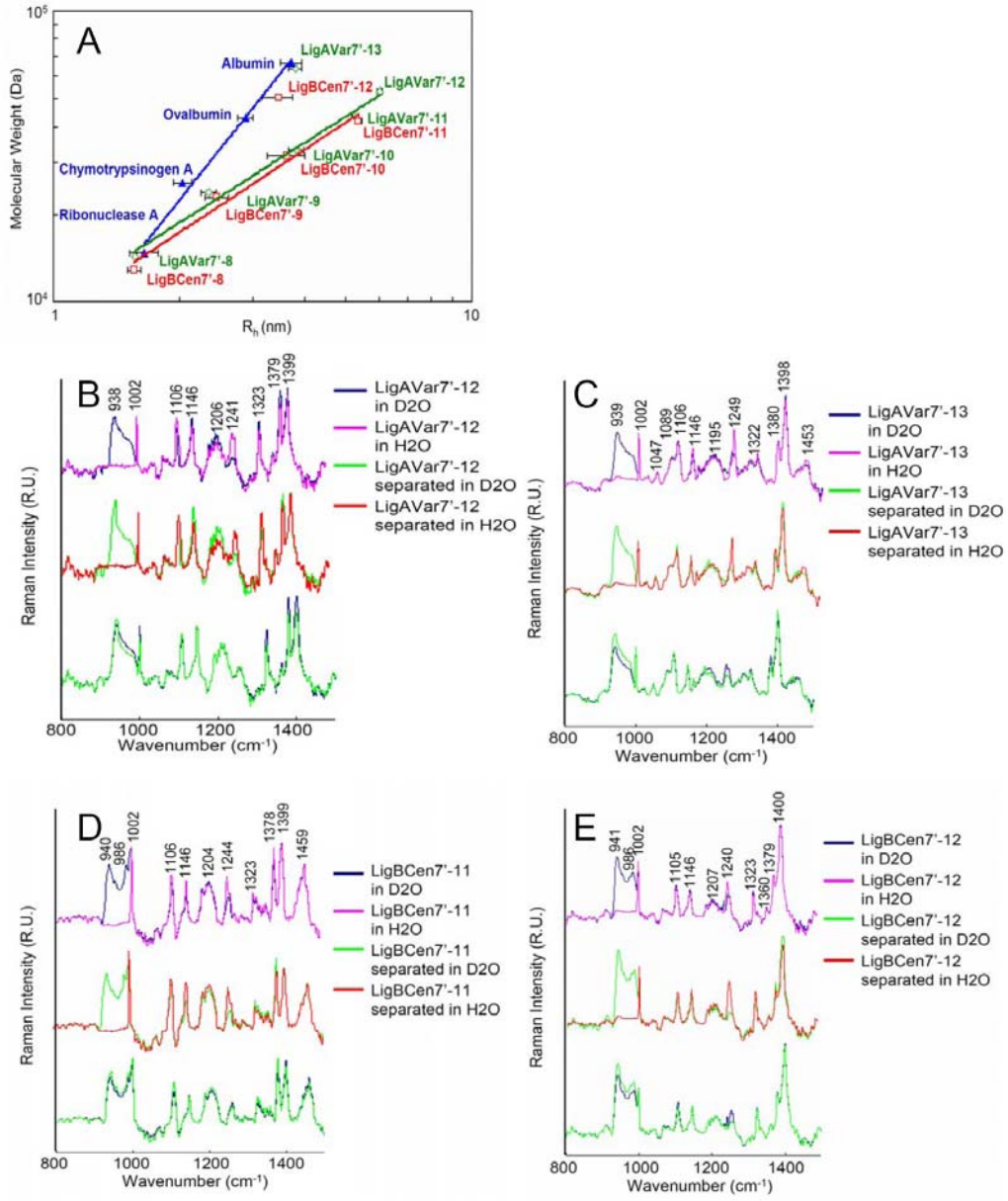
A
Molecular Weight (Da)
10^5
10^4
1
10
R_h (nm)
Albumin
Ovalbumin
Chymotrypsinogen A
Ribonuclease A
LigAVar7'-13
LigBCen7'-12
LigAVar7'-12
LigAVar7'-11
LigBCen7'-11
LigAVar7'-10
LigBCen7'-10
LigAVar7'-9
LigBCen7'-9
LigAVar7'-8
LigBCen7'-8
B
938
1002
1106
1146
1206
1241
1323
1379
1399
LigAVar7'-12 in D2O
LigAVar7'-12 in H2O
LigAVar7'-12 separated in D2O
LigAVar7'-12 separated in H2O
Raman Intensity (R.U.)
800
1000
1200
1400
Wavenumber (cm^{-1})
C
939
1002
1047
1089
1106
1146
1195
1249
1322
1380
1398
1453
LigAVar7'-13 in D2O
LigAVar7'-13 in H2O
LigAVar7'-13 separated in D2O
LigAVar7'-13 separated in H2O
Raman Intensity (R.U.)
800
1000
1200
1400
Wavenumber (cm^{-1})
D
940
986
1002
1106
1146
1204
1244
1323
1378
1399
1459
LigBCen7'-11 in D2O
LigBCen7'-11 in H2O
LigBCen7'-11 separated in D2O
LigBCen7'-11 separated in H2O
Raman Intensity (R.U.)
800
1000
1200
1400
Wavenumber (cm^{-1})
E
941
986
1002
1105
1146
1207
1240
1323
1360
1379
1400
LigBCen7'-12 in D2O
LigBCen7'-12 in H2O
LigBCen7'-12 separated in D2O
LigBCen7'-12 separated in H2O
Raman Intensity (R.U.)
800
1000
1200
1400
Wavenumber (cm^{-1})

Surprisingly, the terminal domains of Lig proteins also proved pivotal since the binding was strongly promoted when the Lig constructs contained the terminal Ig-like domains (Figure. 6.6A and B). Similarly, the inhibition of leptospiral adhesion to MDCK cells was also mediated by multivalent binding between Ig-like domains and cells due to the more significant inhibition when the cells were pre-mixed with the truncated Lig roteins including more Ig-like domains (Figure. 6.6C and D). The ability or Lg proteins to inhibit bind was also significantly increased when the constructs included the last Ig-like domains (Figure. 6.6C and D).

The terminal Ig-like domains contribute to compact structures of Lig proteins

LigAVar13 and LigBCen12, the terminal Ig-like domains of Lig proteins, play a very important role in GBD binding, but the GBD binding affinity of LigAVar13 or LigBCen12 (LigAVar13, K_D=10.39±2.53 uM; LigBCen2R (containing LigBCen12), K_D= 1.91±0.40 uM) alone was not significantly different from that of other Ig-like domains (Table 6.4). Therefore, the global structure of Lig proteins with the terminal domains plays an important role in the binding affinity of Lig protein and GBD. As presented in Table 6.5, the hydrodynamic radii (R_h) of truncated Lig proteins and other standard globular proteins were determined by dynamic light scattering. In addition, the logarithm of R_h was plotted against the molecular mass of each standard using equation 3 in Materials and Methods, and a calibration curve of each globular protein or each truncated Lig protein was constructed (Figure. 6.7A). According to the results in Figure. 6.7A, the R_h values for LigAVar7'-13 and LigBCen7'-12 are comparably closing to that of the calibration curve of the globular protein standard suggesting both LigAVar7'-13 and LigBCen7-12 are globular proteins that possesses compact structures. However, the R_h of truncated Lig proteins without terminal Ig-like domains aligned in calibration curves distinct from the curve established by the R_h of the globular protein standards

indicating that the Lig proteins without the terminal Ig-like domains are not globular proteins (Figure. 6.7A and Table 6.5) but still possess a folded structure, especially with a rich β-strand due to the positive peak in 1241nm and 1244nm (amide III band) of the Raman spectra of LigAVar7'-12 and LigBCen7'-11, respectively (Figure. 6.7B and C).

In order to test if interdomain interactions contribute to the compact structure of truncated Lig proteins with terminal domains, LigAVar7'-13, LigAVar7'-12, LigBCen7'-12, LigBCen7'-11, and stoichiometric mixture of Ig-like domains were pplied to Raman spectrophotometer in H_2O or D_2O. The deuterium-exchange reaction showed a more significant isotopic effect on the amide III band than the amide I band. To elucidate the secondary structure of the proteins (38), the amide III band in the spectra of truncated Lig proteins were specifically identified in this study. As shown on Figure. 6.7B, C, D, and E, the positive peak in 1241 cm^{-1}, 1249 cm^{-1}, 1244 cm^{-1}, 1240 cm^{-1} (amide III) observed in the spectra of full-length or stoichiometrically mixed LigAVar7'-12, LigAVar7'-13, LigBCen7'-11, and LigBCen7'-12 in H_2O indicated that certain Lig truncations harbor a β-strand structure, which confirmed the previous findings for Ig-like domains of LigB (13,15,16,38). The positive peak at 938 cm^{-1}, 939 cm^{-1}, 940 cm^{-1}, 941 cm^{-1}, and 986 cm^{-1} (amide III) in the spectra of Lig proteins measured in D2O support the conclusion that truncated Lig proteins contain a β-strand rich structure (Figure. 6.7B, C, D, and E)(38). Interestingly, the hydrogen-deuterium exchange (NH → ND) in full-length LigAVar7'-13 or LigBCen7'-12 was not as significant as that of stoichiometric mixture of Ig-like domains due to lower intensities of the β-strand marker, 1249 cm-1 and 1240 cm-1 in the spectrum of full-length LigAVar7'-13 or LigBCen7'-12 than stoichiometrically mixed ones (Figure. 6.7C and E), but similar results cannot be found in LigAVar7'-12 or LigBCen7'-11 (1241 cm^{-1} in LigAVar7'-12 1241 cm^{-1} in LigBCen7'-11)(Figure. 6.7B and D). The results indicate that H/D exchange is more protected in full-length LigAVar7'-13 and LigBCen7'-12

compared to stoichiometrically mixed or separated Ig-like domains. However, the protection is the same between full-length LigAVar7'-12 and LigBCen7'-11 and their stoichiometric mixtures of Ig-like domains. Overall, it proposed that more interdomain interactions exist in the truncated Lig proteins with terminal Ig-like domains, and the interdomain interactions might contribute to the compact structures of Lig proteins.

Terminal Ig-like domains assist the formation of the round shaped Lig proteins

To gain more insight into the contribution of the terminal Ig-like domains to the shape of Lig proteins, transmission electron microscope (TEM) was performed to detect the shape of LigAVar7'-12, LigAVar7'-13, LigBCen7'-11, and LigBCen7'-12. As shown on Figure. 6.8A and C, both LigAVar7'-12 and LigBCen7'-11 form elongated structures. However, the shape of LigAVar7'-13 and LigBCen7'-12, which include the terminal Ig-like domains, form round shapes consistent with the above results that the terminal domains aid the formation of compact structures of Lig proteins (Figure. 6.8B and D).

Discussions

Leptospira Ig-like (Lig) proteins are MSCRAMMs that assist pathogen attachment by binding to Fn, collagen, laminin, fibrinogen, elastin, and tropoelastin (11-16). We previously reported that the Lig binding site to the NTD of Fn was located on a disordered region containing 47 amino acids residues of a non-Ig-like domain of LigB called LigBCen2NR (13). In this study, LigBCen2R, containing the partial 11^{th} and full 12^{th} Ig-like domain of LigB, was demonstrated to interact with GBD of Fn (Figure. 6.2). LigBCen2R showed no sequence similarity to any other GBD binding proteins, so a novel GBD binding motif is located on Ig-like domains of LigA and LigB variable regions.

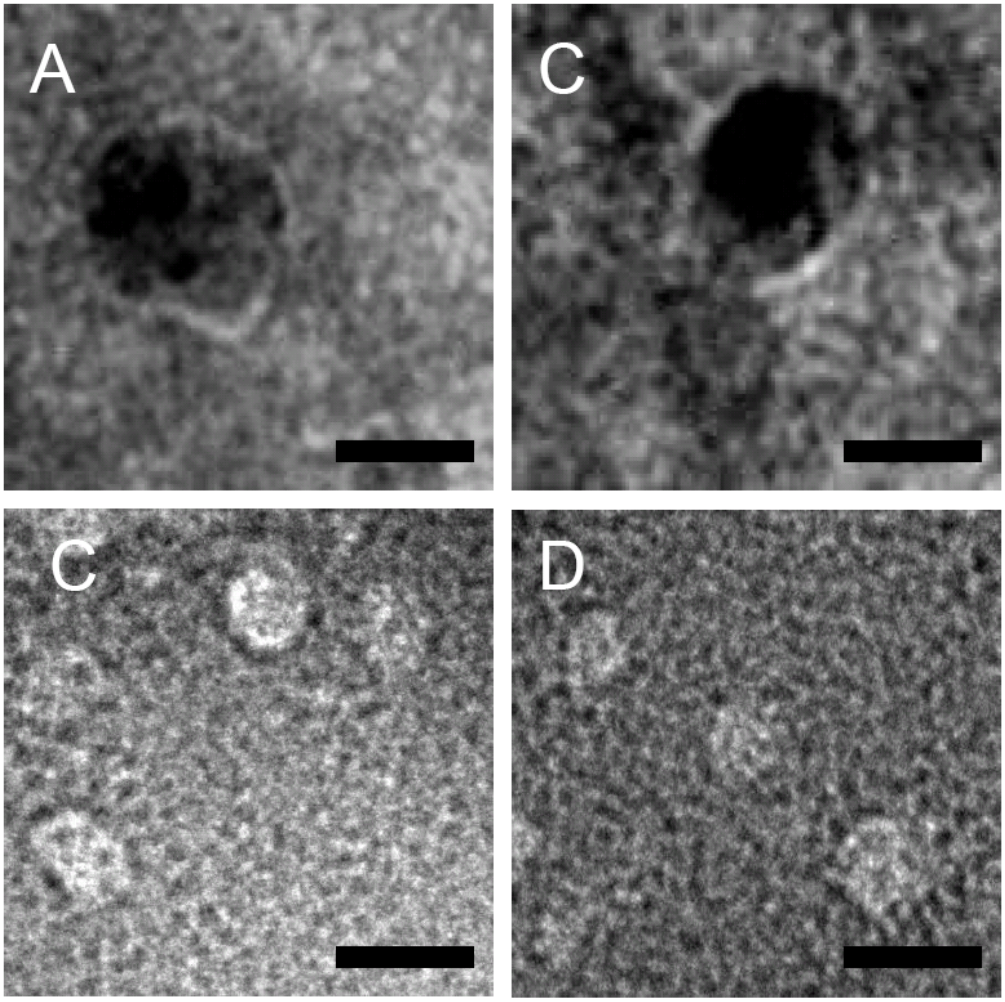

Figure 6.8 Terminal Ig-like domains contribute to the round shape of Lig proteins. Transmission Electron Microscopic image of (A) LigAVar7'-12, (B) LigAVar7'-13, (C) LigBCen7'-11, and (D) LigBCen7'-12. (10nm scale bar).

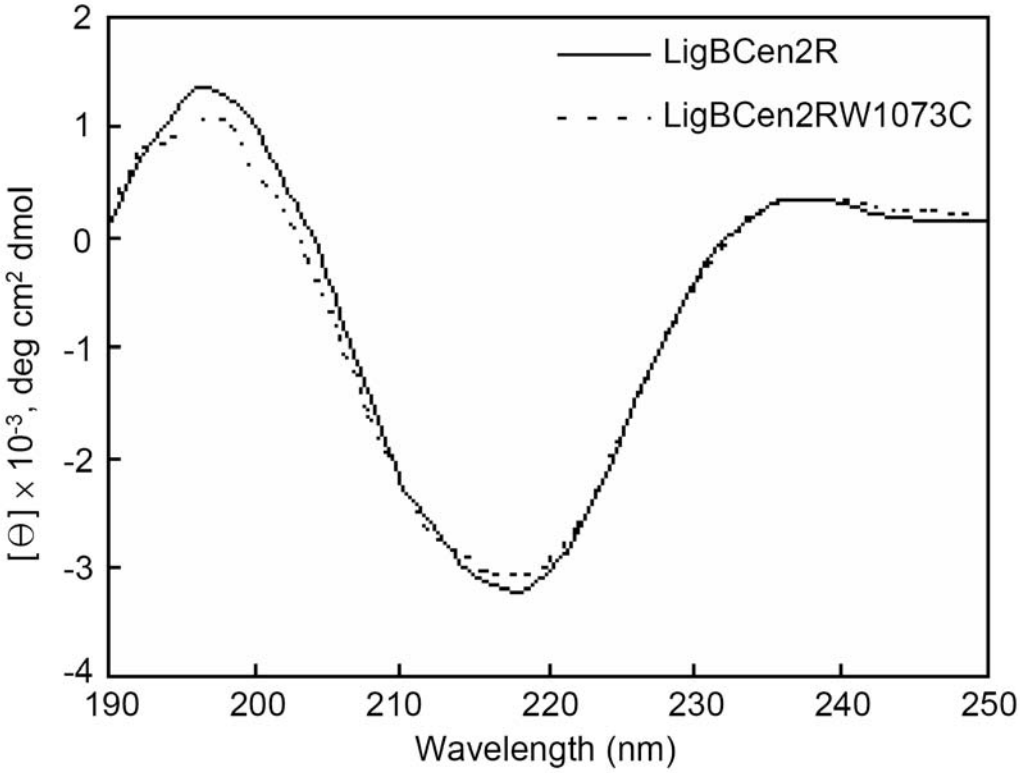

Figure 6.9 W1073C mutation cannot affect the structure of LigBCen2R. Far-UV CD analysis of LigBCen2R and LigBCen2R. The molar ellipticity, Φ, was measured from 190 to 250 nm for 10μM of each protein in Tris buffer with 100μM of calcium chloride.

In addition to LigBCen2R, other variable regions of Ig-like domains of LigA and LigB were also found to possess GBD binding activities but with different strengths (Figure. 6.3 and Table 6.3). Furthermore, the diversified K_D of different variable regions of the Ig-like domains of LigA and LigB characterized by distinct association rate constants (k_{on}) (5×10^{-4} to 5×10^{-3} $M^{-1}S^{-1}$) but similar dissociation rate constants (k_{off})(5×10^{-3} to 9×10^{-3} $M^{-1}S^{-1}$) suggests that there might be a conserved GBD binding motif completely or partially distributed in various variable regions of the Ig-like domains of Lig proteins (Table 6.3). This is not surprising because the amino acid sequences of each Ig-like domain of Lig proteins are divergent (26,27), and this inheritable difference in sequences influences not only the binding affinity to Fn but also to elastin and tropoelastin, as reported previously (15). In addition, similar phenomena were also described in the interaction between a staphylococcal Fn binding rotein, FnBPA, and NTD of Fn (39). On the other hand, the comparably weaker K_D and smaller k_{on} of GBD and Ig-like domains of LigA or LigB compared to other Fn binding proteins indicates a possible role of Lig proteins in transmission of *Leptospira* (40,41), and this phenomenon was also discovered in the NTD binding region of LigB, LigBCen2NR (13).

Multivalency is widely used by bacteria to mediate biomolecular interactions including carbohydrate-protein interaction or protein-protein interaction because it enhances the binding affinity and efficacy between two molecules (33,34). Recently, it was revealed that some bacterial Fn binding proteins with tandem repeated domains can also take advantage of these multivalent domains (39,42,43). For example, 11 Fn binding repeated regions (FnBR) in FnBPA and FnBPB of *Staphylococcus aureus* are associated with the binding of NTD of Fn with various affinities (39,42). Furthermore, the constructs covering three FnBRs of FnBPA have 44 to 250 fold greater affinity to NTD than that of a construct containing just two FnBRs (D1-2, K_D = 0.25μM; D2-3, K_D

= 0.044μM; D1-3, K_D = 0.001μM) (42). In this study, we found that most of the variable regions of LigA and LigB could collaborate to interact with GBD (Figure. 6.4 and Table 6.2), but the slight enhancement of binding affinity contributed by each construct was roughly dependent on the increased number of Ig-like domains it contained (Figure. 6.4, 6.5, and Table 6.4). It is inferred that Lig proteins bind to GBD through both multivalency and a cooperative binding model. On the other hand, the Ig-like domains of Lig proteins collaborated to make attachment to MDCK cells more efficient (Figure. 6.6). Thus, these results indicate multivalent binding of Ig-like domains of Lig proteins to not only Fn but also other ECMs such as elastin, laminin, and collagen. Previously, the repeat domains of Eap (extracellular adherence protein) from *Staphylococcus aureus* were found to cooperatively assist bacterial aggregation, adherence, and host cell invasion (44). Multivalent $EspF_U$ repeats are required to induce the efficient activation of actin polymerization to facilitate the entry of *Escherichia coli* (33). Therefore, multivalent binding of bacterial proteins could be a convergent strategy of different pathogenic bacteria and this strategy may play a pivotal role in the pathogensis bacterial infection.

Surprisingly, Lig proteins lacking the last Ig-like domain bound to GBD much more weakly than the constructs containing the whole variable domain (LigAVar7'-12, K_D = 2.41 μM; LigAVar7'-13, K_D = 0.055 μM; LigBCen7'-11, K_D = 1.39 μM; LigBCen7'-12, K_D = 0.056 μM)(Figure. 6,4E and F, Figure. 6.5D and E, Table 6.3), but the binding affinity between GBD and the last Ig-like domain of LigA or LigB, LigAVar13 or LigBCen2R (LigAVar13, K_D = 10.39 μM; LigBCen2R, K_D = 1.91 μM)(Figure. 6.5 and Table 6.3) was low. Clearly, the terminal domain of Lig protein serves an important role but is not required for GBD binding. In addition, the increased affinity of LigAVar7'-13-GBD or LigBCen7'-12-GBD could be attributed to the precipitously reduced enthalpy compared to LigAVar7'-12-GBD or

LigBCen7'-11-GBD (Table 6.4). Interestingly, the structural differences of the Lig constructs with or without terminal domain were also revealed by DLS, Raman spectrometry, and TEM, and all indicated that Lig protens with the terminal Ig-like domains exhibit compact structures attributable to interdomain interactions (Figure. 6.7 and 6.8). In a previous study, multiple repeat domains of Eap from *Staphylococcus aureus* could form an elongated but structured conformation mediated by interdomain interaction (45). Thus, the structure of protein-ligand interactions requires substantial cooperative interdomain interaction. In addition, this specific compact structure may be important for physiological functions of Lig proteins since the construct with the terminal domains (LigAVar7'-13 and LigBCen7'-12) possess a high affinity binding to GBD and MDCK cells described above (Table 6.4 and Figure. 6.6). It also suggests that the conformation changes of both LigAVar7'-13 and LigBCen7'-12 made them easier to access GBD resulting in a greater reduction in enthalpy due to more charge-charge interactions or hydrogen bonds formed between Lig proteins and GBD.

Fibronectin serves different roles mediated by distinct domains and isoforms. Two Fn isoforms include soluble plasma Fn and insoluble cellular Fn (2,3). MSCRAMMs are a group of proteins that allow pathogens to either attach on host cells by binding to cellular ECMs or to be decorated by plasma Fn to evade the host immune response in the blood stream (1). Multivalency, which promotes higher binding avidity and efficiency, has been described for some MSCRAMMs such as the FnBR of SfbI of *Streptococcus pyogenes* and FnBPA or FnBPB of *Staphylococcus aureus* (39,42,43). Thus, *Leptospira* Lig proteins, which possess 90 amino acid Ig-like repeated domains that bind to Fn, could be reasonably inferred to serve a similar role. Recently, a novel role for MSCRAMMs was ascribed to a 70kDa domain that includes the NTD and GBD of Fn. Both the NTD and GBD contain IGD motifs, called migration stimulating factor (MSF) located on ^{3}F1, ^{5}F1, ^{7}F1, and ^{9}F1, which mediate fibroblast migration (46,47).

Whether Lig proteins aid *Leptospira* spp. infection through this strategy waits to be determined.

In conclusion, we have fine mapped the GBD binding sites on LigBCen2 and found GBD binds to LigBCen2R, the partial 11^{th} and full 12^{th} Ig-like domains. Furthermore, most of the individual Ig-like domains from the variable region of Lig A and LigB were also bound by GBD but with divergent affinities. Multivalent binding was proved to mediate the GBD-Lig proteins interaction and MDCK cell adhesion, and the terminal Ig-like domain serves a role for the formation of compact and round structures and a substantial but nonessential role for the interaction. Further studies on the function of Lig proteins interacting with GBD are needed and are currently being investigated in our laboratory.

REFERENCES

1. **Patti, J. M., B. L. Allen, M. J. McGavin, and M. Hook.** 1994. MSCRAMM-mediated adherence of microorganisms to host tissues. Annu Rev Microbiol **48:**585-617.
2. **Potts, J. R., and I. D. Campbell.** 1994. Fibronectin structure and assembly. Current opinion in cell biology **6:**648-655.
3. **Vakonakis, I., and I. D. Campbell.** 2007. Extracellular matrix: from atomic resolution to ultrastructure. Curr Opin Cell Biol **19:**578-583.
4. **Schwarz-Linek, U., M. Hook, and J. R. Potts.** 2004. The molecular basis of fibronectin-mediated bacterial adherence to host cells. Mol Microbiol **52:**631-641.
5. **Joh, D., P. Speziale, S. Gurusiddappa, J. Manor, and M. Hook.** 1998. Multiple specificities of the staphylococcal and streptococcal fibronectin-binding microbial surface components recognizing adhesive matrix molecules. Eur. J. Biochem. **258:**897-905.
6. **Joh, D., E. R. Wann, B. Kreikemeyer, P. Speziale, and M. Hook.** 1999. Role of fibronectin-binding MSCRAMMs in bacterial adherence and entry into mammalian cells. Matrix Biol **18:**211-223.
7. **Probert, W. S., J. H. Kim, M. Hook, and B. J. Johnson.** 2001. Mapping the ligand-binding region of *Borrelia burgdorferi* fibronectin-binding protein BBK32. Infect. Immun. **69:**4129-4133.
8. **Dabo, S. M., A. W. Confer, B. E. Anderson, and S. Gupta.** 2006. *Bartonella henselae* Pap31, an extracellular matrix adhesin, binds the fibronectin repeat III13 module. Infect Immun **74:**2513-2521.
9. **Kingsley, R. A., A. M. Keestra, M. R. de Zoete, and A. J. Baumler.** 2004. The ShdA adhesin binds to the cationic cradle of the fibronectin 13FnIII repeat

module: evidence for molecular mimicry of heparin binding. Mol Microbiol **52:**345-355.

10. **Choy, H. A., M. M. Kelley, T. L. Chen, A. K. Moller, J. Matsunaga, and D. A. Haake.** 2007. Physiological osmotic induction of *Leptospira interrogans* adhesion: LigA and LigB bind extracellular matrix proteins and fibrinogen. Infect. Immun. **75:**2441-2450.
11. **Lin, Y. P., and Y. F. Chang.** 2007. A domain of the *Leptospira* LigB contributes to high affinity binding of fibronectin. Biochem Biophys Res Commun **362:**443-448.
12. **Lin, Y. P., and Y. F. Chang.** 2008. The C-terminal variable domain of LigB from *Leptospira* mediates binding to fibronectin. J. Vet. Sci. **9:**133-144.
13. **Lin, Y. P., A. Greenwood, L. K. Nicholson, Y. Sharma, S. P. McDonough, and Y. F. Chang.** 2009. Fibronectin binds to and induces conformational change in a disordered region of Leptospira interrogans immunoglobulin-like protein LigB. J. Biol. Chem. **284:** 23547-23557
14. **Lin, Y. P., A. Greenwood, W. Yan, L. K. Nicholson, and Y. F. Chang.** 2009. A novel fibronectin type III module binding motif identified on C-terminus of Leptospira immunoglobulin-like protein, LigB. Biochem. Biophy. Res. Commun. **389:** 57-62
15. **Lin, Y. P., D. W. Lee, S. P. McDonough, L. K. Nicholson, Y. Sharma, and Y. F. Chang.** 2009. Repeated domains of *Leptospira* Immunoglobulin-like proteins interact with elastin and tropoealstin. J. Biol. Chem. **284:** 19380-19391
16. **Lin, Y. P., R. Raman, Y. Sharma, and Y. F. Chang.** 2008. Calcium binds to Leptospiral immunoglobulin-like protein, LigB and modulates fibronectin binding. J. Biol. Chem. **283:**25140-25149.

17. **Hauk, P., F. Macedo, E. C. Romero, S. A. Vasconcellos, Z. M. de Morais, A. S. Barbosa, and P. L. Ho.** 2008. In LipL32, the major leptospiral lipoprotein, the C terminus is the primary immunogenic domain and mediates interaction with collagen IV and plasma fibronectin. Infect. Immun. **76:**2642-2650.

18. **Hauk, P., C. R. Guzzo, H. R. Ramos, P. L. Ho, and C. S. Farah.** 2009. Structure and Calcium-Binding Activity of LipL32, the Major Surface Antigen of Pathogenic *Leptospira* sp. J Mol Biol. **390:** 722-736.

19. **Hoke, D. E., S. Egan, P. A. Cullen, and B. Adler.** 2008. LipL32 is an extracellular matrix-interacting protein of *Leptospira* spp. and *Pseudoalteromonas tunicata*. Infect Immun **76:**2063-2069.

20. **Vivian, J. P., T. Beddoe, A. D. McAlister, M. C. Wilce, L. Zaker-Tabrizi, S. Troy, E. Byres, D. E. Hoke, P. A. Cullen, M. Lo, G. L. Murray, B. Adler, and J. Rossjohn.** 2009. Crystal structure of LipL32, the most abundant surface protein of pathogenic *Leptospira* spp. J Mol Biol **387:**1229-1238.

21. **Barbosa, A. S., P. A. Abreu, F. O. Neves, M. V. Atzingen, M. M. Watanabe, M. L. Vieira, Z. M. Morais, S. A. Vasconcellos, and A. L. Nascimento.** 2006. A newly identified leptospiral adhesin mediates attachment to laminin. Infect. Immun. **74:**6356-6364.

22. **Stevenson, B., H. A. Choy, M. Pinne, M. L. Rotondi, M. C. Miller, E. Demoll, P. Kraiczy, A. E. Cooley, T. P. Creamer, M. A. Suchard, C. A. Brissette, A. Verma, and D. A. Haake.** 2007. Leptospira interrogans Endostatin-Like Outer Membrane Proteins Bind Host Fibronectin, Laminin and Regulators of Complement. PLoS ONE **2:**e1188.

23. **Atzingen, M. V., A. S. Barbosa, T. De Brito, S. A. Vasconcellos, Z. M. Morais, D. M. Lima, P. A. Abreu, and A. L. Nascimento.** 2008. Lsa21, a novel

leptospiral protein binding adhesive matrix molecules and present during human infection. BMC Microbiol **8:**70.

24. **Carvalho, E., A. S. Barbosa, R. M. Gomez, A. M. Cianciarullo, P. Hauk, P. A. Abreu, L. C. Fiorini, M. L. Oliveira, E. C. Romero, A. P. Goncales, Z. M. Morais, S. A. Vasconcellos, and P. L. Ho.** 2009. Leptospiral TlyC is an extracellular matrix-binding protein and does not present hemolysin activity. FEBS Lett **583:**1381-1385.

25. **Matsunaga, J., M. A. Barocchi, J. Croda, T. A. Young, Y. Sanchez, I. Siqueira, C. A. Bolin, M. G. Reis, L. W. Riley, D. A. Haake, and A. I. Ko.** 2003. Pathogenic *Leptospira* species express surface-exposed proteins belonging to the bacterial immunoglobulin superfamily. Mol Microbiol **49:**929-945.

26. **Palaniappan, R. U., Y. F. Chang, F. Hassan, S. P. McDonough, M. Pough, S. C. Barr, K. W. Simpson, H. O. Mohammed, S. Shin, P. McDonough, R. L. Zuerner, J. Qu, and B. Roe.** 2004. Expression of leptospiral immunoglobulin-like protein by *Leptospira interrogans* and evaluation of its diagnostic potential in a kinetic ELISA. J Med Microbiol **53:**975-984.

27. **Palaniappan, R. U., Y. F. Chang, S. S. Jusuf, S. Artiushin, J. F. Timoney, S. P. McDonough, S. C. Barr, T. J. Divers, K. W. Simpson, P. L. McDonough, and H. O. Mohammed.** 2002. Cloning and molecular characterization of an immunogenic LigA protein of *Leptospira interrogans*. Infect. Immun. **70:**5924-5930.

28. **Faisal, S. M., M. A. Khan, T. H. Nasti, N. Ahmad, and O. Mohammad.** 2003. Antigen entrapped in the escheriosomes leads to the generation of CD4(+) helper and CD8(+) cytotoxic T cell response. Vaccine **21:**2383-2393.

29. **Faisal, S. M., W. Yan, C. S. Chen, R. U. Palaniappan, S. P. McDonough, and Y. F. Chang.** 2008. Evaluation of protective immunity of *Leptospira*

immunoglobulin like protein A (LigA) DNA vaccine against challenge in hamsters. Vaccine **26:**277-287.

30. **Faisal, S. M., W. Yan, S. P. McDonough, and Y. F. Chang.** 2009. Variable region of *Leptospira* immunoglobulin like protein A (LigAvar) incorporated in Liposomes and PLGA-Microspheres produces a robust immune response correlating to protective immunity against challenge in hamsters. Vaccine **27:**378-387.
31. **Palaniappan, R. U., S. P. McDonough, T. J. Divers, C. S. Chen, M. J. Pan, M. Matsumoto, and Y. F. Chang.** 2006. Immunoprotection of recombinant leptospiral immunoglobulin-like protein A against *Leptospira interrogans* serovar Pomona infection. Infect. Immun. **74:**1745-1750.
32. **Yan, W., S. M. Faisal, S. P. McDonough, T. J. Divers, S. C. Barr, C. F. Chang, M. J. Pan, and Y. F. Chang.** 2009. Immunogenicity and protective efficacy of recombinant *Leptospira* immunoglobulin-like protein B (rLigB) in a hamster challenge model. Microbes Infect **11:**230-237.
33. **Sallee, N. A., G. M. Rivera, J. E. Dueber, D. Vasilescu, R. D. Mullins, B. J. Mayer, and W. A. Lim.** 2008. The pathogen protein EspF(U) hijacks actin polymerization using mimicry and multivalency. Nature **454:**1005-1008.
34. **Connaris, H., P. R. Crocker, and G. L. Taylor.** 2009. Enhancing the receptor affinity of the sialic acid-binding domain of *Vibrio cholerae* sialidase through multivalency. J. Biol. Chem. **284:**7339-7351.
35. **Vadas, O., and K. Rose.** 2007. Multivalency - a way to enhance binding avidities and bioactivity - preliminary applications to EPO. J. Pept. Sci. **13:**581-587.
36. **Benevides, J. M., Overman, S. A., and Thomas, G. J., Jr.** 2004. *Current protocols in protein science.* Chapter 17, Unit 17 18

37. **Strickland, A. D., and Batt, C. A.** 2009. Detection of carbendazim by surface-enhanced Raman Scattering using cyclodextrin inclusion complexes on gold nanorods. Anal Chem **81:** 2895-2903

38. **Tu, A. T.** 1982. Raman Spectroscopy in Bology: Principles and Applications. In., John Wiley & Sons, New York

39. **Meenan, N. A., L. Visai, V. Valtulina, U. Schwarz-Linek, N. C. Norris, S. Gurusidappa, M. Hook, P. Speziale, and J. R. Potts.** 2007. The tandem beta -zipper model defines high affinity fibronectin-binding repeats within Staphylococcus aureus FnBPA.

40. **Patil, A., and H. Nakamura.** 2006. Disordered domains and high surface charge confer hubs with the ability to interact with multiple proteins in interaction networks. FEBS Lett **580:**2041-2045.

41. **Kreikemeyer, B., S. Oehmcke, M. Nakata, R. Hoffrogge, and A. Podbielski.** 2004. *Streptococcus pyogenes* fibronectin-binding protein F2: expression profile, binding characteristics, and impact on eukaryotic cell interactions. J. Biol. Chem. **279:**15850-15859.

42. **Ingham, K. C., S. Brew, D. Vaz, D. N. Sauder, and M. J. McGavin.** 2004. Interaction of *Staphylococcus aureus* fibronectin-binding protein with fibronectin: affinity, stoichiometry, and modular requirements. J. Biol. Chem. **279:**42945-42953.

43. **Schwarz-Linek, U., E. S. Pilka, A. R. Pickford, J. H. Kim, M. Hook, I. D. Campbell, and J. R. Potts.** 2004. High affinity streptococcal binding to human fibronectin requires specific recognition of sequential F1 modules. J. Biol. Chem. **279:**39017-39025.

44. **Hussain, M., Haggar, A., Peters, G., Chhatwal, G. S., Herrmann, M., Flock, J. I., and Sinha, B.** 2008. More than one tandem repeat domain of the

extracellular adherence protein of *Staphylococcus aureus* is required for aggregation, adherence, and host cell invasion but not for leukocyte activation. Infect. Immun. **76:** 5615-5623

45. **Hammel, M., Nemecek, D., Keightley, J. A., Thomas, G. J., Jr., and Geisbrecht, B. V.** 2007. The *Staphylococcus aureus* extracellular adherence protein (Eap) adopts an elongated but structured conformation in solution. Protein Sci. **16:** 2605-2617

46. **Millard, C. J., I. R. Ellis, A. R. Pickford, A. M. Schor, S. L. Schor, and I. D. Campbell.** 2007. The role of the fibronectin IGD motif in stimulating fibroblast migration. J. Biol. Chem. **282:**35530-35535.

47. **Vakonakis, I., D. Staunton, I. R. Ellis, P. Sarkies, A. Flanagan, A. M. Schor, S. L. Schor, and I. D. Campbell.** 2009. Motogenic sites in human fibronectin are masked by long range interactions. J. Biol. Chem. **284:**15668-15675.

CHAPTER 7

FIBRONECTIN-BINDING ACTIVITY ON A SURFACE-EXPOSED DOMAIN WITHIN THE C-TERMINAL VARIABLE REGION OF *LEPTOSPIRA INTERROGANS* LIGB PROTEIN

Introduction

Leptospirosis, caused by infection with pathogenic *Leptospira* spp., is a serious zoonosis with world-wide distribution [1]. *Leptospira* (from the Greek *leptos*, "thin", and the Latin *spira*, "coil") are thin, filamentous (0.1-0.2 μm wide x 6-12 μm long) spirochetes which can be transmitted to people and animals both by direct and indirect contact [2]. These spirochetes usually penetrate through mucosal surfaces and/or skin wounds and disseminate to several organs, especially the kidney, liver and lungs. Infection may lead to Weil's disease, which results in liver failure (jaundice), renal failure (nephritis), pulmonary hemorrhage and/or meningitis [2]. Human leptospirosis is often waterborne, and most commonly occurs in tropical areas of the world [2] However, studies indicate that leptospirosis is on the rise in the United States, particularly among individuals exposed to the pathogen through recreational swimming or through exposure to infected urban rat populations [3; 4].

Many microbial pathogens produce Microbial Surface Components Recognizing Adhesive Matrix Molecules (MSCRAMM) to facilitate their colonization of host tissues during initial infection [5]. Pathogenic leptospires bind to mammalian cells, such as MDCK cells [6], often via the extracellular matrix (ECM) [7; 8]. Several adhesion molecules have been identified from *Leptospira* spp. including a 36 kDa protein that binds Fn [9], a leptospiral endostatin-like protein (Len) that binds to Fn and laminin [10; 11], Lsa21 and LipL32 which bind to Fn, laminin and collagen [12-14], and Lig proteins, which bind to Fn, laminin, collagen, fibrinogen, elastin, and tropoelastin [15-17].

Leptospiral immunoglobulin-like proteins, LigA and LigB, possess 12 and 13 immunoglobulin-like (Ig-like) domains, respectively [18-20]. Such Ig-like repeats are also found in known bacterial adhesion proteins including invasin from *Yersinia pseudotuberculosis* and intimin from *Escherichia coli* [18-20]. A key environmental signal, i.e., osmolarity, controls the expression of LigA and LigB, enabling pathogenic *Leptospira* to bind to host cells [21; 22]. The binding of LigB to Fn is also modulated by calcium [23]. These studies indicate that Lig proteins are pivotal virulence factors of pathogenic *Leptospira* spp.

In previous studies, LigB has been shown to possess Fn-binding activity [15; 16; 23; 24] which mediates adhesion of *Leptospira* bacteria to host cells [16; 24]. Moreover, high and low affinity Fn-binding sites were located on LigB within the LigBCen and the C-terminal variable (LigBCtv) regions (Figure. 7.1A), respectively [16; 24]. In this study, we have further identified the exact location of Fn binding site of LigBCtv to five amino acid regions from 1708 to1712, with the sequence LIPAD. These residues, located in a surface-exposed domain, are also conserved on LigB and LigC derived from other pathogenic *Leptospira* serovars. Furthermore, this sequence binds to the 15^{th} type III module of Fn, a novel binding site for bacterial Fn-binding proteins. The kinetics of the interaction are strikingly slow, with an off rate (k_{off} = 0.0129 Sec^{-1}, Figure. 7.7) far below typical rates for protein-protein interactions and near the range of rates for drugs, such as inhibitors of HIV-1 protease [25]. *In vitro* binding assays yield a K_D of 8.06 ± 0.11 μM of $LigB_{1706-1716}$ for Fn, and pretreatment of MDCK cells with $LigB_{1706-1716}$, which includes the LIPAD Fn-binding site, inhibits leptospiral binding by 39%. This significant inhibition by a short peptide demonstrates the importance of this sequence in adhesion of the pathogen to target tissues.

Figure 7.1 Identification of the LigB C-terminal Fn-binding region and its Fn-binding residues. (A). A schematic diagram showing the structure of LigB and the truncated LigB C-terminal regions including LigBCtv, LigBCtv1, LigBCtv2, LigBCtv3, and LigBCtv4 used in the Fn-binding assay. (B). The Fn-binding activity of LigBCtv1, LigBCtv2, LigBCtv3, and LigBCtv4 regions. (C). The Fn-binding activity of the peptides (30 mers) corresponding to the amino acids of LigBCtv. (D). The synthetic peptide sequences (11 mers) with overlapping regions used to identify the essential amino acids (indicated in bold) required for Fn-binding. (E). The synthetic peptides as indicated in D used in the Fn-binding assays. (F). wild-type ($LigB_{1706\text{-}1716}$) and mutant ($LigB_{L1708A}$, $LigB_{I1709A}$, $LigB_{P1710A}$, and $LigB_{D1712A}$) peptides used in the identification of the essential amino acids binding to Fn. Various concentrations (40μM, 20μM, 10μM, 5μM, 2.5μM, 1.25μM, 0.625μM) of each tested biotinylated-protein or -peptide, -$BBK32_{56\text{-}205}$ (positive control; B, C, E, and F), -LigBCon (negative control; B) or -scrambled peptide (negative control; C, E and F) were used in this study. The binding of each of these proteins or peptides to Fn was measured by ELISA, and each value represents the mean ± SEM of three trials in triplicate samples (B, C, E, and F)**.**

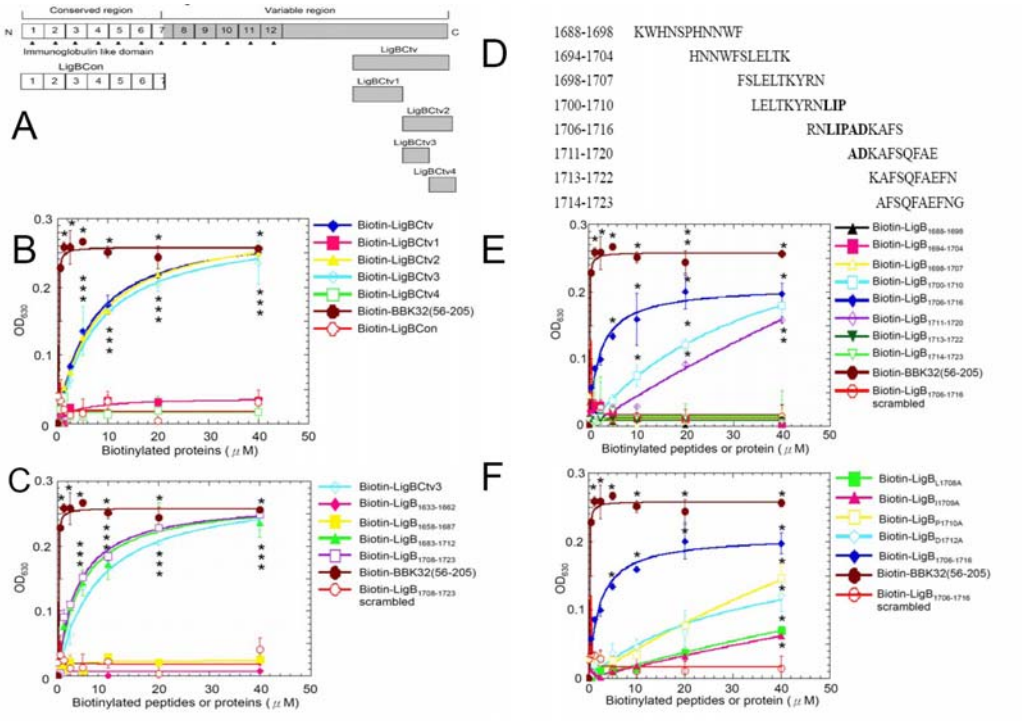
A
Conserved region
Variable region
N
C
Immunoglobulin like domain
LigBCon
LigBCtv
LigBCtv1
LigBCtv2
LigBCtv3
LigBCtv4
B
Biotin-LigBCtv
Biotin-LigBCtv1
Biotin-LigBCtv2
Biotin-LigBCtv3
Biotin-LigBCtv4
Biotin-BBK32(56-205)
Biotin-LigBCon
OD630
Biotinylated proteins (μM)
C
Biotin-LigBCtv3
Biotin-LigB1633-1662
Biotin-LigB1658-1687
Biotin-LigB1683-1712
Biotin-LigB1708-1723
Biotin-BBK32(56-205)
Biotin-LigB1708-1723 scrambled
Biotinylated peptides or proteins (μM)
D
1688-1698 KWHNSPHNNWF
1694-1704 HNNWFSLELTK
1698-1707 FSLELTKYRN
1700-1710 LELTKYRNLIP
1706-1716 RNLIPADKAFS
1711-1720 ADKAFSQFAE
1713-1722 KAFSQFAEFN
1714-1723 AFSQFAEFNG
E
Biotin-LigB1688-1698
Biotin-LigB1694-1704
Biotin-LigB1698-1707
Biotin-LigB1700-1710
Biotin-LigB1706-1716
Biotin-LigB1711-1720
Biotin-LigB1713-1722
Biotin-LigB1714-1723
Biotin-BBK32(56-205)
Biotin-LigB1706-1716 scrambled
Biotinylated peptides or protein (μM)
F
Biotin-LigBL1708A
Biotin-LigB1709A
Biotin-LigBP1710A
Biotin-LigBD1712A
Biotin-LigB1706-1716
Biotin-BBK32(56-205)
Biotin-LigB1706-1716 scrambled
Biotinylated peptides or protein (μM)

Material and Methods

Bacterial strains and Cell Culture

L. interrogans serovar Pomona (NVSL1427-35-093002) was used as previously described [35]. All experiments were performed with virulent, low-passage strains obtained by passage in golden syrian hamsters as previously described [35]. Leptospires were grown in EMJH medium at 30 ^{o}C for less than 5 passages; growth was monitored by dark-field microscopy. A high passage culture of this strain (50 *in vitro* passages) was also used. Madin-Darby canine kidney (MDCK) cells (ATCC CCL34^{TM}) were cultured in Dulbecco's minimum essential medium (DMEM) containing 10% fetal bovine serum (GIBCO Laboratories, Grand Island, N.Y.). Cells were grown at 37^{o}C in a humidified atmosphere with 5% CO_2.

Reagents and antibodies

Horseradish peroxidase (HRP)-conjugated goat anti-hamster antibody and HRP-conjugated goat anti-mouse antibody were purchased from Zymed (San Diego, CA). HRP conjugated streptavidin was purchased from Biosource (Camarillo, CA). Alexa 594 conjugated goat anti-hamster antibody, Alexa 488-conjugated goat anti-hamster antibody, Alexa 647 conjugated goat anti-rabbit antibody, and FITC conjugated streptavidin were purchased from Molecular Probes (Eugene, OR). 120 kDa cell-binding domain (CBD: F1904) or 40 kDa domain containing heparin-binding domain and type III module 15 (40 kDa; F1903) of Fn were purchased from Chemicon International (Temecula, CA). Rabbit anti-LipL32 antibody were prepared by intramuscular inoculation with 100 µg of recombinant LipL32 in Freund's complete adjuvant (first vaccination) followed by 100 µg intramuscularly in Freund's incomplete adjuvant (booster) three weeks later. Three weeks after the second booster, the rabbit

was sacrificed and serum was collected. Anti-*L. interrogans* antibodies were prepared in hamsters from the challenge controls [35]. The anti-LigBCen and LigBCtv antibodies were prepared in hamsters as previously described [36]. N-terminal domain (NTD) or gelatin-binding domain (GBD) of Fn were purchased from Sigma (St. Louis, MO), and Keyhole limpet haemocyanin (KLH) and biotin labeling kit were purchased from Pierce (Rockford, IL). Full length human plasma fibronectin was purchased from GIBCO (Carlsbad, CA). Heparin was purchased from MP biomedicals (Solon, OH).

Plasmid construction and protein purification

Rat 12^{th}-13^{th}, 14^{th}, or 15^{th} type III modules were purified as MBP fusion proteins (Figure. 7.5A) [40]. The DNA fragments of LigBCon and BBK32 (AA 56-205) were inserted into pGEX4T2 (Amersham Pharmacia Biotech, Piscataway, NJ) and pQE30 (Qiagen, Valencia, CA), respectively [35]. LigBCtv sequence was analyzed with Jpred to predict the secondary structure for truncation construction [49]. Constructs for the expression of GST-fused with LigBCtv1 (AA 1418-1632), LigBCtv2 (AA 1633-1889), LigBCtv3 (AA 1633-1723) and LigBCtv4 (AA 1724-1889) were generated using the vector pGEX-4T-2 (Figure. 7.1A). Relevant fragments of DNA were amplified by PCR using primers (Table 7.1) based on the *ligB* sequence [19]. Primers were engineered to introduce a *BamH*I site at the 5' end of each fragment and a stop codon followed by a *Sal*I site at the 3' end of each fragment, except LigBCtv1. For LigBCtv1, primers were engineered to introduce a *Sal*I site at the 5' end of each fragment and a stop codon followed by a *Not*I site at the 3' end. PCR products were digested sequentially with *BamH*I /*Sal*I or *Sal*I /*Not*I for the indicated fragment and then ligated into pGEX-4T-2 cut with *BamH*I/*Sal*I or *Sal*I/*Not*I, respectively. In this study, we purified the soluble form of the four GST fusion peptides from *E. coli* as described earlier [19; 20].

Table 7.1 Primers.

Primer	Sequence
LigBCtv1fp	GTCGACTCAAGCAGCTCGATTC
LigBCtv1rp	GCGGCCGCTTATATTCCCACA
LigBCtv2fp	GGATCCGATTCTCTATTCGTT
LigBCtv2rp	GTCGACTTATTGATTCTGTTG
LigBCtv3fp	GGATCCGATTCTCTATTCGTTTTT
LigBCtv3rp	GTCGACTTATCCGTTAAATTCTGC
LigBCtv4fp	GGATCCAGATTGTATGTAACAAGA
LigBCtv4rp	GTCGACTTATTGATTCTGTTGTCT

Binding assays by ELISA

To determine the binding of truncated LigB (LigBCtv1, LigBCtv2, LigBCtv3, or LigBCtv4) or LigB peptides to Fn, 1 μg of Fn or BSA (negative control) was coated onto microtiter plate wells as previously described [16; 24]. The plates were incubated at 4^{o}C for 16 h and subsequently blocked with blocking buffer (50 μl/well) containing 3% BSA in PBS at room temperature (RT) for 2 h. Then, various concentrations (0.625, 1.25, 2.5, 5, 10, 20, 40 μM) of biotinylated LigB truncated protein, LigB peptide, (as indicated in Figure. 7.1B, C, E, F and 7.5), scrambled peptide (negative control, as indicated in Table 7.2), BBK32 (56-205) or LigBCon was added to each microtiter plate wells for 1 hour at 37^{o}C. BBK32 (56-205) or LigBCon serve as positive and negative control due to the strong or no Fn-binding activities reported previously [15; 14; 50]. To measure the binding of biotinylated LigB protein, HRP-conjugated streptavidin was added into microtiter plate wells (1:1,000).

To identify the binding site of $LigB_{1706\text{-}1716}$ on Fn, 1 μg of each of full length Fn, NTD, GBD, CBD, 40 kDa domain of Fn, or MBP fused with 12th- 13th type III modules (MBP-12-13F_3), 14th type III modules (MBP-14F_3), or 15th type III modules (MBP-15F_3) of Fn were coated onto microtiter plate wells. 1 μg of BSA or maltose binding protein (MBP) was coated as a negative control. Then, various concentrations (as indicated in Figure. 7.6B and C) of biotin conjugated $LigB_{1706\text{-}1716}$ (biotin-$LigB_{1706\text{-}1716}$) or biotin (negative control, data not shown) were added to microtiter plate wells. To measure the binding of $LigB_{1706\text{-}1716}$ to MDCK cells, MDCK cells (10^5) were incubated with various concentrations (as indicated in Figure. 7.3 A.) of biotin-$LigB_{1706\text{-}1716}$ or biotin (negative control) in 100 μl PBS for 1 hour at 37^{o}C. To measure the binding inhibition of *Leptospira* to MDCK cells treated with $LigB_{1706\text{-}1716}$, MDCK cells (10^5) were pretreated with various concentrations (as indicated in Figure. 7.3 B.) of biotin-$LigB_{1706\text{-}1716}$ or biotin (negative control) in 100 μl PBS for 1 hour at 37^{o}C. Then, *Leptospira* (10^7) were

added to each well and incubated for 6 hours at 37°C. Following incubation, the plates were washed three times with phosphate-buffered saline (PBS) containing 0.05% Tween-20 (PBST). To measure the binding of *Leptospira,* hamster anti-*Leptospira* (1:200) and HRP-conjugated goat anti-hamster IgG (1:1,000) were used as primary and secondary antibodies, respectively. To detect the binding of biotin-$LigB_{1706-1716}$ or biotin to Fn or MDCK cells, HRP conjugated streptavidin (1:1,000) was added and incubated for 30 min at 25°C. After washing the plates thrice with PBST, 100µL of TMB (KPL, Gaithersburg, MD) was added to each well and incubated for 5 min. The reaction was stopped by adding 100 µl of 0.5% hydrofluoric acid in each well. Each plate was read at 630 nm using an ELISA plate reader (Bioteck EL-312, Winoski, VT). Each value represented the mean ± SEM of three trials in triplicate samples. Statistically significant ($P<0.05$) differences are indicated by asterisks. In order to determine the dissociation constant (K_D), the data were fitted by the following equation using KaleidaGraph software (Version 2.1.3 Abelbeck software). The K_D value represents the mean ± SEM of three trials in triplicate samples.

$$OD_{630} = \frac{OD_{630max}\,[\,\text{Biotin-LigB}_{1706-1716}\,]}{K_D + [\,\text{Biotin-LigB}_{1706-1716}\,]} \quad \text{(Eq. 1)}$$

Binding assays by confocal laser-scanning microscopy (CLSM)

To determine the binding inhibition of *Leptospira* to MDCK cells by $LigB_{1706-1716}$ by CLSM, MDCK cells (10^6) were preincubated with 10 µM of biotin-$LigB_{1706-1716}$ or biotin (negative control) as previously described [24]. Untreated MDCK cells served as negative control as well (data not shown). To quantify the attachment of *Leptospira* (Figure. 7.3C), hamster anti-*Leptospira* antibodies (1:250) served as the primary antibody, and Alexa 594-conjugated goat anti-hamster IgG (1:250) was used as the secondary antibody. To reveal the binding of biotin-$LigB_{1706-1716}$ or biotin, 150µl of FITC-conjugated streptavidin was added (1:250). Fixation and immunofluorescence

staining were followed as previously described [24]. For measuring the reduced attachment of *Leptospira* to biotin-$LigB_{1706-1716}$ treated MDCK cells, three fields were selected to count the number of binding organisms. All studies were repeated three times and the number of *Leptospira* attached to the MDCK cells were counted by an investigator blinded to the treatment group. The value of reduced leptospiral attachment represents the mean ± SEM of three trials performed in triplicate samples.

Generation of polyclonal antibodies against LIPAD-containing peptides

Keyhole limpet haemocyanin (KLH) conjugated LigB-derived peptides LigB AA 1698-1712 ($LigB_{1698-1712}$), LigB AA 1703-1717 ($LigB_{1703-1717}$), and LigB AA 1708-1722 ($LigB_{1708-1722}$) were ordered from Genemed Synthesis (San Antonio, TX). Ten female BALB/c mice were immunized intramuscularly once with a cocktail (10 μg of each peptide) of three conjugated peptides ($LigB_{1698-1712}$, $LigB_{1703-1717}$, and $LigB_{1708-1722}$) in Freud's complete adjuvant and twice with these three conjugated peptides in Freud's incomplete adjuvant. After that, the mice were immunized one more time with a single conjugated peptide ($LigB_{1703-1717}$) in Freud's incomplete adjuvant.

Two weeks after the second booster, all mice were sacrificed and the sera were collected. All the experimental work was conducted in compliance with the regulations, policies, and principles of the Animal Welfare Act, the Public Health Service Policy on Humane Care and Use of Laboratory Animals used in Testing, Research, and Training, the NIH Guide for the Care and Use of Laboratory Animals and the New York State Department of Public Health.

Determining whether LIPAD-containing peptide was surface-exposed by CLSM

Both low passage and high passage *L. interrogans* serovar Pomona were harvested from EMJH medium, pelleted by centrifugation and washed once with PBS. 10^8 bacteria were suspended in 100 μL of 0.3% BSA in PBS and placed on glass culture slides. Bacteria were fixed in 2% paraformaldehyde for 60 min at room temperature (RT). For antibody labeling, fixed bacteria were incubated in PBS containing 0.3% BSA for 10 min at RT. Rabbit anti-LipL32 antibody (1:250), mouse anti-$LigB_{1703-1717}$ antibody (LigB peptide pAb; 1:250), and hamster anti-LigBCen and LigBCtv antibody (1:250) served as primary antibodies. Alexa 647-conjugated goat anti-rabbit IgG, Texas Red-conjugated goat anti-mouse IgG, and Alexa 488-conjugated goat anti-hamster IgG were used as secondary antibodies (1:250). The glass slides were mounted with coverslips using Prolong Antifade (Molecular Probe, Eugene, OR) and viewed with a 60x objective by CLSM (Olympus, America, Inc., Melville, NY). The settings were identical for all captured images. Images were processed using Adobe Photoshop CS2.

Fluorescence Spectrometry

Fluorescence emission spectra were measured on a Hitachi F4500 spectrofluorometer (Hitachi. San Jose, CA). All spectra were recorded in correct spectrum mode of the instrument using excitation and emission band passes of 5 nm. The intrinsic Trp fluorescence of protein was recorded by exciting the solution at 295 nm and measuring the emission in the 305-400 nm regions. For $LigB_{1706-1716}$ titration, 0.625, 1.25, 2.5, 5, 10, 20, 40 μM of $LigB_{1706-1716}$ was mixed with 1 μM of 15^{th} type III module of Fn and spectra were recorded after 5 minutes. In order to determine the dissociation constant (K_D), the fluorescence intensities at 350 nm were recorded and fitted in following equation using KaleidaGraph software (Version 2.1.3 Abelbeck software).

$$F_{max}\text{-}F = \frac{(F_{max}\text{-}F_{min})\,[\,LigB_{1706\text{-}1716}\,]}{K_D + [\,LigB_{1706\text{-}1716}\,]} \quad \text{(Eq. 2)}$$

where F_{max} is the fluorescence intensity of 15F3 in the absence of $LigB_{1706\text{-}1716}$ and F_{min} is the fluorescence intensity in the presence of 40 μM of $LigB_{1706\text{-}1716}$. In addition, F is the fluorescence intensity in the presence of various concentrations of $LigB_{1706\text{-}1716}$. All of the measurements were corrected for dilution and for inner filter effect.

Stopped-flow Measurements

Stopped-flow measurements were performed using a KinTek stopped flow system (Austin, TX) with 1-ms dead time. Protein Trp fluorescence emission above 320 nm was monitored using an excitation wavelength of 295 nm. A cut-off filter was used to prevent the detection of fluorescence signal below 320 nm. The observation cell was maintained at 25 °C during the stopped-flow measurements. The stopped-flow experiments were performed by mixing Fn 15^{th} type III modules ($15F_3$) in a PBS buffer after rapidly mixing with 25, 50, 100, 200, or 400 μM of $LigB_{1706\text{-}1716}$; the time course of fluorescence intensity change was recorded by computer data acquisition. In each experiment 1000 pairs of data were recorded, and sets of data from three experiments were averaged. The apparent observed rate (k_{obs}) was obtained by fitting the stopped-flow trace (average of five repeated runs) with a single exponential equation as shown follows.

$$F_t = A \exp(-k_{obs}t) + F_\infty \quad \text{(Eq. 3)}$$

where F_t is the fluorescence observed at any time, t, and A is the signal amplitude. F_∞ is the final value of fluorescence, and k_{obs} is the observed first order rate constant. In

Table 7.2. Peptides used in this study

Peptide name	Amino acid no.	Source of sequence	Residues
$LigB_{1633-1662}$	AA 1633-1662	LigB / *L. interrogans* serovar Pomona	DSLFVFKEKLYAANGGFPNSLHNGSIIHST
$LigB_{1658-1687}$	AA 1658-1687	LigB / *L. interrogans* serovar Pomona	IIHSTSANPSPCEGINRCSSWKDTAPRSNP
$LigB_{1683-1712}$	AA 1683-1712	LigB / *L. interrogans* serovar Pomona	PRSNPKWHNSPHNNWFSLELTKYRNLIPAD
$LigB_{1708-1723}$	AA 1708-1723	LigB / *L. interrogans* serovar Pomona	LIPADKAFSQFAEFNG
$LigB_{1688-1698}$	AA 1688-1698	LigB / *L. interrogans* serovar Pomona	KWHNSPHNNWF
$LigB_{1694-1704}$	AA 1694-1704	LigB / *L. interrogans* serovar Pomona	HNNWFSLELTK
$LigB_{1698-1707}$	AA 1698-1707	LigB / *L. interrogans* serovar Pomona	FSLELTKYRN
$LigB_{1700-1710}$	AA 1700-1710	LigB / *L. interrogans* serovar Pomona	LELTKYRNLIP
$LigB_{1706-1716}$	AA 1706-1716	LigB / *L. interrogans* serovar Pomona	RNLIPADKAFS
$LigB_{1711-1720}$	AA 1711-1720	LigB / *L. interrogans* serovar Pomona	ADKAFSQFAE
$LigB_{1713-1722}$	AA 1713-1722	LigB / *L. interrogans* serovar Pomona	KAFSQFAEFN
$LigB_{1714-1723}$	AA 1714-1723	LigB / *L. interrogans* serovar Pomona	AFSQFAEFNG
$LigB_{1698-1712}$	AA 1698-1712	LigB / *L. interrogans* serovar Pomona	FSLELTKYRNLIPAD
$LigB_{1703-1717}$	AA 1703-1717	LigB / *L. interrogans* serovar Pomona	TKYRNLIPADKAFSQ
$LigB_{1708-1722}$	AA 1708-1722	LigB / *L. interrogans* serovar Pomona	LIPADKAFSQFAEFN

Table 7.2 (Continued)

Peptide name	Amino acid no.	Source of sequence	Residues
$LigB_{harjo1713}$	AA 1713-1723	LigB / *L. borgpetersenii* serovar Hardjo-bovis	RDLIPADKAFS
$LigC_{1773-1783}$	AA 1773-1783	LigC / *L. interrogans* serovar Pomona	YNLIPGDKAFA
$LigB_{L1708A}$			RNAIPADKAFS
$LigB_{I1709A}$			RNLAPADKAFS
$LigB_{P1710A}$			RNLIAADKAFS
$LigB_{D1712A}$			RNLIPAAKAFS
$LigB_{1708-1723}$			LASEGIDFANAKQPFF
scrambled			
$LigB_{1706-1716}$			ASDLARIKFNP
scrambled			

Table 7.3. Thermodynamic parameters for the interaction of Fn and $LigB_{1706-1716}$

[LigB1706-1716]	[Fn]	ΔH	TΔS	K_d	ΔG
μM	μM	kcal mol^{-1}	kcal mol^{-1}	μM	kcal mol^{-1}
8	40	-3.31±0.32	3.61±0.29	8.06±0.11	-6.92

Figure. 7.7D, each value represents the mean ± SEM of three trials in triplicate samples. The residuals were measured by the differences between the calculated fit and the exponential data. In order to calculate k_{on} and k_{off} of the binding reaction, the concentrations of $LigB_{1706-1716}$ used in this experiment were at least 25 fold higher than that of 15F3 to fulfill the requirement of pseudo-first order so kobs obtained from different concentrations of $LigB_{1706-1716}$ could fit the following equation to determine the value of k_{on} and k_{off}.

$$k_{obs} = k_{on} [LigB_{1706-1716}] + k_{off} \quad \text{(Eq. 4)}$$

Isothermal Titration Calorimetry

Calorimetric experiments were carried out with CSC 5300 microcalorimeter (Calorimetry Science Corp. Lindon, UT, USA) at 25℃ as previously described [23; 24]. The cell contained 1 ml of a solution containing $LigB_{1706-1716}$; the syringe contained 250 µl of a solution of full length Fn at a concentration indicated in Table 7.3. Both solutions were in phosphate based saline, pH 7.5. The titration was performed as follows: 25 injections of 10 µl (Table 7.3) with a stirring speed of 250 rpm, with delay time between the injections at 5 min. Data were analyzed using Titration Binding Work 3.1 software (Calorimetry Science Corp. Lindon, UT, USA) fitting them to an independent binding model. The concentration of Fn and $LigB_{1706-1716}$ used in this study was based on our preliminary dose titration experiment (data not shown).

Statistical analysis

Significance between samples was determined using the Student's t-test following logarithmic transformation of the data. Two-tailed P-values were determined for each sample and a P-value <0.05 was considered significant. Each data point represents the

mean ± standard error of the mean (SEM) of sample tested in triplicate. An (*) indicates the result was statistically significant.

NMR Sample Preparation and Experiments

Cysteine conjugated $LigB_{1703-1717}$ used to immunize mice was prepared by dissolving lyophilized powder in a solution of PBS (pH 6.0) in either H_2O or D_2O to apply to NMR. The pH was adjusted by phosphoric acid or sodium hydroxide to a final concentration of 2.51 mM.

NMR spectra were recorded at 25°C on a Varian Inova 600 MHz spectrometer using the States-Haberkorn hypercomplex method of frequency discrimination [51]. Two-dimensional homonuclear total correlation spectroscopy (TOCSY) [52] and nuclear Overhauser enhancement spectroscopy (NOESY) [53] spectra were recorded with spectral widths of 6 kHz in t1 (1024 real + imaginary data points in the TOCSY and H_2O NOESY experiments, 800 real + imaginary in the D_2O NOESY experiment) and 8 kHz in t2 (2048 real + imaginary data points). Two-dimensional TOCSY spectra were acquired with a DIPSI-2 [54] isotropic mixing period (t_{mix}) of 55 ms, and NOESY spectra were acquired with a t_{mix} of 200 ms. For both experiments, the spectra were processed to a final data size of 1024 by 2048 real points.

NMR data were processed and analyzed using the software tools nmrPipe and nmrDraw [55]. Solvent subtraction was obtained by subtraction of a fourth-order polynomial fit in the time domain. The free induction decay (FID) was generally multiplied by a 72° shifted squared sine-bell function before zero-fitting and Fourier transformation. Linear baseline correction was applied in the acquisition dimension of all spectra. Analysis of the resulting TOCSY and NOESY spectra yielded proton resonance assignments for all 16 LigB-derived residues (Table 7.4). Cys1 and Thr2 lack δ_{HN} assignments because of fast proton exchange of the N-terminal amino group.

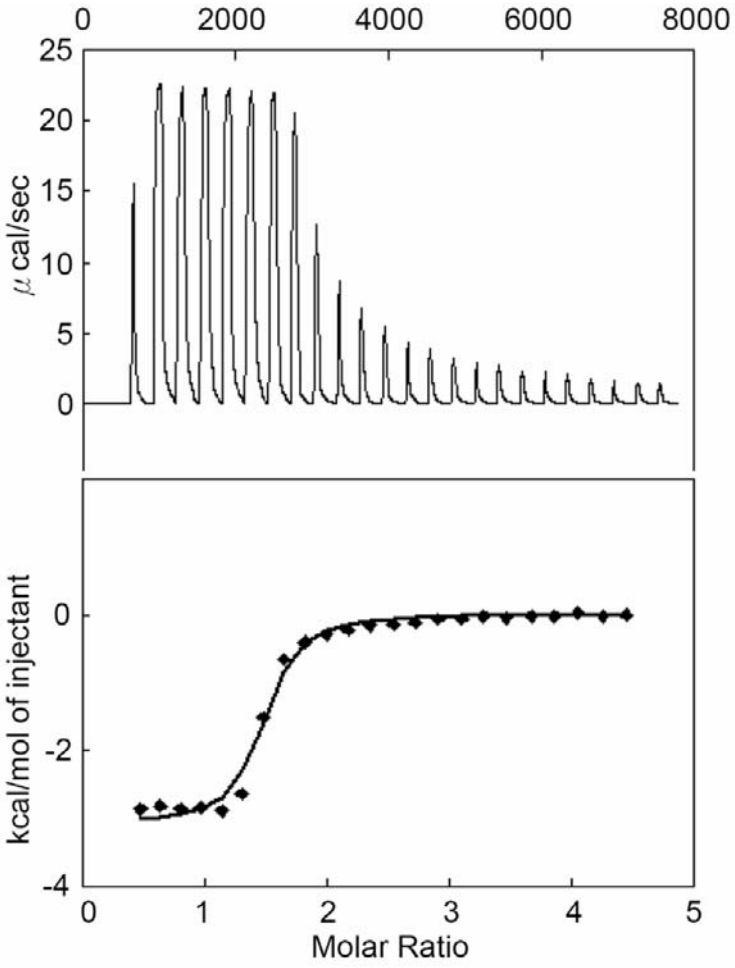

Figure 7.2 Binding affinity determined by the ITC profile of $LigB_{1706-1716}$ with Fn. Data of heat change obtained with Fn titration is shown in the upper panel. In the lower panel, the solid lines represent the best fits to a single-site binding model data after peak (◆) integration, subtraction of blank titration data (not shown), and concentration normalization. Molar heats of binding are plotted vs. the molar ratio of Fn to $LigB_{1706-1716}$. Binding potency of protein with ligand K_D is 8.06μM. The thermodynamic data that were obtained from ITC are shown in Table 7.3.

Construction of a Ribbon model of the 15th type III module of Fn

A Ribbon model was made with the program CPHmodels 2.0 (http://www.cbs.dtu.dk/services/CPHmodels) for residues 2116-2189 (corresponding to the 15F3) of rat fibronectin using data previously published, coordinated, and retrieved from the Protein Data Bank (PDB http://www.rcsb.org) [56].

Results

LigB Residues from 1708-1712 (LIPAD) possess Fn-binding activity

To identify the Fn-binding region, truncated forms of LigBCtv including LigBCtv1, LigBCtv2, LigBCtv3, and LigBCtv4 (Figure. 7.1A) were purified and assayed for Fn-binding capability using ELISA. Only LigBCtv2 and LigBCtv3 bind to Fn (Figure. 7.1B). The Fn-binding region was more finely mapped to LigB residues 1688-1723 using synthesized peptides corresponding to the LigBCtv sequence (Figure. 7.1C, Table 7.2). To identify the specific residues required for Fn-binding activity, peptides corresponding to AA 1688-1723 were synthesized with overlapping regions of 5 amino acids (Figure. 7.1D and Table 7.2). As presented in Figure. 7.1D, $LigB_{1706-1716}$ displayed the highest Fn-binding activity, while both $LigB_{1700-1710}$ and $LigB_{1711-1720}$ had moderate Fn-binding affinities. Based on the alignment of these three peptides, the residues LIPAD ($LigB_{1708-1712}$) of LigBCtv were found to be essential for Fn binding (Figure. 7.1E).

In order to investigate the importance of each residue of $LigB_{1708-1712}$, LIPAD, to Fn-binding, peptide variants of $LigB_{1706-1716}$ with individual residues substituted with alanine were synthesized. These peptides, designated $LigB_{L1708A}$, $LigB_{I1709A}$, $LigB_{P1710A}$, and $LigB_{D1712A}$, were screened for Fn-binding activity with ELISA (Table 7.2). The binding activities of each of these peptides was significantly decreased (Figure. 7.1F),

suggesting that polar or charge-charge interactions involving D1712 and hydrophobic interactions involving L1708 and I1709 may serve important roles in binding.

The binding of $LigB_{1706-1716}$ to Fn was also confirmed using isothermal titration calorimetry (ITC), which yielded a K_D of 8.06 ± 0.11 μM (Figure. 7.2 and Table 7.3). As seen in Table 7.3, the ΔH of binding is negative while the ΔS is positive, consistent with the release of water molecules upon binding. This indicates that the binding of $LigB_{1706-1716}$ to Fn is driven by favorable changes in both entropy and enthalpy, in agreement with our finding that both polar and hydrophobic residues are critical for the binding event (Figure. 7.1F).

To further explore the role of the LIPAD residues in Fn-binding activity, a competitive ELISA assay was performed where the LigBCtv-Fn interaction was inhibited by treating Fn-coated microtiter plate wells with various concentrations of $LigB_{1706-1716}$, LigBCtv, and BSA. We found that $LigB_{1706-1716}$ as well as LigBCtv could block the binding of LigBCtv to Fn (data not shown).

$LigB_{1708-1712}$ LIPAD residues mediate the attachment of Leptospira to MDCK cells

To investigate the role of the LIPAD residues in cell binding, 100 μl of various concentrations (0, 1.25, 2.5, 5, or 10 μM) of biotin-conjugated $LigB_{1706-1716}$ or biotin were added to MDCK cells; binding levels were detected using ELISA and immunofluorescence staining. Our results clearly show that biotin-$LigB_{1706-1716}$, but not biotin alone, binds to MDCK cells in a dose-dependent manner (K_D = 2.23 μM, Figure. 7.3A, 7.3C). Pretreatment of MDCK cells with 10 μM biotin-$LigB_{1706-1716}$ for 1 hour reduced the attachment of *Leptospira* by approximately 39% compared to either untreated (data not shown) or biotin-treated MDCK cells, also in a dose-dependent manner (Figure. 7.3B).

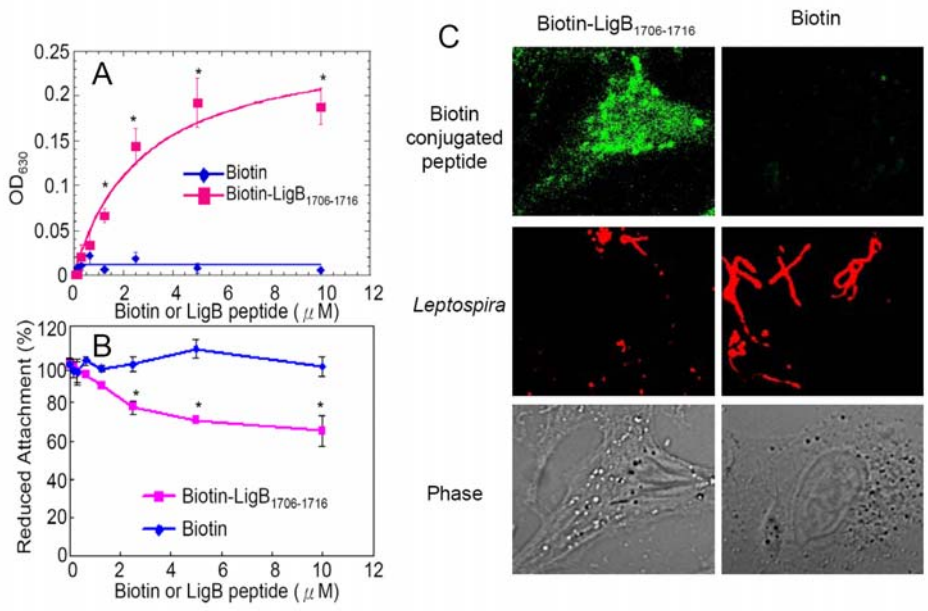

Figure. 7.3 The binding of $LigB_{1706-1716}$ to MDCK cells reduces leptospiral adhesion. (A) Binding of $LigB_{1706-1716}$ to MDCK cells. Various concentrations (0, 2, 4, 6, 8, or 10 μM) of biotin-$LigB_{1706-1716}$, or biotin (negative control) were added to MDCK cells (10^5), and binding was measured by ELISA. (B) $LigB_{1706-1716}$ inhibits the binding of *Leptospira* to MDCK cells. MDCK cells were incubated with various concentrations (0, 2, 4, 6, or 8, 10 μM) of biotin-$LigB_{1706-1716}$, or biotin (negative control) prior to the addition of *Leptospira* (10^7). The adhesion of *Leptospira* to MDCK cells (10^5) was detected by ELISA. The reduced percentage of attachment was determined relative to the attachment of *Leptospira* on untreated MDCK cells. (C). $LigB_{1706-1716}$ inhibits the binding of *Leptospira* to MDCK cells. MDCK cells (10^6) were pre-treated with 10 μM of biotin-$LigB_{1706-1716}$, and biotin (negative control) prior to the addition of *Leptossira* (10^8). The adhesion of *Leptospira* or the binding of these proteins to MDCK cells was detected by CLSM. In (A) and (B), each value represents the mean± SEM of three trials in triplicate samples. Statistically significant values ($P<0.05$) are indicted by *. In (C), the CLSM settings were identical for all the captured images. Images were processed using Adobe Photoshop CS2.

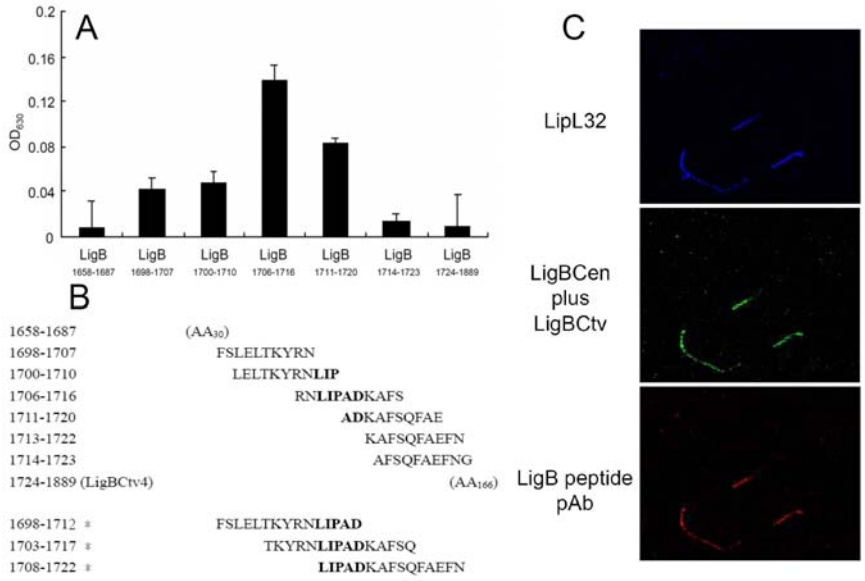

Figure 7.4 LigBCtv residues encompassing the LIPAD domain are surface-exposed. (A) To test for binding of the polyclonal antibody against peptides containing the LIPAD residues, ELISAs were performed with various overlapping LigB peptides or BSA (negative control, data not shown). The polyclonal serum was only reacted to those peptides containing all or part of the sequence used for immunization. (B) Alignment of peptide sequences used in the ELISA revealed that the LigB peptide pAb recognized a region of LigB protein that was no greater than 16 amino acids. The three peptides marked with the asterisks were used to generate the LigB peptide pAb. The residues indicated in bold were the five residues in LigB peptides that are essential for Fn-binding activity. (C) 10^8 of low passage *L. interrogans* were cultured in EMJH with 150mM of NaCl overnight and were sequentially fixed and incubated with rabbit anti-LipL32, mouse anti-LIPAD containing peptide (LigB peptide pAb), and hamster anti-LigBCen plus LigBCtv polycolonal serum as primary antibodies and Alexa647 conjugated goat anti-rabbit IgG, Texas red conjugated goat anti-mouse IgG, and Alexa 488 conjugated goat anti-hamster IgG as secondary antibodies. The CLSM settings were identical for all the captured images. Images were processed using Adobe Photoshop CS2.

$LigB_{1708-1712}$ LIPAD residues are surface-exposed *in vivo*

To determine whether the $LigB_{1708-1712}$ LIPAD residues are surface-exposed in the pathogen, mouse anti-LigB peptide polyclonal antibodies (LigB peptide pAb) were generated using three peptides spanning residues 1698-1722 of LigB, which include the LIPAD sequence. To determine the binding specificity of these LigB peptide pAbs, ELISA was performed with a variety of LigB-derived peptides (Figure. 7.4B). As shown in Figure. 7.4A, the LigB peptide pAb recognize a stretch of about 16 amino acids within LigBCtv which contain the LIPAD sequence. To determine if the $LigB_{1708-1712}$ LIPAD residues are surface-exposed, immunofluorescence staining was performed and visualized using confocal laser-scanning microscopy. High- and low-passage *Leptospira* were incubated with LigB peptide pAb as well as polyclonal antibodies against LigBCtv, LigBCen, and LipL32. The high passage Leptospira was used as negative reference (data not shown). *Leptospira* were cultured in EMJH medium with 150 mM sodium chloride to enhance expression levels of LigB [21; 22]. We have observed that LigB is expressed in low passage *Leptospira* cultured in EMJH medium supplemented with sodium chloride (data not shown), and is recognized by anti-LigB peptide pAb and polyclonal antibodies against LigBCtv and LigBCen (Figure. 7.4C) [18; 20]. The constitutively-expressed LipL32 served as a positive control (Figure. 7.4C and data not shown) [26]. These results indicate that the $LigB_{1708-1712}$ LIPAD residues are surface-exposed.

The LigB LIPAD Fn-binding motif is conserved in various serovars of pathogenic *Leptospira* and also present in LigC

Sequence analysis reveals that the LIPAD motif is conserved in LigB proteins from several serovars of pathogenic *Leptospira,* including Pomona, Copenhageni, Lai, and Hardjo (Figure. 7.5A). Surprisingly, LIPAD sequence is also present in LigC proteins

Figure 7.5 LIPAD Fn-binding motif distributed in LigB and LigC from different *Leptospira* serovars show similar Fn-binding activity. (A) Sequence alignment of LigB from *L. interrogans* serovar Pomona type kennewicki (GenBank™ AAP74956) (LigB_Pomona), *L. interrogans* serovar Copenhageni (GenBank™ AAS69085) (LigB_Copenhageni), *L. interrogans* serovar Lai (GenBank™ AAN50976) (LigB_Lai), *L. borgpetersenii* serovar Hardjo-bovis JB197 (GenBank™ ABJ75289) (LigB_Hardjo-bovis), *L. kirschneri* serovar Grippotyphosa (GenBank™ AAP04736) (LigB_Grippotyphosa), and LigC from *L. interrogans* serovar Lai (GenBank™ AAN50273) (LigC_Lai), *L. interrogans* serovar Pomona type kennewicki (GenBank™ AAP92092) (LigC_Pomona) were aligned along the of LIPAD Fn-binding motif. Sequence alignments were performed using the programs ClustalW [57] and BioEdit [58]. Black and gray outlines indicate identical and similar amino acid residues, respectively, and the sequence number is presented on the side. (B) Various concentrations (40μM, 20μM, 10μM, 5μM, 2.5μM, 1.25μM, 0.625μM) of biotinylated $LigB_{1706\text{-}1716}$, $LigB_{hardjo1713}$, $LigC_{1773\text{-}1783}$, scrambled LigB peptide (negative control), or BBK32 (56-205) (positive control) (10nM in 100μL PBS) was added to wells coated with one μg of Fn. The binding of each of these proteins or peptides to Fn was determined by ELISA. Each value represents the mean ± SEM of three trials in triplicate samples. Statistically significant ($P<0.05$) binding of peptides compared to BSA by Fn is indicted by *.

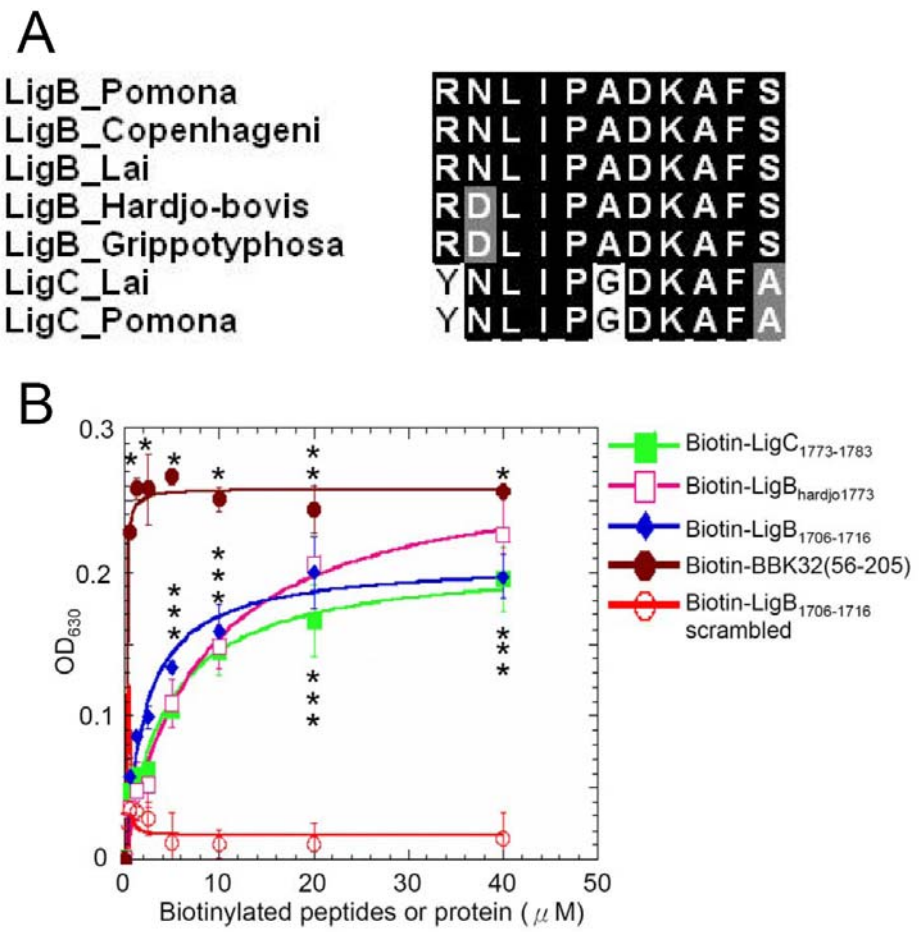
A
LigB_Pomona
LigB_Copenhageni
LigB_Lai
LigB_Hardjo-bovis
LigB_Grippotyphosa
LigC_Lai
LigC_Pomona
RNLIPADKAFS
RNLIPADKAFS
RNLIPADKAFS
RDLIPADKAFS
RDLIPADKAFS
YNLIPGDKAFA
YNLIPGDKAFA
B
OD630
0.3
0.2
0.1
0
0
10
20
30
40
50
Biotinylated peptides or protein (μM)
Biotin-LigC1773-1783
Biotin-LigBhardjo1773
Biotin-LigB1706-1716
Biotin-BBK32(56-205)
Biotin-LigB1706-1716 scrambled

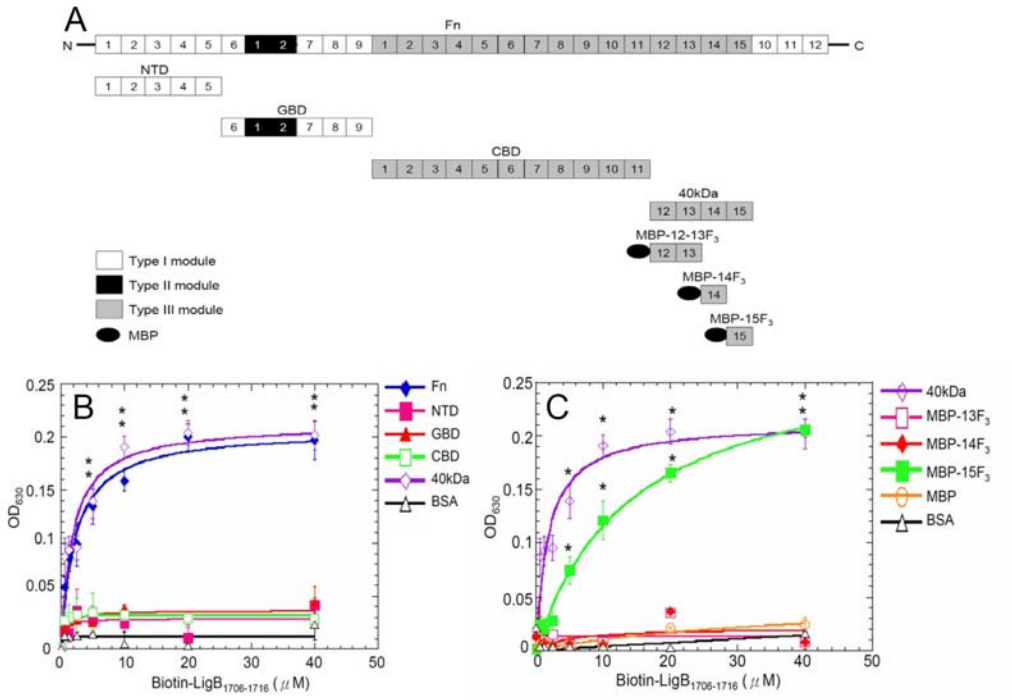

Figure 7.6 Mapping the LIPAD binding site in Fn. (A) A chart presenting the location of Fn and truncated Fn used in this study. (B and C) Binding of LigB LIPAD motif to various concentration of immobilized Fn and 40kDa domain. Various concentration of biotin-$LigB_{1706-1716}$ and biotin (negative control and data not shown) (0.625, 1.25, 2.5, 5, 10, 20, 40μM) were added to 1μg of (B) full length Fn, NTD, GBD, CBD, 40kD domain (40kDa), or BSA (negative control) (C) 40kDa domain, MBP-12-$13F_3$, MBP-$14F_3$, MBP-$15F_3$, MBP(negative control), or BSA (negative control) in 100μL PBS coated microtiter plate wells. Bound proteins were measured by ELISA.

of serovars Pomona type kennewicki and Lai (Figure. 7.5A). As shown in Figure. 7.5B, LIPAD peptide analogs corresponding to the sequences from these serovars exhibit similar Fn-binding activity.

The LigB LIPAD motif binds to the 15th type III module of Fn and exhibits slow binding kinetics

In order to identify the specific region of Fn recognized by the LigB LIPAD motif, ELISA was performed with biotin-$LigB_{1706-1716}$ and full-length Fn or different truncated domains of Fn including NTD, GBD, CBD, and a 40 kDa domain containing the last four type III module repeats (Figure. 7.6A). The results (Figure. 7.6B) show that $LigB_{1706-1716}$ binds exclusively to intact Fn (K_D = 5.45 ± 0.64 μM) and the 40 kDa domain (K_D = 5.31 ± 0.96 μM). To further locate the binding site on the 40 kDa domain, the assay was repeated with biotin-$LigB_{1706-1716}$ and MBP-12-$13F_3$, MBP-$14F_3$, MBP-$15F_3$, BSA, MBP (negative control), and the 40 kDa domain (positive control) (Figure. 7.6A). Only the 40 kDa domain and MBP-$15F_3$ (K_D = 14.31 ± 0.76 μM) were observed to immobilize $LigB_{1706-1716}$, though the binding of MBP-$15F_3$ was slightly weaker than that of the 40 kDa domain (Figure. 7.6C). Quenching of the intrinsic Trp fluorescence intensity of $15F_3$ in the presence of $LigB_{1706-1716}$ is in agreement with the results (K_D = 11.70 ± 2.23 μM), indicating that the LigB LIPAD motif binds to $15F_3$ (Figure. 7.7A, 7.7B). Furthermore, stopped flow techniques were used to obtain kinetic rates for the $LigB_{1706-1716}$:$15F_3$ interaction. As shown in Figure. 7.7C and D, the concentrations of all the reactant species fulfilled the requirement for a pseudo-first order rate equation. The kinetic rates of $LigB_{1706-1716}$-$15F_3$ (k_{on} = 600 ± 12 M^{-1} Sec^{-1} and k_{off} = 0.0129 ± 0.0003 Sec^{-1}), are very slow relative to typical rates for protein-protein interactions [27]. These results indicate that the LIPAD motif binds to the 15th type III module ($15F_3$) with unusually slow binding kinetics.

Figure 7.7 Kinetic analysis of the binding of LIPAD Fn-binding motif and 15th type III modules of Fn. (A) Intrinsic fluorescence spectrum of $15F_3$ in the presence and absence of LigB LIPAD motif. 1 μM of $15F_3$ in PBS was excited at 295 nm. Aliquots of $LigB_{1706-1716}$ were added. The figure shows Trp fluorescence in the presence of 0, 0.625, 1.25, 2.5, 5, 10, 20 and 40 μM of $LigB_{1706-1716}$. (B) The determination of K_D of $15F_3$ and LigB LIPAD motif by monitoring quenching fluorescence intensities. The emission wavelength recorded in this figure was 350nm, and K_D was obtained by fitting the data to Eq. 2. (K_D= 10.70±2.23μM). Each value represents the mean ± SEM of three trials in triplicate samples. (C) Time course of the intrinsic fluorescence intensity caused by binding of $15F_3$ to $LigB_{1706-1716}$. Single-exponential fit to the fluorescence data. Excitation wavelength was 295nm. The signal represents the total fluorescence emission above 320nm. The residuals were measured by the differences between the calculated fit and the exponential data. (D) The kinetic plot of k_{obs} versus concentration of 1μM $15F_3$ under different $LigB_{1706-1716}$ concentrations (25, 50, 100, 200, 400μM). k_{on} and k_{off} were obtained as the intercept (k_{on} = 600±12$M^{-1}Sec^{-1}$) and the y intercept (k_{off} = 0.0129±0.0003Sec^{-1}). (E) A ribbon model showing the surface-exposed tryptophan, W_{2122}, in 15th type III module of rat Fn.

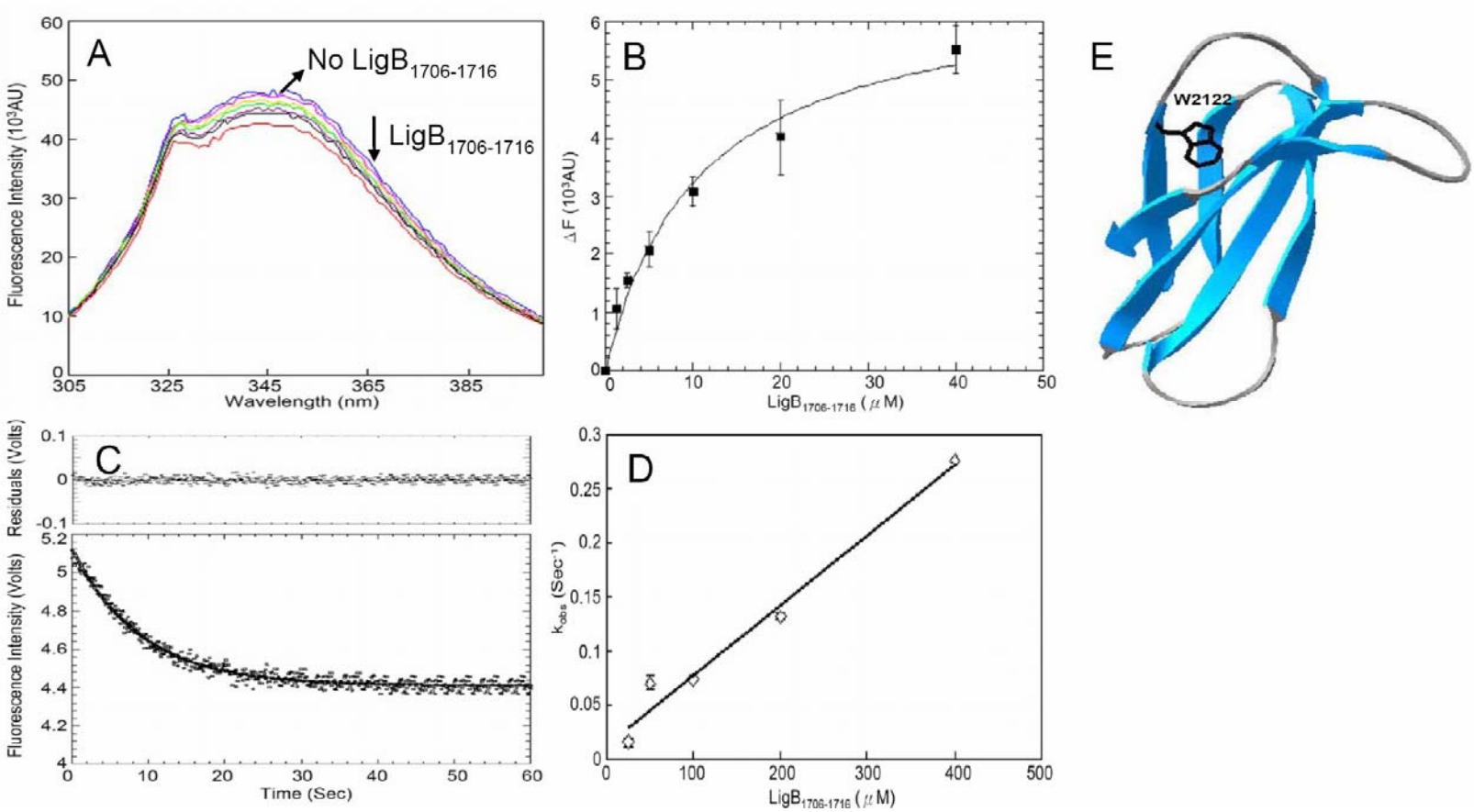
A
No LigB1706-1716
LigB1706-1716
Fluorescence Intensity (10³AU)
Wavelength (nm)
B
ΔF (10³AU)
LigB1706-1716 (μM)
E
W2122
C
Residuals (Volts)
Fluorescence Intensity (Volts)
Time (Sec)
D
kobs (Sec⁻¹)
LigB1706-1716 (μM)

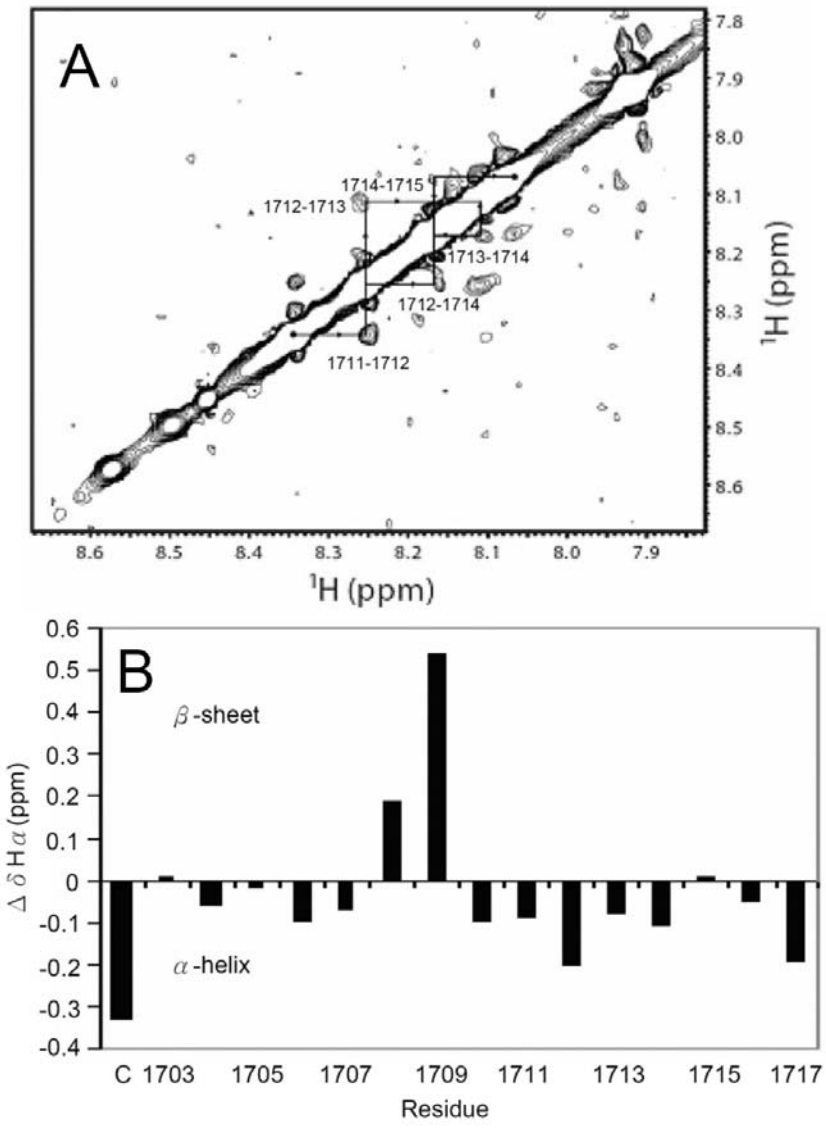

Figure 7.8 (A) H^N-H^N region of the homonuclear NOESY spectrum (t_{mix} = 200 ms, pH = 6.0) of $LigB_{1703\text{-}1717}$ in PBS in H_2O. The d_{NN} cross-peaks are labeled with residue numbers, and arrows indicate sequential connectivities. The NOEs between sequential residues in residues A_{1711} through F_{1715} indicate nascent helical character. (B) Plot of the difference in H^{α} chemical shifts, or $\Delta\delta_{H\alpha}$, between observed and random coil values for $LigB_{1703\text{-}1717.}$ C indicated the first cysteine conjugated on $LigB_{1703\text{-}1717.}$ A stretch of $\Delta\delta_{H\alpha}$ values below -0.1 indicates nascent α-helical structure, and a stretch of values above 0.1 indicates preference for β-strand conformation.

Table 7.4. Proton chemical shift assignments for $LigB_{1703-1717}$ (error ± 0.01 ppm)

residue	δ_{HN}	$\delta_{H\alpha}$	$\delta_{H\beta}$	$\delta_{H\gamma}$	$\delta_{H\delta}$	$\delta_{H\varepsilon}$
Cys	--	4.32	3.35, 3.11			
Thr1703	--	4.36	4.11	1.14		
Lys1704	8.41	4.28	1.68	1.27	1.34	2.97
Tyr1705	8.18	4.58	3.04, 2.89	2,6H: 7.12	3,5H: 6.84	
Arg1706	8.24	4.28	1.79, 1.71	1.55	3.17	
Asn1707	8.38	4.68	2.85, 2.73			
Leu1708	8.17	4.36	1.57	1.63	0.84, 0.91	
Ile1709	8.15	4.49	1.89	1.48, 1.17, 0.94	0.86	
Pro1710	--	4.34	2.29	1.95, 2.06	3.66, 3.88	
Ala1711	8.34	4.26	1.40			
Asp1712	8.26	4.56	2.70			
Lys1713	8.11	4.28	1.74, 1.85	1.44	1.69	3.01
Ala1714	8.18	4.24	1.29			
Phe1715	8.08	4.67	3.07, 3.21	2,6H: 7.30	3,5H: 7.38	4H: 7.33
Ser1716	8.10	4.45	3.83			

Table 7.4 (Continued)

residue	δ_{HN}	$\delta_{H\alpha}$	$\delta_{H\beta}$	$\delta_{H\gamma}$	$\delta_{H\delta}$	$\delta_{H\varepsilon}$
Gln1717	7.92	4.18	1.95	2.14, 2.31		

β-Strand and nascent helical characters are present in a peptide containing the LIPAD motif

The structure of $LigB_{1703\text{-}1717}$ was investigated with solution NMR. The nuclear Overhauser effect, or NOE, is a useful structural probe for identifying spatially close residues. A NOE cross-peak between two atoms indicates that they are separated by a distance of less than 5 Å. Sequential through-space NOE cross-peaks between successive amide protons, or $d_{NN}(i,i+1)$ NOEs, were observed for residues $A_{1711}D_{1712}K_{1713}A_{1714}F_{1715}$ in the NOESY spectra of $LigB_{1703\text{-}1717}$, shown in Figure 8A. An additional cross-peak between the amide protons of D_{1712} and A_{1714}, or $d_{NN}(i,i+2)$ NOE, was also observed. This pattern of local NOEs is indicative of nascent helical structure, which is defined as an equilibrium between a series of turn-like structures and unfolded states [28]. No other d_{NN} NOEs were observed, and other $d_{N\alpha}$ NOEs did not reveal any additional structure, although more peaks may be present but unresolved due to overlap.

An additional probe of backbone structure is provided by the resonance frequency of alpha protons ($\delta_{H\alpha}$). Because of the distance between an alpha proton and the side chains of its preceding and following residues, its electronic environment is dominated by its own side chain identity and φ and ψ torsion angles but not the identities of neighboring residues. The difference between an observed Hα chemical shift and the corresponding random coil value for a given type of amino acid residue, or $\Delta\delta_{H\alpha}$, gives an accurate measure of the secondary structure of proteins and peptides[29]. Three or more sequential $\Delta\delta_{H\alpha}$ values greater than +0.1 indicate -strand conformation, whereas four or more sequential $\Delta\delta_{H\alpha}$ values less than -0.1 indicate helical conformation. Values of $\Delta\delta_{H\alpha}$ were determined for $LigB_{1703\text{-}1717}$ and the results are depicted in Figure 8B. The low value for cysteine, the first amino acid in the peptide (conjugated for mouse immunization) is most likely due to its position near the positive N terminus. The plot

reveals $\Delta\delta_{H\alpha}$ values greater than +0.1 for sequential residues L_{1708} and I_{1709} (+0.19 and +0.54, respectively), indicating that this segment of the peptide may transiently adopt a β-strand conformation. Although minor corrections to $\Delta\delta_{H\alpha}$ have been rationalized in the interpretation of $\Delta\delta_{H\alpha}$ for residues directly preceding a proline, the large positive value for I_{1709} observed here far exceeds the typical correction (+.11 ppm) [30]. This region is followed by a nascent helical region for residues $A_{1711}D_{1712}K_{1713}A_{1714}$. Although not all below -0.1 ppm, the sequential negative values of $\Delta\delta_{H\alpha}$ are consistent with the nascent helical character deduced from the observed NOEs involving these residues as described above.

Discussion

Various bacterial MSCRAMMs possess Fn-binding activity [31; 32] which is often pivotal for host cell colonization and bacterial infection. Molecular interactions of bacterial pathogens and Fn have been extensively studied in recent years, especially with *S. aureus* and *Streptococcus* spp. These studies have made progress towards a greater understanding of how these interactions lead to host cell signaling and physiological changes and can result in bacterial uptake [5]. Leptospiral LigB has emerged as an important Fn binding protein that can serve as a protective antigen against *Leptospira* infection [33-36] and its Fn-binding regions have been found to be localized to two regions, LigBCen and LigBCtv [15; 16; 24]. This study sought to finely map the Fn binding site of LigBCtv.

Based on the results from this study, the sequence LIPAD ($LigB_{1708\text{-}1712}$) on LigBCtv is required for Fn-binding. The Fn-binding capabilities of LIPAD alanine-substituted peptides including $LigB_{L1708A}$, $LigB_{I1709A}$, $LigB_{P1710A}$, and $LigB_{D1712A}$ were greatly reduced compared to the wild-type $LigB_{1706\text{-}1716}$, indicating that the LIPAD residues are important for LigBCtv's interaction with Fn. These results are

consistent with the reduced binding of LigBCtv to Fn that was observed upon pretreatment of Fn with $LigB_{1706-1716}$ (data not shown). The binding affinity of $LigB_{1706-1716}$ and Fn measured by ITC also confirms these results (K_D = 8.06 μM, Figure. 7.2 and Table 7.3). It should be noted that this is within the error of the K_D of the interaction between whole LigBCtv and Fn (K_D = 8.55 ± 0.75 μM) as measured by ITC [24]. This strongly suggests that the residues of $LigB_{1706-1716}$ are predominantly responsible for the interaction between LigBCtv and Fn and that long-range structure-dependent interactions were not overlooked as a result of the truncation-based screening process.

LigBCtv mediates *Leptospira* adhesion to MDCK cells, as evidenced by the reduced attachment of *Letpospira* to LigBCtv-treated cells [24]. In this study, the adhesion of *Leptospira* to MDCK cells pretreated with a LIPAD-containing peptide ($LigB_{1706-1716}$) was also decreased (Figure. 7.3C). We hypothesized that AA 1708-1712 of LigBCtv are responsible for *Leptospira* adhesion. Adhesion inhibition caused by $LigB_{1706-1716}$ was 39 ± 5% (Figure. 7.3B), slightly less than 47% ± 5% for cells pretreated with LigBCtv [24] though the errors of these measurements overlap. This may be due to other regions of LigBCtv, in addition to $LigB_{1706-1716,}$ mediating the interaction between LigBCtv and ECM components or cell-surface elements. This study also demonstrates that the LIPAD residues of LigB are highly immunogenic (Figure. 7.4) and surface-exposed. The LIPAD Fn-binding motif is present in LigB and LigC of various pathogenic serovars of *Leptospira*, and peptides corresponding to these serovars all display similar Fn-binding affinities (Figure. 7.5).

Most bacterial Fn-binding proteins have been found to bind to the NTD or GBD of Fn [37]. Recently, it was shown that the *Staphylococcus dysgalactiae* fibronectin-binding protein B3 binds to the first two F1 modules in the N-terminal domain of Fn by contributing an additional antiparallel strand to a β-sheet in each

module [38]. A few bacterial Fn-binding proteins have also been shown to bind to the 40 kDa domain. For example, ShdA of *Salmonella enterica* binds the cationic cradle of the 13th type III module of Fn [39]. Here, we show that the LIPAD motif of LigB binds to the 15th type III module (Figure. 7.6B and C). Our study describes for the first time a bacterial MSCRAMM binding to this module. A previous report indicated that dipeptidyl peptidase IV (DPPIV), a transmembrane sialoglycoprotein from various epithelial tissues, binds to a consensus motif, T(I/L)TGLX(P/R)G(T/V)X in the 13th, 14th, and 15th type III modules of Fn [40]. Since the LIPAD motif binds to the 15th and not the 13th or 14th type III modules (Figure. 7.6C), it can be inferred that the binding site of LIPAD should involve sequence(s) unique to the 15th type III module. Therefore, the LigB LIPAD motif is not expected to interact with the DPPIV binding site. The long wavelength (350 nm) of the maximum intensity of the fluorescence spectrum (Figure. 7.7A), and a homology model of $15F_3$ based on residues 1431 to 1505 of the 10th type III module (Figure. 7.7E) suggest that the sole tryptophan in the 15th type III module, W_{2122}, is in a polar and surface-exposed environment. The observed sensitivity of Trp fluorescence to the binding event suggests that the binding site may be near $W_{2122.}$ These results suggest that $LigB_{1706\text{-}1716}$ may exploit a novel mechanism to bind a region of Fn distinct from the previously identified DPPIV binding sites.

The immunoglobulin-like repeat regions of LigA and LigB, including LigBCen2, strongly bind to the N-terminal (NTD) and gelatin binding domains (GBD) of Fn, as well as to other ECM components [15; 16; 24]. This study identifies a Fn-binding LIPAD motif located in the C-terminal non-repeat region of LigB that binds, in comparison to interactions between LigB and other ECM components, with moderate affinity (K_D = 10.70 μM), to the 15th type III module of Fn (Figure. 7.6C, 7.7B and data not shown). This binding event has unusually slow association and dissociation rates

(k_{on} = 600 $M^{-1}Sec^{-1}$, k_{off} = 0.0129 Sec^{-1}), in agreement with the retarded equilibrium of each interaction obtained from ITC (Figure. 7.2).

The modest affinity of LigBCtv for fibronectin *in vitro* appears to be at odds with the appreciable ability of $LigB_{1706-1716}$ to block leptospiral cell binding. It is possible that environmental factors *in vivo* such as pH, ionic strength, cofactors, or other binding partners may play an important role in the binding event. As measured by ELISA (Figure 3A), the *ex vivo* binding affinity of $LigB_{1706-1716}$ for MDCK cells (K_D = 2.23 μM) is higher, albeit only modestly, than its affinity for Fn *in vitro* (K_D = 8.06 μM). Such factors assisting *ex vivo* binding may not be crucial to rectify the cell-binding inhibition data and the *in vitro* K_D measurements. Micromolar affinities are by no means unusual in biologically relevant protein-protein interactions. For example, the SH3 domain, a highly-characterized and widespread protein-interaction module important in signal transduction pathways, has K_D values in the low μM range for optimized synthetic peptide ligands. This low binding affinity is frequently compensated for by additional binding domains, such as SH2 or other SH3 domains, that act in synergy to promote biding [41]. Likewise, LigB has multiple regions that bind to different parts of fibronectin and to other components of the extracellular matrix [15; 16; 24]. It has been indicated a *ligB* mutant with an insertion containing a Spc^r cassette into the 3' end of the *ligB* gene is still virulent in a hamster model [42]. The reasons are unknown. However, there are several possibilities: 1). The truncated LigB is expressed, but at a lower level since the insertion is only in the far 3' end of *ligB* 2). Since the first 630 amino acids of LigA and LigB are identical, LigA may compensate for LigB in this mutant even with a similar LigA expression level. 3). LigB is not required for virulence in a hamster or rat model. 4). LigB is only needed for initial adhesion and invasion of *Leptospira* spp. moving from the environment through mucous membranes and injured skin. 5). The presence of several other putative adhesins with potentially redundant functions in the

pathogen. In order to answer these questions, it is essential to knockout the complete *ligA* and *ligB* genes (in frame deletion of the complete *ligA* and *ligB* genes) and perform a virulence test using different animal models, such as in dogs or monkeys or any other suitable animals.

The kinetic rates of $LigB_{1706\text{-}1716}$ binding to the 15^{th} type III module of Fn are at least 100 fold slower than rates seen with any other bacterial Fn-binding proteins (Figure. 7.6C and D) [37; 43-45]. The slow dissociation rate, k_{off}, may be an important factor in retention of the bound state in the biological system. In an *in vivo* system where the concentration of ligand is not constant, but rather influenced by factors such as absorption, distribution, metabolism, and excretion (ADME), the residence time of a receptor-ligand complex is not necessarily appropriately described by the equilibrium dissociation constant K_D [46]. Current experimental evidence has pointed to the dissociation rate constant k_{off} as a more relevant parameter in some cases. For example, recent kinetic studies [47] of peptide inhibitors of HER2, a member of the epidermal growth factor receptor family, showed that the k_{off} of the peptide-receptor complex was a better predictor of the *in vivo* efficacy of the peptides than the K_D. This has led to arguments that the dissociation rate constant may be an important parameter to be considered in drug design and screening. In light of this, it is tempting to interpret the slow dissociation rate of the $LigB_{1706\text{-}1716}$:Fn complex as an example of an evolutionarily optimized k_{off} for a bacterial adhesin/target complex, which is challenged by many of the same limitations to overall ligand concentration as drug/target complexes are.

In light of our findings that the LIPAD motif of LigB binds the 15^{th} type III module of Fn and that LigBCen2 binds the NTD of Fn, we speculate that LigB may interact with fibronectin via different binding mechanisms during different stages of infection, or possibly via both simultaneously. It is possible that LigB might bind the

NTD and 15th type III module of the same Fn molecule simultaneously, but this would require substantial bending of Fn. Alternatively, each LigBCen2 and the LIPAD motif might bind a separate Fn molecule. Binding to two different Fn molecules together might allow LigB to cluster the cell-binding regions of Fn, which in turn can cluster integrins on the surface of a host cell. This is thought to be important for the entry of invasive bacteria such as *S. pyogenes* and *S. aureus* into host cells [48]. However, unlike the multiple Fn binding sites on SfbI from *S. pyogenes* and FnBPA from *S. aureus*, the two binding sites on LigB attach to different regions of Fn, which would not seem to be ideal for such clustering.

We have demonstrated that the sequence LIPAD located on the C-terminus of LigB is a Fn-binding motif that interacts with the 15th type III module of Fn with slow binding kinetics. Furthermore, this Fn-binding motif is surface-exposed, and a peptide corresponding to this region displays β-strand and nascent helix character when free in solution. The specificity of the motif for the 15th type III module of Fn suggests a novel mode of bacterial Fn binding. The slow dissociation rate of the complex may be important for evading clearance *in vivo*, analogous to the importance of k_{off} in drug efficacy. Further studies should include the identification of the binding site within the type III module, using NMR, X-ray crystallography and/or mutagenesis studies. Work to further elucidate this interaction is in progress in our lab.

REFERENCES

1. **Levett PN** 2001 Leptospirosis. Clin Microbiol Rev **14**: 296-326.
2. **Faine SB, Adher B, Bolin C, Perolat P, editors** 1999 *Leptospira* and Leptospirosis. Medbourne, Australia: MedSci.
3. **Meites E, Jay MT, Deresinski S, Shieh WJ, Zaki SR et al.** 2004 Reemerging leptospirosis, California. Emerg Infect Dis **10:** 406-412.
4. **Vinetz JM, Glass GE, Flexner CE, Mueller P, Kaslow DC** 1996 Sporadic urban leptospirosis. Ann Intern Med **125**: 794-798.
5. **Schwarz-Linek U, Hook M, Potts JR** 2004 The molecular basis of fibronectin-mediated bacterial adherence to host cells. Mol Microbiol **52:** 631-641.
6. **Barocchi MA, Ko AI, Reis MG, McDonald KL, Riley LW** 2002 Rapid translocation of polarized MDCK cell monolayers by *Leptospira interrogans*, an invasive but nonintracellular pathogen. Infect Immun **70:** 6926-6932.
7. **Ito T, Yanagawa R** 1987 Leptospiral attachment to four structural components of extracellular matrix. Nippon Juigaku Zasshi **49**: 875-882.
8. **Ito T, Yanagawa R** 1987 Leptospiral attachment to extracellular matrix of mouse fibroblast (L929) cells. Vet Microbiol **15**: 89-96.
9. **Merien F, Truccolo J, Baranton G, Perolat P** 2000 Identification of a 36-kDa fibronectin-binding protein expressed by a virulent variant of *Leptospira interrogan*s serovar icterohaemorrhagiae. FEMS Microbiol Lett **185**: 17-22.
10. **Stevenson B, Choy HA, Pinne M, Rotondi ML, Miller MC et al.** 2007 Leptospira interrogans Endostatin-Like Outer Membrane Proteins Bind Host Fibronectin, Laminin and Regulators of Complement. PLoS ONE **2**: e1188.

11. **Barbosa AS, Abreu PA, Neves FO, Atzingen MV, Watanabe MM et al.** 2006 A newly identified leptospiral adhesin mediates attachment to laminin. Infect Immun **74**: 6356-6364.

12. **Atzingen MV, Barbosa AS, De Brito T, Vasconcellos SA, Morais ZM et al.** 2008 Lsa21, a novel leptospiral protein binding adhesive matrix molecules and present during human infection. BMC Microbiol **8**: 70.

13. **Hauk P, Macedo F, Romero EC, Vasconcellos SA, de Morais ZM et al.** 2008 In LipL32, the major leptospiral lipoprotein, the C terminus is the primary immunogenic domain and mediates interaction with collagen IV and plasma fibronectin. Infect Immun **76**: 2642-2650.

14. **Hoke DE, Egan S, Cullen PA, Adler B** 2008 LipL32 is an extracellular matrix-interacting protein of *Leptospira* spp. and *Pseudoalteromonas tunicata*. Infect Immun **76**: 2063-2069.

15. **Choy HA, Kelley MM, Chen TL, Moller AK, Matsunaga J et al.** 2007 Physiological osmotic induction of *Leptospira interrogans* adhesion: LigA and LigB bind extracellular matrix proteins and fibrinogen. Infect Immun **75:** 2441-2450.

16. **Lin YP, Chang YF** 2007 A domain of the *Leptospira* LigB contributes to high affinity binding of fibronectin. Biochem Biophys Res Commun **362**: 443-448.

17. **Lin YP, Lee DW, McDonough SP, Nicholson LK, Sharma Y et al.** 2009 Repeated domains of *Leptospira* Immunoglobulin-like proteins interact with elastin and tropoealstin. J. Biol. Chem. **284:** 19380-19391.

18. **Matsunaga J, Barocchi MA, Croda J, Young TA, Sanchez Y et al.** 2003 Pathogenic *Leptospira* species express surface-exposed proteins belonging to the bacterial immunoglobulin superfamily. Mol Microbiol **49:** 929-945.

19. **Palaniappan RU, Chang YF, Hassan F, McDonough SP, Pough M et al.** 2004 Expression of leptospiral immunoglobulin-like protein by *Leptospira interrogans* and evaluation of its diagnostic potential in a kinetic ELISA. J Med Microbiol **53**(Pt 10): 975-984.

20. **Palaniappan RU, Chang YF, Jusuf SS, Artiushin S, Timoney JF et al.** 2002 Cloning and molecular characterization of an immunogenic LigA protein of *Leptospira interrogans*. Infect Immun **70**: 5924-5930.

21. **Matsunaga J, Lo M, Bulach DM, Zuerner RL, Adler B et al.** 2007 Response of *Leptospira interrogans* to Physiologic Osmolarity: Relevance in Signaling the Environment-to-Host Transition. Infect Immun **75** 2864-2874.

22. **Matsunaga J, Sanchez Y, Xu X, Haake DA** 2005 Osmolarity, a key environmental signal controlling expression of leptospiral proteins LigA and LigB and the extracellular release of LigA. Infect Immun **73:** 70-78.

23. **Lin YP, Raman R, Sharma Y, Chang YF** 2008 Calcium binds to Leptospiral immunoglobulin-like protein, LigB and modulates fibronectin binding. J. Biol. Chem. **283**: 25140-25149.

24. **Lin YP, Chang YF** 2008 The C-terminal variable domain of LigB from *Leptospira* mediates binding to fibronectin. J. Vet. Sci. **9:** 133-144.

25. **Markgren PO, Schaal W, Hamalainen M, Karlen A, Hallberg A et al.** 2002 Relationships between structure and interaction kinetics for HIV-1 protease inhibitors. J. Med. Chem. **45:** 5430-5439.

26. **Haake DA, Chao G, Zuerner RL, Barnett JK, Barnett D et al.** 2000 The leptospiral major outer membrane protein LipL32 is a lipoprotein expressed during mammalian infection. Infect Immun **68**: 2276-2285.

27. **Schreiber G** 2002 Kinetic studies of protein-protein interactions. Curr Opin Struct Biol **12**: 41-47.

28. **Dyson HJ, Rance M, Houghten RA, Wright PE, Lerner RA** 1988 Folding of immunogenic peptide fragments of proteins in water solution. II. The nascent helix. J Mol Biol **201:** 201-217.

29. **Wishart DS, Sykes BD, Richards FM** 1992 The chemical shift index: a fast and simple method for the assignment of protein secondary structure through NMR spectroscopy. Biochemistry **31:** 1647-1651.

30. **Schwarzinger S, Kroon GJ, Foss TR, Chung J, Wright PE et al.** 2001 Sequence-dependent correction of random coil NMR chemical shifts. J Am Chem Soc **123:** 2970-2978.

31. **Joh D, Wann ER, Kreikemeyer B, Speziale P, Hook M** 1999 Role of fibronectin-binding MSCRAMMs in bacterial adherence and entry into mammalian cells. Matrix Biol **18:** 211-223.

32. **Patti JM, Allen BL, McGavin MJ, Hook M** 1994 MSCRAMM-mediated adherence of microorganisms to host tissues. Annu Rev Microbiol **48:** 585-617.

33. **Faisal SM, Yan W, Chen CS, Palaniappan RU, McDonough SP et al.** 2008 Evaluation of protective immunity of *Leptospira* immunoglobulin like protein A (LigA) DNA vaccine against challenge in hamsters. Vaccine **26:** 277-287.

34. **Faisal SM, Yan W, McDonough SP, Chang YF** 2009 Variable region of *Leptospira* immunoglobulin like protein A (LigAvar) incorporated in Liposomes and PLGA-Microspheres produces a robust immune response correlating to protective immunity against challenge in hamsters. Vaccine **27:** 378-387.

35. **Palaniappan RU, McDonough SP, Divers TJ, Chen CS, Pan MJ et al.** 2006 Immunoprotection of recombinant leptospiral immunoglobulin-like protein A against *Leptospira interrogans* serovar Pomona infection. Infect Immun **74:** 1745-1750.

36. **Yan W, Faisal SM, McDonough SP, Divers TJ, Barr SC et al.** 2009 Immunogenicity and protective efficacy of recombinant *Leptospira* immunoglobulin-like protein B (rLigB) in a hamster challenge model. Microbes Infect **11:** 230-237.

37. **Joh HJ, House-Pompeo K, Patti JM, Gurusiddappa S, Hook M** 1994 Fibronectin receptors from gram-positive bacteria: comparison of active sites. Biochemistry **33:** 6086-6092.

38. **Schwarz-Linek U, Werner JM, Pickford AR, Gurusiddappa S, Kim JH et al.** 2003 Pathogenic bacteria attach to human fibronectin through a tandem beta-zipper. Nature **423:** 177-181.

39. **Kingsley RA, Keestra AM, de Zoete MR, Baumler AJ** 2004 The ShdA adhesin binds to the cationic cradle of the fibronectin 13FnIII repeat module: evidence for molecular mimicry of heparin binding. Mol Microbiol **52:** 345-355.

40. **Cheng HC, Abdel-Ghany M, Pauli BU** 2003 A novel consensus motif in fibronectin mediates dipeptidyl peptidase IV adhesion and metastasis. J Biol Chem **278:** 24600-24607.

41. **Mayer BJ** 2001 SH3 domains: complexity in moderation. J Cell Sci **114:** 1253-1263.

42. **Croda J, Figueira CP, Wunder EA, Jr., Santos CS, Reis MG et al.** 2008 Targeted mutagenesis in pathogenic *Leptospira* species: disruption of the LigB gene does not affect virulence in animal models of leptospirosis. Infect Immun **76:** 5826-5833.

43. **Kreikemeyer B, Oehmcke S, Nakata M, Hoffrogge R, Podbielski A** 2004 *Streptococcus pyogenes* fibronectin-binding protein F2: expression profile,

binding characteristics, and impact on eukaryotic cell interactions. J Biol Chem **279:** 15850-15859.

44. **Hardy DM, Garbers DL** 1994 Species-specific binding of sperm proteins to the extracellular matrix (zona pellucida) of the egg. J Biol Chem **269:** 19000-19004.

45. **Pankov R, Yamada KM** 2002 Fibronectin at a glance. J Cell Sci **115:** 3861-3863.

46. **Copeland RA, Pompliano DL, Meek TD** 2006 Drug-target residence time and its implications for lead optimization. Nat Rev Drug Discov **5:** 730-739.

47. **Berezov A, Zhang HT, Greene MI, Murali R** 2001 Disabling ErbB receptors with rationally designed exocyclic mimetics of antibodies: structure-function analysis. J Med Chem **44:** 2565-2574.

48. **Schwarz-Linek U, Hook M, Potts JR** 2006 Fibronectin-binding proteins of gram-positive cocci. Microbes and infection / Institut Pasteur **8:** 2291-2298.

49. **Cuff JA, Clamp ME, Siddiqui AS, Finlay M, Barton GJ** 1998 JPred: a consensus secondary structure prediction server. Bioinformatics **14:** 892-893.

50. **Kim JH, Singvall J, Schwarz-Linek U, Johnson BJ, Potts JR et al.** 2004 BBK32, a fibronectin binding MSCRAMM from *Borrelia burgdorferi*, contains a disordered region that undergoes a conformational change on ligand binding. J Biol Chem **279:** 41706-41714.

51. **States DJ, R.A. H, Rubena DJ** 1982 Two-dimensional nuclear overhauser experiment with pure absorption phase in four quadrants. J Magn Reson **48:** 286-292.

52. **Bax A, Davis DG** 1985 MLEV-17 based two-dimensional homonuclear magnetization transfer spectroscopy. J Magn Reson **65:** 355-360.

53. **Bodenhausen G, Kogler H, Ernst RR** 1984 Selection of Coherence Transfer Pathways in NMR Pulse Experiments. J Magn Reson **58:** 370-388.

54. **Shaka AJ, Lee CL, Pines A** 1988 Iterative schemes for bilinear operators; application to spin decoupling. J Magn Reson **77:** 274-293

55. **Delaglio F, Grzesiek S, Vuister GW, Zhu G, Pfeifer J et al.** 1995 NMRPipe: a multidimensional spectral processing system based on UNIX pipes. J Biomol NMR **6:** 277-293.

56. **Leahy DJ, Aukhil I, Erickson HP** 1996 2.0 A crystal structure of a four-domain segment of human fibronectin encompassing the RGD loop and synergy region. Cell **84:** 155-164.

57. **Thompson JD, Higgins DG, Gibson TJ** 1994 CLUSTAL W: improving the sensitivity of progressive multiple sequence alignment through sequence weighting, position-specific gap penalties and weight matrix choice. Nucleic Acids Res **22:** 4673-4680.

58. **Hall TA** 1999 BioEdit: a user-friendly biological sequence alignment editor and analysis program for windows 95/98/NT. Nucleic Acids Symp Ser **41:** 95-98.

CHAPTER 8

THE REPEATED DOMAINS OF *LEPTOSPIRA* IMMUNOGLOBULIN-LIKE PROTEINS INTERACT WITH ELASTIN AND TROPOEALSTIN

Introduction

Pathogenic *Leptospira* spp. are spirochetes that cause leptospirosis, a serious infectious disease of people and animals (1,2). Weil's syndrome, the severe form of leptospiral infection, leads to multi-organ damage including liver failure (jaundice), renal failure (nephritis), pulmonary hemorrhage, meningitis, abortion and uveitis (3,4). Furthermore, this disease is not only prevalent in many developing countries, it is reemerging in the United States (3). Although leptospirosis is a serious world-wide zoonotic disease, the pathogenic mechanisms of *Leptospira* infection remain enigmatic. Recent breakthroughs in applying genetic tools to *Leptospira* promise to speed studies into the molecular pathogenesis of leptospirosis (5-8).

The attachment of pathogenic *Leptospira* spp. to host tissues is critical in the early phase of *Leptospira* infection. *Leptospira* spp. adhere to host tissues to overcome mechanical defense systems at tissue surfaces and to initiate colonization of specific tissues, such as the lung, kidney, and liver. *Leptospira* invade hosts tissues through mucous membranes or injured epidermis, coming in contact with subepithelial tissues. Here, certain bacterial outer surface proteins serve as microbial surface components recognizing adhesive matrix molecules (MSCRAMMs) to mediate the binding of bacteria to different extracellular matrices (ECMs) of host cells (9). Several leptospiral MSCRAMMs have been identified (10-18) and we speculate that more will be identified in the near future.

Lig proteins are distributed on the outer surface of pathogenic *Leptospira* and the expression of Lig protein is only found in low passage strains (14,16,17), probably induced by environmental cues such as osmotic or temperature changes (19). Lig proteins can bind to fibrinogen and a variety of ECMs including fibronectin (Fn), laminin, and collagen, thereby mediating adhesion to host cells (20-23). Lig proteins also constitute good vaccine candidates (24-26).

Elastin is a component of ECM critical to tissue elasticity and resilience and is abundant in skin, lung, blood vessels, placenta, uterus and other tissues (27-29). Tropoelastin is the soluble precursor of elastin (28). During the major phase of elastogenesis, multiple tropoelastin molecules associate through coacervation (30-32). Due to the abundance of elastin or tropoelastin on the surface of host cells, several bacterial MSCRAMMs use elastin and/or tropoelastin to mediate adhesion during the infection process (33-35).

Since leptospiral infection is known to cause severe pulmonary hemorrhage (36,37) and abortion (38), we hypothesize that some leptospiral MSCRAMMs may interact with elastin and/or tropoelastin in these elastin-rich tissues. This is the first report that Lig proteins of *Leptospira* interact with elastin and tropoelastin, and the interactions are mediated by several specific immunoglobulin-like domains of Lig proteins including LigBCon4, LigBCen7'-8, LigBCen9, LigBCen12 which bind to the 17^{th} to 27^{th} exons of human tropoelastin (HTE).

Materials and Methods

Bacterial strains

L. interrogans serovar Pomona (NVSL1427-35-093002) was used in this study (18). All experiments were performed with virulent, low-passage strains obtained by infecting golden Syrian hamsters as previously described (24). *Leptospires* were grown in EMJH

medium at 30℃ for less than 5 passages; growth was monitored by dark-field microscopy.

Reagents and antibodies

rabbit anti-GST antibody and Alexa488-conjugated goat anti-hamster antibody were ordered from Molecular Probes (Eugene, OR). Horseradish peroxidase (HRP)-conjugated goat anti-hamster antibody, HRP-conjugated goat anti-horse antibody, HRP-conjugated goat anti-rabbit antibody, and HRP-conjugated streptavidin were ordered from KPL (Gaithersburg, MD). Human lung, aortic and skin elastins, and bovine serum albumin (BSA) were ordered from Sigma-Aldrich (St. Louis, MO). The Quickchange mutagenesis kit was purchased from Stratagene (La Jolla, CA). Elastin peptide was ordered from Elastin Products Company (Owensville, MO). Hamster anti-*L. interrogans* antibodies were previously prepared in hamsters from the challenge controls (24).

Plasmid construction and Protein purification

N2-N3 domain of FnBPA (rFnBPA$_{194\text{-}511}$) gene from *Staphylococcus aureus* (34,39) and full length human tropoelastin (HTE) gene (40) were cloned into pQE30 and pTrcHis-TOPO vectors, respectively, and purified as histidine-tag fusion proteins. Construction for expression as histidine-tag, GST or MBP fused with truncated HTE including 1-18 HTE (1st to 18th exons of HTE), 17-27 HTE (17th to 27th exons of HTE), and 27-36 HTE (27th to 36th exons of HTE) is schematized in Figure. 8.5A. Truncated LigB constructs including LigBCon (amino acids 47-630 in LigB), LigAVar (amino acids 631-1225 in LigA), LigBCen (amino acids 631-1417 in LigB), LigBCtv (amino acids 1418-1889 in LigB), LigBCen1 (amino acids 631-1013 in LigB),

LigBCen2(amino acids 1014-1165 in LigB), LigBCen3(amino acids 1166-1417 in LigB), LigBCon1-3 (amino acids 47-316 in LigB), LigBCon4-7'(amino acids 307-630 in LigB), LigBCon4 (amino acids 307-403 in LigB), LigBCon5 (amino acids 397-492 in LigB), LigBCon6-7'(amino acids 486-630 in LigB), LigB7'-8 (amino acids 631-756 in LigB), LigB9 (amino acids 755-850 in LigB), LigB10(amino acids 846-941 in LigB), LigB11(amino acids 942-1028 in LigB), LigB12 (amino acids 1047-1119 in LigB), and LigBCen2NR (amino acids 1120-1165 in LigB) is schematized in Figure. 8.2. Each PCR amplified fragment was inserted into vectors pET-THGT, pET-THMT, pQE30 (Qiagen, Alencia, CA) and/or pGEX-4T-2 (GE Healthcare, Piscataway, NJ) as previously described (21,22,26). Constructs for the expression of histidine-tag or GST fused LigBCon, LigAVar, LigBCen, LigBCtv, LigBCen1, LigBCen2, LigBCen3, LigBCen2NR and GST were obtained from previous studies (21, 22, 26, 41;Figure. 8.1). Other constructs including 1-18HTE, 17-27HTE, 27-36HTE, LigBCon1-3, LigBCon4-7, LigBCon4, LigBCon5, LigBCon6-7', LigB7'-8, LigB9, LigB10, LigB11, and LigB12 were amplified by PCR using primers described in Table 8.1 and are based on the DNA sequences derived from Genbank (*L. interrogan* serovar Pomona: FJ030916)
and human tropoelastin (42). For constructing LigBCon1-3 and LigBCon4-7', primers were engineered to introduce a *Sal*I site at the 5' end and a stop codon followed by a *Not*I site at the 3' end of each fragment. For LigBCon4, LigBCon5, LigBCon6, LigBCen7'-8, LigB9, LigB10, LigB11, and LigB12 fragments, primers were engineered to introduce a *Sphl*I site at the 5' end and a stop codon followed by a *Sal*I site at the 3' end of each fragment (Table 8.1). PCR products were sequentially digested with either *Sal*I and *Not*I or *Sph*I and *Sal*I, and inserted into pQE30 or pGEX-4T-2 cut with appropriate matching restriction enzyme sets. Sets of primers were engineered to introduce an *EcoR*I site at the 5' end and a stop codon followed by a *Not*I site at the 3'

Table 8.1. Primers.

Primer/Vector	Sequence*
LigBCon1-3fp/pGEX4T2**	CGGTCGACTGGTAACTCTAATCCG
LigBCon1-3rp	CGGCGGCCGCAATAGAAACTAAGGC
LigBCon4-7'fp/pGEX4T2	CGGTCGACTATCGTTACTCCAGCA
LigBCon4-7'rp	CGGCGGCCGCAATATCCGTATTAGA
LigBCon4fp/pQE30***	CGGCATGCATCGTTACTCCAGCA
LigBCon4rp	CGGTCGACTAATACCTCTTGTGT
LigBCon5fp/pQE30	CGGCATGCAAAGTTACACAAGAG
LigBCon5rp	CGGTCGACGAGAACCGCAGGAAC
LigBCon6-7'fp/pQE30	CGGCATGCACTGTAGTTCCTGCG
LigBCon6-7'rp	CGGTCGACAATATCCGTATTAGA
LigBCen7'-8fp/pQE30	CGCGGATCCATTGCTGAAATT
LigBCen7'-8rp	CGCCCTGCAGGACATTCAAAAC
LigBCen9fp/pQE30	CGGCATGCAATGTCACTCCTGCA
LigBCen9rp	CGGTCGACTAAGTCAGTGACTGT
LigBCen10fp/pQE30	CGGCATGCACAGTCACTGACTTA
LigBCen10rp	CGGTCGACGGCAGCACTTACATT
LigBCen11fp/pQE30	CGGGATCCACGTTAGATTCCATT
LigBCen11rp	CGAAGCTTTTAGACCGTTATGTC
LigBCen12fp/pQE30	CGGGATCCACCCTTTCTTCGATT
LigBCen12rp	CGAAGCTTTTATACTGTGAGAATTGT
LigBCon4D341Nf****	GGGATCTTTACAAATAATTCAAACTCG
LigBCon4D341Nr****	CGAGTTTGAATTATTTGTAAAGATCCC
1-18HTEfp/pET-THGT#	CGGAATTCATGGCGGGTCTGACGGCG
1-18HTErp/	CGGCGGCCGCTGGAACCGCAGCACC

Table 8.1 (Continued)

Primer/Vector	Sequence*
17-27HTEfp/pET-THGT	CGGAATTCGGCGTTGGGACTCCA
17-27HTErp/	CGGCGGCCGCTCCATATTTGGCTGC
27-36HTEfp/pET-THMT$	CGGAATTCGTACCTGGAGCCCTG
27-36HTErp	CGGCGGCCGCTTTTCTCTTCCGGCC

* The restriction enzyme cutting sites were underlined. ** GE Healthcare, Piscataway, NJ, ***Qiagen Inc., Volencia,CA,**** Primers used for site directed mutagenesis. # and $: Obtained from the Cornell protein production and characterization core facility, Cornell University).

end of each fragment in constructing 1-18HTE, 17-27HTE, and 27-36HTE clones. (Table 8.1). PCR products were sequentially digested with *EcoR*I and *Not*I then ligated into pET-THMT or pET-THGT (obtained from the Cornell protein production and characterization core facility, Cornell University) cut with *EcoR*I and *Not*I, respectively. For LigBCon4D35N mutant construction, the pQE30 expression plasmid containing the DNA sequence encoding LigBCon4 was subjected to site-directed mutagenesis using the Quickchange mutagenesis kit following the manufacturer's instructions (Strategene, La Jolla, CA). Resulting PCR products were digested with *Dpn*I to remove contaminating wild-type plasmid and then transformed into *E.coli* XL-1 Blue (Strategene, La Jolla, CA). Transformants were screened and subjected to DNA sequencing. In this study, we purified the soluble form of the histidine-tag, GST, or MBP fusion proteins from *E. coli* as previously described (21,23,41).

Bacterial Adhesion to Immobilized Elastin or Tropoelastin measured by ELISA and Epifluorescence Microscope (EPM)

To measure the binding of *Leptospira* to elastin or tropoelastin, 100μL of 10 μg/mL of human lung elastin, chicken tropoelastin, or BSA (negative control) were coated onto microtiter plate wells. For dose dependent binding experiments, 100μL of different concentrations of each human lung, aortic and skin elastins, chicken tropoelastin, or BSA were coated onto microtiter plate wells. In order to immobilize elastin, all of the elastins were dissolved in coating buffer (0.1M sodium bicarbonate, pH 9.4), and then air-dried under UV light (355nm) at room temperature (RT) for 18 hours as previously described (35). To immobilize tropoelastin or BSA, tropoelastin or BSA was dissolved in Tris buffer (25mM Tris and 150mM sodium chloride at pH7.5), added to microtiter plate wells and incubated at 4^{o}C overnight (21,22,43). After the plates were subsequently blocked with blocking buffer (100μL/well) containing 3% BSA in Tris

buffer at RT for 2 hours, *Leptospira* (10^7) were added to each well and further incubated at 37^{o}C for 6 hours. Following incubation, the plates were washed three times with Tris buffer containing 0.05% Tween-20 (TBST). To measure the binding of *Leptospira*, hamster anti-*Leptospira* (1:200) and HRP-conjugated goat anti-hamster IgG (1:1000) were used as primary and secondary antibodies, respectively. After washing the plates thrice with TBST, 100µL of TMB (KPL, Gaithersburg, MD) was added to each well and incubated for 5 min. The reaction was stopped by adding 100µl of 0.5% hydrofluoric acid to each well. Each plate was read at 630nm by an ELISA plate reader (Bioteck EL-312, Winoski, VT). Each value represents the mean ± SEM of three trials in triplicate samples. Statistically significant ($P<0.05$) differences are indicated by *.

To measure the binding of *Leptospira* to elastin or tropoelastin by Epifluorescene microscopy (EPM), *Leptospira* (10^8) were added to each well (eight well culture slides) coated with 1µg of human lung elastin, chicken tropoelastin, or BSA (negative control) in 100µL of Tris buffer and incubated at 37^{o}C for 6 hour. For the detection of *Leptospira* binding in Figure. 8.2B, hamster anti-*Leptospira* antibodies (1:100) and Alexa 488-conjugated goat anti-hamster IgG (1:250) were used as primary and secondary antibodies, respectively. Fixation and immunofluorescence staining were performed as previously described (22) with slight modifications. Briefly, *Leptospira* were fixed in 2% paraformaldehyde for 60min at RT. For antibody labeling, fixed bacteria were incubated in Tris buffer containing 0.3% BSA for 10min at RT. The primary and secondary antibodies, diluted in Tris buffer containing 0.3% BSA, were incubated sequentially for 60min at RT. After incubation with the primary and secondary antibodies, the glass slides were mounted with coverslips using Prolong Antifade (Molecular Probe, USA) and viewed with a 60 × objective by EPM (Nikon, Japan). The settings were identical for all captured images. Images were processed using Adobe Photoshop CS2.

Table 8.2. The dissociation constant (K_D) obtained from the Elastin and HTE binding by Lig proteins determined by ELISA.

Truncated Lig	K_D				
	Elastin	HTE	1-18HTE	17-27HTE	27-36HTE
LigBCon	166 ± 38 nM	n/d[b]	n/d[b]	n/d[b]	n/d[b]
LigBCon1-3	n/b[a]	n/d[b]	n/d[b]	n/d[b]	n/d[b]
LigBCon4-7	181 ± 33 nM	n/d[b]	n/d[b]	n/d[b]	n/d[b]
LigBCon4	179 ± 29 nM	475 ± 80 nM	n/b[a]	501 ± 51 nM	n/b[a]
LigBCon5	n/b[a]	n/d[b]	n/d[b]	n/d[b]	n/d[b]
LigBCon6-7’	n/b[a]	n/d[b]	n/d[b]	n/d[b]	n/d[b]
LigAVar	n/b[a]	n/d[b]	n/d[b]	n/d[b]	n/d[b]
LigBCen	101 ± 11 nM	n/d[b]	n/d[b]	n/d[b]	n/d[b]
LigBCen1	189 ± 21 nM	n/d[b]	n/d[b]	n/d[b]	n/d[b]
LigBCen7’-8	750 ± 56 nM	824 ± 17 nM	n/b[a]	833 ± 13 nM	n/b[a]
LigBCen9	1230 ± 15 nM	1390 ± 11 nM	n/b[a]	1540 ± 351 nM	n/b[a]
LigBCen10	n/b[a]	n/d[b]	n/d[b]	n/d[b]	n/d[b]
LigBCen11	n/b[a]	n/d[b]	n/d[b]	n/d[b]	n/d[b]
LigBCen12	208 ± 25 nM	726 ± 20 nM	n/b[a]	742 ± 31 nM	n/b[a]

Table 8.2 (Continued)

Truncated Lig	K_D				
	Elastin	HTE	1-18HTE	17-27HTE	27-36HTE
LigBCen2	212 ± 34 nM	n/d[b]	n/d[b]	n/d[b]	n/d[b]
LigBCen2NR	n/b[a]	n/d[b]	n/d[b]	n/d[b]	n/d[b]
LigBCen3	n/b[a]	n/d[b]	n/d[b]	n/d[b]	n/d[b]
LigBCtv	n/b[a]	n/d[b]	n/d[b]	n/d[b]	n/d[b]
$rFnBPA_{194-511}$	42 ± 1.5 nM	133 ± 22 nM	n/d[b]	n/d[b]	n/d[b]

n/b[a], no binding.

n/d[b], not determined.

Elastin and Tropoelastin binding assays

100 µL of 10µg/mL human lung elastin, HTE, or BSA (negative control and data not shown) were coated onto microtiter plate wells as described above. 100µL of different concentrations of biotinylated LigBCon, LigAVar, LigBCen, LigBCtv, LigBCon1-3, LigBCon4-7', LigBCen1, LigBCen2, LigBCen3, LigBCon4, LigBCon5, LigBCon6-7', LigBCen7'-8, LigBCen9, LigBCen10, LigBCen11, LigBCen12, LigBCen2NR, or $rFnBPA_{194-511}$ (positive control), or biotin (negative control) were added subsequently (Figure. 8.3). To reveal the HTE binding sites of Lig protein, 100µL of 1µM full length HTE and truncated HTE including 1-18HTE, 17-27HTE, 27-36HTE or BSA (negative control) were coated onto microtiter plate wells, and 100µL of different concentrations of biotinylated LigBCon4, LigBCen7'-8, LigBCen9, LigBCen12 or biotin (negative control) were added subsequently (Figure. 8.5). To detect binding of biotinylated proteins, HRP-conjugated streptavidin (1:1000) was added to each well at RT for 1 hour prior to washing the wells thrice with TBST. The measurement of binding by ELISA was as described above. To determine the dissociation constant (K_D), the data were fitted by the following equation using KaleidaGraph software (Version 2.1.3 Abelbeck software, Reading, PA), and the calculated K_D are listed in Table 8.2.

$$OD_{630} = \frac{OD_{630max}\,[\text{Lig proteins}]}{K_D + [\text{Lig proteins}]} \quad \text{(Eq. 1)}$$

Inhibition of LigBCon4, LigBCen7'-8, LigBCen9, LigBCen12, and $rAFnBPA_{194-511}$ Binding to Immobilized Elastin or Tropoelastin with Soluble Elastin peptides or Tropoelastin

The wells of a microtiter plate were coated with 100µL of 10µg/mL of human lung elastin, HTE, or BSA (negative control) as described previously. 100µL of 1µM of biotinylated LigBCon4, LigBCen7'-8, LigBCen9, LigBCen12, $rAFnBPA_{194-511}$

(positive control), or biotin (negative control) were mixed with different concentrations of soluble lung elastin peptides or HTE at RT for 1 hour prior to be added to elastin or HTE coated wells (Figure. 8.4). The binding of biotinylated proteins was measured by ELISA described above.

Steady State Fluorescence Measurement

Steady state fluorescence emissions were measured on a Hitachi F4500 spectrofluorometer (Hitachi. San Jose, CA). All spectra were recorded in correct spectrum mode of the instrument using excitation and emission band passes of 2 nm. The intrinsic tryptophan fluorescence of 1μM wild type LigBCon4 or LigBCon4D35N was recorded by exciting the solution at 295 nm and measuring the emission in the 305-400 nm regions. For truncated tropoelastin titration, 0.4, 0.8, 1.6, 3.2, 6.4, or 12.8 μM of 1-18HTE, 17-27HTE, 27-36HTE in Tris buffer (25mM Tris-150 mM sodium chloride, pH 7.5) was mixed with 1μM of LigBCon4 or LigBCon4D35N. For measuring the pH effect on LigBCon4 (1μM) binding to 17-27 HTE, the same serial dilution of 17-27HTE mentioned above using Tris buffer with pH ranging from 4.5 to 9.5 as described in Figure. 8.7C were used. All spectra were recorded at 25^{o}C after 5 minutes. Furthermore, the spectra of the various concentrations of HTE indicated above were also recorded and used to subtract the spectra of each Lig protein in the addition of certain concentrations of HTE. To determine the dissociation constant (K_D), the fluorescence intensities at 320nm were recorded and fitted by the following equation using KaleidaGraph software (Version 2.1.3 Abelbeck sotware):

$$F_{max}\text{-}F = \frac{(F_{max}\text{-}F_{min})\,[\,\text{Tropoelastin}\,]}{K_D + [\,\text{Tropoelastin}\,]} \quad \text{(Eq. 2)}$$

Where F_{max} is the fluorescence intensity of Lig proteins in absence of HTE, F_{min} indicates the fluorescence intensities of Lig proteins saturated with HTE. In addition,

Table 8.3. Thermodynamic parameters for the interaction of 17-27 HTE and LigBCon4 or LigBCon4D341N

	[Proteins]	[HTE]	ΔH	TΔS	K_D	ΔG	n
	μM	μM	kcal mol^{-1}	kcal mol^{-1} K^{-1}	μM	kcal mol^{-1}	
LigBCon4	20	1	-46.39	-37.88	0.54±0.02	-8.51	1.01
LigBCon4D341N	20	1	-56.68	-49.05	2.51±0.48	-7.63	0.99

F is the fluorescence intensities of Lig proteins in presence of various concentration of HTE. All of the measurements were corrected for dilution and for inner filter effect.

Calculation of Charges on LigBCon4 and 17-27HTE at different pH

The charges on LigBCon4 at different pHs and 17-27HTE was determined using ABIM, a Web Service for remote and automatic data processing,. The analyses were performed using default values.

Isothermal Titration Calorimetry (ITC)

The experiments were carried out with a CSC 5300 microcalorimeter (Calorimetry Science Corp. Lindon, UT, USA) at 25^{o}C as previously described (21,22). In a typical experiment, the cell contained 1 ml of a solution of LigBCon4 or LigBCon4D35N and the syringe contained 250 µl of a solution of 17-27HTE. The concentration of Lig proteins and 17-27HTE are detailed in Table 8.3. Both solutions were in Tris buffer (pH 7.5). The titration was performed as follows: 25 injections of 10 µl with a stirring speed of 250 rpm with a delay time between injections of 5min. Data were analyzed using Titration Binding Work 3.1 software (Calorimetry Science Corp. Lindon, UT, USA) fitting them to an independent binding model.

Circular dichroism (CD) spectroscopy

CD analysis was performed on an Aviv 215 spectropolarimeter (Lakewood, NJ) under N_2 atmosphere. CD spectra were measured at RT (25^{o}C) in a 1-cm path length quartz cell. Spectra of LigBCon4 and LigBCon4D35N were recorded in Tris buffer, pH7.5, at a protein concentration of 10 µM. Three spectra were recorded for each condition from 190 to 250 nm for far-UV CD in 1 nm increments. To reveal the effect of pH, 10 µM of LigBCon4 or 17-27HTE in Tris buffer ranging from pH 4.5 to 9.5 were used in all CD

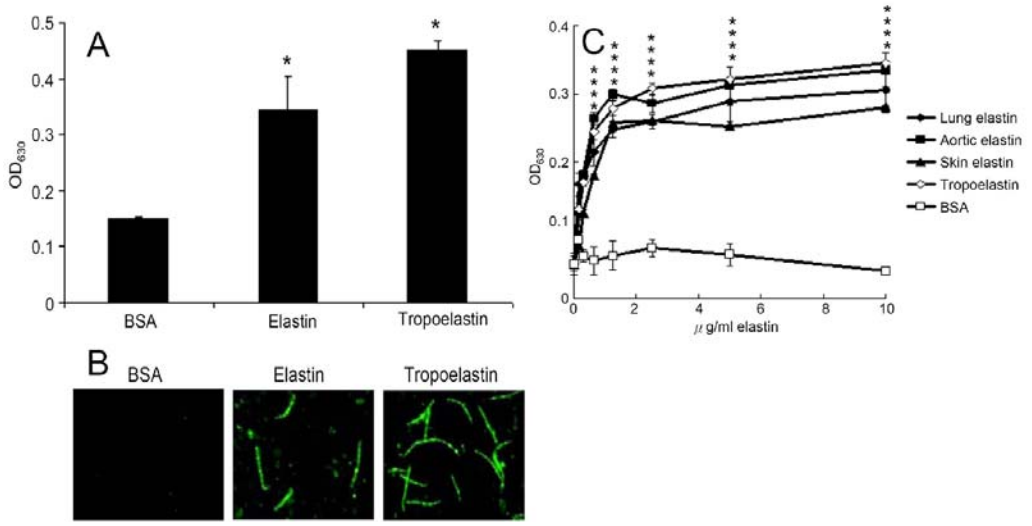

Figure 8.1 Binding of *L. interrogans* serovar Pomona (NVSL 1427-35-093002) to elastin and tropoelastin. (A) Binding of *Leptospira* to BSA, elastin, or tropoelastin. *Leptospira* (10^7) were added to wells coated with BSA, human lung elastin, or HTE (1μg in 100μL Tris buffer). (B) Binding of *Leptospira* to immobilized elastin or HTE. *Leptospira* (10^8) cultured in human lung elastin, HTE, or BSA (negative control) coated (1μg in 100 Tris buffer) or un-coated wells (negative control). Leptospiral immobilization was assayed by immunofluorescence microscopy. (C) Binding of *Leptospira* (10^7) to various concentrations of human lung elastin, human aortic elastin, human skin elastin, HTE, or BSA (0 , 0.25, 0.5, 1, 2, 4, 8, 16μg/mL in 100μL Tris buffer). BSA serves as negative control. In (A) and (C), the binding *Leptospira* was estimated by ELISA, and each value represents the mean± SEM of three trials performed in triplicate samples. Statistically significant ($p < 0.05$) differences compared to the negative reference are indicated by an asterisk.

experiments. The background spectrum of buffer without protein was subtracted from the protein spectra. CD spectra were initially analyzed by the software accompanying the spectrophotometer. Analysis of spectra to extrapolate secondary structures was performed by Dichroweb (44) (http://www.cryst.bbk.ac.uk/cdweb/html/home.html) using the K2D and Selcon 3 analysis programs (45,46).

Statistical analysis

Significant differences between samples were determined using the Student's t-test following logarithmic transformation of the data. Two-tailed P-values were determined for each sample and a P-value <0.05 was considered significant. Each data point represents the mean $\pm$ standard error of the mean (SEM) for each sample tested in triplicate. An (*) indicates the result was statistically significant.

Results

Leptospira can be immobilized by elastin and tropoelastin

To determine if leptospiral adherence is mediated by elastin, ELISA-based and immunofluorescence assays were performed. As shown on Figure. 8.1A and B, both elastin and its precursor, tropoelastin, can immobilize *Leptospira* on microtiter plate wells or culture slides.

To reveal whether elastin derived from different tissues affect the immobilization of *Leptospira*, *Leptospira* were incubated over various concentrations of human lung, aortic or skin elastin coated onto microtiter plate wells. Based on the results of Figure. 8.1C, *Leptospira* can bind to elastin from all different sources including lung, skin, and blood vessels.

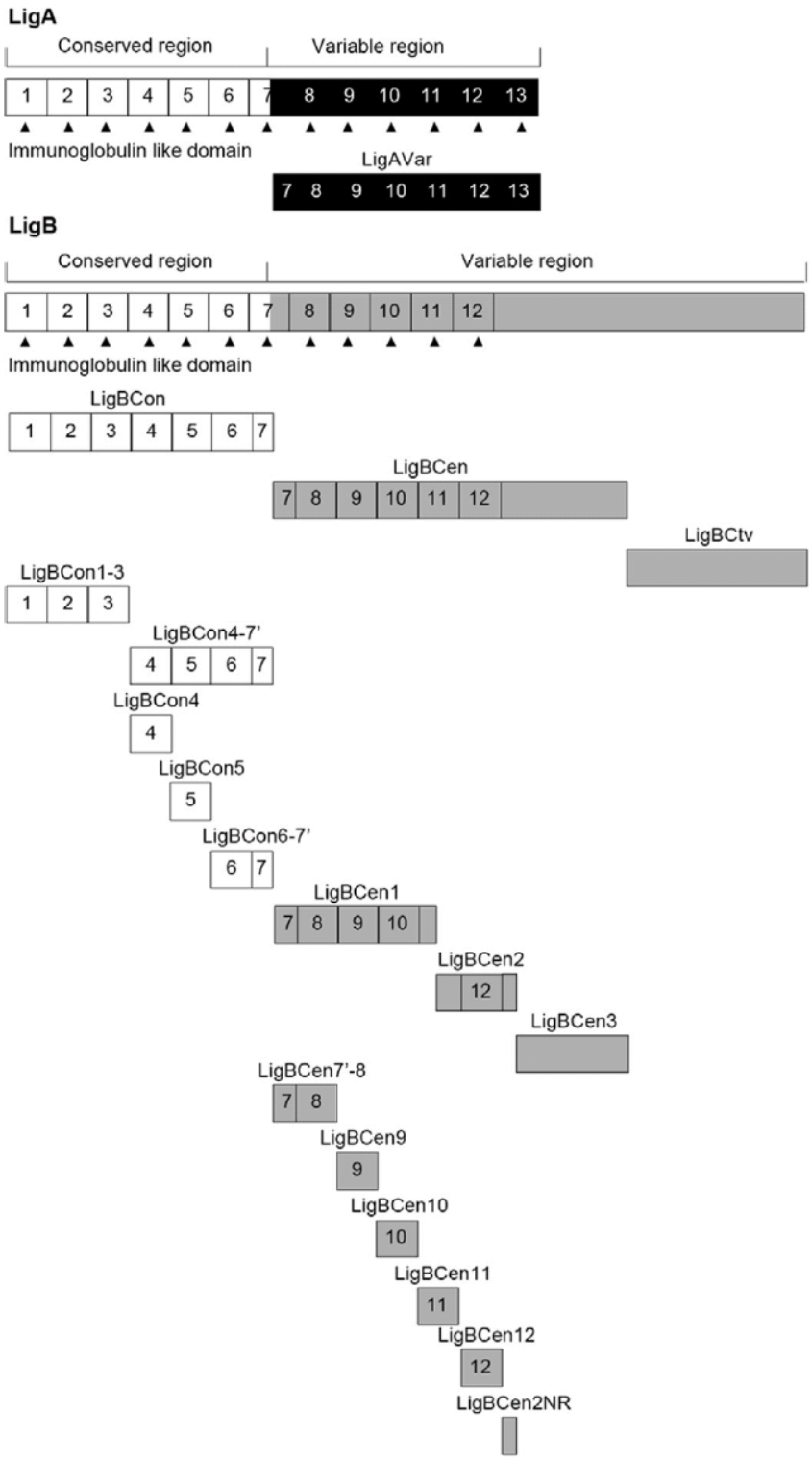

Figure 8.2 A schematic diagram showing the structure of Lig proteins and the truncated Lig proteins used in this study.

Figure. 8.3 Localization of the elastin or HTE-binding domains on Lig proteins. Various concentrations (0.0156, 0.03125, 0.0625, 0.125, 0.25, 0.5, 1μM) of biotin (negative control), biotinylated rAFnBPA$_{194\text{-}511}$, (A) LigBCon, LigAVar, LigBCen, LigBCtv, (B) LigBCon, LigBCon1-3, LigBCon4-7', (C) LigBCen, LigBCen1, LigBCen2, LigBCen3, (D) LigBCon4'-7, LigBCon4, LigBCon5, LigBCon6-7', (E) LigBCen1, LigBCen7'-8, LigBCen9, LigBCen10, LigBCen11, (F) LigBCen2, LigBCen12, or LigBCen2NR, (G) LigBCon4, LigBCen7'-8, LigBCen9, LigBCen12 were added to wells coated with 1μg of BSA (negative control and data not shown), (A-F) human lung elastin or (G) HTE in Tris buffer. The binding of biotinylated proteins to elastin or HTE was measured by ELISA. For all experiments, each value represents the mean± SEM of three trials in triplicate samples. Statistically significant ($p < 0.05$) differences compared to negative control are indicated by an asterisk.

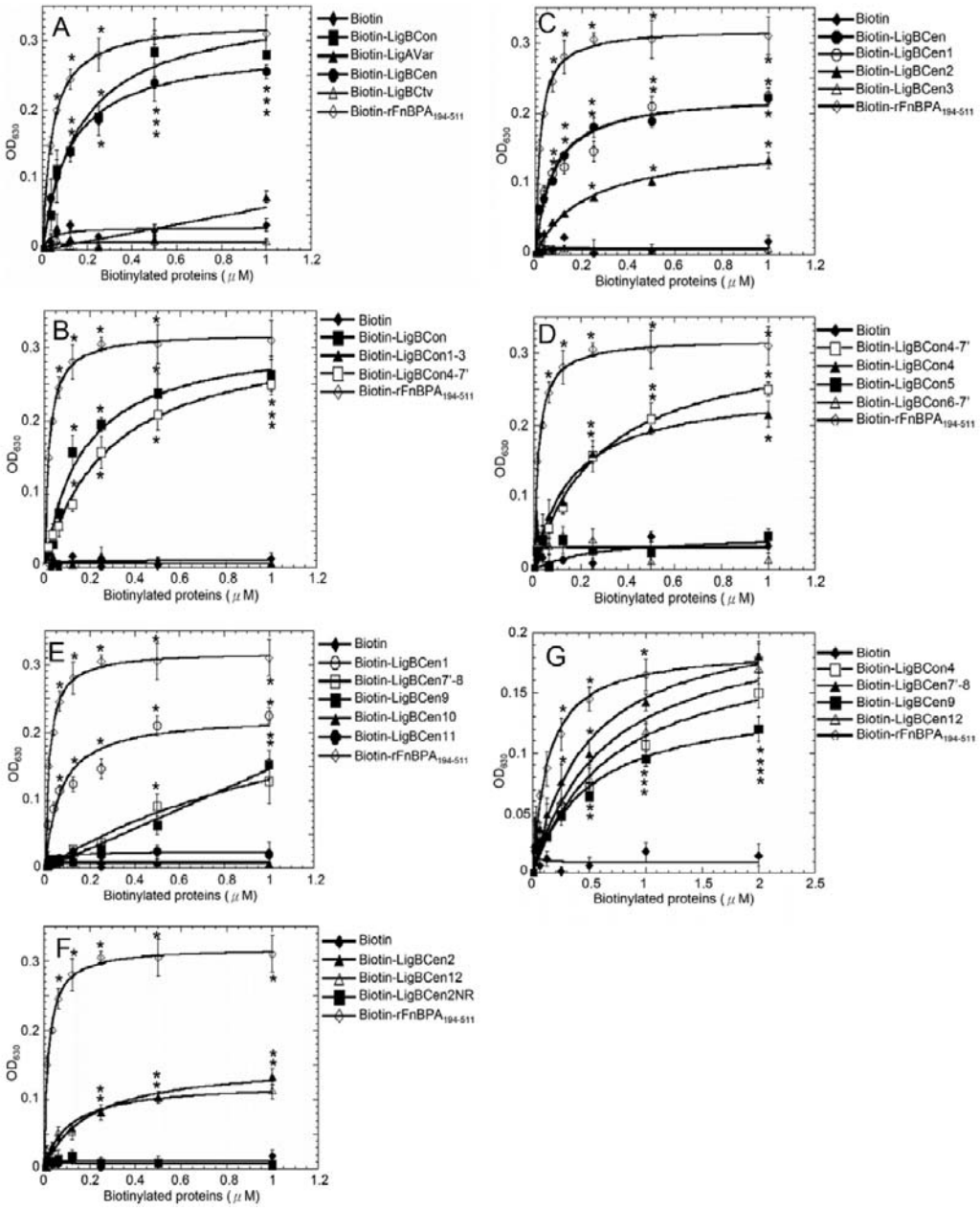
A
Biotin
Biotin-LigBCon
Biotin-LigAVar
Biotin-LigBCen
Biotin-LigBCtv
Biotin-rFnBPA194-511
B
Biotin
Biotin-LigBCon
Biotin-LigBCon1-3
Biotin-LigBCon4-7'
Biotin-rFnBPA194-511
C
Biotin
Biotin-LigBCen
Biotin-LigBCen1
Biotin-LigBCen2
Biotin-LigBCen3
Biotin-rFnBPA194-511
D
Biotin
Biotin-LigBCon4-7'
Biotin-LigBCon4
Biotin-LigBCon5
Biotin-LigBCon6-7'
Biotin-rFnBPA194-511
E
Biotin
Biotin-LigBCen1
Biotin-LigBCen7'-8
Biotin-LigBCen9
Biotin-LigBCen10
Biotin-LigBCen11
Biotin-rFnBPA194-511
F
Biotin
Biotin-LigBCen2
Biotin-LigBCen12
Biotin-LigBCen2NR
Biotin-rFnBPA194-511
G
Biotin
Biotin-LigBCon4
Biotin-LigBCen7'-8
Biotin-LigBCen9
Biotin-LigBCen12
Biotin-rFnBPA194-511
OD630
Biotinylated proteins (μM)

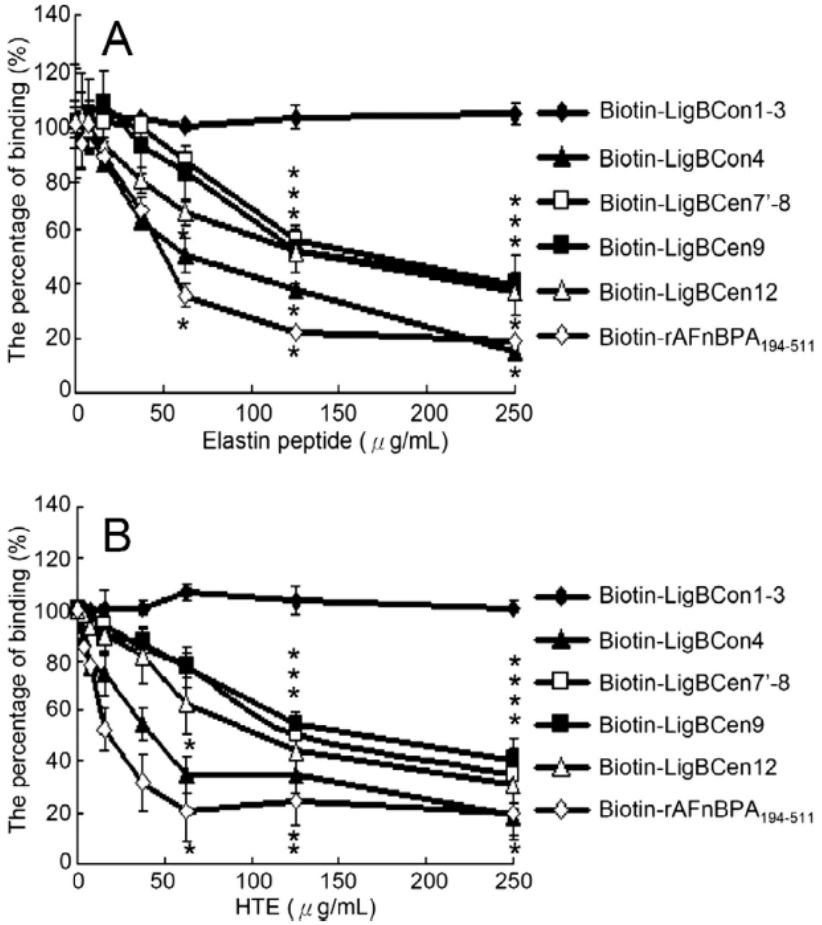

Figure 8.4 Soluble elastin peptide or HTE inhibited LigBCon4, LigBCen7'-8, LigBCen9, LigBCen12 binding to immobilized elastin or HTE. One μM of LigBCon1-3 (negative control), biotinylated rAFnBPA$_{194-511}$ (positive control) LigBCon4, LigBCen7'-8, LigBCen9, LigBCen12 treated with various concentrations (3.90, 7.81, 15.62, 31.25, 62.5, 125, 250μg/mL in 100μL of Tris buffer) of soluble elastin peptide or HTE were added to each well coated with 1 μg of BSA (negative control and data not shown), (A) human lung elastin or (B) HTE in Tris buffer. The binding of biotinylated proteins to wells was measured by ELISA. The percentage of binding was determined relative to the binding of biotinylated proteins in the untreated well. For all experiments, each value represents the mean± SEM of three trials in triplicate samples.

LigBCon4, LigBCen7'-8, LigBCen9, LigBCen12 mediate the binding of Leptospira to elastin and tropoelastin

To examine LigA and LigB mediated leptospiral adhesion to elastin, Lig proteins were truncated and expressed as shown in Figure. 8.2. First, biotinylated LigBCon, LigAVar, LigBCen, LigBCtv, or biotin (negative control) was added to elastin coated microtiter plate wells. In addition, rFnBPA$_{194\text{-}511}$ was used as a positive control (33,35). As indicated in Figure. 8.3A, only LigBCon and LigBCen can bind to elastin (LigBCon; K_D= 166 ± 38 nM, LigBCen; K_D= 101 ± 11 nM). In order to further localize the elastin binding sites on LigBCon or LigBCen, truncated significant ($p < 0.05$) differences compared to the negative reference are indicated by an asterisk. elastin peptide blocked the interaction of LigBCon4, LigBCen7'-8, LigBCen9, and LigBCen12 with elastin. Pretreatment of these four fragments with HTE also inhibited binding (Figure. 8.4B), suggesting that these fragments contain both HTE and elastin binding sites. LigBCon and LigBCen were constructed, expressed, purified, biotinylated (Figure. 8.2), and ELISA assays were performed to map the elastin binding sites. As shown in Figure. 8.3B and D, the elastin binding site on LigBCon was determined as LigBCon4, the fourth immunoglobulin repeated region of LigBCon (LigBCon4; K_D= 179 ± 29 nM). On the other hand, unlike LigBCon, there were three elastin binding sites on LigBCen including LigBCen7'-8, LigBCen9, and LigBCen12 (LigBCen7'-8; K_D= 750 ± 56 nM, LigBCen9; K_D= 1230 ± 15 nM, LigBCen12; K_D= 208 ± 25 nM) (Figure. 8.3C, E, and F).

To investigate whether tropoelastin also binds to similar Lig protein binding sites as elastin, biotinylated LigBCon4, LigBCen7'-8, LigBCen9, or LigBCen12 was added to human tropoelastin (HTE) coated microtiter plate wells in a binding assay. As presented in Figure. 8.3G, all four of these regions can also bind to HTE (LigBCon4;

K_D= 475 ± 80 nM, LigBCen7'-8; K_D= 824 ± 17 nM, LigBCen9; K_D= 1390 ± 11 nM, LigBCen12; K_D= 726 ± 20 nM).

Soluble elastin or HTE block LigBCon4, LigBCen7'-8, LigBCen9, LigBCen12 binding to elastin or HTE

To further confirm the association of specific lig domains with elastin or HTE, biotin (negative control) and biotinylated LigBCon4, LigBCen7'-8, LigBCen9, or LigBCen12 were incubated in the presence of soluble elastin or HTE prior to be added to elastin or HTE coated microtiter plate wells. As shown in Figure. 8.4A, soluble

LigBCon4, LigBCen7'-8, LigBCen9, LigBCen12 bind to 17th to 27th exons of HTE

To locate the binding domain on HTE, biotin (negative control), biotinylated LigBCon4, LigBCen7'-8, LigBCen9, or LigBCen12 was incubated with either full length HTE or different truncated fragments of HTE including 1-18HTE(1st to 18th exons of HTE), 17-27HTE(17th to 27th exons of HTE), and 27-36HTE(27th to 36th exons of HTE) (Figure. 8.5A) and assayed for their binding activity using ELISA. As indicated in Figure. 8.5, all four Lig protein fragments only bind to 17-27HTE (LigBCon4; K_D= 0.50±0.051μM, LigBCen7'-8; K_D= 0.83±0.13μM, LigBCen9; K_D= 1.54±0.35μM, LigBCen12; K_D= 0.74±0.031μM).

Since the binding affinity of LigBCon4 to 17-27HTE is highest, further studies using steady state fluorescence spectrometry and ITC were used; the results confirm those from the ELISA tests. We found that the tryptophan fluorescence intensity of LigBCon4 in the presence of 17-27HTE (compared with 1-17HTE or 27-36HTE) was quenched; this is in agreement with our ELISA results, indicating that LigBCon4 binds to 17-27HTE (Figure. 8.6A and B). The K_D obtained from the quenched fluorescence spectra (K_D= 0.49 ± 0.07μM) matched the data obtained with ELISA very closely

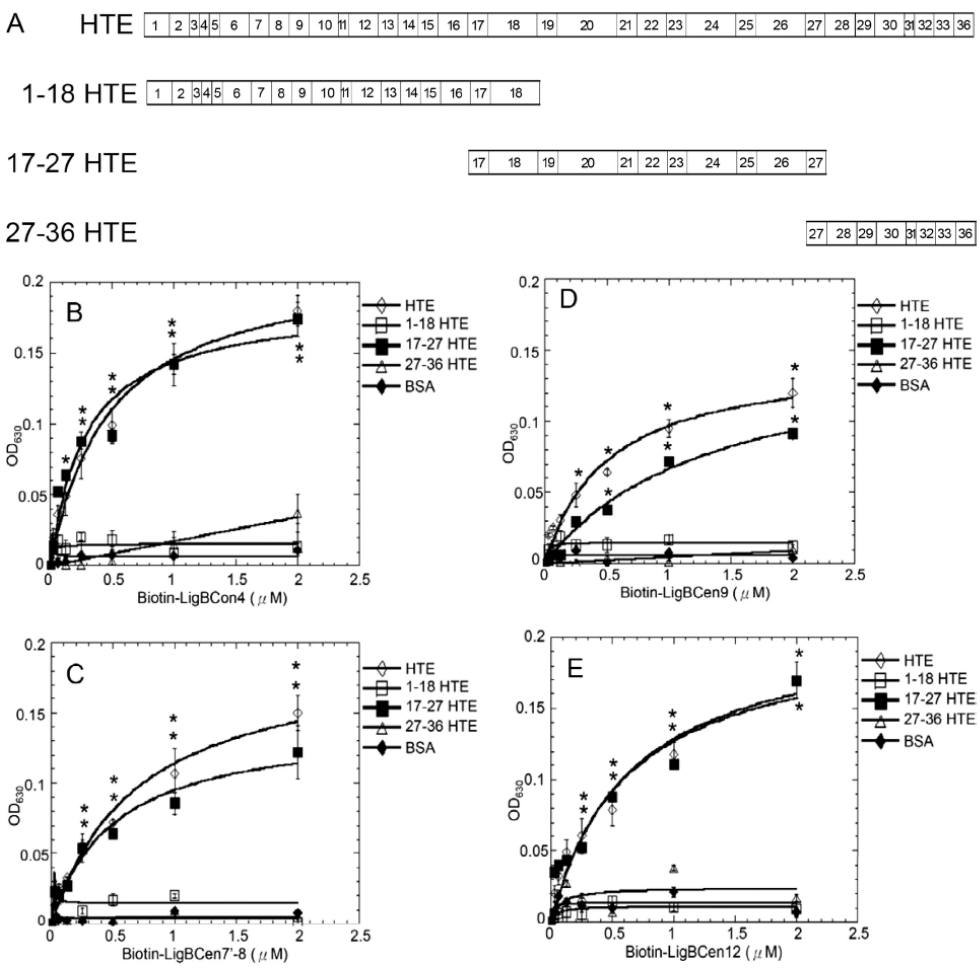

Figure 8.5 Mapping the binding site of LigBCon4, LigBCen7'-8, LigBCen9, LigBCen12 on HTE. (A) A chart presenting the location of HTE and truncated HTE used in this study. (B-E) Binding of LigBCon4, LigBCen7'-8, LigBCen9, and LigBCen12 to various concentrations of immobilized truncated HTE. Various concentrations (0.03125, 0.0625, 0.125, 0.25, 0.5, 1, 2μM) of biotin (negative control and data not shown), biotinylated (B) LigBCon4, (C) LigBCen7'-8, (D) LigBCen9, or (E) LigBCen12 were added to 1μM of full length HTE, 1-18HTE, 17-27HTE, 27-36HTE, or BSA (negative control) in 100μL PBS coated microtiter plate wells. Bound proteins were measured by ELISA. For all experiments, each value represents the mean± SEM of three trials in triplicate samples. Statistically significant ($p < 0.05$) differences compared to the negative control are indicated by an asterisk.

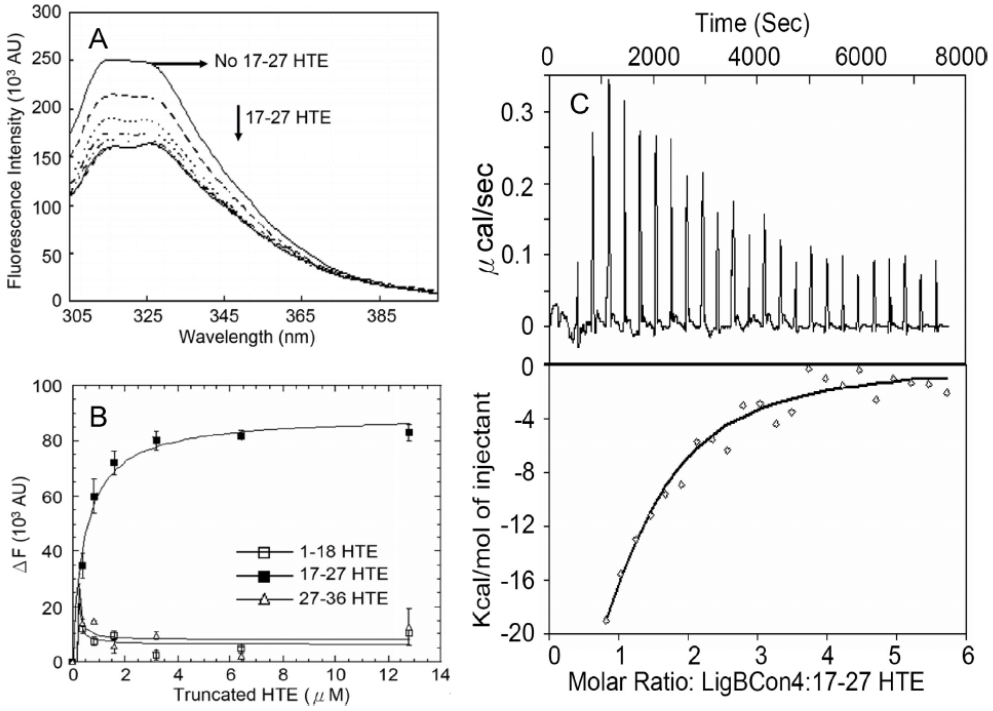

Figure 8.6 Interaction of 17-27HTE and LigBCon4 by steady state fluorescence spectroscopy and isothermal titration calorimetry (ITC). (A) Intrinsic fluorescence spectrum of LigBCon4 in the presence and absence of 17-27HTE. One μM of LigBCon4 in Tris buffer was excited at 295 nm. Aliquots of 17-27HTE from respective stock solutions were added. The figure shows Trp fluorescence in the presence of 0, 0.4, 0.8, 1.6, 3.2, 6.4, 12.8μM of 17-27HTE. (B) The determination of K_D of LigBCon4 and truncated HTE by monitoring the quenching fluorescence intensities of LigBCon4 titrated by 1-18HTE, 27-36HTE (data not shown), or 17-27HTE shown in (A). The emission wavelength recorded in this figure was 327nm, only the titration of 17-27HTE can quench the spectrum of LigBCon4. K_D was determined by fitting the data point into the equation described in materials and methods (K_D= 0.49±0.07μM). (C) ITC profile of LigBCon4 with 17-27HTE as a typical ITC profile in this study. (Upper panel) Heat difference obtained from 25 injections. (Lower panel) Integrated curve with experimental point (◇) and the best fit (—). The thermodynamic parameters are shown in Table 8.3.

(Figure. 8.6B). Furthermore, K_D values from ITC measurements confirmed the binding nature of LigBCon4 to 17-27HTE (K_D= 0.54 ± 0.02μM) (Figure. 8.6C and Table 8.3). On the other hand, the negative values of both enthalpy and entropy shown on table 8.2 indicated that the binding of LigBCon4 to 17-27HTE was a enthalpy favorable and entropy unfavorable interaction. The binding was only driven by enthalpy through charge-charge interactions or by Van der Waal forces. That is, the surface charges of interface of LigBCon4-17-27HTE might contribute to the binding.

Effect of pH on the LigBCon4-17-27HTE interaction

Due to the possibility of surface charges for the binding of LigBCon4 to 17-27HTE (Table 8.3), we further investigated the influence of pH on the interaction of both proteins. An ABIM software program was used to analyze the titration curve of LigBCon4 and 17-27HTE (http:\\www.iut-arles.up.univ-mrs.fr/w3bb/d_abim/compo-p.html). As shown in Figure. 8.7A, 17-27HTE undergoes a sharp isoelectric transition at pH 9.5, and maintains a positive charge up to pH 9.5. However, there are two step of transitions from the titration curve of LigBCon4 located around pH4 and pH11, and the surface charge of LigBCon4 is kept slightly negative from pH 4 to pH10 (Figure. 8.7A). The effect of pH on the LigBCon4-17-27HTE interaction was also measured by the quenching of fluorescence intensity of LigBCon4 in the presence of various concentrations of 17-27HTE. As presented in Figure. 8.7B and C, the highest affinity was found in the range of pH 6.5 to 7.5 (pH6.5; K_D= 0.60±0.08μM, pH7.5; K_D= 0.49±0.07μM). When pH was lower than 6.5 or higher than 7.5, the binding affinity of LigBCon4-17-27HTE was considerably lower (pH4.5; K_D= 4.84±0.20μM, pH5.5; K_D= 2.53±0.27μM, pH8.5; K_D= 2.30±0.20μM) (Figure. 8.7B); interaction was found to be negligible at pH9.5 or higher (data not shown).

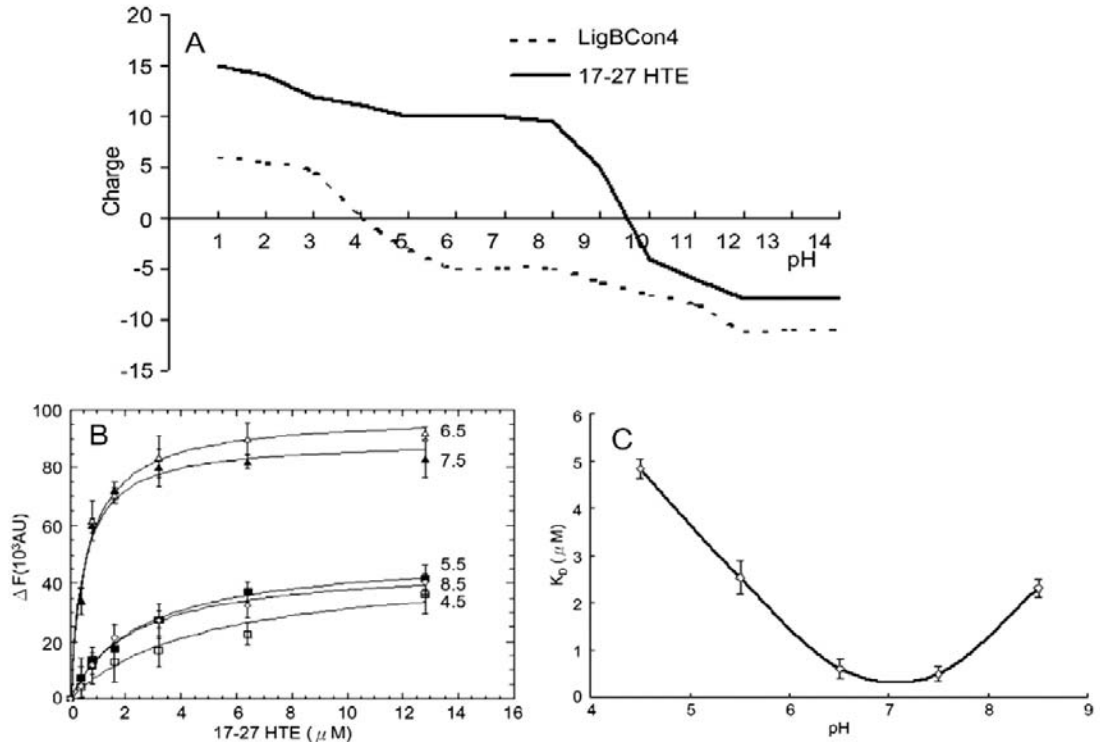

Figure 8.7 The effect of different pH values on the binding of LigBCon4 to 17-27HTE. (A) Titration curve for LigBCon4 and 17-27HTE. LigBCon4 (broken line) undergoes two step charge transition at pH 4 and 11. 17-27 HTE (solid line) undergoes a charge transition at pH 9.5. (B) The determination of K_D of LigBCon4 and 17-27HTE by monitoring the quenching fluorescence intensities of LigBCon4 at various concentrations (0, 0.4, 0.8, 1.6, 3.2, 6.4, and 12.8μM) of 17-27HTE in Tris buffer at different pH (4.5, 5.5, 6.5, 7.5, and 8.5). One μM of LigBCon4 in Tris buffer was excited at 295 nm, and the emission wavelength recorded in this figure was 327nm. The K_D was determined by fitting the data point into the equation described in materials and methods (C) LigBCon4 binding to 17-27HTE from pH 4.5 to 8.5. A plot of K_D against pH indicates that the interaction is strongly dependent on pH.

To determine if the observed reduced affinity was due to conformational changes by LigBCon4 and 17-27HTE when the pH was outside the 6.5 -7.5 range, we performed a CD analysis. Results from our undifferentiated CD spectra recorded from pH4.5 to 9.5 indicate that the reduced affinity was not the result of disruption of the structure of LigBCon4 and 17-27HTE (Figure. 8.9). Furthermore, the secondary structures of LigBCon4 and 17-27HTE were shown to be unaffected by various pH environments (Figure. 8.9). This indicates that the interaction of LigBCon4 and 17-27HTE is largely influenced by charge-charge interaction via the environmental pH.

Asp341 is critical for the association of LigBCon4 and 17-27HTE

The results of surface charge prediction showed that the negatively charged amino acids of LigBCon4 at physiological pH might contribute to the interaction of Lig/HTE by charge-charge interaction (Figure. 8.7A). The sequence alignment was performed on LigBCon4, LigBCen7'-8, LigBCen9, and LigBCen12 to identify potential conserved acidic amino acids that may contribute to the binding of Lig proteins to HTE. Surprisingly, Asp341 in LigBCon4 was the only acidic amino acid conserved in all four elastin binding immunoglobulin-like domains (Asp341 in LigBCon4, Asp703 in LigBCen7'-8, Asp789 in LigBCen9, and Asp1061 in LigBCen12) (Figure. 8.8A) To determine whether this aspartate plays a role in binding to 17-27HTE, a mutant, LigBCon4D341N was constructed. The intrinsic fluorescence spectra of LigBCon4D341N in the absence or presence of various concentrations of 17-27HTE were recorded and our results showed the binding affinity of LigBCon4D341N and 17-27HTE was fitted by the quenching of fluorescence intensities with a K_D of 2.44±0.21μM (Figure. 8.8B). ITC was performed to measure the binding affinity of LigBCon4D341N to 17-27HTE (K_D = 2.51±0.48μM) (Figure. 8.8C and Table 8.3). Interestingly, the binding affinity of LigBCon4D341N to 17-27HTE was 4.6-fold lower

Figure 8.8 Asp341 is one of the important residues contributing to the LigBCon4-17-27HTE interaction. (A) Sequence alignment of LigBCon4 (Asp341), LigBCen7'-8(Asp703), LigBCen9(Asp789), and LigBCen12(Asp1061)shows that an arspartate is conserved in these four doamins as indicated by an asterisk. The gaps were introduced to maximize the alignment. Black and gray colored residues indicate the conserved residues, and the homology analysis was performed with EMBL-EBI ClustalW (http://www.ebi.ac.uk/clustalw/). (B) Intrinsic fluorescence spectrum of LigBCon4D341N in the presence and absence of 17-27HTE. One μM of LigBCon4D341N in Tris buffer was excited at 295 nm. Aliquots of 17-27HTE from respective stock solutions were added. The figure shows Trp fluorescence in the presence of 0, 0.4, 0.8, 1.6, 3.2, 6.4, 12.8μM of 17-27HTE (Inner plot). The determination of K_D of LigBCon4D35N and 17-27HTE by monitoring the quenching fluorescence intensities of LigBCon4D35N titrated by 17-27HTE. The emission wavelength recorded in this figure was 327nm, and K_D was revealed by fitting the data point into the equation described in materials and methods (K_D= 2.44±0.21μM). (C) ITC profile of LigBCon4D35N with 17-27HTE as a typical ITC profile in this study. (Upper panel) Heat difference obtained from 25 injections. (Lower panel) Integrated curve with experimental point (◇) and the best fit (—). The thermodynamic parameters are shown in Table 8.3.

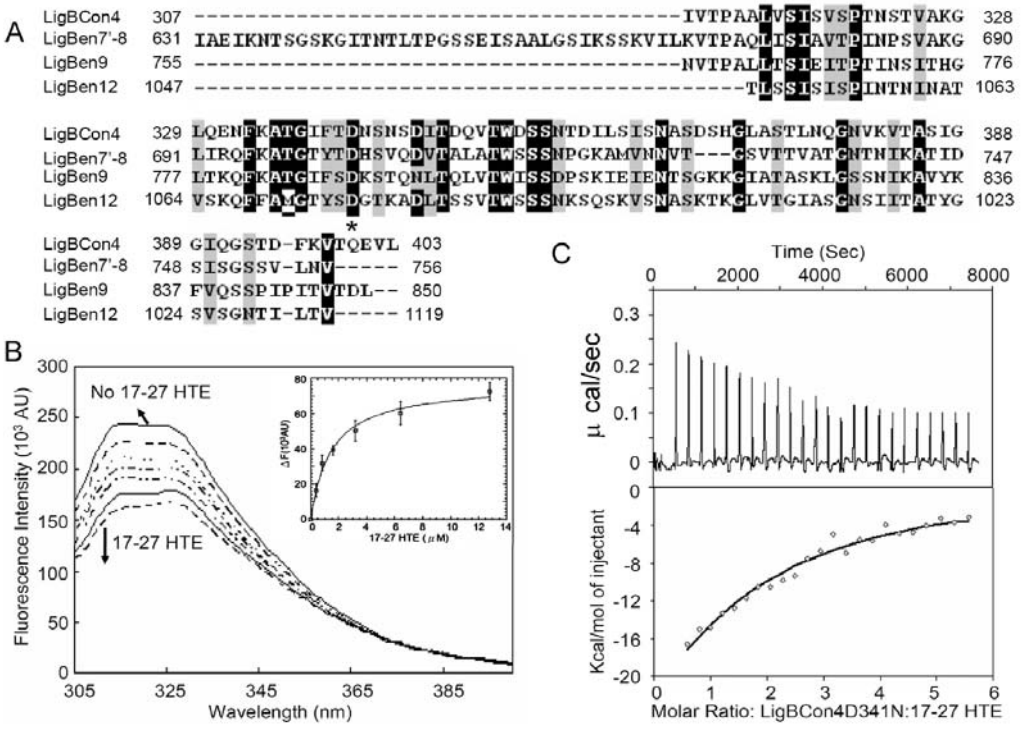
A
LigBCon4 307 IVTPAALVSISVSPTNSTVAKG 328
LigBen7'-8 631 IAEIKNTSGSKGITNTLTPGSSEISAALGSIKSSKVILKVTPAQLISIAVTPINPSVAKG 690
LigBen9 755 NVTPALLTSIEITPTINSITHG 776
LigBen12 1047 TLSSISISPINTNINAT 1063
LigBCon4 329 LQENFKATGIFTDNSNSDITDQVTWDSSNTDILSISNASDSHGLASTLNQGNVKVTASIG 388
LigBen7'-8 691 LIRQFKATGTYTDHSVQDVTALATWSSSNPGKAMVNNVT---GSVTTVATGNTNIKATID 747
LigBen9 777 LTKQFKATGIFSDKSTQNLTQLVTWISSDPSKIEIENTSGKKGIATASKLGSSNIKAVYK 836
LigBen12 1064 VSKQFFAMGTYSDGIKADLTSSVTWSSSNKSQSKVSNASKTKGLVTGIASGNSIITATYG 1023
*
LigBCon4 389 GIQGSTD-FKVTQEVL 403
LigBen7'-8 748 SISGSSV-LNV----- 756
LigBen9 837 FVQSSPIPITVTDL-- 850
LigBen12 1024 SVSGNTI-LTV----- 1119
B
No 17-27 HTE
17-27 HTE
Fluorescence Intensity (10³ AU)
Wavelength (nm)
ΔF(10³AU)
17-27 HTE (μM)
C
Time (Sec)
μ cal/sec
Kcal/mol of injectant
Molar Ratio: LigBCon4D341N:17-27 HTE

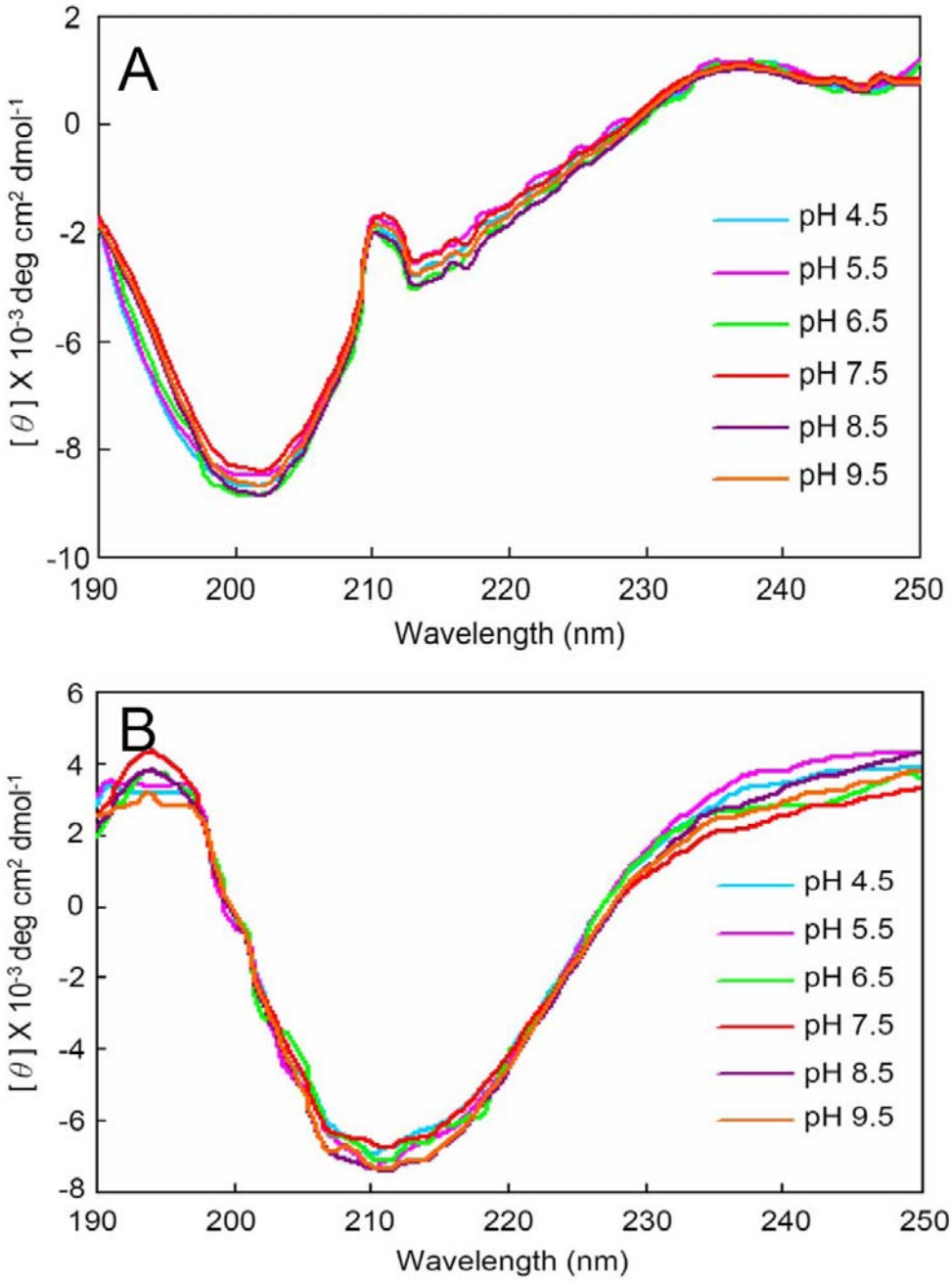

Figure 8.9 Environmental pH cannot affect the secondary structures of 17-27HTE and LigBCon4. Far-UV CD analysis of (A) 17-27HTE and (B) LigBCon4 at different pH (4.5, 5.5, 6.5, 7.5, and 8.5). The molar ellipticity, Φ, was measured from 190 to 250 nm for 10 μM of each protein in Tris buffer.

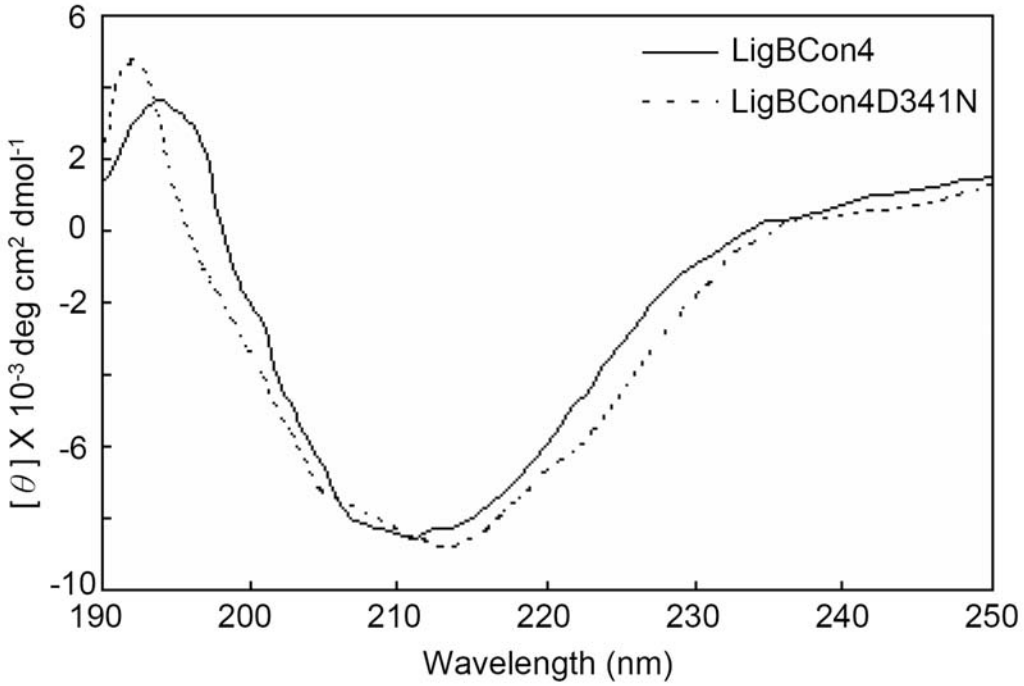

Figure 8.10 D341N mutation cannot affect the structure of LigBCon4. Far-UV CD analysis of LigBCon4 and LigBCon4D341. The molar ellipticity, Φ, was measured from 190 to 250 nm for 10μM of each protein in Tris buffer.

compared to wild type LigBCon4 (K_D = 0.50μM from ELISA, K_D = 0.49μM from fluorescence spectroscopy, K_D = 0.54μM from ITC) (Figure. 8.5A, 6 and Table 8.3). Moreover, the far-UV CD data of LigBCon4D341N to17-27HTE was similar to that of wild-type LigBCon4. This result rules out the possibility that the reduction of binding activity of LigBCon4D341N is due to a conformation change (Figure. 8.10). This data indicates that Asp341 is a pivotal residue in LigBCon4 -17-27HTE binding.

Discussion

The colonization of host tissues by pathogenic *Leptospira* spp. is a pivotal factor in leptospiral pathogenesis. *Leptospira* spp. express a number of MSCRAMMs on their surfaces that promote binding to host ECMs, and likely play an important role in leptospiral pathogensis (10-13,18,20-23). *Leptospira* spp. causes severe pulmonary hemorrhage with significant mortality rates in several countries, (36,37,47,48) and abortion with placentitis (38,49,50). The lung and placenta are elastin-rich tissues; this led us to examine the interaction of *L. interrogans* with elastin. Our results clearly show that *L. interrogans* can adhere to both immobilized elastin peptides and tropoelastin, the precursor of elastin (Figure. 8.1A, B), and that elastin peptides extracted from tissues including lung, skin, and blood vessels can immobilize *Leptospira* as well (Figure. 8.1C). This data indicates that *L. interrogans* can bind to immobilized elastin peptides and tropoelastin.

We and others have shown that Lig proteins bind to Fn, laminin, collagen, and fibrinogen (20,21). We, therefore, wanted to know if Lig proteins can bind to elastin. Our ELISA data show that coated elastin peptides can bind to the Lig protein fragements LigBCon and LigBCen, but not LigAVar or LigBCtv (Figure. 8.3A). Additionally, LigBCon and LigBCen can only partially block leptospiral binding to elastin, raising the possibility that *L. interrogans* may possess other elastin binding

proteins on its surface (Figure. 8.3B). Further studies confirming this are needed. To our surprise, LigBCon was recently shown to have no binding capacity for Fn, laminin, fibrinogen or collagen (20,21), but it proved capable of binding to elastin. This may explain why LigBCon is a protective antigen against *L. interrogans* serovar Pomona challenge (41). This study clearly demonstrated that Lig proteins bind to elastin, thus proving our hypothesis that one or more leptospiral MSCRAMMs bind to elastin. A recent study indicated a *ligB* mutant with an insertion containing a Spc^r cassette into the 3' end of the *ligB* gene is still virulent in a hamster model(5). Although The reasons are unknown, there are several possibilities: 1). The truncated LigB is expressed, but at a lower level since the insertion is only in the far 3' end of *ligB* 2). Since the first 630 amino acids of LigA and LigB are identical, LigA may compensate for LigB in this mutant even with a similar LigA expression level. 3). LigB is not required for virulence in a hamster or rat model. 4). LigB is only needed for initial adhesion and invasion of *Leptospira* spp. moving from the environment through mucous membranes and injured skin. In order to answer these questions, it is essential to knockout the complete *ligA* and *ligB* genes (in frame deletion of the complete *ligA* and *ligB* genes) and perform a virulence test using different animal models, such as dogs or monkeys.

To map the potential binding sites of Lig proteins to elastin, LigBCon and LigBCen were further truncated into several fragments and the recombinant proteins were purified for use in an ELISA assay to identify the potential elastin binding domains. From our truncated constructs, we found that only LigBCon4, LigBCen7'-8, LigBCen9, and LigBCen12 can bind to elastin (Figure. 8.3D-F). Furthermore, soluble elastin peptides can block the binding of these four truncated proteins to elastin. This data clearly indicates that there are four elastin binding sites located on the LigB moiety(Figure. 8.4A). Although LigA and LigB contain twelve and thirteen immunoglobulin-like domains, respectively, only LigBCon4, LigBCen7'-8, LigBCen9,

and LigBCen12 are able to bind to elastin. This is not surprising, given that the amino acids of each immunoglobulin-like domain of LigA and LigB are so divergent (14,16,17).

Apart from elastin, the binding regions of LigB to human tropoelastin (HTE), the precursor of elastin, were examined by ELISA and competition binding assays, and our results indicated that the elastin binding domains of LigB, LigBCon4, LigBCen7'-8, LigBCen9, and LigBCen12, can also bind to HTE (Figure. 8.3G and 8.4B). Moreover, we demonstrated that the HTE binding region for LigBCon4, LigBCen7'-8, LigBCen9, LigBCen12 resides in 17-27HTE, the central region of HTE (Figure. 8.5B, C, D, and E). Interestingly, FnBPA, the elastin binding protein of *Staphylococcus aureus*, was found to bind to 1-18HTE and 17-27HTE, N-termini and central region of HTE (33). It suggests that binding to elastin or tropoelastin is a common mechanism for pathogen adhesion (33). However, HTE is also involved in elastogenesis, the process of elastin formation, which is pivotal for tissue repair and the regeneration of host cells. Basically, monomer HTE is expressed and excreted into the extracellular area, undergoing a rapid ordered assembly to form tropoelastin packages, a self-association process called coacervation. Lysine oxidation by lysyl oxidase facilitates cross-linking and then incorporation into microfibrils to generate elastic fibers (28,32). HTE is tethered to the cell surface and probably binds to ligands, including glycosaminoglycans, integrins and other non-ECM molecules, by its C-terminal region, 27-36HTE (43,51). Thus, Lig protein binding to 17-27HTE may not only mediate leptospiral adhesion but may also inhibit tissue regeneration by blocking the network formation (from HTE) of elastin fibers. Moreover, failed tissue repair may further facilitate the invasion of *L. interrogans* during infection.

In order to gain more insight into the interaction of Lig proteins with HTE, LigBCon4 was chosen for further characterization using steady state fluorescence

spectroscopy and ITC techniques (Figure. 8.6). The K_D obtained from both experiments are close to each other and to our ELISA results (ELISA; K_D= 0.50±0.05μM, ITC; K_D= 0.49±0.07μM , Fluroescence spectroscopy; K_D= 0.54±0.02μM). The spectrum of LigBCon4 possesses a doublet maximum in 315nm and 326nm similar to that of LigBCen2. LigBCen2 contains a tryptophan in an immunoglobulin-like domain; indications are that this tryptophan is buried in a highly hydrophobic core (23), but the quenching of the spectra in the presence of 17-27HTE suggest the binding site of LigBCon4 may be close to this hydrophobic core containing a tryptophan. Also, the interaction of 17-27HTE and LigBCon4 is driven by enthalpy as determined by ITC (Table 8.3). Since enthalpy-driven reactions are generally due to charge-charge interactions or Van der Waal forces, the examination of the influences of surface charges on LigBCon4 and 17-27HTE were conducted by adjusting the environmental pH. Interestingly, the optimal binding of LigBCon4 to 17-27HTE corresponds to pH 6.5 to 7.5, where the charge of LigBCon4 and 17-27HTE are opposite to each other and implies that binding between the two is governed by charge-charge interaction (Figure. 8.7). Furthermore, the structure of LigBCon4 or 17-27HTE and the binding activities of LigBCon4-17-27HTE are properly maintained from pH4.5 to pH8.5 when detected by CD and fluorescence spectroscopy; this indicates that the interaction can occur in slightly basic and/or acidic environments (Figure. 8.7B and C and supplemental Figure. 8.9). *Leptospira* spp. usually invade the host through mucous membranes or injured skin and then are distributed to different organs such as the lung, liver, kidney or placenta through spirochetemia (1). The normal range of pH in plasma is 7.38-7.42 and that of urine ranges from 4.5 to 8.5 (52) . We conclude that the pH range from 4.5 to 8.5 allows the optimal environment for LigBCon4-17-27HTE binding, facilitating adhesion of *Leptospira* spp. to tissues in these organs.

In this study, it was inferred that the interaction of LigBCon4/17-27HTE can partly be attributed to charge-charge interaction due to the enthalpy driven interaction found by ITC (Table 8.3), and the acidic amino acids of LigBCon4, LigBCen7'-8, LigBCen9, and LigBCen12 participate in the binding because of the negative charge on the surface of LigBCon4 as predicted in Figure. 8.7A. The results obtained from alignment of LigBCon4, LigBCen7'-8, LigBCen9, and LigBCen12 indicate that D341 of LigBCon4 is conserved in all four elastin binding immunoglobulin-like domains (Figure. 8.8A). A mutant, LigBCon4D341N, was constructed and the binding activity of the mutated protein to 17-27HTE was analyzed by ITC and fluorescence spectroscopy to determine if an aspartate residue is involved in the binding of LigBCon4 to 17-27HTE. The ITC and fluorescence spectroscopy results show a 4.6-fold reduction of binding activity when LigBCon4D341N was used instead of the wild type LigBCon4 (LigBCon4; K_D= 0.54±0.02μM, LigBCon4D341N; K_D= 2.51±0.48μM) (Figure. 8.8C, Table 8.3). This result further supports that the charge-charge interaction of LigBCon4 to 17-27 HTE is due to the negative charge of aspartate at physiological pH (Asp; pKa = 3.9). However, the binding of 17-27HTE to LigBCon4D341N is not completely eliminated. This strongly indicates that other residues of LigBCon4 also contribute to the binding of HTE, but to a lesser degree. It is not surprising that Lig proteins interact with HTE mainly through charge-charge interactions because of the biochemical nature of HTE. There are two major types of domains found in tropoelastin including hydrophobic domains rich in nonpolar amino acids as well as hydrophilic domains rich in basic amino acids like lysine, so HTE can inherently bind to many partners via charge-charge interaction; examples include FnBPA binding to 17-27HTE and glycosaminoglycans binding to HTE (32,53,54).
In conclusion, we have identified that Lig proteins contribute leptospiral adhesion to elastin and HTE. Elastin and HTE binding regions on the immunoglobulin-like domains

of LigBCon4, LigBCen7'-8, LigBCen9, and LigBCen12 were mapped. Among these binding regions, LigBCon4 was found to bind to elastin and HTE with the highest affinity and the residue Asp^{341} of LigBCen4 was determined to be involved in HTE binding through charge-charge interactions. This is the first report that elastin and tropoelastin can bind to LigBCon, the conserved region of Lig from *Leptospira* spp. Further study of the interaction of Lig protein with elastin and tropoelastin is in progress in our laboratory.

REFERENCES

1. **Levett, P. N.** Leptospirosis 2001 Clin. Microbiol. Rev. **14**: 296-326
2. **Palaniappan, R. U., Ramanujam, S., and Chang, Y. F.** 2007 Leptospirosis: pathogenesis, immunity, and diagnosis. Curr Opin Infect Dis **20**: 284-292
3. **Faine, S. B., Adher, B., Bolin, C., and Perolat, P**. (eds). 1999 *Leptospira and Leptospirosis.*, MedSci, Medbourne, Australia
4. **Verma, A., Rathinam, S. R., Priya, C. G., Muthukkaruppan, V. R., Stevenson, B., and Timoney, J. F.** 2008 LruA and LruB antibodies in sera of human with leptospiral uvieitis. Clin Vaccine Immunol **15**, 1019-1023
5. **Croda J, Figueira CP, Wunder EA, Jr., Santos CS, Reis MG et al.** 2008 Targeted mutagenesis in pathogenic *Leptospira* species: disruption of the LigB gene does not affect virulence in animal models of leptospirosis. Infect Immun **76:** 5826-5833.
6. **Murray, G. L., Ellis, K. M., Lo, M., and Adler, B**. 2008 *Leptospira interrogans* requires a functional heme oxygenase to scavenge iron from hemoglobin. Microbes Infect **10**, 791-797
7. **Murray, G. L., Srikram, A., Henry, R., Puapairoj, A., Sermswan, R., and Adler, B.** 2008 *Leptospira interrogans* requires heme oxygenase for disease pathogenesis. Microbes Infect **11:** 311-314
8. **Murray, G. L., Srikram, A., Hoke, D. E., Wunder, E. A., Jr., Henry, R., Lo, M., Zhang, K., Sermswan, R. W., Ko, A. I., and Adler, B.** 2008 Major surface protein LipL32 is not required for either acute or chronic infection with *Leptospira interrogans*. Infect. Immun. **77:** 952-958
9. **Patti, J. M., B. L. Allen, M. J. McGavin, and M. Hook.** 1994. MSCRAMM-mediated adherence of microorganisms to host tissues. Annu Rev Microbiol **48:**585-617

10. **Atzingen MV, Barbosa AS, De Brito T, Vasconcellos SA, Morais ZM et al.** 2008 Lsa21, a novel leptospiral protein binding adhesive matrix molecules and present during human infection. BMC Microbiol **8**: 70.

11. **Barbosa AS, Abreu PA, Neves FO, Atzingen MV, Watanabe MM et al.** 2006 A newly identified leptospiral adhesin mediates attachment to laminin. Infect Immun **74**: 6356-6364.

12. **Hauk P, Macedo F, Romero EC, Vasconcellos SA, de Morais ZM et al.** 2008 In LipL32, the major leptospiral lipoprotein, the C terminus is the primary immunogenic domain and mediates interaction with collagen IV and plasma fibronectin. Infect Immun **76**: 2642-2650.

13. **Hoke DE, Egan S, Cullen PA, Adler B** 2008 LipL32 is an extracellular matrix-interacting protein of *Leptospira* spp. and *Pseudoalteromonas tunicata*. Infect Immun **76**: 2063-2069.

14. **Matsunaga J, Barocchi MA, Croda J, Young TA, Sanchez Y et al.** 2003 Pathogenic *Leptospira* species express surface-exposed proteins belonging to the bacterial immunoglobulin superfamily. Mol Microbiol **49:** 929-945.

15. **Merien, F., Truccolo, J., Baranton, G., and Perolat, P.** 2000 Identification of a 36-kDa fibronectin-binding protein expressed by a virulent variant of *Leptospira interrogans* serovar icterohaemorrhagiae. FEMS Microbiol Lett **185**, 17-22

16. **Palaniappan RU, Chang YF, Hassan F, McDonough SP, Pough M et al.** 2004 Expression of leptospiral immunoglobulin-like protein by *Leptospira interrogans* and evaluation of its diagnostic potential in a kinetic ELISA. J Med Microbiol **53**(Pt 10): 975-984.

17. **Palaniappan RU, Chang YF, Jusuf SS, Artiushin S, Timoney JF et al.** 2002 Cloning and molecular characterization of an immunogenic LigA protein of *Leptospira interrogans*. Infect Immun **70**: 5924-5930.

18. **Stevenson B, Choy HA, Pinne M, Rotondi ML, Miller MC et al.** 2007 Leptospira interrogans Endostatin-Like Outer Membrane Proteins Bind Host Fibronectin, Laminin and Regulators of Complement. PLoS ONE **2**: e1188.

19. **Matsunaga J, Lo M, Bulach DM, Zuerner RL, Adler B et al.** 2007 Response of *Leptospira interrogans* to Physiologic Osmolarity: Relevance in Signaling the Environment-to-Host Transition. Infect Immun **75** 2864-2874.

20. **Choy HA, Kelley MM, Chen TL, Moller AK, Matsunaga J et al.** 2007 Physiological osmotic induction of *Leptospira interrogans* adhesion: LigA and LigB bind extracellular matrix proteins and fibrinogen. Infect Immun **75:** 2441-2450.

21. **Lin YP, Chang YF** 2007 A domain of the *Leptospira* LigB contributes to high affinity binding of fibronectin. Biochem Biophys Res Commun **362**: 443-448.

22. **Lin YP, Chang YF** 2008 The C-terminal variable domain of LigB from *Leptospira* mediates binding to fibronectin. J. Vet. Sci. **9:** 133-144.

23. **Lin YP, Raman R, Sharma Y, Chang YF** 2008 Calcium binds to Leptospiral immunoglobulin-like protein, LigB and modulates fibronectin binding. J. Biol. Chem. **283**: 25140-25149.

24. **Faisal SM, Yan W, Chen CS, Palaniappan RU, McDonough SP et al.** 2008 Evaluation of protective immunity of *Leptospira* immunoglobulin like protein A (LigA) DNA vaccine against challenge in hamsters. Vaccine **26:** 277-287.

25. **Faisal SM, Yan W, McDonough SP, Chang YF** 2009 Variable region of *Leptospira* immunoglobulin like protein A (LigAvar) incorporated in Liposomes and PLGA-Microspheres produces a robust immune response

correlating to protective immunity against challenge in hamsters. Vaccine **27:** 378-387.

26. **Palaniappan RU, McDonough SP, Divers TJ, Chen CS, Pan MJ et al.** 2006 Immunoprotection of recombinant leptospiral immunoglobulin-like protein A against *Leptospira interrogans* serovar Pomona infection. Infect Immun **74:** 1745-1750.

27. **Graf, R., Neudeck, H., Gossrau, R., and Vetter, K.** 1996 Elastic fibres are an essential component of placental stem villous stroma and an integrated part of perivascular contractile sheath. Cell .Tissue Res. **283**: 133-141

28. **Mithieux, S. M., and Weiss, A. S.** 2005 Elastin Adv. Protein Chem. **70**: 437-461

29. **Starcher, B. C.** 1986 Elastin and the lung. Thorax **41**: 577-585

30. **Vrhovski, B., Jensen, S., and Weiss, A. S.** 1997 Coacervation characteristics of recombinant human tropoelastin. Eur. J. Biochem. **250**: 92-98

31. **Vrhovski, B., and Weiss, A. S.** 1998 Biochemistry of tropoelastin. Eur. J. Biochem. **258**: 1-18

32. **Wise, S. G., and Weiss, A. S.** 2009 Tropoelastin. Int. J. Biochem. Cell. Biol. **41**: 494-497

33. **Keane, F. M., Clarke, A. W., Foster, T. J., and Weiss, A. S.** 2007 The N-terminal A domain of *Staphylococcus aureus* fibronectin binding protein A binds to tropoelastin. Biochemistry **46**: 7226-7232

34. **Keane, F. M., Loughman, A., Valtulina, V., Brennan, M., Speziale, P., and Foster, T. J.** 2007 Fibrinogen and elastin bind to the same region within the A domain of fibronectin binding protein A, an MSCRAMM of *Staphylococcus aureus.* Mol. Microbiol. **63**: 711-723

35. **Roche, F. M., Downer, R., Keane, F., Speziale, P., Park, P. W., and Foster, T. J.** 2004 The N-terminal A domain of fibronectin-binding protein A and B promotes adhesion of *Staphylococcus aureus* to elastin. J. Biol. Chem. **279**: 38433-38440

36. **Dolhnikoff, M., Mauad, T., Bethlem, E. P., and Carvalho, C. R.** 2007 Leptospiral pneumonias Curr Opin Pulm Med **13**: 230-235

37. **Seijo, A., Coto, H., San Juan, J., Videla, J., Deodato, B., Cernigoi, B., Messina, O. G., Collia, O., de Bassadoni, D., Schtirbu, R., Olenchuk, A., de Mazzonelli, G. D., and Parma, A.** 2002 Lethal Leptopiral pulmonary hemorrhage: an emerging disease in Buenos Aires, Argentina. Emerg Infect Dis **8**: 1004-1005

38. **Donahue, J. M., and Williams, N. M.** 2000 Emerging causes of placentitis and abortion. Vet Clin North Am Equine Pract **16**: 443-456, viii

39. **Walsh, E. J., Miajlovic, H., Gorkun, O. V., and Foster, T. J.** 2008 Identification of *Staphylococcus aureus* MSCRAMM clumping factor B (ClfB) binding site in the alphaC-domain of human fibrinogen. Microbiology **154**: 550-558

40. **Wachi, H., Sato, F., Nakazawa, J., Nonaka, R., Szabo, Z., Urban, Z., Yasunaga, T., Maeda, I., Okamoto, K., Starcher, B. C., Li, D. Y., Mecham, R. P., and Seyama, Y.** 2007 Domain 16 and 17 of tropoelastin in elastic fibre formation. Biochem J **402**: 63-70

41. **Yan W, Faisal SM, McDonough SP, Divers TJ, Barr SC et al.** 2009 Immunogenicity and protective efficacy of recombinant *Leptospira* immunoglobulin-like protein B (rLigB) in a hamster challenge model. Microbes Infect **11:** 230-237.

42. **Sandell, L. J., and Boyd, C. D. (eds).** 1990 Extracellular matrix genes. pp 224-231. 1st Ed., Academic Press Inc., San Diego, CA

43. **Rodgers, U. R., and Weiss, A. S.** 2004 Integrin alpha v beta 3 binds a unique non-RGD site near the C-terminus of human tropoelastin *Biochimie* **86**, 173-178

44. **Bohm, G., Muhr, R., and Jaenicke, R.** 1992 Quantitative analysis of protein far UV circular dichroism spectra by neural network. Protein Eng **5**: 191-195

45. **Sreerama, N., and Woody, R. W.** 1994 Protein secondary structure from circular dichroism spectroscopy Combining variable selection principle and cluster analysis with neural network, ridge regression and self-consistent methods. J Mol Biol **242**: 497-507

46. **Pervushin, K., Riek, R., Wider, G., and Wuthrich, K.** 1997 Attneuated relaxation by mutual cancellation of dipole-dipole coupling and chemical shift anisotropy indicates an avenue to NMR structures of very large biological macromolecules in solution. *Proc Natl Acad Sci U S A* **94**: 12366-12371

47. **Marotto, P. C., Nascimento, C. M., Eluf-Neto, J., Marotto, M. S., Andrade, L., Sztajnbok, J., and Seguro, A. C.** 1999 Acute lung injury in leptospirosis: clinical and laboratory features, outcome, factors associated with mortality. Clin Infect Dis **29**, 1561-1563

48. **Wagenaar, J. F., de Vries, P. J., and Hartskeerl, R. A.** 2004 Leptospirosis with pulmonary hemorrhage, caused by a new strain of serovar Lai: Langkawi. J Travel Med **11**: 379-381

49. **Hong, C. B., Donahue, J. M., Giles, R. C., Jr., Petrites-Murphy, M. B., Poonacha, K. B., Roberts, A. W., Smith, B. J., Tramontin, R. R., Tuttle, P. A., and Swerczek, T. W.** 1993 Etiology and pathology of equine placentitis. Journal of veterinary diagnostic investigation **5**: 56-63

50. **Sebastian, M., Giles, R., Roberts, J., Poonacha, K., Harrison, L., Donahue, J., and Benirschke, K.** 2005 Funisitis associated with leptospiral abortion in an equine placenta. Veterinary pathology **42**: 659-662

51. **Broekelmann, T. J., Kozel, B. A., Ishibashi, H., Werneck, C. C., Keeley, F. W., Zhang, L., and Mecham, R. P.** 2005 Tropoelastin interacts with cell-surface glyacosaminoglycans via its COOH-terminal domain. J. Biol. Chem. **280**: 40939-40947

52. **Silverthorn, D. U.** (ed) 2001 Human physiology, An integrated approach., 2nd Ed., Prentice Hall, New Jersey

53. **Piontkivska, H., Zhang, Y., Green, E. D., and Elnitski, L.** 2004 Multi-species sequence comparison reveals dynamic evolution of the elastin gene that has involved purifying selection and lineage-specific insertion/deletions. BMC genomics **5**: 31

54. **Wu, W. J., Vrhovski, B., and Weiss, A. S.** 1999 Glycosaminoglycan mediates the coacervation of human tropoelastin through dominant charge interaction involving lysine side chain. J. Biol. Chem. **274**: 21719-21724

CHAPTER 9

LEPTOSPIRA IMMUNOGOBULIN-LIKE PROTEINS BIND TO THE C-TERMINAL FIBRINOGEN AC DOMAIN INHIBITING FIBRIN CLOT FORMATION, PLATELET ADHESION AND AGGREGATION

Introduction

Leptospira spp are pathogenic spirochetes that can cause acute or chronic infections in both humans and animals. The disease is widespread in developing countries and is reemerging in the United States (1, 2). Patients with Weil's syndrome, a severe form of leptospirosis, may develop liver failure (jaundice), renal failure (nephritis), pulmonary hemorrhage, meningitis, abortion and uveitis (3). Several potential virulence factors from *Leptospira* spp. have been identified including LipL32 (4, 5), Lsa21 (6), Lsa27 (7), HlyC (8), Lp95 (9), *Leptospira* endostatin-like proteins (Len) (10,11), and *Leptospira* immunoglobulin-like (Lig) proteins (12-16). Among these molecules, only Lig proteins possess fibrinogen (Fg) binding activity (12,13). Lig proteins, including LigA, LigB, and LigC, contain 13, 12, and 13 Ig-like domains (17-19). The N-terminal 630 amino acids of LigA and LigB are highly conserved (LigBCon), but the C-terminals are variable (18,19). In addition, a non-Ig-like region is located in the C-terminals of LigB and LigC (18,19). Lig proteins bind calcium, which aids their binding to fibronectin (Fn) (20,21). LigBCen2NR, a disordered region of LigBCen2 binds to the N-terminal of Fn (21). Apart from Fn, LigBCen2 also binds to elastin, laminin, collagen, and Fg (13-16). A recent study indicated that knockout of the C-terminal of the LigB gene does not affect the virulence of this organism (22). Therefore, the role of LigB in the pathogenesis of leptospirosis is still unclear.

Fibrinogen (Fg) is a 340 kDa plasma glycoprotein composed of α, β, and γ chains crosslinked by 29 disulfide bonds (1-3). Fg interacts with activated $\alpha_{IIb}\beta 3$ integrin on the

surface of platelets thereby inducing platelet aggregation, which is intimately associated with blood coagulation (23-25). Activation of prothrombin to thrombin by the coagulation cascade converts soluble Fg into a three-dimensional network of insoluble fibrin to form a clot (23,25). The fibrinolytic cascade limits the extent of the resulting thrombus. Plasminogen (PLG) is converted to plasmin by tissue-type plasminogen activator (tPA) and decomposes the fibrin clot by breaking down fibrin and interfering with fibrinogen polymerization (25). Several microbial adhesins classified as either Microbial Surface Components Recognizing Adhesive Matrix Molecules (MSCRAMMs) or secreted adhesins termed Secretable Expanded Repertoire Adhesive Molecules (SERAMs) are able to interfere with blood coagulation and thrombosis by binding to Fg (26,27). We hypothesized that Lig proteins could play a similar role in the pathogenesis of leptospirosis.

In this study, we demonstrate that LigBCen2R, the partial 11th and entire 12th Ig-like domain of LigB, is able to bind to the C-terminus of Fg α (FgαCC) and fibrin, and the binding is expanded to other Ig-like domains of Lig proteins. The LigBCen2R-FgαCC interaction may prevent Fg binding to integrin $\alpha_{IIb}\beta3$ on platelets and platelet aggregation. Furthermore, LigBCen2R could disrupt fibrin clot formation but did not affect the binding of PLG and tPA to FgαCC.

Materials and Methods

Reagents and antibodies

rabbit anti-GST antibody, mouse anti-integrin $\alpha_{IIb}\beta3$, Texas Red conjugated streptavidin, and FITC-conjugated goat anti-mouse antibody were ordered from Invitrogen (Eugene, OR). HRP-conjugated goat anti-rabbit antibody and HRP-conjugated streptavidin were ordered from KPL (Gaithersburg, MD). Integrin $\alpha_{IIb}\beta3$ was purchased from Millipore (Billerica, MA). Thrombin and protein A HP

spintrap column were ordered from GE healthcare (Piscataway, NJ). Human plasma fibrinogen, human fibrin, plasminogen from human plasma, and human tissue plasminogen activator, bovine serum albumin (BSA), Tris-HCl, sodium phosphate dehydrate, and sodium chloride were obtained from Sigma-Aldrich (St. Louis, MO).

Plasmid construction and protein purification

$ClfAN_2N_3$, N2-N3 domain of ClfA (amino acids 1131-1225 in ClfA) were from *Staphylococcus aureus* (28). All constructs used in this study were cloned into pGEX-4T-2 (GE healthcare) or pQE-30 (Qiagen, Alencia, CA) described in Table 9.1 and schematized in Figure. 9.1 and overexpressed proteins purified as Glutathione-S-Transferase (GST) or histidine tagged fusion proteins, respectively (16,20,29). To clone all above constructs, PCR reactions were performed by using the primers listed in Table 9.2 and is based on the DNA sequence in *L. interrogans* serovar Pomona (Genbank number: FJ030916) for all subconstructs of LigA. FgαC, FgαD, FgαE, FgαCC, and FgαCN were amplified from the α chain of human Fg (gifts from Dr. Timothy J. Foster) using primers as indicated in Table 9.1 and 9.2. For constructing all clones described above, primers were engineered to introduce a BamHI site at the 5' end and a SalI site at the 3' end of each fragment. PCR products were sequentially digested with BamHI and SalI and then ligated into pQE30 or pGEX-4T-2 digested with same restriction enzymes. For LigBCen2RW1073C and FgαCCY570W mutant constructions, a Quickchange mutagenesis kit (Strategene, La Jolla, CA) was used and followed the manufacturer's instructions as previously described (16). In this study, the soluble form of the histidine-tag and GST fusion proteins were purified from *E. coli* as previously described (29).

Table 9.1. The sources of clones used in this study

Clone	Source	Tag
LigAVar7'-8	Residues 631-765 of LigA from *L. interrogans*	GST tag
LigAVar9	Residues 756-856 of LigA from *L. interrogans*	Histidine tag
LigAVar10	Residues 847-946of LigA from *L. interrogans*	Histidine tag
LigAVar11	Residues 938-1038 of LigA from *L. interrogans*	Histidine tag
LigAVar12	Residues 1029-1140 of LigA from *L. interrogans*	Histidine tag
LigAVar13	Residues 1131-1225 of LigA from *L. interrogans*	Histidine tag
FgαC	Residues 198-644 of Fgα chain from human	Histidine tag
FgαD	Residues 111-197 of Fgα chain from human	Histidine tag
FgαE	Residues 1-110 of Fgα chain from human	Histidine tag
FgαCN	Residues 198-391 of Fgα chain from human	GST-tag
FgαCC	Residues 392-644 of Fgα chain from human	GST-tag

Table 9.2. Primer Table

Primer/Vector	Sequence
LigAVar7'-8fp/pGEX4T2	GCGGATCCCTTACCGTTTCCAAC
LigAVar7'-8rp	GCGTCGACATTGAAGTAAGAATT
LigAVar9fp/pQE30	GCGGATCCTACCGTTACTCCCGC
LigAVar9rp	GCGTCGACCTCAATAAGTTCCGC
LigAVar10fp/pQE30	GCGGATCCTTATCCGTTACCGCA
LigAVar10rp	GCGTCGACCGAAACTACTTTAGC
LigAVar11fp/pQE30	GCGGATCCTTCCAAGTTACTCCG
LigAVar11rp	GCGTCGACGTAACGAAGAAGCGC
LigAVar12fp/pQE30	GCGGATCCTTGAATGTCACTCCA
LigAVar12rp	GCGTCGACATTTACTATACCACT
LigAVar13fp/pQE30	GCGGATCCGTTACGGTTACGGAA
LigAVar13rp	GCGTCGACTTATGGCTCCGTTTT
LigBCen2RW1073Cf	TCTTCGGTTACATGTTCCAGCTCAAAT
LigBCen2RW1073Cr	ATTTGAGCTGGAACATGTAACCGAAGA
FgαCfp/pQE30	CGGGATCCGAAGATCAGCAGAAG
FgαCrp	CGGTCGACCTAGGGGGACAGGGA
FgαDfp/pQE30	CGGGATCCGAAATTTTGAGAGGC
FgαDrp	CGGTCGACATAGTCCTTCAGATC
FgαEfp/pQE30	CGGGATCCATGTTTTCCATGAG
FgαErp	CGGTCGACCATTATATTAGTGGT
FgαCCfp/pGEX4T2	CGGGATCCGGCACATTTGAAGAG
FgαCCrp	CGGTCGACCTAGGGGGACAGGGA
FgαCNfp/pGEX4T2	CGGGATCCGAAGATCAGCAGAAG
FgαCNrp	CGGTCGACCCAGTCTGGGTTGTT

Fig. 9.2 (Continued)

Primer/Vector	Sequence
FgαCCY570Wf	AGCACGAGTTGGAACAGAGGA
FgαCCY570Wr	TCCTCTGTTCCAACTCGTGCT

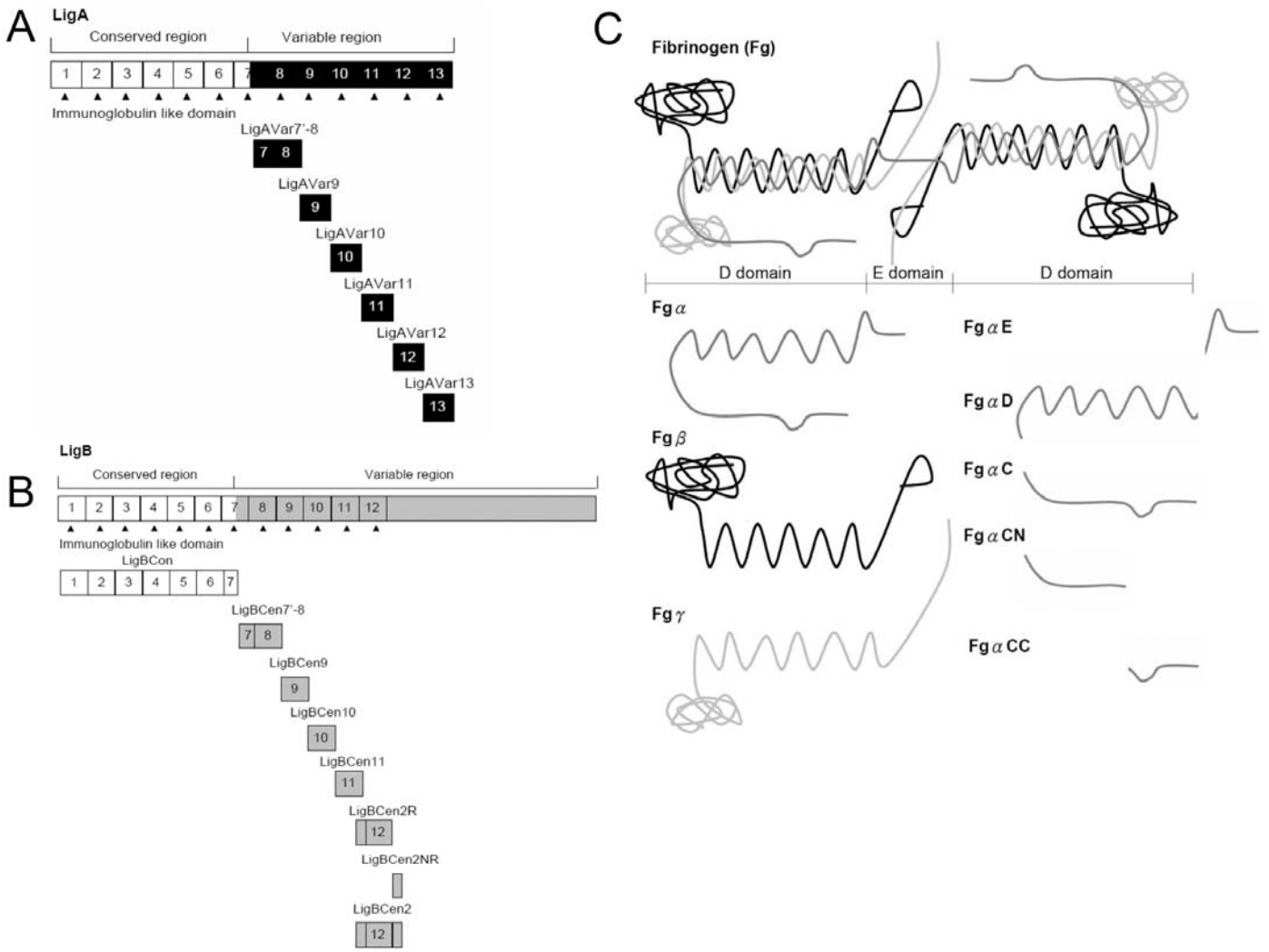

Figure 9.1 A schematic diagram showing the structure of truncated (A) LigA, (B) LigB , and (C) Fg used in this study.

Platelet preparation

All studies were performed in healthy blood donors without anti-platelet medication for at least four weeks. The preparation of platelets was performed using published methods (30). Briefly, 5 mL of blood was collected into citrated vacuum tubes, centrifuged at 140 x g for 10 minutes and platelet rich plasma (PRP) was aspirated from the upper layer. Platelet poor plasma (PPP) was obtained after centrifuging the lower phase at 200 x g for 20 min. The number of platelets used in this study was adjusted by mixing different volumes of PRP and PPP and counted using a hemocytometer. In order to remove Fg on the surface of platelets, the platelets were spun down at 1,000 x g for 1 min and then treated with 1μM of PGE1 and 1.0 U/ml of apyrase. After removing the upernatant, the platelet pellets were gently resuspended in 10 mL of wash buffer (134mM NaCl, 5 mM Glucose, 1 mM EDTA, 15 mM Tris, pH 6.3) containing 1.0 U/mL apyrase and subsequently centrifuged at 800 x g for 15 min. The Fg depleted platelets were resuspended in buffer (145 mM NaCl, 5 mM KCl, 0.5 mM EGTA, 1 mM $MgSO_4$, 10 mM Glucose, 25 mM HEPES, pH 7.3) containing 1.0 U/mL of apyrase.

Binding assays by ELISA

To identify the Fg binding site on Lig proteins, 1 μM of Fg (Figure. 9.2A, 9.3A and B) or BSA (negative control and data not shown) in Tris buffer (25 mM of Tris and 150 mM of sodium chloride at pH 7.0) were coated onto microtiter plate wells as previously described (21). Subsequently 100 μL of a serial dilution of biotinylated LigBCon (negative control), $ClfAN_2N_3$ (positive control in Figure. 9.2A) (28), LigBCen2 (positive control in Figure. 9.2A) (13), LigBCen2NR, or LigBCen2R (Figure. 9.2A and positive control in Figure. 9.3A and B), LigAVar7'-8, LigAVar9, LigAVar10, LigAVar11, LigAVar12, LigAVar13, LigBCen7'-8, LigBCen9, LigBCen10, or LigBCen11 was added (Figure. 9.3A and B). To analyze the fibrin binding site of

LigBCen2R, 1μM of biotinylated LigBCon (negative control), ClfAN_2N_3 (positive control) (31), LigBCen2, LigBCen2R, or LigBCen2NR was added to a serial dilution of fibrin coated onto microtiter plate wells (Figure. 9.2B). To map the binding site of Lig proteins to Fg, 1 μM of Fg (positive control), BSA (negative control), Fgα, Fgβ, Fgγ (Figure. 9.4A), FgαC, FgαD, FgαE (Figure. 9.4B), FgαCC, or FgαCN (Figure. 9.4C) in Tris buffer were coated onto microtiter plate wells. A 100 μL aliquot of a serial dilution of GST fused LigBCon (negative control and data not shown) or LigBCen2R in Tris buffer was added subsequently (Figure. 9.4A, B, and C). To study the effect of LigBCen2R-Fg interaction on the binding of PLG and tPA on FgαCF, 100 μL of a serial dilution of GST fused LigBCon (negative control and data not shown) or LigBCen2R was mixed with 200 nM of PLG, tPA, LigBCen2R (positive control), or LigBCon (negative control) immediately before being added to microtiter plate wells coated with 1 μM of FgαCC (Figure. 9.8B). To measure the interaction of Fg or fibrin with Lig proteins by ELISA, rabbit anti-GST (1:200) and horseradish peroxidase-conjugated goat anti-rabbit IgG (1:1000) were used as primary and secondary antibodies. To detect the binding of the biotinylated proteins, HRP-conjugated streptavidin (1:1000) was added to each well at RT for 1 hour prior to washing the wells three times with TBST. The measurement of binding by ELISA was performed as previously described (21). To determine the dissociation constant (K_D), the data were fitted by the following equation using KaleidaGraph software (Version 2.1.3 Abelbeck software, Reading, PA), and the calculated K_D are listed in Table 9.3.

$$OD_{630} = \frac{OD_{630max}\,[\text{Lig proteins}]}{K_D + [\text{Lig proteins}]} \quad \text{(Eq. 1)}$$

Table 9.3. The dissociation constant (K_D) obtained from the Fibrinogen binding by Lig proteins determined by ELISA.

Truncated Lig	K_D								
	Fg	Fgα	Fgβ	Fgγ	FgαC	FgαD	FgαE	FgαCC	FgαCN
LigBCen2	116 ± 15 nM	n/d[b]	n/d[b]	n/d[b]	n/d[b]	n/d[b]	n/d[b]	n/d[b]	n/d[b]
LigBCen2R	110 ± 12 nM	165 ± 33 nM	n/b[a]	n/b[a]	200 ± 43 nM	n/b[a]	n/b[a]	355 ± 43 nM	n/b[a]
LigBCen2NR	n/b[a]	n/d[b]	n/d[b]	n/d[b]	n/d[b]	n/d[b]	n/d[b]	n/d[b]	n/d[b]
LigAVar7'-8	n/b[a]	n/d[b]	n/d[b]	n/d[b]	n/d[b]	n/d[b]	n/d[b]	n/d[b]	n/d[b]
LigAVar9	n/b[a]	n/d[b]	n/d[b]	n/d[b]	n/d[b]	n/d[b]	n/d[b]	n/d[b]	n/d[b]
LigAVar10	207 ± 9 nM	n/d[b]	n/d[b]	n/d[b]	n/d[b]	n/d[b]	n/d[b]	n/d[b]	n/d[b]
LigAVar11	n/b[a]	n/d[b]	n/d[b]	n/d[b]	n/d[b]	n/d[b]	n/d[b]	n/d[b]	n/d[b]
LigAVar12	303 ± 44 nM	n/d[b]	n/d[b]	n/d[b]	n/d[b]	n/d[b]	n/d[b]	n/d[b]	n/d[b]
LigAVar13	755 ± 12 nM	n/d[b]	n/d[b]	n/d[b]	n/d[b]	n/d[b]	n/d[b]	n/d[b]	n/d[b]

Table 9.3 (Continued)

Truncated Lig	K_D								
	Fg	Fgα	Fgβ	Fgγ	FgαC	FgαD	FgαE	Fgα CC	FgαCN
LigBCen7'-8	3170 ±15nM	n/d[b]	n/d[b]	n/d[b]	n/d[b]	n/d[b]	n/d[b]	n/d[b]	n/d[b]
LigBCen9	758 ± 26 nM	n/d[b]	n/d[b]	n/d[b]	n/d[b]	n/d[b]	n/d[b]	n/d[b]	n/d[b]
LigBCen10	295 ± 78 nM	n/d[b]	n/d[b]	n/d[b]	n/d[b]	n/d[b]	n/d[b]	n/d[b]	n/d[b]
LigBCen11	n/b[a]	n/d[b]	n/d[b]	n/d[b]	n/d[b]	n/d[b]	n/d[b]	n/d[b]	n/d[b]
LigBCon	n/b[a]	n/d[b]	n/d[b]	n/d[b]	n/d[b]	n/d[b]	n/d[b]	n/d[b]	n/d[b]

n/b[a], no binding.

n/d[b], not determined.

Inhibition assays by ELISA

To confirm that Fg- or fibrin-Lig protein interactions reflected specific binding, the microtiter plate wells were coated with 100 μL of 1 μM of Fg (Figure. 9.2C, 3C and D), fibrin (Figure. 9.2D) or BSA (negative control) as previously described (21). 100 μL of 1 μM of biotinylated LigA10, LigA12, LigA13 (Figure. 9.3C), LigB7'-8, LigB9, LigB10 (Figure. 9.3D), LigBCen2R (Figure. 9.2C and D and positive control in 3C and D), $ClfAN_2N_3$ (positive control in Figure. 9.2C and D) (28) or LigBCon, LigBCen2R, LigBCon (negative control), or integrin $\alpha_{IIb}\beta_3$ (positive control) prior to being added to microtiter plate wells coated with 200 nM of integrin $\alpha_{IIb}\beta_3$ or containing 10^5 human platelets treated with 1 μM ADP (Figure. 9.5C and D). To elucidate if PLG or tPA binding to FgαCC affects the LigBCen2R-Fg interaction, 1 μM of FgαCC was coated on microtiter plate wells and treated with a serial dilution of PLG, tPA, LigBCen2R (positive control), or LigBCon (negative control) before incubation with 1 μM of GST fused LigBCen2R (Figure. 9.8A). The binding of GST fused or biotinylated proteins was measured by ELISA as described above.

Isothermal Titration Calorimetry (ITC)

The experiments were carried out with a CSC 5300 microcalorimeter (Calorimetry Science Corp. Lindon, UT, USA) at 25^{o}C as previously described (21). In a typical experiment, the cell contained 1 ml of a solution of LigBCen2R and the syringe contained 250 μl of a solution of FgαCC. The concentration of LigBCen2R and FgαCC are 2.4 μM and 40 μM in Tris buffer. The titration was performed as follows: 25 injections of 10 μl with a stirring speed of 250 rpm with a delay time between injections of 5 min. Data were analyzed using Titration Binding Work 3.1 software (Calorimetry Science Corp. Lindon, UT, USA) fitting them to an independent binding model.

Steady State Fluorescence Measurement

Steady state fluorescence emissions were measured on a Hitachi F4500 spectrofluorometer (Hitachi. San Jose, CA). All spectra were recorded in correct spectrum mode of the instrument using excitation and emission band passes of 2 nm. For titration experiments of LigBCen2R, 0.15, 0.3125, 0.625, 1.25, 2.5, or 5 μM of FgαCC were incubated with 1 μM LigBCen2R for 5 min. For the titration experiments of FgαCCY570W, 1 μM was mixed with 0.15, 0.3125, 0.625, 1.25, 2.5, or 5 μM of LigBCen2RW1073C for 5 minutes. The emission spectra were taken as the excitation wavelength at 295 nm and the emission wavelength recorded from 310 nm to 400 nm in Tris buffer (Figure. 9.5A). All spectra were recorded at 25^{o}C after 5 min. To determine the dissociation constant (K_D), the fluorescence intensities at 330 nm were recorded and fitted by the following equation using KaleidaGraph software (Version 2.1.3 Abelbeck software):

$$F_{max}\text{-}F = \frac{(F_{max}\text{-}F_{min})\,[\,\text{LigBCen2RW1073C}]}{K_D + [\,\text{LigBCen2RW1073C}\,]} \quad \text{(Eq. 2)}$$

Where F_{max} is the fluorescence intensity of LigBCen2R or FgαCCY570W proteins in the absence of FgαCC or LigBCen2RW1073C, F_{min} indicates the fluorescence intensities of FgαCCY570W saturated with LigBCen2RW1073C or LigBCen2R saturated with FgαCC. In addition, F is the fluorescence intensities of LigBCen2R or FgαCCY570W in the presence of various concentrations of FgαCC or LigBCen2RW1073C. All of the measurements were corrected for dilution and for inner filter effect.

Circular dichroism (CD) spectroscopy

CD analysis was performed on an Aviv 215 spectropolarimeter (Lakewood, NJ) under N_2 atmosphere. CD spectra were measured at RT (25℃) in a 1-mm path length quartz

cell. Spectra of LigBCen2R, LigBCen2RW1073C, FgαCC (10 μM), and FgαCCY570W (10 μM) were recorded in Tris buffer at 25°C, and three far-UV CD spectra were recorded from 190 to 250 nm for far-UV CD in 1 nm increments. The background spectrum of buffer without protein was subtracted from the protein spectra. CD spectra were initially analyzed by the software accompanying the spectrophotometer. Analysis of spectra to extrapolate secondary structures was performed by Dichroweb (http://www.cryst.bbk.ac.uk/cdweb/html/home.html) using the K2D and Selcon 3 analysis programs (20).

Binding assays by Confocal Laser Scanning Microscopy (CLSM)

To determine the binding inhibition of FgαC to platelets by LigBCen2R, 1 μM of GST-FgαCC was treated by 50 μM of LigBCen2R or LigBCon (negative control) in 100 μl of Tris buffer for 1 hour at 37℃ prior to being added to wells containing 10^6 platelets treated with 1 μM ADP and incubated at 37℃ for 1 hour. Fixation and immunofluorescence staining were performed as described previously with slight modification (21). Briefly, platelets were fixed in 2% paraformaldehyde for 60 min at room temperature (RT) and then incubated in PBS containing 0.3% BSA for 10 min at RT. The primary and secondary antibodies in PBS containing 0.3% BSA were incubated sequentially for 60 min at RT. To detect the expression of integrin $\alpha_{IIb}\beta_3$ and its binding to GST- FgαC, mouse anti-integrin $\alpha_{IIb}\beta_3$ (1:250x) and rabbit anti-GST antibodies (1:250x) served as primary antibodies, and FITC conjugated goat anti-mouse IgG (1:250x) and Texas Red-conjugated goat anti-rabbit IgG (1:250x) were used as secondary antibodies. To measure the binding by CLSM, the glass slides were mounted with coverslips using Prolong Antifade (Molecular Probe, Eugene, OR) and viewed with an Olympus Fluoview 500 confocal laser-scanning imaging system equipped with

krypton, argon, and He-Ne lasers on an Olympus IX70 inverted microscope with a PLAPO 60X objective (Olympus, America, Inc., Melville, NY). Confocal images were processed using Adobe Photoshop CS2 (San Jose, CA). The settings were identical for all captured images.All studies were repeated three times.

Platelet aggregation

IgG depleted human serum was produced from the flowthrough of the human serum passed through protein A HP spin trap column. and ELISA and SDS-PAGE were used to test that IgG has been depleted from IgG as previously described (32). To inactivate complement proteins, human serum was incubated at 56℃ for 30 min (32,33). To measure platelet aggregation in serum, PRP (10^6) was treated with various concentration (1.5 μM, 3.125 μM, 6.25 μM, 12.5 μM, 25 μM, 50 μM, 100 μM) of LigBCen2R, LigBCon (negative control), or $ClfAN_2N_3$ (positive control) (34) for 1 hour, and treated PRP was mixed with 1 μM ADP and incubated for 1 hour subsequently. All the procedures were performed in 37℃. To measure the platelet aggregation in IgG depleted or complement protein inactivated serum, platelets were washed by spinning down and washing through washed buffer prior to be suspended in IgG depleted or complement inactivated human serum. The number of platelets can be adjusted by the added volume of certain serum. Light microscopy was used to measure the platelet aggregation (35). Basically, the platelet aggregation was immediately analyzed using 60× objective by epifluorescence microscope (Nikon, Japan). This setting was identical for all captured image. The aggregation size was measured by counting the area of each aggregate in one field (1,024×1,024 μm). The total area covered by all aggregates was calculated and normalized to the total surface measured, and the percentage of reduced aggregation surface coverage is relative to the area covered by the aggregates of untreated platelets.

Fibrin clot formation assay

The fibrin clot formation assay was performed as previously described (34). For the time course study of fibrin clot formation, each reaction contained 10 µL of Fg (10 U/mL) mixed with 90 µL of thrombin (1 mg/mL) with 30 µM of LigBCen2R, $ClfAN_2N_3$ (positive control) (34), or LigBCon (negative control) in the presence of 2 mM calcium chloride on microtiter plates wells (Figure. 9.7A). The OD_{600} values were recorded every 1 min by an ELISA plate reader (Bioteck EL-312; BioTeck, USA). To determine the effect of LigBCen2R binding to Fg on clot formation, 10 µL of thrombin (10 U/mL) mixed with 90 µL of Fg (1 mg/mL) that was pre-treated with a serial dilution of LigBCen2R, $ClfAN_2N_3$ (positive control), or LigBCon (negative control) in the presence of 2 mM calcium chloride at 25℃ was incubated for 1 hour in microtiter plate wells (Figure. 9.7B). The OD_{600} values were recorded described above.

Statistical analysis

Significance between samples was determined using the Student's t-test following logarithmic transformation of the data. Two-tailed P-values were determined for each sample and a P-value <0.05 was considered significant. Each data point represents the mean $\pm$ standard error of the mean (SEM) of samples tested in triplicate. An (*) indicates the result was statistically significant.

Results

The Ig-like domains of Lig proteins interact with Fg

LigBCen2 includes a well-folded region, LigBCen2R, which contains part of the 11th and all of the 12th Ig-like domains, and a disordered region, LigBCen2NR (Figure. 9.1B) (20). To further map the Fg binding site on LigBCen2, LigBCen2R and LigBCen2NR

Figure 9.2 Determination the binding sites of Fg and fibrin on LigBCen2. (A and B) Binding of serial concentrations of LigBCen2R to immobilized Fg or fibrin by ELISA. 0.015, 0.03125, 0.0625, 0.125, 0.25, 0.5, 1μM of biotinylated LigBCen2R, LigBCen2NR, LigBCen2 (positive reference), LigCon (negative reference), or $ClfAN_2N_3$ (positive reference) was added to 1μM of Fg or BSA (negative control, data not shown) coated wells in Tris buffer. (B) 1μM of biotinylated LigBCen2R, LigBCen2NR, LigBCen2, $ClfAN_2N_3$ (positive reference), or LigCon (negative reference) was added to the microtiter plate wells coated with 0.062, 0.125, 0.25, 0.5, 1, 2, 4μg/mL of Fibrin or BSA (negative control, data not shown) coated wells in Tris buffer. (C and D) Fg or fibrin inhibited LigBCen2R binding to immobilized Fg or fibrin. One μM of biotinylated $ClfAN_2N_3$ (positive control), LigBCon (negative control), or LigBCen2R was incubated with various concentrations of (C) Fg (0.031, 0.0625, 0.125, 0.25, 0.5, 1, 2μM in Tris buffer), (D) fibrin (0.062, 0.125, 0.25, 0.5, 1, 2, 4μg/mL in Tris buffer), or GST (negative control and data not shown) at RT for 1 hour prior to be added to wells coated with (C) 1μM of Fg, (D) 4μg/mL of fibrin, or BSA (negative control and data not shown). The percentage of binding was determined relative to the binding of biotinylated proteins in the LigBCon treated wells. The binding of biotinylated proteins to Fg or fibrin was measured by ELISA. For all experiments, each value represents the mean± SEM of three trials in triplicate samples. Statistically significant ($p < 0.05$) differences compared to negative control are indicated by an asterisk.

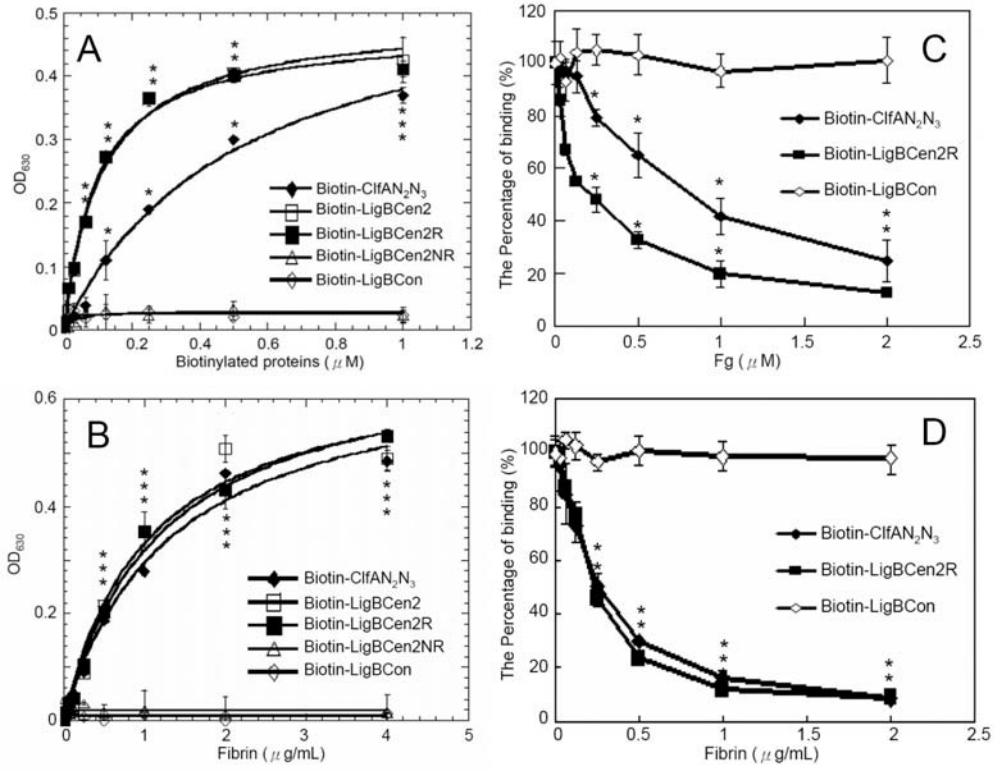
A
B
C
D
OD630
Biotinylated proteins (μM)
Fibrin (μg/mL)
The Percentage of binding (%)
Fg (μM)
Biotin-ClfAN2N3
Biotin-LigBCen2
Biotin-LigBCen2R
Biotin-LigBCen2NR
Biotin-LigBCon

Figure 9.3 Localization of the Fg-binding domains on Lig proteins. (A and B) Various concentrations (0, 0.015, 0.03125, 0.0625, 0.125, 0.25, 0.5, 1μM) of biotinylated LigCon (negative control), LigBCen2R (positive control), and (A) LigAVar7'-8, LigAVar9, LigAVar10, LigAVar11, LigAVar12, LigAVar13, (B) LigBCen7'-8, LigBCen9, LigBCen10, LigBCen11 were added to wells coated with 1μM of Fg or BSA (negative control and data not shown) in Tris buffer. The binding of biotinylated proteins to Fg was measured by ELISA. For all experiments, each value represents the mean± SEM of three trials in triplicate samples. Statistically significant ($p < 0.05$) differences compared to negative control are indicated by an asterisk. (C and D) Soluble Fg inhibited Fg-binding Ig-like domains of Lig proteins to immobilized Fg. One μM of biotinylated LigBCen2R (positive control), LigBCon (negative control), (A) LigA10, LigA12, LigA13, (B) LigB7'-8, LigB9, LigB10 was incubated with various concentrations (0.031, 0.0625, 0.125, 0.25, 0.5, 1, 2μM in Tris buffer) of Fg or GST (negative control and data not shown) at RT for 1 hour prior to be added to 1μM of Fg or BSA coated wells (negative control and data not shown) The percentage of binding was determined relative to the binding of biotinylated proteins in the LigBCon wells. The binding of biotinylated proteins to Fg was measured by ELISA. For all experiments, each value represents the mean± SEM of three trials in triplicate samples. Statistically significant ($p < 0.05$) differences compared to negative control are indicated by an asterisk.

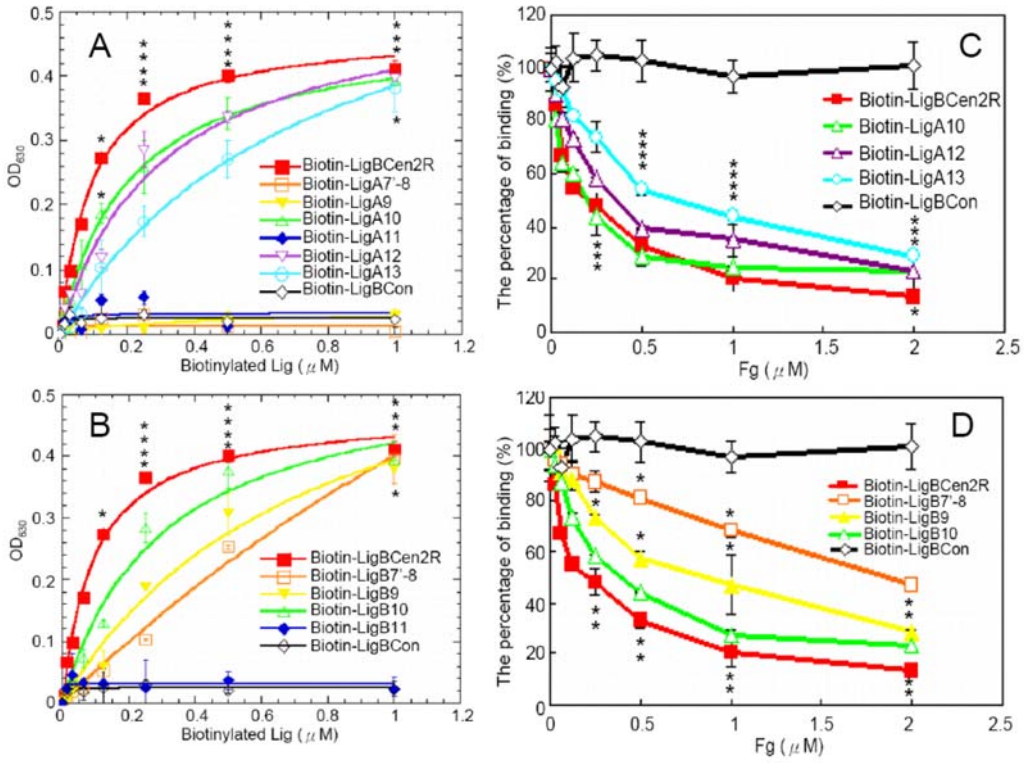
A
B
C
D
OD630
Biotinylated Lig (μM)
The percentage of binding (%)
Fg (μM)
Biotin-LigBCen2R
Biotin-LigA7'-8
Biotin-LigA9
Biotin-LigA10
Biotin-LigA11
Biotin-LigA12
Biotin-LigA13
Biotin-LigBCon
Biotin-LigB7'-8
Biotin-LigB9
Biotin-LigB10
Biotin-LigB11

were examined for their Fg binding activities by ELISA, which shows that the Fg binding site on LigBCen2 is located on LigBCen2R (K_D = 0.11±0.012 μM) (Figure. 9.2A). The binding of LigBCen2R and fibrin was also analyzed and as shown in Figure. 9.2B, LigBCen2 and LigBCen2R can also interact with fibrin. This indicates that the Fg binding site is preserved when fibrinogen is converted to fibrin. In addition, the interaction of LigBCen2R with Fg or fibrin is specific since pretreatment of Fg or fibrin with LigBCen2R abrogates binding (Figure. 9.2C and D).

Since Fg binds to LigBCen2R, the Ig-like domain containing fragment of LigBCen2, it is rational to speculate that Fg may also bind to other Ig-like domains. To test this hypothesis, each Ig-like domain of LigA and LigB was purified and their ability to bind to Fg was assayed by ELISA. LigA10, LigA12, LigA13, LigB7'-8, LigB9, and LigB10 can bind Fg with different binding affinities (LigA10, K_D = 0.207±0.009 μM; LigA12, K_D = 0.303±0.044 μM; LigA13, K_D = 0.755±0.012 μM; LigB7'-8, K_D = 3.17±0.015 μM; LigB9, K_D = 0.758±0.026 μM; LigB10, K_D = 0.295±0.078 μM; Figure. 9.3A and B). Moreover, the treatment of Fg with LigA10, LigA12, LigA13, LigB7'-8, LigB9, or LigB10 reduced their binding to Fg in a dose dependent manner, thus confirming that Fg binds to certain Ig-like domains of LigA and LigB (Figure. 9.3C and D).

The Fg binding site for Lig proteins is located on the C-terminal tail of Fg αC domain (FgαCC)

To elucidate the Fg binding site for Lig proteins, the binding of various truncated forms of Fg, including α (Fgα), β (Fgβ), and γ (Fgγ) chains, with LigBCen2R were examined by ELISA (Figure. 9.1C). The results showed that only Fgα could bind to LigBCen2R (K_D = 0.165±0.033 μM; Figure. 9.4A). To map the LigBCen2R binding region, Fgα was further truncated into C (FgαC), D (FgαD), and E (FgαE) domains

Figure 9.4 Characterization the LigBCen2R binding site on Fg exhibited by ELISA, ITC, and steady state fluorescence spectroscopy. (A-D) Various concentrations (0.0156, 0.03125, 0.0625, 0.125, 0.25, 0.5, 1μM) of GST-LigCon (negative control and data not shown) or GST-LigBCen2R was added to wells coated with 1μM of BSA (negative control), (A) Fg (positive control), Fgα, Fgβ, Fgγ, (B) Fgα (positive control), FgαC, FgαD, FgαE, (C) FgαC (positive control), FgαCC, FgαCN in Tris buffer. (D) FgαCC inhibited LigBCen2R binding to immobilized Fg. One μM of GST-LigBCon (negative control and data not shown), or GST-LigBCen2R was incubated with various concentrations (0.031, 0.0625, 0.125, 0.25, 0.5, 1, 2μM in Tris buffer) of GST (negative control), Fg (positive control) or FgαCC at RT for 1 hour prior to be added to wells coated with 1μM of Fg or BSA (negative control and data not shown). The percentage of binding was determined relative to the binding of GST fused proteins in the GST treated wells. The binding of GST fused proteins to Fg was measured by ELISA. For all experiments, each value represents the mean± SEM of three trials in triplicate samples. Statistically significant ($p < 0.05$) differences compared to negative control are indicated by an asterisk. (E) Determination of the binding affinity by ITC. The cell contained 1 ml of 2.5μM of LigBCen2R and the syringe contained 250 μl of 40μM of FgαCC (upper panel) Heat differences obtained from 25 injections of FgαCC; (lower panel) Integrated curve with experimental data (◇) and the best fit (—). The thermodynamic parameters are shown by the average of duplicate experiments (Kd = 0.382 ± 0.045μM, ΔH = -5.57 ± 0.57 kcal mol^{-1}, $T\Delta S$ = 3.14 ± 0.5 kcal mol^{-1} K^{-1}), and the molar ratio of FgαCC to LigBCen2R is 1.02. (F) and (G) Intrinsic fluorescence spectrum of LigBCen2R in the presence and absence of FgαCC. One μM of LigBCen2R in Tris buffer was excited at 295 nm. Aliquots of FgαCC from respective stock solutions were added. The figure shows Trp fluorescence in different concentration of FgαCC.

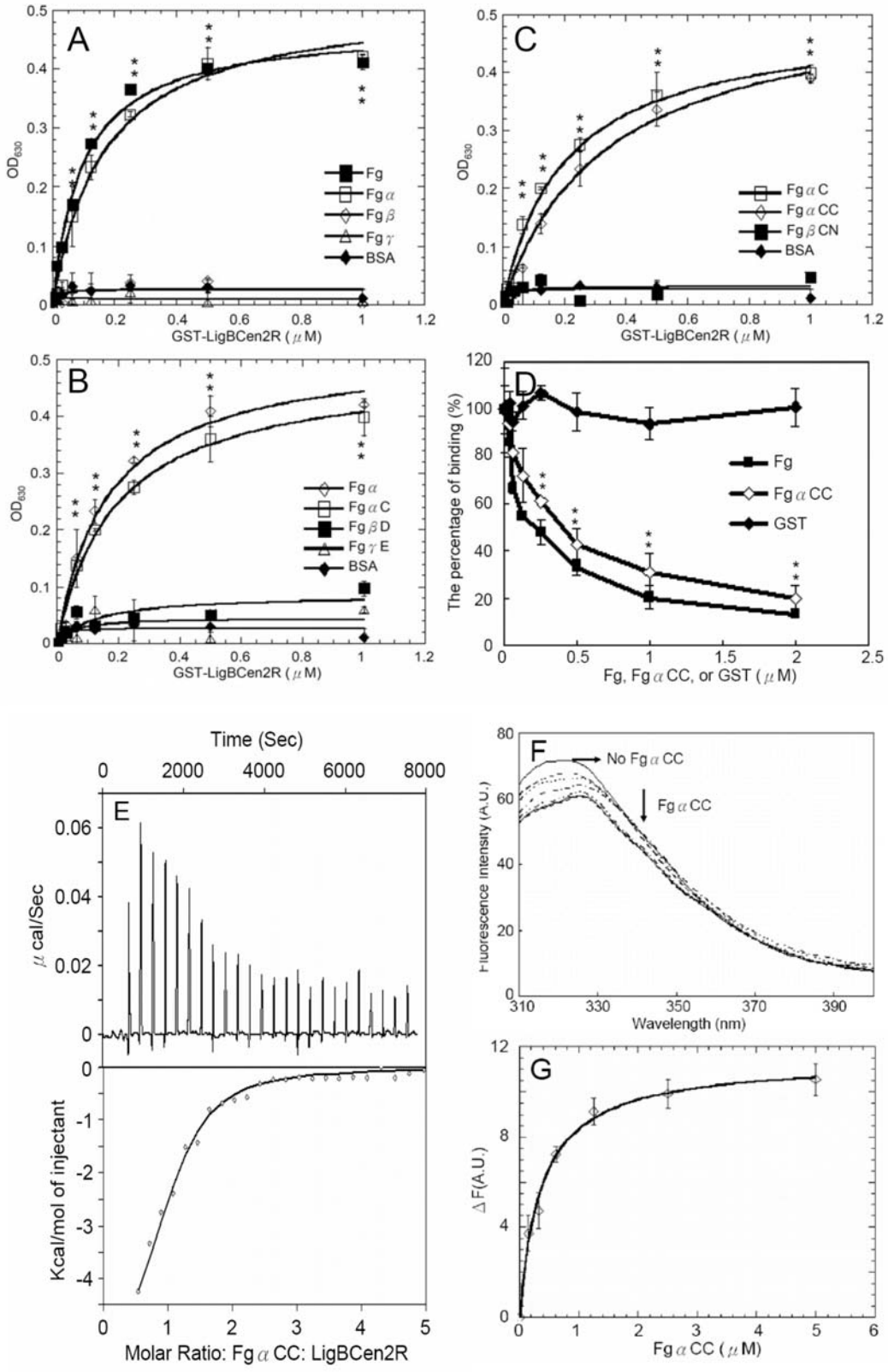
A
OD630
GST-LigBCen2R (μM)
Fg
Fgα
Fgβ
Fgγ
BSA
B
Fgα
FgαC
FgβD
FgγE
BSA
C
FgαC
FgαCC
FgβCN
BSA
D
The percentage of binding (%)
Fg, FgαCC, or GST (μM)
Fg
FgαCC
GST
E
Time (Sec)
μcal/Sec
Kcal/mol of injectant
Molar Ratio: FgαCC: LigBCen2R
F
No FgαCC
FgαCC
Fluorescence intensity (A.U.)
Wavelength (nm)
G
ΔF(A.U.)
FgαCC (μM)

(Figure. 9.1C) and it was found that LigBCen2R binds only FgαC (K_D = 0.20±0.043 μM; Figure. 9.4B). FgαC was truncated into 2 fragments, including an N-terminal disordered connecting region (FgαCN) and a C-terminal folded region with a hydrophobic collapsed region formed by two pairs of anti-parallel β-sheets (FgαCC) (Figure. 9.1C) (44-46). The results showed that LigBCen2 could bind only to FgαCC (K_D = 0.355±0.043 μM; Figure. 9.4C). Also, the treatment of LigBCen2R with FgαCC reduced its binding to Fg, indicating that the Fg binding site for LigBCen2R is on the FgαCC domain (Figure. 9.4D).

To gain more insight into the binding nature between LigBCen2R and FgαCC, ITC was performed to measure the binding affinity. As presented in Figure. 9.4E, the LigBCen2R- FgαCC interaction is driven by both enthalpy and entropy because of the negative values obtained, and the dissociation constant is in agreement with that obtained from ELISA (ITC, K_D = 0.382±0.045 μM; ELISA, K_D = 0.355±0.043 μM). On the other hand, the intrinsic fluorescence of LigBCen2R was also measured by the titration of FgαCC due to its absence of tryptophan. As shown in Figure. 9.4F and G, the K_D of LigBCen2R- FgαCC interaction was obtained from the quenched tryptophan fluorescence of LigBCen2R upon the increased binding of FgαCC (K_D = 0.364±0.037 μM). A red shift of the wavelength in the maximum fluorescence intensity from 321 nm to 325 nm observed in FgαCC- -LigBCen2R inferred a conformational change led by FgαCC binding. This conformational change offers a solvent-exposed environment close to the tryptophan on LigBCen2R (Figure. 9.4F).

LigBCen2R- FgαCC interaction prevents the binding of Fg to integrin on platelets due to a conformation change

It is known that Fg can bind to activated integrin $\alpha_{IIb}\beta3$ on the surface of platelets by its RGD motif located on FgαD and FgαCC to activate the functions of platelets (3).

Figure 9.5 LigBCen2R prevents the binding of FgαCC to integrin on platelets by altering the conformation close to RGD motif on FgαCC. The conformational change close to RGD motif of FgαCC induced by the binding of LigBCen2R observed in intrinsic fluorescence spectra. (A) A blue shift and quenching of the maximum wavelength of the spectra (339 to 330nm) of FgαCCY570W in the addition of LigBCen2RW1073C. One μM of FgαCCY570W in Tris buffer was excited at 295 nm. Aliquots of LigBCen2W1073C from respective stock solutions were added. The figure shows Trp fluorescence in the presence of 0.15, 0.3125, 0.625, 1.25, 2.5, 5μM of FgαCF. (B) The determination of K_D of LigBCen2RW1073C and FgαCCY570W by monitoring the quenching fluorescence intensities of FgαCCY570W titrated by LigBCen2RW1073C or GST (data not shown) shown in (A). The emission wavelength recorded in this figure was 330nm. K_D was determined by fitting the data point into the equation described in materials and methods (K_D= 0.349±0.011μM). (C and D) LigBCen2R binding to FgαCC inhibits its interacting with integrin or platelets measured by ELISA. One μM of GST-FgαCC was mixed with various concentrations (0.015, 0.031, 0.0625, 0.125, 0.25, 0.5, 1μM in Tris buffer) of LigBCon (negative control), integrin (positive control) or LigBCen2R at RT for 1 hour prior to be added to wells (C) coated with 1μM of integrin or BSA (negative control and data not shown) or (D) containing 10^5 human platelets (negative control and data not shown). (E) LigBCen2R binding to FgαCC blocks its adhesion to platelets detected by immunoflourescence microscopy. 1μM of GST-FgαCC was treated with 50μM of LigBCen2R or LigBCon (negative control) prior to be incubated with 10^6 human platelets. The expression of integrin and the binding of FgαCC was examined by CLSM. In (C) and (D), the percentage of binding was determined relative to the binding of GST fused proteins in the LigBCon treated wells. The binding of GST fused proteins to integrin or platelets were measured by ELISA. For all experiments, each value represents the mean± SEM of three trials in triplicate samples.

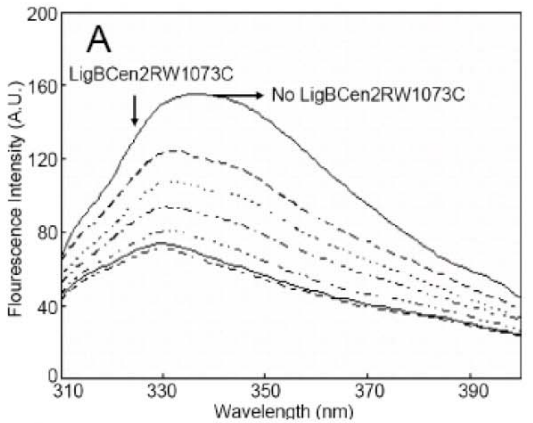
A
LigBCen2RW1073C
No LigBCen2RW1073C
Flourescence Intensity (A.U.)
Wavelength (nm)

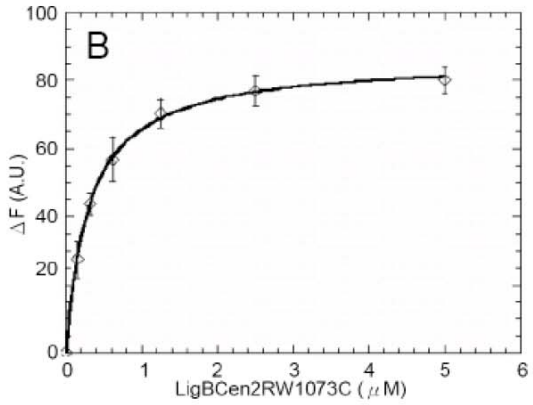
B
ΔF (A.U.)
LigBCen2RW1073C (μM)

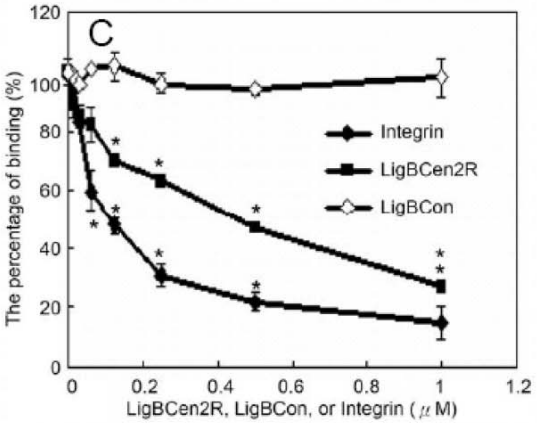
C
The percentage of binding (%)
Integrin
LigBCen2R
LigBCon
LigBCen2R, LigBCon, or Integrin (μM)

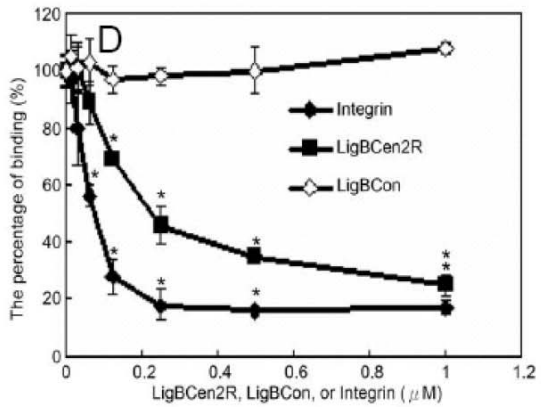
D
The percentage of binding (%)
Integrin
LigBCen2R
LigBCon
LigBCen2R, LigBCon, or Integrin (μM)

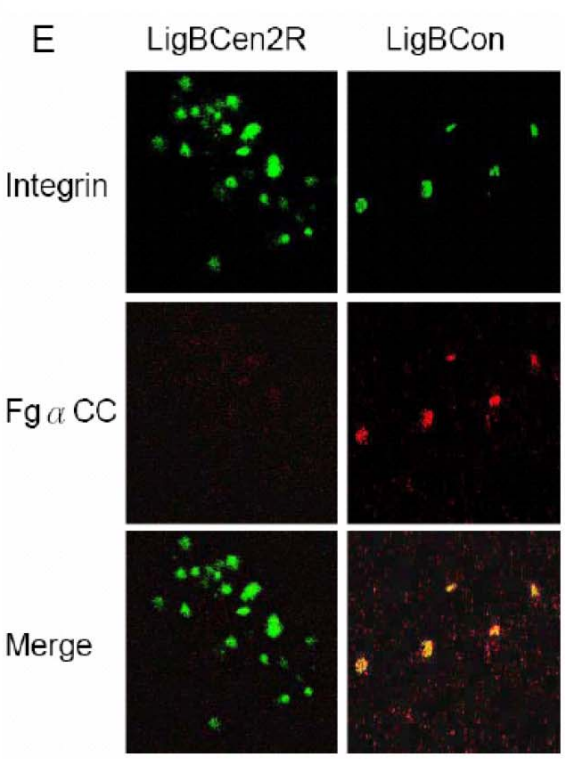
E
LigBCen2R
LigBCon
Integrin
Fg α CC
Merge

Due to the presence of an RGD motif in FgαCC (RGDS within α572-574), the possibility ofinhibiting binding to integrin by LigBCen2R- FgαCC interaction was tested. To test whether blocking the FgαCC RGD binding site inhibited binding to integrin, FgαCCY570W, a FgαCC mutant with tryptophan close to the RGD motif, and LigBCen2RW1073C, a LigBCen2R mutant without tryptophan, were constructed. The undistinguishable secondary structures of the LigBCen2RW1073 and FgαCCY570W mutants were measured by CD spectroscopy and compared to wild type LigBCen2 and FgαCC to eliminate the possibility that the mutations changed their structure (data not shown). As indicated in Figure. 9.5A and B, the intrinsic fluorescence spectrum of FgαCCY570W was quenched after the addition of LigBCen2RW1073C in a dose dependent manner with a K_D (K_D = 0.349±0.011 μM) consistent with the value reported above, which suggested that the mutations did not affect the nature of the binding (ITC, K_D = 0.382±0.045 μM; ELISA, K_D = 0.355±0.043 μM; Fluorescence spectrometry of LigBCen2R and FgαCC, K_D = 0.364±0.037 μM). Furthermore, the wavelength of the maximum fluorescence intensity in the spectrum of FgαCCY179W recorded in the absence of LigBCen2RW1073C was located at 339 nm indicating that the environment close to this sole tryptophan (RGD motif) is polar and exposed, which is in agreement with previous studies (Figure. 9.5A) (36). However, a significant blue shift of the wavelength in the maximum fluorescence intensity from 339nm to 330nm was found in the spectrum of FgαCCY179W upon the addition of 5μM LigBCen2RW1073C, which indicates that the environment close to the tryptophan (RGD motif) on FgαCCY179W was buried and became hydrophobic upon the binding of LigBCen2RW1073C (Figure. 9.5A).

To determine whether the buried RGD motif of FgαCC after saturation with LigBCen2R blocks the interaction of FgαCC and integrin, the binding of FgαCC treated with a serial dilution of LigBCen2R was measured by ELISA. As revealed in

Figure 9.6 Platelet aggregation inhibited by LigBCen2R- FgαCC interaction. Platelets (10^6) in (A to D) PRP or in (E to G) IgG depleted and complement inactivated serum was treated with 100μM of (A and E) LigBCen2R, (B and F) $ClfAN_2N_3$, or (C and G) LigBCon, or (D and H) various concentration (1.56 μM, 3.125 μM, 6.25 μM, 12.5 μM, 25 μM, 50 μM, 100 μM) of LigBCon, LigBCen2R, or $ClfAN_2N_3$. Aggregation was observed by light microscopy. For all experiments, each value represents the mean± SEM of three trials in triplicate samples. The light microscopic settings were identical for all the captured images. In (D) and (H), the area covered by the aggregates in one field normalized to the total surface measured, and the percentage of reduced aggregation surface coverage corresponds to the area covered by the aggregates of untreated platelets. Statistically significant ($p < 0.05$) differences compared to negative control are indicated by an asterisk.

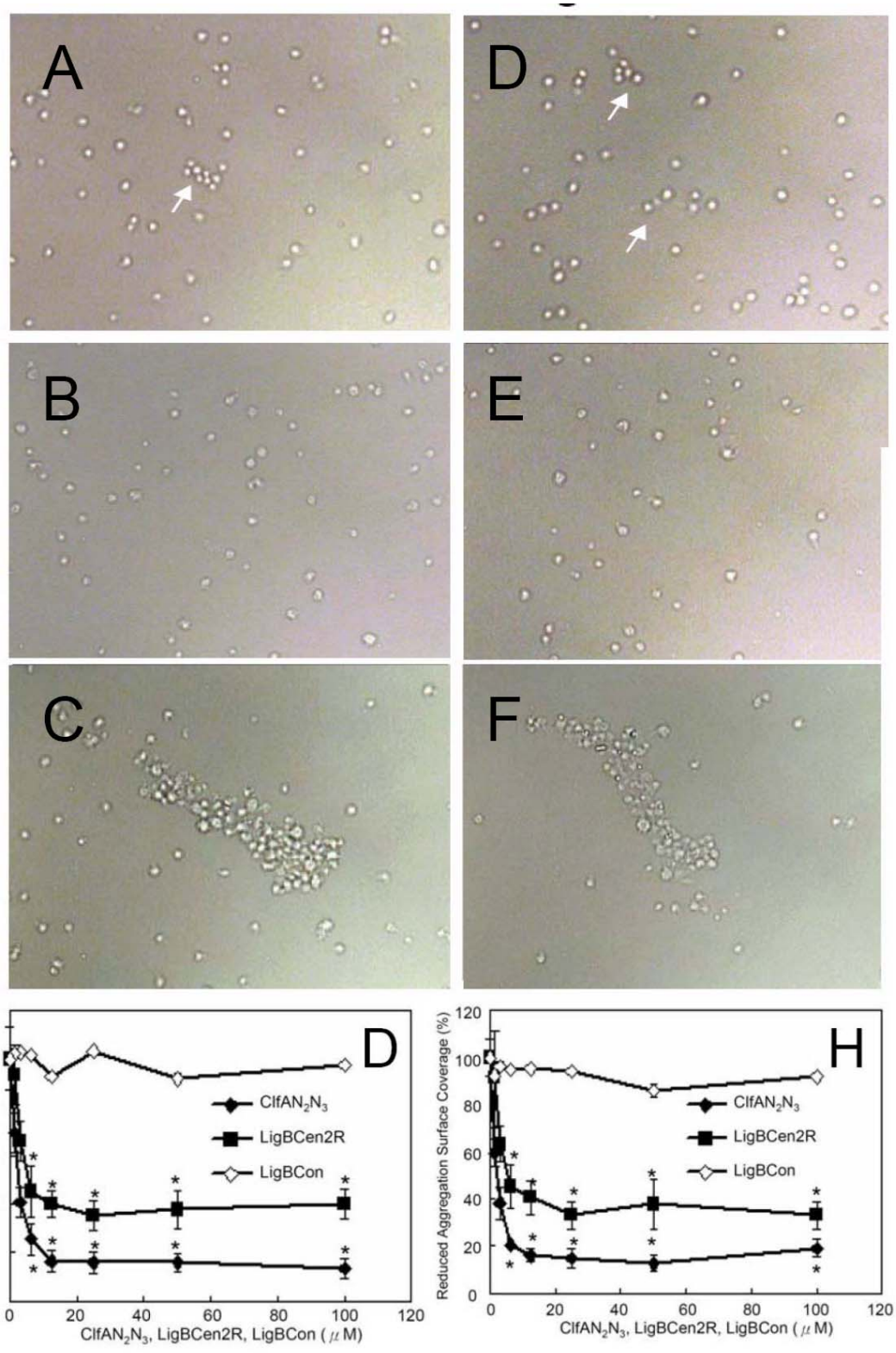
A
D
B
E
C
F
D
ClfAN2N3
LigBCen2R
LigBCon
0
20
40
60
80
100
120
ClfAN2N3, LigBCen2R, LigBCon (μM)
H
Reduced Aggregation Surface Coverage (%)
0
20
40
60
80
100
120
ClfAN2N3, LigBCen2R, LigBCon (μM)

Figure 9.7 Effect of LigBCen2R on thrombin-induced fibrin clot. (A) Dose dependent reduced fibrin clot formation by premixing with LigBCen2R. 90μL of fibrinogen (0.9 mg/mL) was mixed with various concentrations (0.23, 0.46, 0.93, 1.875, 3.75, 7.5, 15, 30μM in Tris buffer with 2mM of $CaCl_2$) of $ClfAN_2N_3$ (positive control), LigBCon (negative control), or LigBCen2R at RT for 5min. Then, the mixture was incubated with 10μL of thrombin (1unit/mL) for 1 hour. The fibrin clot was measured by the optical density of the reaction at 600nm. (B) Time course of fibrin formation affected by LigBCen2R. 90μL of fibrinogen (0.9 mg/mL) was mixed with 30μM of $ClfAN_2N_3$ (positive control), LigBCon (negative control), or LigBCen2R in Tris buffer with 2mM of $CaCl_2$ at RT for 5min. Then, the mixture was incubated with 10μL of thrombin (1unit/mL). The optical density of the reaction at 600nm was recorded at 1 min intervals over 30 min. All above experiments was performed thrice, and each value represents the mean± SEM of three trials in triplicate samples. Statistically significant ($p < 0.05$) differences compared to negative control are indicated by an asterisk.

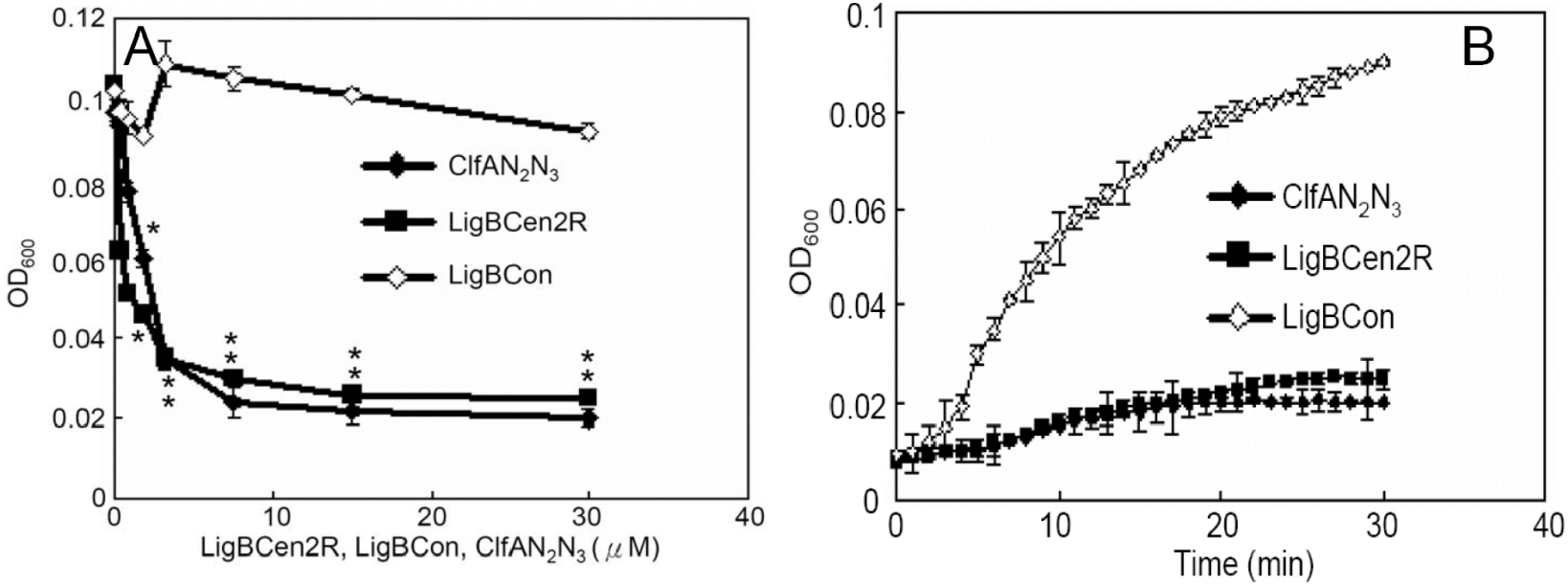
A
B
OD_{600}
$ClfAN_2N_3$
LigBCen2R
LigBCon
LigBCen2R, LigBCon, $ClfAN_2N_3$ (μM)
Time (min)
0.12
0.1
0.08
0.06
0.04
0.02
0
10
20
30
40

Figure. 9.5C, the binding of LigBCen2R to FgαCC prevented the interaction of FgαCC with integrin. Furthermore, LigBCen2R interfered with the binding of FgαCC to platelets as shown by both ELISA and immunofluorescence microscopy (Figure. 9.5D and E).

LigBCen2R- FgαCC interaction blocks platelet aggregation

To gain more insight into the influence of LigBCen2R- FgαCC binding on platelet aggregation, PRP was treated with LigBCon, LigBCen2R, or $ClfAN_2N_3$. Platelet aggregation was significantly decreased in a dose-dependent manner in PRP treated with LigBCen2R but not LigBCon, which indicates LigBCen2R inhibits platelet aggregation (Figure. 9.6A-D). Furthermore, platelet aggregation in IgG depleted and complement inactivated serum was also evaluated in order to elucidate the role of Lig protein binding to Fg in platelet aggregation. As shown in Figure. 9.6 E-H, the addition of LigBCen2R could block the aggregation ADP induced platelet aggregation in IgG depleted and complement inactivated serum and is dose dependent. Therefore, LigBCen2R- FgαCC interaction inhibits platelet aggregation.

LigBCen2R- FgαCC interaction inhibits clot formation

To determine if LigBCen2R could interfere with Fg function, a thrombin-induced clot formation experiment was performed (Figure. 9.7). Pretreatment of LigBCen2R with fibrinogen before the addition of thrombin reduced the turbidity of the fibrin forming reaction in a dose dependent manner (Figure. 9.7 A). Furthermore, fibrin clot formation upon the addition of LigBCen2R was time dependent. As shown in Figure. 9.7B, clot formation in response to the addition of LigBCon was slow initially but was followed by a rapid increase in the reaction. Similarly, pretreatment of LigBCen2R or

Figure 9.8 Competition experiments on the binding of LigBCen2 and PLG or tPA to the immunoblized FgαCC performed by ELISA. (A) PLG or tPA cannot compete with LigBCen2R for the binding of FgαCC. The microtiter plate wells coated with 1μM of FgαCC or BSA (negative control and data not shown) were treated by various concentrations (0.031, 0.0625, 0.125, 0.25, 0.5, 1, 2μM in Tris buffer) of PLG, tPA, LigBCen2R (positive control) Fg or LigBCon (negative control) at RT for 1 hour prior to be incubated with 1 μM of GST fused LigBCen2R, LigBCon (negative control and data not shown). The percentage of binding was determined relative to the binding of GST fused proteins in the LigCon treated wells. (B) The pre-mixture of PLG or tPA to LigBCen2R doesn't change its binding affinity to FgαCC. Increased concentrations (0, 0.015, 0.03125, 0.0625, 0.125, 0.25, 0.5, 1μM) of GST-LigCon (negative control and data not shown), GST-LigBCen2R was treated with 200nM of PLG, tPA, LigBCen2R (positive control), or LigBCon (negative control) before added to wells coated with 1μM of FgαCC or BSA (negative control and data not shown) in Tris buffer. The binding of GST fused proteins to FgαCC was measured by ELISA. For all experiments, each value represents the mean± SEM of three trials in triplicate samples. Statistically significant ($p < 0.05$) differences compared to negative control are indicated by an asterisk

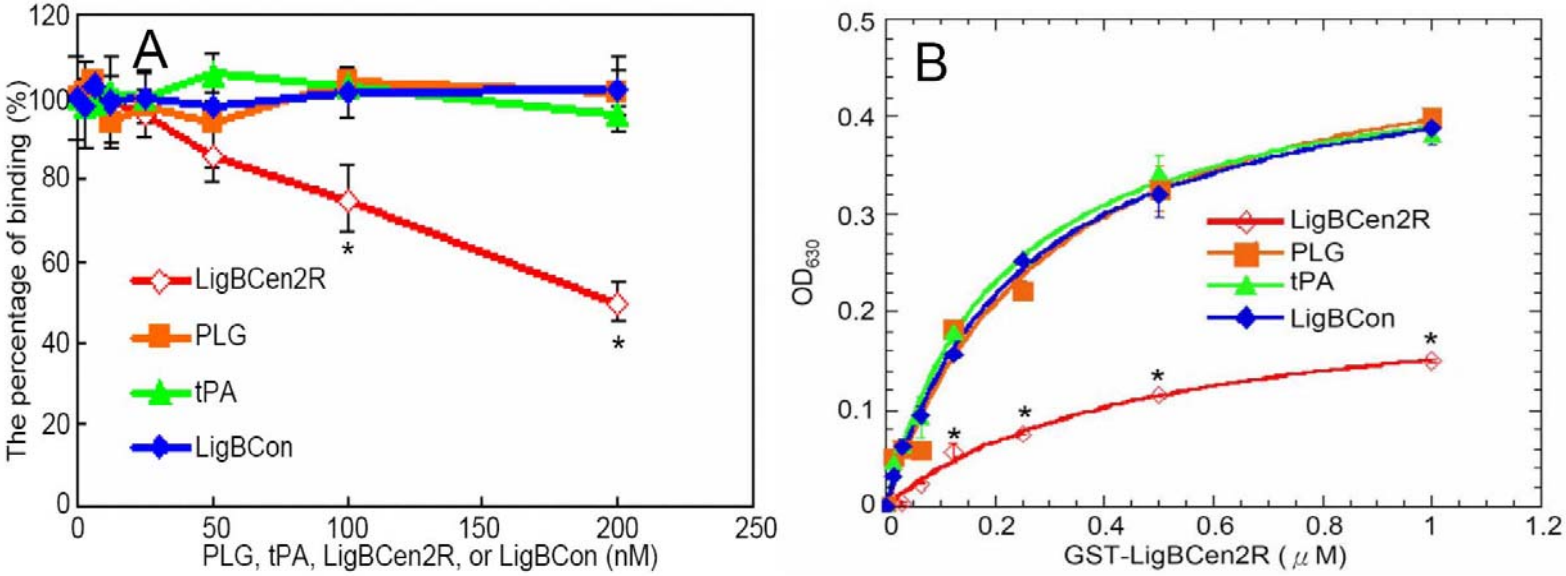
A
The percentage of binding (%)
PLG, tPA, LigBCen2R, or LigBCon (nM)
LigBCen2R
PLG
tPA
LigBCon
B
OD630
GST-LigBCen2R (μ M)
LigBCen2R
PLG
tPA
LigBCon

ClfAN_2N_3 also resulted in slow initial clot formation similar to the results seen with LigBCon pretreatment (negative control). However, after the initial stage, there was no further increase in turbidity indicating that LigBCen2R pretreatment of Fg had an inhibitory effect on fibrin clot formation (Figure. 9.7B).

LigBCen2R cannot compete with PLG or tPA for FgαCC binding

To determine if LigBCen2R competes with PLG or tPA for binding to FgαCC, competition ELISA of LigBCen2R binding to PLG or tPA saturated FgαCC was performed. The binding of LigBCen2R to FgαCC was not affected by the pre-treatment with PLG or tPA (Figure. 9.8). Moreover, the K_D values of LigBCen2R interaction with FgαCC in the presence or absence of tPA or PLG were statistically insignificant, which confirmed that the binding sites of tPA, PLG, and LigBCen2R on FgαCC are distinct (PLG treated GST-LigBCen2R, K_D = 0.358±0.062 μM; tPA treated GST-LigBCen2R, K_D = 0.347±0.019 μM; LigBCon treated GST-LigBCen2R as negative control, K_D = 0.341±0.012 μM) (Figure. 9.8B).

Discussion

In a previous study, a high affinity fibronectin binding site on LigB was localized to amino acids 1014-1165 within LigBCen2. This LigBCen2 site also binds to fibrinogen, collagen, and laminin (13). LigBCen2 consists of two regions, LigBCen2R, which contains part of the 11th and the entire 12th Ig-like domains, and a disordered region, designated LigBCen2NR, which contains 47 non-repeated amino acids (20). In this study, the Fg binding site was fine-mapped to LigBCen2R, and this binding expanded to other Ig-like domains of LigA and LigB. Furthermore, the LigBCen2R binding site on Fg was mapped to the C-terminal αC domain of Fg (FgαCC). Recently, several bacterial Fg binding proteins were described, and the binding sites are

distributed on various regions of Fg including FgαD (31), FgαCN (37), Fgβ (38), and Fgγ (34,39). This is the first Fg binding protein isolated from a spirochete proven to interact with FgαCC. Interestingly, the major tertiary structures of Lig proteins, the Ig-like domains, are similar to those of ClfA, FnBPA and SdrG, the Fg binding proteins of *S. aureus* (40,41). A general model called "dock, lock, and latch" can describe the interaction of ClfA, FnBPA, and SdrG with Fg, although their binding sites are distinct (Fgγ for ClfA and FnBPA, and Fgβ for SdrG) (41-43). However, it is unclear whether the interaction of Lig-Fg is similar to this model due to the absence of sequence similarities between Lig proteins and ClfA, FnBPA and SdrG. Further structural studies are needed to demonstrate the binding model of LigBCen2R and FgαCC.

Fibrinogen serves a key role in blood coagulation and thrombosis (23-25). Fg binding to platelets is responsible for platelet aggregation, which is essential for primary hemostasis (25), and integrin $\alpha_{IIb}\beta 3$ is the most important platelet surface protein that mediates the interaction of Fg with platelets (23-25). Fg contains three potential integrin binding sites including two RGD motifs on Fgα (RGDS Fgα572-575 and RGDF Fgα95-98) and a non-RGD sequence on Fg γ (HHLGGAKQAGDV Fgγ400-411) (23-25). The synthetic peptides RGDS Fgα572-575 and RGDF Fgα95-98 block Fg binding to platelets indicating that the two RGD motifs in Fgα are pivotal for the interaction of human Fg with human platelets (44). Previously, it was proposed that an extracellular Fg-binding protein, Efb, from *S. aureus* either blocks the RGD sequence on FgαD (amino acids 95-97 in Fgα) or causes a nearby conformational change when it binds to FgαD (31,45). In this study, LigBCen2R was found to interact with FgαCC, which also contains one of the RGD motifs, RGDS in Fgα572-575. Surprisingly, the binding studies using mutant fragments found that LigBCen2RW1073C induces a transition in the environment close to the sole mutated tryptophan, W570, of FgαCCY570W near the RGD motif from an exposed position to one that is buried.

These results suggest that LigBCen2R either binds directly to the RGD motif or to amino acids at other locations and then induces a conformational change. However, the lack of binding activity of LigBCen2R and the peptide containing the RGD motif of FgαCC and LigCen2 with the cell binding domain (CBD) of Fn, which contains a RGD motif, suggests that LigBCen2R does not bind to the RGD domain, but binds to other regions of FgαCC and induces a conformational change close to the RGD motif (13 and data not shown)

Fg-integrin binding on platelets promotes platelet aggregation and induces primary hemostasis (23-25). To date, several bacterial Fg binding proteins are known and they may play a role in the pathogenesis of bacterial infection. ClfA, ClfB, FnBPA, and SdrG are able to bind to platelets and induce platelet aggregation and activation mediated by interacting with Fg (46-49). In contrast, Efb binding to Fg inhibits platelet aggregation and activation by interfering with Fg-integrin interaction (34,50), although Efb can still attach to platelets via Fg or unknown components (50). In this study, LigBCen2R reduced the binding of FgαCC to integrin, which led to decreased binding of Fg to platelets. This phenomenon can be attributed to the inability of the integrin to bind to the buried RGD motif on FgαCC that result from a LigBCen2R binding induced conformational change. Platelet adhesion is required for platelet aggregation or activation (25) so it is not surprising that LigBCen2R inhibited platelet aggregation by interacting with FgαCC. However, platelet aggregation was not completely blocked by treatment with LigBCen2R since other two platelet binding sites of Fg, Fgγ and FgαD, are still active (Figure. 9.6). Platelet aggregation was found in some cases of human leptospirosis associated with pulmonary hemorrhage and the authors speculated that leptospiral induced capillary damage led to platelet activation (51). Conversely, in another study the authors concluded that platelet aggregation was not important in the pathogenesis of leptospirosis because of the lack of platelet aggregation in organs

usually infected by *Leptospira* spp., such as kidney or lung, or only limited platelet aggregation observed in liver (52). Our results suggest that Lig proteins may block the binding of Fg to platelets, thereby inhibiting platelet aggregation, which may account for the pulmonary hemorrhage noted in severe, often fatal cases of leptospirosis.

During thrombosis, soluble Fg is converted to insoluble fibrin, which contributes to clot formation (25). Initially, thrombin binds to and digests the E domain of Fg yielding fibrinopeptides A and B to form A and B knobs in the FgE domain and a and b holes in the C-terminals of Fgγ and Fgβ, respectively (25). Knob-hole interaction results in the formation of one dimensional fibrin (25). Subsequently, lateral aggregation due to the intermolecular interaction of FgαC domains from adjacent Fg molecules stabilizes the mechanical properties of the fibrin clot to form a two- and three-dimensional fibrin network (25). Several bacterial Fg binding proteins inhibit thrombosis by using different mechanisms. ClfA and FnBPA bind to the C-terminal domain of the Fgγ chain to block the b hole bound by the B knob (39,53), while SdrG, another Fg binding protein, binds to the N-terminal domain of the Fgβ chain, the thrombin targeting site, and prevents fibrin clot formation (38). As presented in Figure. 9.7, the initial stages of clot formation (0 to 3 minutes) upon the addition of LigBCen2R to Fg is similar to the results obtained with untreated Fg. Importantly, thrombin-induced fibrin clot formation was decreased at later time points, which suggests that Lig protein binding to FgαCC obstructs the sites needed for lateral aggregation of fibrin during the later stages of clot formation.

Fibrinolysis clears the temporary hemostatic plug (25). Plasmin, a protease which digests fibrin, is converted from inactive plasminogen (PLG) through the action of tPA (25). PLG usually binds to the end-to-end junction of two fibrin molecules including FgαD (amino acids 148-160 in Fg α chain), and the tPA binding site on fibrin was identified on Fgγ (amino acids 312-324 in Fg γ chain). Interestingly, both tPA and PLG

also bind to the C-terminal FgαC domain (FgαCC) within fibrin, and this binding is physiologically relevant due to the surface exposed structure of FgαCC in firbrin (25,54). Since PLG and tPA do not compete with each other for their Fg binding sites on FgαCF, a ternary complex model for PLG-tPA-FgαCC was proposed (54). LigBCen2R of Lig proteins is known to interact not only with fibrin, but also with FgαCC of Fg, and LigBCen2R- FgαCC interaction does not affect the binding of PLG or tPA to FgαCC. This "dynamic equilibrium" permits fibrin clot removal as there is no inhibitory effect on PLG or tPA binding to FgαCC (25). The significantly reduced clot formation caused by LigBCen2R- FgαCC interaction suggests that leptospiral Lig proteins push this "dynamic equilibrium" toward fibrinolysis. This may help explain the pulmonary hemorrhage that is observed in most recent *Leptospira* spp. fatal cases, since decreased fibrin clot formation may lead to the severe pulmonary hemorrhage that often occurs in fatal cases of leptospirosis (51,55-57).

Massive hemoptysis, either alone or in combination with acute respiratory death syndrome, has emerged as the leading mechanism of death among people infected with pathogenic leptospires. Similarly, pulmonary hemorrhage is a prominent feature in the hamster model of leptospirosis (58,59). We propose that Lig proteins bind to FgαCC, which prevents Fg from binding to $\alpha_{IIb}\beta3$ on platelets thereby inhibiting platelet aggregation. Furthermore, Lig proteins do not interfere with the binding of tPA and PLG to fibrin, which would preserve the fibrinolytic machinery. The net result of platelet aggregation inhibition and maintenance of fibrinolysis would be a bleeding diathesis.

In conclusion, we report a high affinity Fg binding site located on LigBCen2R and expanded to most of Ig-like domains of LigA and LigB. Furthermore the binding sites of the Ig-like domains within Lig proteins mapped to the C-terminal tail of FgαC (FgαCC). The binding of LigBCen2R leads to a conformational change close to RGD

motifs within FgαCC, blocking the interaction of integrin and LigBCen2R and preventing platelet aggregation. In addition, the LigBCen2R-FgαCC interaction can also reduce clot formation but not influence the binding of PLG and tPA to Fg. Taken together, Lig proteins may modulate thrombosis and fibrinolysis by binding to Fg. Further work to elucidate the Lig-Fg binding structure site with high resolution should offer further insights into this interaction.

REFERENCES

1. **Meites, E., Jay, M. T., Deresinski, S., Shieh, W. J., Zaki, S. R., Tompkins, L., and Smith, D. S.** 2004. Remerging leptospirosis, California. Emerg Infect Dis **10:** 406-412

2. **Palaniappan, R. U., Ramanujam, S., Chang, Y. F.** 2007. Leptospirosis: pathogenesis, immunity, and diagnosis. Curr. Opin. Infect. Dis. **20:** 284-292.

3. **Levett, P. N.** 2001. Leptospirosis. Clin. Microbiol. Rev. **14:**296-326.

4. **Hauk, P., Guzzo, C. R., Ramos, H. R., Ho, P. L., and Farah, C. S.** 2009. Structure and calcium-binding activity of LipL32, the major outer surface antigen of pathogenic *Leptospira* sp. J. Mol. Biol. **390:** 722-736.

5. **Vivian, J. P., Beddoe, T., McAlister, A. D., Wilce, M. C., Zaker-Tabrizi, L., Troy, S., Byres, E., Hoke, D. E., Cullen, P. A., Lo, M., Murray, G. L., Adler, B., and Rossjohn, J.** 2009. Crystal structure of LipL32, the most abundant surface protein of pathogenic Leptospira spp. J Mol Biol **387:** 1229-1238

6. **Atzingen, M.V.**, **Barbosa, A.S.**, **De Brito, T.**, **Vasconcellos, S.A.**, **de Morais, Z.M.**, **Lima, D.M.**, **Abreu, P.A.**, **Nascimento, A.L**. 2008. Lsa21, a novel leptospiral protein binding adhesive matrix molecules and present during human infection. BMC Microbiol. **8:** 70.

7. **Longhi, M. T., Oliveira, T. R., Romero, E. C., Goncales, A. P., Morais, Z. M., Vasconcellos, S. A., and Nascimento, A. L.** 2009. A newly identified protein of Leptospira interrogans mediates binding to laminin. J Med Microbiol **58:** 1275-1282.

8. **Carvalho, E., Barbosa, A. S., Gomez, R M., Cianciarullo, A. M., Hauk, P., Abreu, P. A., Fiorini, L. C., Oliveira, M. L., Romero, E. C., Goncales, A. P., Morais, Z. M., Vasconcellos, S. A., Ho, P. L.** 2009. Leptospiral TlyC is an extracellular-matrix binding protein and does not present hemolysin activity.

FEBS Lett. **583:** 1381-1385.

9. **Atzingen, M. V., Gomez, R. M., Schattner, M., Pretre, G.,Goncales, A. P., Morais, Z. M., Vasconcellos, S. A., Nascimento, A. L.** 2009. Lp95, a novel leptospiral protein that binds extracellular matrix components and activates e-selectin on endothelial cells. J. Infect. **In Press.**

10. **Barbosa, A. S., Abreu, P. A., Neves, F. O., Atzingen, M. V., Watanabe, M. M., Vieira, M. L., Morais, Z. M., Vasconcellos, S. A., and Nascimento, A. L.** 2006. A newly identified leptospiral adhesin mediates attachment to laminin. Infect. Immun. **74:** 6356-6364

11. **Stevenson, B., Choy, H. A., Pinne, M., Rotondi, M. L., Miller, M. C., Demoll, E., Kraiczy, P., Cooley, A. E., Creamer, T. P., Suchard, M. A., Brissette, C. A., Verma, A., and Haake, D. A.** 2007 *Leptospira interrogans* endostatin-like outer membrane proteins bind host fibronectin, laminin and regulators of complement. PLoS ONE **2:** e1188

12. **Choy, H. A., Kelley, M. M., Chen, T. L., Moller, A. K., Matsunaga, J., and Haake, D. A.** 2007. Physiological osmotic induction of *Leptospira interrogans* adhesion: LigA and LigB bind extracellular matrix proteins and fibrinogen. Infect. Immun. **75:** 2441-2450

13. **Lin, Y. P., and Chang, Y. F.** 2007. A domain of the *Leptospira* LigB contributes to high affinity binding of fibronectin. Biochem. Biophys. Res. Commun. **362:** 443-448

14. **Lin, Y. P., and Chang, Y. F.** 2008. The C-terminal variable domain of LigB from *Leptospira* mediates binding to fibronectin. J. Vet. Sci. **9:** 133-144.

15. **Lin, Y. P., Greenwood, A., Yan, W., Nicholson, L. K., Sharma, Y., McDonough, S. P., Chang, Y. F.** 2009. A novel type III module binding motif identified on C-terminus *Leptospira* Immunoglobulin-like protein LigB.

Biochem. Biophys. Res. Commun. **389:** 57-62

16. **Lin, Y. P., Lee, D. W., McDonough, S. P., Nicholson, L. K., Chang, Y. F.** 2009. The repeated domains of *Leptospira* immunoglobulin-like proteins interact with elastin and tropoelastin. J. Biol. Chem. **284:** 19380-19391.

17. **Matsunaga, J., Barocchi, M. A., Croda, J., Young, T. A., Sanchez, Y., Siqueira, I., Bolin, C. A., Reis, M. G., Riley, L. W., Haake, D. A., and Ko, A. I.** 2003. Pathogenic *Leptospira* species express surface-exposed proteins belonging to the bacterial immunoglobulin superfamily. Mol Microbiol **49**: 929-945.

18. **Palaniappan, R. U., Chang, Y. F., Hassan, F., McDonough, S. P., Pough, M., Barr, S. C., Simpson, K. W., Mohammed, H. O., Shin, S., McDonough, P., Zuerner, R. L., Qu, J., and Roe, B.** 2004. Expression of leptospiral immunoglobulin-like protein by *Leptospira interrogans* and evaluation of its diagnostic potential in a kinetic ELISA. J Med Microbiol **53**: 975-984

19. **Palaniappan, R. U., Chang, Y. F., Jusuf, S. S., Artiushin, S., Timoney, J. F., McDonough, S. P., Barr, S. C., Divers, T. J., Simpson, K. W., McDonough, P. L., and Mohammed, H. O.** 2002. Cloning and molecular characterization of an immunogenic LigA protein of *Leptospira interrogans*. Infect. Immun. **70**: 5924-5930

20. **Lin, Y. P., Greenwood, A., Nicholson, L. K., Sharma, Y., McDonough, S. P., Chang, Y. F.** 2009 Fibronectin binds to and induces conformational change in a disordered region of *Leptospira interrogans* immunoglobulin-like protein LigB. J. Biol. Chem. **284:** 23547-23557.

21. **Lin, Y. P., Raman, R., Sharma, Y., Chang, Y. F.** 2008. Calcium binds to Leptospiral immunoglobulin-like protein, LigB, and modulates fibronectin

binding. J. Biol. Chem. **283:** 25140-25149.

22. **Croda, J., Figueira, C. P., Wunder, E. A. Jr, Santos, C. S., Reis, M. G., Ko, A. I., Picardeau, M.** 2008. Targeted mutagenesis in pathogenic *Leptospir*a species: disruption of the LigB gene does not affect virulence in animal models of leptospirosis. Infect. Immun. **76:** 5826-5833.
23. **Doolittle, R. F.** 1984. Fibrinogen and fibrin. Ann. Rev. Biochem. **53:** 195-229.
24. **Herrick, S., Blanc-brude, O., Gray, A., Laurent, G..** 1999. Fibrinogen. Int. J. Biochem. Cell Biol. **31:** 741-746.
25. **Weisel, J. W.** 2005. Fibrinogen and fibrin. Adv. Prot. Chem. **70:** 247-299.
26. **Chavakis, T., Wiechmann, K., Preissner, K. T., and Herrmann, M.** 2005 Staphylococcus aureus interactions with the endothelium: the role of bacterial "secretable expanded repertoire adhesive molecules (SERAM)" in disturbing host defense system. Thromb. Haemost. **94:** 278-285
27. **Rivera, J., Vannakambadi, G., Hook, M., Speziale, P.** 2007. Fibrinogen-binding poteins of Gram-positive bacteria. Thromb Haemost **98:** 503-511
28. **McDevitt, D., Francois, P., Vaudaux, P., Foster, T. J.** 1995. Identification of the ligand binding domain of the surface located fibrinogen receptor (Clumping factor) of *Staphylococcus aureus*. Mol. Microbiol. **16:** 895-907.
29. **Palaniappan, R. U., McDonough, S. P., Divers, T. J., Chen, C. S., Pan, M. J., Matsumoto, M., and Chang, Y. F.** 2006. Immunoprotection of recombinant leptospiral immunoglobulin-like protein A against *Leptospira interrogans* serovar Pomona infection. Infect. Immun. **74**: 1745-1750
30. **Miajlovic, H., Loughman, A., Brennan, M., Cox, D., Foster, T. J.** 2007. Both complement- and fibrinogen-depedent mechanisms contribute to platelet aggregation mediated by *Staphylococcus aureus* clumping factor B. Infect. Immun.

75: 3335-3343.

31. **Palma, M., Shannon, O., Quezada, H. C., Berg, A., Flock, J. –I.** 2001. Extracellular fibrinogen-binding protein, Efb, from *Staphylococcus aureus* blocks platelet aggregation due to its binding to the α chain. J. Biol. Chem. **276:** 31691-31697.

32. **Loughman, A., Fitzgerald, J. R., Brennan, M. P., Higgins, J., Downer, R., Cox, D., and Foster, T. J.** 2005. Role of fibrinogen, immunoglobulin, and complement in platelet activation promoted by Staphylococcus aureus clumping factor A. Mol Microbiol **57:** 804-818

33. **Ford, I., Douglas, C. W., Heath, J., Rees, C., and Preston, F. E.** 1996. Evidence for the involvement of complement proteins in platelet aggregation by Streptococcus sanguis NCTC 7863 Br. J. Haematol. **94:** 729-739

34. **Liu, C. Z., Shih, M. H., Tsai, P. J.** 2005. ClfA221-550, a fibrinogen-binding segment of *Staphylococcus aureus* clumping factor A, disupts fibrinogen function. Thromb. Haemost. **94:** 286-294.

35. **Vanhoorelbeke, K., De Meyer, S. F., Pareyn, I., Melchior, C., Plancon, S., Margue, C., Pradier, O., Fondu, P., Kieffer, N., Springer, T. A., and Deckmyn, H.** 2009. The novel S527F mutation in the integrin beta3 chain induces a high affinity alphaIIbbeta3 receptor by hindering adoption of the bent conformation. J. Biol. Chem. **284:** 14914-14920

36. **Doolittle, R. F., Goldbaum, D. M., Doolittle, L. R.** 1978. Designation of the sequence involved in coiled-coil interdomainal connections in fibrinogen: Construction of an atomic scale model. J. Mol. Biol. **120:** 311-325.

37. **Walsh, E. J., Miajlovic, H., Gorkun, O. V., Foster, T. J.** 2008. Identification of the Staphylococcus aureus MSCRAMM clumping factor B (ClfB) binding site in the αC-domain of human fibrinogen. Microbiology **154:** 550-558.

38. **Davis, S. L., Gurusiddappa, S., McCrea, K. W., Perkins, S., Hook, M.** 2001. SdrG, a fibrinogen-binding bacterial adhesin of the microbial surface components recognizing adhesive matrix molecules subfamily from *Staphylococcus epidermidis*, tagets the thrombin cleavage site in the Bβ chain. J. Biol. Chem. **276:** 27799-27805.

39. **Wann, E. R., Gurusiddappa, S., Hook, M.** 2000. The fibronectin-binding MSCRAMM FnbpA of *Staphylococcus aureus* is a bifunctional protein that also binds to fibrinogen. J. Biol. Chem. **275:** 13863-13871.

40. **Deivanayagam, C. C., Wann, E. R., Chen, W., Carson, M., Rajashankar, K R., Hook, M., Narayana, S. V.** 2002. A novel variant of the immunoglobulin fold in surface adhesins of *Staphylococcus aureus*: crystal structure of the fibrinogen-binding MSCRAMM, clumping factor A. EMBO J. **21:** 6660-6672.

41. **Ponnuraj, K., Bowden, M. G., Davis, S., Gurusiddappa, S., Moore, D., Choe, D., Xu, Y., Hook, M., Narayana, S. V.** 2003 A "dock, lock, and latch" structure model for a Staphylococcal adhesin binding to fibrinogen. Cell **115:** 217-228.

42. **Bowden, M. G., Heuck, A. P., Ponnuraj, K., Kolosova, E., Choe, D., Gurusiddappa, S., Narayana, S. V., Johnson, A. E., Hook, M.** 2008. Evidence for the "dock, lock, and latch" logand binding mechanism of the Staphylococcal Microbial Surface Component Recognizing Adhesive Matrix Molecules (MSCRAMM) SdrG. J. Biol. Chem. **283:** 638-647.

43. **Gangadhar, N. L., Prabhudas, K., Bhushan, S., Sulthana, M., Barbuddhe, S. B., and Rehaman, H.** 2008. Revue scientifique et technique (International Office of Epizootics) **27:** 885-892

44. **Hawiger, J., Kloczewiak, M., Bednarek, M. A., Timmons, S.** 1989. Platelet receptor recognition domains on the α chain of human fibrinogen: structure-function analysis. **28:** 2909-2914

45. **Shannon, O., Flock, J-I.** 2004. Extracellular fibrinogen binding protein, Efb, from *Staphylococcus aureus* binds to platelets and inhibits platelet aggregation. Thromb. Haemost. **91:** 779-789.

46. **Brennan, M. P., Loughman, A., Dovocelle, M., Arasu, S., Chubb, A. J., Foster, T. J., Cox, D.** 2009. Elucidating the role of *Staphylococcus epidermidis* serine-aspartate repeat protein G in platelet activation. J. Thromb. Haemost. **7:** 1364-1372.

47. **Fitzgerald, J. R., Loughman, A., Keane, F., Brennan, M., Knobel, M., Higgins, J., Visai, L., Speziale, P., Cox, D., Foster, T. J.** 2006. Fibronectin-binding proteins of *Staphylococcus aureus* mediate activation of human platelets via fibrinogen and fibronectin bridges to integrin GPIIb/IIIa and IgG binding to the FcγRIIa receptor. Mol. Microbiol. **59:** 212-230.

48. **O'brien, L., Kerrigan, S. W., Kaw, G., Hogan, M., Penades, J., Litt, D.** 2002. Multiple mechanisms for the activation of human platelet aggregation by Staphylococcus aureus: roles for the clumping factors ClfA and ClfB, the serine-aspartate repeat protein SdrE and protein A. Mol. Microbiol. **44:** 1033-1044.

49. **Siboo, I. R., Cheung, A. L. Bayer, A. S., Sullam, P. M.** 2001. Clumping factor A mediates binding of *Staphyloccus aureus* to human platelets. Infect. Immun. **69:** 3120-3127.

50. **Shannon, O., Uekotter, A., and Flock, J. I.** 2005. Extracellular fibrinogen binding protein, Efb, from Staphylococcus aureus as an antiplatelet agent in vivo. Thrombosis and haemostasis **93:** 927-931

51. **Nicodemo, A. C., Duarte, M. I., Alves, V. A., Takakura, C. F., Santos, R. T., and Nicodemo, E. L.** 1997. Lung lesions in human leptospirosis: microscopic,

immunohistochemical, and ultrastructral features related to thrombocytopenia. Am. J. Trop. Med. Hyg. **56:** 181-187

52. **Yang, H. L., Jiang, X. C., Zhang, X. Y., Li, W. J., Hu, B. Y., Zhao, G. P., Guo, X. K.** 2006. Thrombocytopenia in the experimental leptospirosis of guinea pig is not related to disseminated intravascular coagulation. BMC Infect. Dis. **6:**19-27

53. **McDevitt, D., Nanavaty, T., House-Pompeo, K., Bell, E., Turner, N., Mcintire, L., Foster, T. J., Hook, M.** 1997. Characterization of the interaction between the *Staphylococcus aureus* clumping factor (ClfA) and fibrinogen. Eur. J. Biochem. **247:** 416-424.

54. **Tsurupa, G., Tsonev, L., Medved, L.** 2002. Structural organization of the fibrin(ogen) αC-domain. Biochemistry **41:** 6449-6459.

55. **Lepilleur, B., and Zohir, A. H.** 2000. Case of pulmonary hemorrhage due to Leptospira icterohaemorrhagiae a fatal outcome. Ann Biol Clin (Paris) **58:** 624-626

56. **Seijo, A., Coto, H., San Juan, J., Videla, J., Deodato, B., Cernigoi, B., Garcia Messina, O., Collia, O., de Bassadoni, D., Schtirbu, R., Olenchuk, A., de Mazzonelli, D. G., and Parma, A.** 2002. Respiratory distress due to pulmonary hemorrhage in leptospirosis. Medicina **62:** 135-140

57. **Trevejo, R. T., Rigau-Perez, J. G., Ashford, D. A., McClure, E. M., Jarquin-Gonzalez, C., Amador, J. J., de los Reyes, J. O., Gonzalez, A., Zaki, S. R., Shieh, W. J., McLean, R. G., Nasci, R. S., Weyant, R. S., Bolin, C. A., Bragg, S. L., Perkins, B. A., and Spiegel, R. A.** 1998. Epidemic leptospirosis associated with pulmonary hemorrhage-Nicaragua, 1995 *J.* Infect. Dis. **178:** 1457-1463

58. **Faisal, S. M., Yan, W., McDonough, S. P., Mohammed, H. O., Divers, T. J., and Chang, Y. F.** 2009. Immune response and prophylactic efficacy of

smegmosomes in a hamster model of leptospirosis. Vaccine **27:** 6129-6136.

59. **Faisal, S. M., Yan, W., McDonough, S. P., Pan, M. J., Chang, C. F., and Chang, Y. F.** 2009. Leptosome-entrapped leptospiral antigens conferred significant higher levels of protection than those entrapped with PC-liposomes in a hamster model. Vaccine **In Press.**

CHAPTER 10

CONCLUSIONS

Leptospirosis is a serious worldwide zoonosis and is reemerging in the United States. *Leptospira* spp. infect humans and animals by penetrating mucous membranes or injured skin. Adhesion to host tissues is a crucial step in the pathogenesis of bacterial infection. To date, a variety of bacterial adhesins, termed MSCRAMM or SERAM, have been identified to interact with host extracellular matrix (ECM). Prior to these studies, the molecular mechanisms that mediate leptospiral adhesion were unknown. Previously, our laboratory discovered a group of leptospiral outer surface proteins, for which we coined the name "*Leptopsira* immunoglobulin-like protein (Lig)", that includes LigA, LigB, and LigC. Due to similarities between Lig proteins and other bacterial adhesins, we speculated that these molecules might serve as ECM binding proteins. LigB was truncated into N-terminal, central and C-terminal regions and we demonstrated that the C-terminal LigB region, which includes LigBCen (amino acids 631-1417) and LigBCtv (amino acids 1418-1889) can bind to fibronectin (Fn). Further studies confirmed that the binding of Fn-LigBCen or Fn-LigBCtv promotes the adhesion of *Leptopsira* to MDCK cells. A high affinity Fn binding region was also localized to LigBCen2, which consists of amino acids 1014-1165. LigBCen2 binds strongly to the N-terminal domain (NTD) of Fn (K_D = 272nM), but binds only weakly to the gelatin binding domain (GBD) of Fn (K_D = 1200nM). Furthermore, we determined that the LigBCen2 binding sites for NTD and GBD of Fn do not overlap. In addition, LigBCen2 can interact with MDCK cells and binds to other ECMs including laminin, fibrinogen and collagens. Metal ions usually serve a pivotal role as cofactors for bacterial virulence factors, such as bacterial adhesins. In this study, LigBCen2 was found to bind calcium with a K_D of 7μM. Calcium plays an important role in

maintaining the stability of LigBCen2 and promoting the binding of LigBCen2 to Fn by altering its conformation. Since calcium concentrations are higher *in vivo*, calcium binding to LigB may aid *Leptopsira* infection as the organism adapts from the external environment to the internal environment of the host. Interestingly, LigBCen2 contains a well-folded region, LigBCen2R, which includes the 12^{th} and half of 11^{th} immunoglobulin-like domains (amino acids 1014-1119) and a disordered region, LigBCen2NR, composed of 46 amino acid residues in the C-terminal of LigBCen2 (amino acids 1120-1165). In this study, NTD of Fn was found to bind to LigBCen2NR while LigBCen2R binds to GBD only. Surprisingly, the binding of NTD of Fn to LigBCen2NR will dramatically change this disordered region to a β-strand-rich folded structure. NTD-LigBCen2NR binding may follow a β–zipper mechanism, the general rule of Fn binding protein binding to NTD. The disordered-ordered transition found in protein-protein interactions greatly increases their flexibility and receptor binding specificity.

In contrast to the order to disorder transition found in LigBCen2NR upon NTD binding, the binding of LigBCen2R to GBD changes its folded regions to a disordered form. In addition to LigBCen2R, other immunoglobulin-like domains from LigA and LigB are able to bind GBD. Thus, the order to disorder transition observed when LigBCen2R binds to GBD could likely be expanded to most of the immunoglobulin-like domains of LigAVar and LigBCen. Furthermore, most of the immunoglobulin-like domains bind to GBD through a multivalent binding mechanism, and multivalent binding enhances the binding affinities between Fn and LigA or LigB. Interestingly, the terminal immunoglobulin-like domains of LigAVar, LigAVar13, and LigBCen, LigBCen12, serve a greater role in Fn binding as compared to other immunoglobulin-like domains. The binding affinity of GBD or MDCK cells and LigA or LigB truncated protein containing the terminal domains is stronger than that without

the terminal domains. (LigAVar7'-12, K_D= 2.41μM; LigAVar7'-13, K_D= 0.055μM; LigBCen7'-11, K_D= 1.39μM; LigBCen7'-12, K_D= 0.056μM). This may be due to the compact structure contributed to by the inter-domain interactions in LigAVar7'-13 and LigBCen7'-12 instead of LigAVar7'-12 and LigBCen7'-11.

There are two Fn binding sites located on LigB, namely LigBCen and LigBCtv. In this study, a weak Fn binding site is also localized to $LigB_{1706-1716}$ containing LIPAD residues, and binds on 15 type III modules of Fn. $LigB_{1706-1716}$ is surface exposed and can also partially mediate leptopsiral adhesion to host cells. Cooperative binding led by conformational changes are a well recognized mechanism for protein-protein interaction. Although $LigB_{1706-1716}$ binds to Fn weakly, the potential role of this binding in the pathogenesis of leptospiral infection requires further study. Thus, the multivalent interaction of Lig-GBD, LigBCen2NR-NTD, and LigBCtv-15 type III modules of Fn mentioned above may mediate leptospiral adhesion to host cells to initiate infections.

Apart from Fn, the binding activity of LigB to elastin was also elucidated. In this study, elastin and its monomer, tropoelastin, were found to bind to immunoglobulin-like domains of Lig proteins. Four elastin binding immunoglobulin-like domains were identified including LigCon4, LigBCen7'-8, LigBCen9, and LigBCen12. The binding between elastin and Lig was found to be mediated by charge-charge interaction. Since *Leptospira* usually preferentially localize in elastin-rich organs such as lung, skin, and uterus, Lig-elastin interaction may enhance the attachment of *Leptospira* spp. to lung and placenta elastic fibers. The interaction of various virulence factors of *Leptospira* spp. with lung and placenta may lead to pulmonary hemorrhage and/or abortion. Moreover, elastin plays a pivotal role for tissue repair and reorganization. The binding of Lig protein and tropoelastin may block the elastogenesis to repair the tissue injury caused by *Leptospira* spp. infection. Therefore, this may facilitate the penetration and migration of this organism in host tissue.

Fibrinogen (Fg), a plasma proteins involved in blood coagulation, was also proved to bind to Lig proteins in this study. Platelet aggregation, adhesion, and fibrin clot formation can be blocked by the buried RGD motif on FgαCC domains led by the binding of Lig proteins. Due to the inability of the inhibition of plasminogen or tissue plaminogen activator to FgαCC domains by the binding of Lig proteins, a fibrin clot could not be formed stably. This may explain a possible reason for pulmonary and mammary gland hemorrhage..

To date, Ig like domains of Lig proteins possess a limited size (90 amino acids residues) but bind to various ECM including fibronctin, laminin, collegen, elastin, tropoelastin, and fibrinogen. The molecular mechanism of the interaction of Lig protein with multiple ECMs needs further study to understand the role of each ECM in the pathogenesis of *Leptospira* spp. infection in animals and humans. In conclusion, the study of the interaction of Lig protein and their ECMs has helped elucidate the important role of these virulence factors in the pathogenesis of leptospirosis.